Gene regulation in methanotrophs: Evidence from *Methylococcus capsulatus* (Bath) and *Methylosinus trichosporium* (OB3b)

Ashraf Khalifa

A thesis submitted to the School of Life Sciences in fulfilment of the requirements for the degree of Doctor of Philosophy

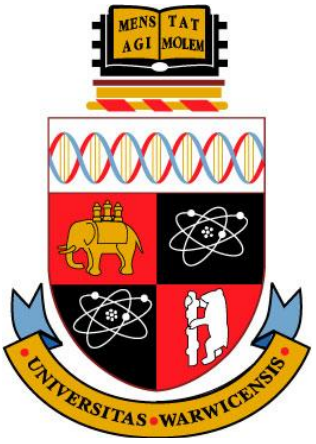

February 2012
University of Warwick
Coventry, UK

Contents

List of figures

List of tables

Acknowledgements

I am very grateful to my supervisor, Professor J. Colin Murrell, for giving me the opportunity to be part of this exciting project, for his extraordinary help and constructive support throughout my PhD project.

I am very indebted to Dr. Andrew Crombie, Mrs Julie Scanlan and Dr. Yin Chen for their endless help, encouragement and fruitful discussions, and for their critical reading of thesis chapters. Special thanks should go to Dr. Kevin Purdy for assistance in statistical analysis. In addition, I would like to thank all past and present members of D14 (Helene, Rich, Elizabetta, Nataliia, Tanvir, Myriam, Jason, Jean, Dani and Antonia) for their friendship and for making my time at Warwick enjoyable. I am grateful to Dr. Paul Norris for copper measurements and to Dr Christophe Corre, Chemistry department for LC/MS analysis. I am also grateful to Professor David Hodgson for fruitful discussions and advice in genetics. I must thank Professor Alan DiSpirito at Iowa State University and Dr. Jeremy Semrau at Michigan University for Mb analysis for some of the mutants and valuable discussions. Thanks should extend to Professor Stephane Vuilleumier, University of Strasbourg, France, for sending us the sequences of the putative precursor for the Mb in *Methylosinus trichosporium*.

In addition, I am very indebted to my family for their patience, support and encouragement. Finally, I would like to acknowledge the Ministry of Higher Education and Research, Egypt for funding this PhD studentship.

Declaration

I declare that the work described herein was conducted by me under the supervision of Professor J. Colin Murrell and none of the work has been previously submitted for any other degree. Contribution from others has been specifically acknowledged.

Part of the work presented in Chapter 3 is in preparation for publication for FEMS Microbiology Letters. The title has been proposed to be:
Mutagenesis of a copper P-type ATPase encoding gene in *Methylococcus capsulatus* (Bath) results in copper-sensitivity, Ashraf Y. Z. Khalifa, M. Hanif Ali and J. Colin Murrell, (in preparation).

In addition, part of the work done in Chapter 4 is in preparation for publication, probably to FEMS Microbiology Letters. This will be a joint-publication, with our collaborators Alan DiSpirito, Jeremy Semrau and others. The following title has been proposed;
Mutagenesis of polyketide synthetase (PKS) of *Methylococcus capsulatus* (Bath): Further evidence that methanobactin may be ribosomally synthesized, (in preparation).

Ashraf Khalifa

Abbreviations

A	actuator domain
A_{540}	absorbance at A_{540} nm
ACP	phosphopantethienylated acyl carrier protein
A-domain	adenylation domain
$Amp^{(R)}$	ampicillin (resistance)
AT	acyltransferase
ATP	adenosine triphosphate
ATPBD	ATP binding domain
P-type ATPases	ion translocating membrane transporters
BCCP	bacterial diheme cytochrome c peroxidase
BLAST	basic local alignment search tool
bp	nucleotide base pairs
C	cyclase
C-domain	condensation domain
CAS	chrome azurol S
DH	dehydratase
DMSO	dimethyl sulfoxide
DNA	deoxyribonucleic acid
DNase	deoxyribonuclease
dNTP	deoxynucleotide triphosphate
EDTA	ethylendiaminetetraacetic acid
EICs	extracted ion chromatograms
dw	dry weight
EPR	electron paramagnetic resonance
FAD	flavin-adenine dinucleotide
g	gram
$Gm^{(R)}$	gentamicin (resistance)
h	hour
HEPES	4-(2-hydroxyethyl)-1-piperazineethanesulfonic acid
HDTMA	hexadecyltrimethylammonium bromide
kDa	kilo Daltons
$Km^{(R)}$	kanamycin (resistance)
KO	knock-out
KR	ketoreductase
KS	β-ketoacylsynthase
ICM	intracytoplasmic membranes
l	litre

LB	Luria-Bertani
LC-MS	Liquid chromatography-mass spectrometry
ln2	natural logarithm of 2
M	molar
Mb	methanobactin
MCS	multiple cloning site
MDH	methanol dehydrogenase
mg	milligram
min	minute
ml	millilitre
mM	millimolar
mRNA	messenger RNA
MS	mass spectrometry
m/z	mass-to-charge ratio
ng	nanogram
nmol	nanomole
N	nucleotide domain
NanoLC-ESI-MS/MS	Nano liquid chromatoghraphy electrospray ionization tandem mass spectrometry
NCBI	National Centre for Biotechnology Information
NMS	nitrate mineral salts
NRP	non-ribosomal peptide
NRPS	non-ribosomal peptide synthetase
OD_{540}	optical density at 540 nm
orf	open reading frame
ori	origin of replication
oriT	origin of transfer
P-domain	phosphorylation domain
PAGE	polyacrylamide gel electrophoresis
PCR	polymerase chain reaction
PK	polyketide
PKS	polyketide synthetase
pMMO	particulate methane monooxygenase
pmol	picomole
PQQ	pyrroloquinoline quinone
qPCR	quantitative real-time polymerase chain reaction
RNA	ribonucleic acid
RNase	ribonuclease
r.p.m.	revolutions per minute
rRNA	ribosomal ribonucleic acid
RT-PCR	reverse transcriptase PCR
RuMP	ribulose monophosphate
s	seconds
SCP	single-cell protein

SDS	sodium dodecyl sulfate
sMMO	soluble methane monooxygenase
T-domain	a thiolation domain
TAE	tris acetate EDTA
TBE	tris borate EDTA
TCE	trichloroethylene
t_D	doubling time
TE	tris-EDTA
TE-domain	a thioesterase domain
TEMED	*N*, *N*, *N'*, *N'*-tetramethyl-ethane-1,2-diamine
Tg	a teragram, 10^{12} grams
TM	transmembrane
TMMBS	transmembrane metal binding site
TMPD	N, N, N′, N′-tetramethyl-p-phenylenediamine
v/v	volume to volume
w/v	weight to volume
µg	microgram
µl	microlitre
X-gal	5-bromo-4-chloro-3-indoyl-β-D-galactoside

Abstract

Methylococcus capsulatus (Bath) is a Gram-negative, spherical-shaped bacterium that gains its needs of carbon and energy via oxidation of methane, a potent greenhouse gas, thus alleviating global warming. This bacterium oxidises methane to methanol using a membrane-bound particulate methane monooxygenase (pMMO) or a soluble, cytoplasmic methane monooxygenases (sMMO). Copper-to-biomass-ratios significantly affect the expression and activity of both enzymes; the biosynthesis of sMMO is switched on when copper-to-biomass ratios are low, while pMMO is up-regulated when they are high. The exact mechanisms by which copper regulates the switching between sMMO and pMMO are not fully elucidated. Therefore, the main aim of this study was to shed some light on this copper switch, taking the advantage of the availability of the genome sequence of this organism, together with mutagenesis and transcriptional regulation studies.

Three potential copper transport *Mc. capsulatus* mutants; Δ*copA1*, Δ*copA2* and Δ*copA3* were generated. The genes inactivated encode three different P-type ATPase homologs.This revealed that CopA1, CopA2 and CopA3 have roles in copper homeostasis, although disruption of genes encoding these proteins individually did not result in constitutive sMMO expression.

In addition, three mutants; Δ*nrpS-1*, Δ*nrpS-2* and *pkS* were constructed. *pkS* encodes for a polyketide synthase, *nrpS-1* and *nrpS-2* encode for two non-ribosomal peptide synthetases. The products of these genes were proposed to be involved in biosynthesis of methanobactin, a short peptide that scavenges copper when it is limited. Results suggested that *nrpS-2* and *pkS* might be involved in production of a functional methanobactin.

Putative coding sequences predicted to be involved in methanobactin biosynthesis in another methane-oxidising bacterium, *Methylosinus trichosporium* (OB3b), were also mutated. The mutant was unable to produce methanobactin, could not express sMMO, and was copper resistant compared to the wild-type organism. Therefore, methanobactin is ribosomally-produced in *Ms. trichosporium*. Corresponding genes were not identified in the genome of *Mc. capsulatus*.

A microarray-based comparative expression profiling study of whole-genome transcriptomics of *Mc. capsulatus* expressing sMMO versus pMMO was carried out to identify genes involved in regulation of MMO by copper. This identified 53 genes that were differentially expressed and hence promising candidate genes for future studies of MMO regulation. For example, *tetR*, a down-regulated gene, encodes a putative transcriptional regulator and *tonB*, an up-regulated gene, which encodes a protein that is a part of a membrane transporter. Interestingly, a cluster of six genes 5' of sMMO was up-regulated; five of them were found to be co-transcribed. A mutant was made in an up-regulated gene encoding ScO protein (synthesis of cytochrome c). The mutant could tolerate high concentrations of copper compared to the wild-type strain.

The work presented in this study is considered a step forward towards understanding the regulatory mechanisms of the copper switch in methanotrophs and provided the basis for new lines of future research to fully understand this phenomenon.

Chapter 1

Introduction

1.1 Introduction

The term methanotrophs is applied to a group of ubiquitous bacteria capable of growth on methane as their sole energy and carbon source (Hanson and Hanson, 1996; Semrau *et al*., 2010). Methanotrophic bacteria represent a subdivision of the methylotrophs, which are a diverse group of organisms able to utilize different compounds containing a single-carbon atom *e.g*., methanol, methylated amines, halomethanes (Murrell and McDonald 2000; Chistoserdova, 2011). Additionally, an interesting novel genus of facultative methylotrophs *Methylorosula polaris* that grows on methanol, methylamines, a wide range of sugars and polysaccharides has recently been isolated from tundra wetland (Berestovskaya *et al*., 2011). The majority of methanotrophs are considered as obligate methylotrophs although some of them can grow on methanol (Trotsenko and Murrell, 2008). Nonetheless, facultative methanotrophs that grow on compounds containing more than one carbon atom (*e.g*., ethanol, acetate) have been isolated. *Methylocella silvestris* BL2 is the notable example (Dunfield *et al*., 2003; Theisen and Murrell, 2005). Also, some species belonging to *Methylocystis* (Im *et al*., 2010; Belova *et al*., 2011) and *Methylocapsa* (Dunfield *et al*., 2010) showed relatively weak growth on ethanol or acetate.

Methane monooxygenase (MMO) is the pivotal enzyme that methanotrophs contain since it catalyses the oxidation methane to methanol (reviewed in Trotsenko and Murrell (2008); Smith *et al*. (2010); Semrau *et al*., (2010)). There are two types of MMO: a particulate methane monooxygenase (pMMO) and a cytoplasmic or soluble methane monooxygenase enzyme (sMMO). Details about both enzymes are outlined later on this chapter. Methanotrophs possess at least one of the two MMOs although some genera contain both. In general, the majority of methanotrophs contain a

particulate methane monooxygenase enzyme. However, a few methanotrophic species contain only soluble methane monooxygenase enzyme *e.g.*, *M. silvestris* (Dunfield *et al.*, 2003; Theisen *et al.*, 2005) and a recently isolated methanotroph, *Methyloferula stellata* (Vorobev *et al.*, 2010). Some methanotrophs, including *Methylococcus capsulatus* (Bath) and *Methylosinus trichosporium* (OB3b), possess both types of MMO, pMMO and sMMO. In the last two examples, the expression of the two types of MMO is significantly affected by the bioavailability of copper (Stanley *et al.*, 1983; Prior and Dalton, 1985b). Under high copper-biomass ratios, the biosynthesis of pMMO is switched on, while sMMO is up-regulated during growth at low copper-to biomass ratio. Although *Mc. capsulatus* has been studied extensively over the past 40 years, the exact role of copper in regulation of MMO is still unclear. Therefore, the basis of this study was to shed new light on the role of copper in regulating the expression of MMO, especially in *Mc. capsulatus* and *Ms. trichosporium*. This chapter presents a brief introduction to different aspects of methanotrophs.

1.2 A brief history of the taxonomy of methanotrophs

Söhngen, a Dutch microbiologist, in 1906 isolated the first methane-oxidizing bacterium, *Bacillus methanicus*, from aquatic plant material. A half century later, this bacterium was re-designated as *Pseudomonas methanica* (Dworkin and Foster, 1956) and a novel methane oxidizer was also isolated from sewage sludge, *Mc. capsulatus* which was able to grow at 50 ºC (Foster and Davis, 1966). This revived the interests of researchers into this group of microorganisms. Whittenbury *et al.* (1970) provided the scientific community with the first detailed

study about isolation, classification, and physiology of methanotrophs. They isolated more than 100 methane-oxidising

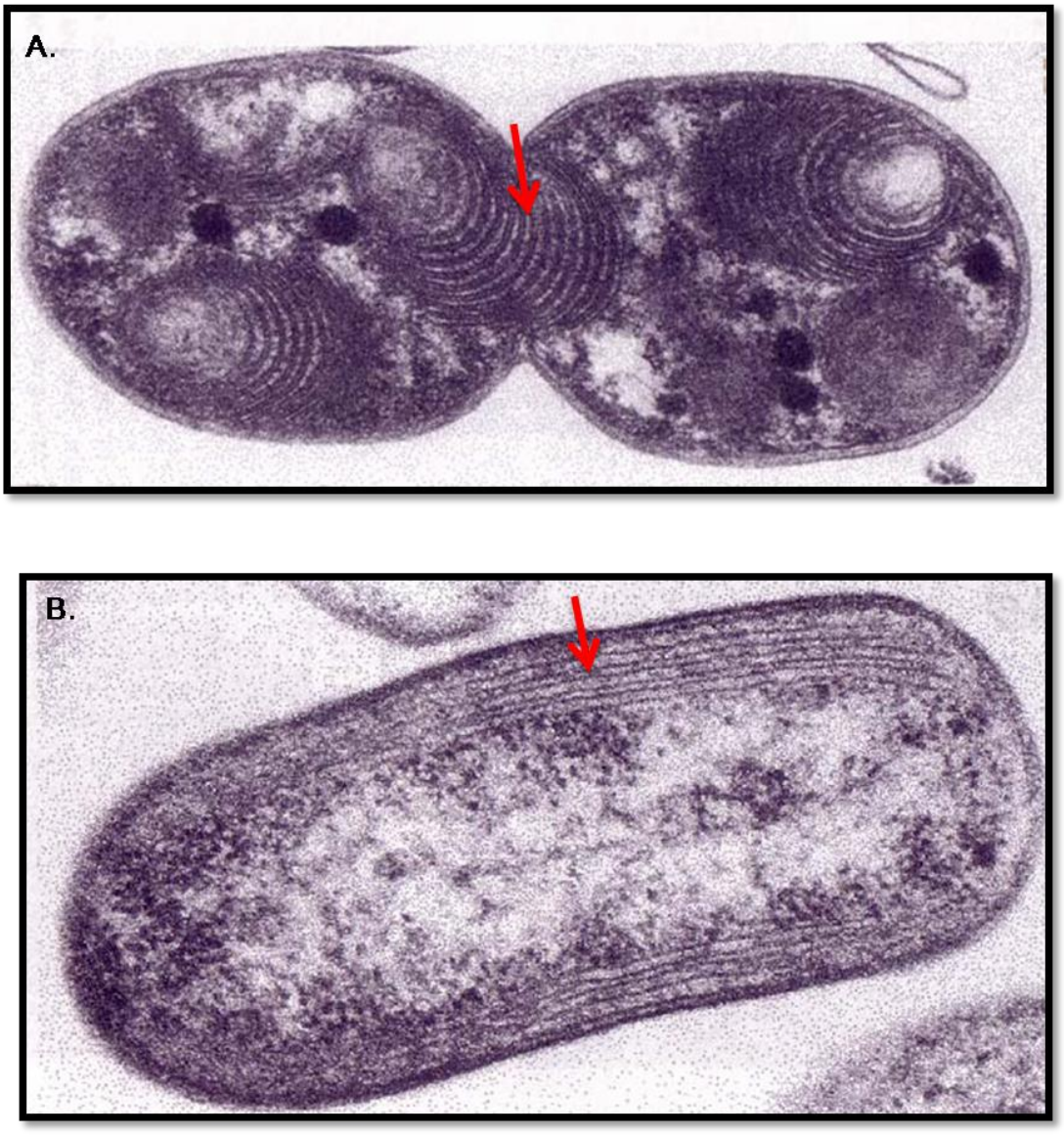

Figure 1.1 Electron micrographs showing intracytoplasmic membranes (ICM) arranged as disc-shaped membrane vesicles in the cells (A. Type I methanotrophs) and around the cell periphery (B. Type II methanotroph). Red arrows point out the ICM. Taken from Green (1992).

bacteria and classified them based on morphological features and ultra-structure of cells. These bacteria were assigned to five genera, which were divided into two

types. Type I methanotrophs have intracytoplasmic membranes, which form disc-like shaped vesicles in the cells (Figure 1.1A). Three genera comprised the Type I methanotroph; *Methylococcus*, *Methylobacter* and *Methylomonas*. In addition, Type II methanotrophs included *Methylosinus* and *Methylocystis* and were characterized by intracytoplasmic membranes organized on periphery of the cells (Figure 1.1B), (Davies and Whittenbury 1970; Whittenbury *et al.*, 1970).

Bowman and his colleagues (Bowman *et al.*, 1993a, 1993b and 1995) revised the taxonomy of methanotrophs and rearranged Type I and II methanotrophs using more reliable polyphasic approaches which included phenotypic, genotypic, biochemical characteristics and their phylogenetic relationships. For example, they combined three species; *Methylobacter albus*, *Methylobacter agilis* and *Methylobacter pelagicus* into a novel genus *Methylomicrobium*.

Hanson and Hanson (1996) summarized what was known about methanotrophs including their physiology, ecology, biotechnological applications, as well as their taxonomy. In addition, Semrau *et al.* (2010) have presented a recent and comprehensive review. This covers almost all topics included in Hanson and Hanson (1996), in addition to methanotrophs phylogeny and the significant role of copper in the physiology of methanotrophs (pMMO, Mb, and specific copper acquisition systems). A considerable deal of concern was given to the two reviews as both fitted with the line of the current study.

Currently, the number of the known methanotroph genera and species is increasing. The reason for this is due, in part, to their isolation from new and diverse environments and modern techniques used for their analysis. The recent discovery of diverse novel methanotrophs confirms that this group of bacteria is more diverse than

previously thought. A list of all currently recognized methanotrophic genera is presented in Table 1.1.

Table 1.1 A list of the current genera of methanotrophs.

Genus	Phylogenetic group	Reference
Methanotrophs that contain both sMMO and pMMO		
Methylococcus	*Gammaproteobacteria*	Foster and Davis (1966)
Methylocystis	*Alphaproteobacteria*	Whittenbury *et al.* (1970)
Methylosinus		Whittenbury *et al.* 1970)
Methylovulum		Iguchi *et al.* (2011)
Methylorosula		Berestovskaya *et al.* (2011)
Methanotrophs that contain pMMO only		
Methylobacter	*Gammaproteobacteria*	Bowman *et al.* (1993b)
Methylocaldum		Bodrossy *et al.* (1997)
Methylohalobius		Heyer *et al.* (2005)
Methylomicrobium		Bowman *et al.* (1995)
Methylomonas		Leadbetter (1974), Whittenbury and Krieg (1984)
Methylosoma		Rahalkar *et al.* (2007)
Methylosphaera		Bowman *et al.* (1997)
Methylosarcina		Wise *et al.* (2001)
Methylothermus		Tsubota *et al.* (2005)
Methylogaea		Geymonat *et al.* (2011)
Crenothrix		Stoecker *et al.* (2006)
Clonothrix		Vigliotta *et al.* (2007)
Methylacidiphilum	*Verrucomicrobia*	Pol *et al.* (2007), Dunfield *et al.* (2007) and Islam *et al.* (2008)
Methanotrophs that contain sMMO only		
Methylocapsa	*Alphaproteobacteria*	Dedysh *et al.* (2002)
Methylocella		Dedysh *et al.* (2000)
Methyloferula		Vorobev *et al.* (2010)

1.3 Phylogeny of methanotrophs

Molecular phylogeny has a pivotal role in classifying and understanding microorganisms based on their evolutionary relationships (Ludwig and Schleifer, 1994). Analyses of sequences of ribosomal RNA genes are commonly used for constructing phylogenetic trees amongst all types of organisms. The reasons for this are largely due to the fact that rRNAs are abundant, universally distributed in cells (Ingraham *et al.*, 1983) and conserved and evolutionarily homologous (Pace *et al.*, 1986).

The first study that addressed the phylogenetic affiliations amongst methylotrophs was carried out by Wolfrum and Stolp (1987), who used 5S rRNA sequences analysis in their study. Subsequently, analysis of 16S rRNA sequences (~ 1,500 bases) rather than 5S rRNA sequences (~ 120 bases) has led to more meaningful phylogenetic inferences (Woese, 1987).

In the early 1990s, comparative 16S rRNA sequence analysis was used successfully to separate methylotrophs into groups (Tsuji *et al.*, 1990 and Bratina *et al.*, 1992) that fitted those obtained by classical taxonomic means (Whittenbury and Krieg 1984). Hanson and Hanson (1996) classified methanotrophs based on the 16S rRNA gene sequence analyses into six genera in the *Proteobacteria*. The four genera that formed Type I methanotrophs; *Methylobacter, Methylococcus, Methylomicrobium* and *Methylomonas*, were found to be *Gammaproteobacteria* while *Alphaproteobacteria* included the two Type II methanotroph genera; *Methylocystis, Methylosinus*.

Currently, the *Gammaproteobacteria* (Type I) and *Alphaproteobacteria* (Type II) methanotrophs have been extended to include new genera (Table 1.1) and a third group *Verrucomicrobia* has been introduced, based on phylogenetic analyses of 16S

rRNA gene sequences (Figure 1.2). Thermoacidophilic methanotrophs have been isolated; *Methylacidiphilum infernorum* strain V4 (Dunfield *et al.*, 2007), *Methylacidiphilum fumarolicum* strain SolV (Pol *et al.*, 2007) and *Methylacidiphilum kamchatkense* strain Kam1 (Islam *et al.*, 2008). These strains clustered phylogenetically as *Verrucomicrobia*. Details about Verrucomicrobial methanotrophs are discussed in a review by Op den Camp *et al.* (2009). Recently, a novel facultative methylotroph *Methylorosula polaris* (not shown in Figure 1.2) has been classified as a member of the *Alphaproteobacteria* and situated in a separate cluster within the *Beijerinckiaceae* (Berestovskaya *et al.*, 2011).

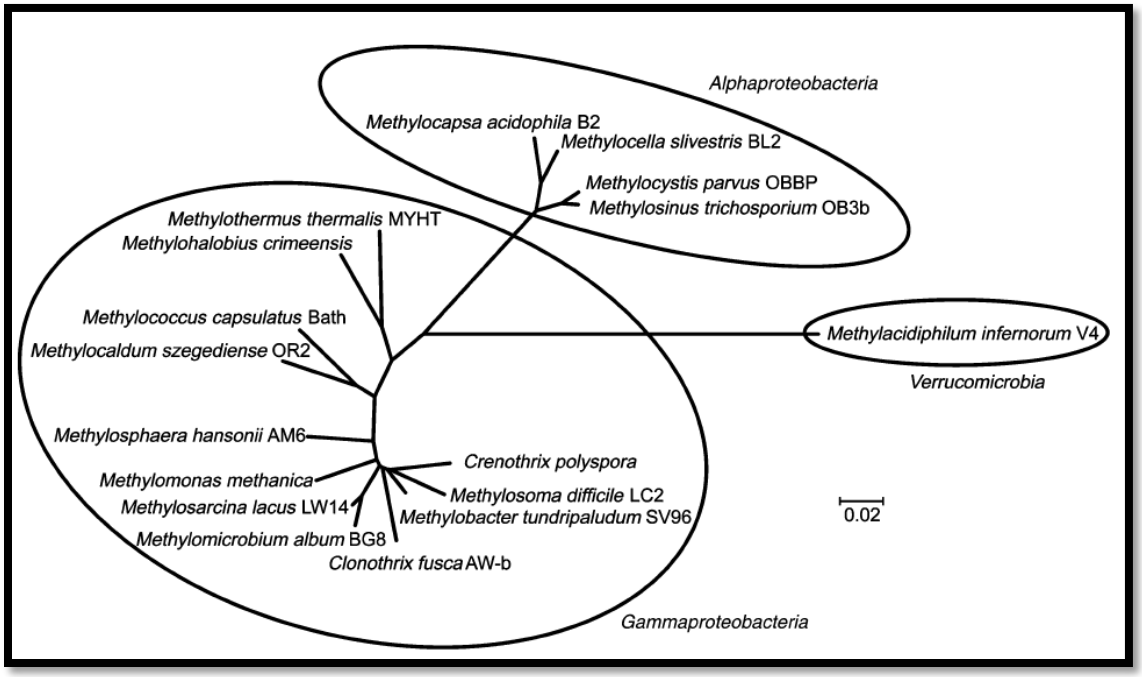

Figure 1.2 Phylogenetic relationships between methanotrophs based on 16S rRNA gene sequences. The scale bar indicates 0.02 base substitutions per site. Taken from Semrau *et al.* (2010).

Another approach that has been used in studying phylogenetic relationships amongst methanotrophic organisms is the use of *pmoA*, as a functional gene, which encodes for the β-subunit of the pMMO hydroxylase (reviewed in Semrau *et al.*,

2010). The phylogeny of *pmoA* was consistent with that of 16S rRNA gene. It has been revealed that *pmoA* from *Crenothrix*, a filamentous methanotroph (Stoecker *et al*., 2006; Vigliotta *et al*., 2007), diverges from *pmoA* of the *Gammaproteobacteria* methanotrophs. Significant divergence (more than 40%) between *pmoA* in the *Verrucomicrobia*, *Alphaproteobacteria* and *Gammaproteobacteria* was also found (Dunfield *et al*., 2007).

1.4 Distribution of methanotrophs

Methanotrophs are ubiquitous organisms found in many diverse environments. Methanotrophic species have been found in peat bogs (Dedysh *et al*., 1998), landfills (Wise *et al*., 1999), plant rhizosphere (Gilbert and Frenzel, 1995), freshwater and seawater (Fliermans *et al*., 1988; Holmes *et al*., 1995; Khmelenina *et al*., 1996; Bodrossy *et al*., 1997), sediments (Smith *et al*., 1997; Auman *et al*., 2000) and soils (Whittenbury *et al*., 1970; Iguchi *et al*., 2011; Rahman *et al*., 2011).

Many soil properties and climatic factors affect methanotrophic distribution in the environment, *e.g*. temperature and pH (Amaral and Knowles, 1995; Han *et al*., 2009a). For more details on such factors, see Hanson and Hanson (1996) and Semrau *et al*. (2010).

Methanotrophic bacteria are in general mesophilic organisms, however, some genera are moderately thermophilic *e.g*., *Mc*. *capsulatus*, *Methylothermus thermalis* and *Methylocaldum* spp. (Medvedkova *et al*., 2007). Furthermore, *Methylosphaera hansonii, Methylomonas scandinavica* and *Methylobacter psychrophilus* are examples of psychrophilic methanotrophs (Bowman *et al*., 1997; Kalyuzhnaya *et al*., 1999). *Verrucomicrobia* are thermoacidophilic methanotrophs that can grow at high temperature (65 ^{o}C) and low pH (pH 1.0) (Op den Camp *et al*., 2009).

Methanotrophs are also found in association with other organisms; as endosymbionts of marine invertebrates such as mussels (DeChaine and Cavanaugh, 2006; Duperron *et al.*, 2008), tubeworms and sponges (Petersen and Dubilier, 2009). Furthermore, *Methylocella* and *Methylocapsa* spp. probably establish symbiotic relationships with some nonvascular plants such as *Sphagnum* mosses (Raghoebarsing *et al.*, 2005).

1.5 Ecological significance of methanotrophs

Methane, a one-carbon compound, occurs in the atmosphere at the highest concentration of any of the trace gases (Cicerone and Oremland, 1988; Crutzen, 1994). One important characteristic of methane is its efficient capacity as a greenhouse gas (heat-trapping gas) in comparison to carbon dioxide (Wuebbles and Hayhoe, 2002). Therefore, methane contributes to global warming (Lelieveld *et al.*, 1998).

Methanotrophs, through the efficient activity of methane monooxygenases, are major players in removal of methane from the atmosphere, therefore mitigating the global warming. Furthermore, the cosmopolitan distribution of methanotrophs (see section 1.4) is an indication of their significant role in oxidation of methane and global carbon cycling. Several approaches have been proposed to increase the activity of methanotrophs in order to decrease the amount of methane emitted to the atmosphere (*e.g.*, biocovers and biofilters). For more details, refer to Scheutz *et al.* (2009), Jiang *et al.* (2010) and Chiemchaisri *et al.* (2012).

1.6 Biotechnological application of methanotrophs

Methanotrophs are microorganisms that have many potential applications in industry *e.g.*, biodegradation of pollutants, and production of biofuels and microbial proteins. Several studies have described extensively the different applications of methanotrophs (Smith and Murrell, 2009; Jiang *et al.*, 2010; Semrau *et al.*, 2010).

1.6.1 Pollutant degradation

Methanotrophs have a potential role in bioremediation. Methanotrophs co-oxidize trichloroethylene (TCE), a toxic compound commonly used as a solvent (Tsien *et al.*, 1989). sMMO is capable of oxidising a variety of hydrocarbons including alkanes, alkenes, heterocyclic compounds and aromatic ethers (Colby *et al.*, 1977). The main disadvantage of using the wide-substrate specificity of sMMO in bioremediation is its repression by copper. This highlights the need to elucidate of the mechanisms of copper regulation of MMO, which were the focus of this study. Furthermore, some chlorinated ethanes and propanes can be degraded by methanotrophs that express pMMO (Oldenhuis *et al.*, 1989). Details about the uses of methanotrophs as biocatalysis and the different co-substrates of sMMO and pMMO are reviewed by Smith and Dalton (2004) and Smith and Murrell (2010).

1.6.2 Production of fuels

It has been reported that methanotrophs can be used to produce methanol under ambient conditions, which could be used as fuel or in chemical production. For example, *Methylosinus trichosporium* was used to produce methanol from methane in the presence of 40% carbon dioxide for best results (Xin *et al.*, 2004). One of the

major limitations is that the growth of *Ms. trichosporium* is relatively slow and the cell density can be low. However, a novel approach to overcome this problem is by increasing the methane solubility in the growth medium using paraffin oil, an immiscible organic solvent (Han *et al.*, 2009b). It has been shown that addition of 5% paraffin oil led to an increase in the cell density of *Ms. trichosporium* seven times more than the control (Han *et al.*, 2009b). Extending this approach to other methanotrophs and in particular slow growers may enhance the potential use of these organisms in biotechnological applications. Furthermore, two strategies have been proposed for maximizing the bioproduction of methane by methanotrophs: using appropriate genetically modified strains or adding a specific inhibitor to slow down the rate of methanol dehydrogenase, an enzyme responsible for conversion of methanol to formaldehyde (reviewed in Smith and Murrell, 2010). Taking these suggested approaches and considering technical and engineering issues, production of biofuels on an industrial scale using methanotrophs shows some promise.

1.6.3 The pharmaceutical industry

Enantiopure chemical compounds have a paramount importance particularly in the pharmaceutical industry, *e.g.*, in treating diseases with minimal side effects. This is because one enantiomeric form of a compound could be an effective drug against certain diseases while the other enantioner of the same compound might be fatal (Perri and Hsu, 2003). Despite the fact that sMMO oxidation is not exceedingly stereospecific, the stereospecificity of sMMO oxidations might be improved via site-directed mutagenesis of the active site (Smith *et al.*, 2002; Borodina *et al.*, 2007). Research in the Murrell lab and in the Smith lab is directed at obtaining

pharmaceutically important chemicals via genetically modified methane monooxygenase.

1.6.4 Single cell protein (SCP)

Methanotrophs can be used as an alternative source for proteins for consumption as feedstocks by animals and fish. A notable attempt has been made by Norferm Danmark A/S in Norway to produce 8,000 tons y^{-1} of single-cell protein known as BioProtein using *Mc. capsulatus* (Winder, 2004). The future may bring more biotechnological applications of methanotrophs through improving their genetic manipulating systems, using efficient homologous expression system and extending the uses of the sMMO (Smith *et al*., 2010).

1.7 The methane oxidation pathway

Methane metabolism involves either complete oxidation of methane into CO_2 in a catabolic processes or partial oxidation to formaldehyde, which is then converted into cell biomass via anabolic processes (Figure 1.3).

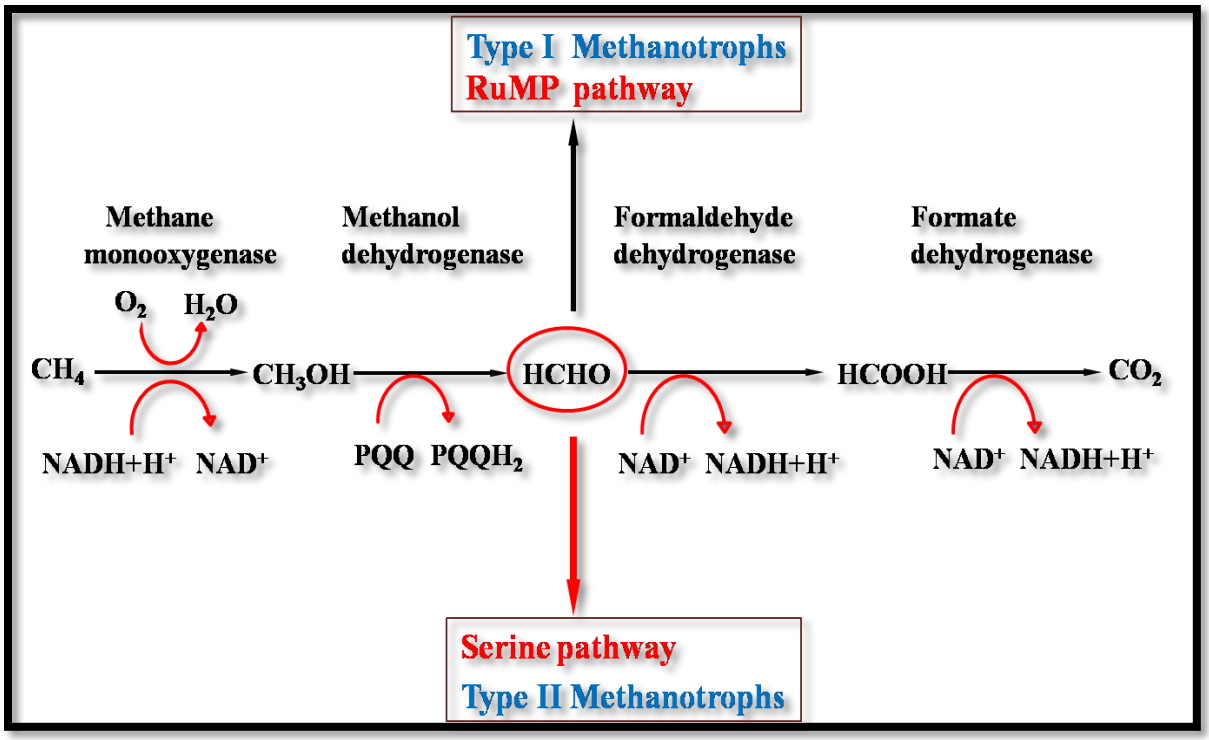

Figure 1.3 Different pathways of methane metabolism in methanotrophs.

Methane monooxygenase (sMMO or pMMO) mediates the first step in metabolism of methane in methanotrophs by oxidizing methane to methanol. In this step, two reducing equivalents are involved in breaking the dioxygen bond. Incorporation of one of the two resulting oxygen atoms into methane forms methanol while the other atom is reduced, forming water (Hanson and Hanson 1996). Further oxidation of the methanol produced in the first step, into formaldehyde, is mediated by the periplasmic pyrroloquinoline quinone (PPQ)-dependent methanol dehydrogenase (MDH) (Anthony, 2004) (Figure 1.3). Formaldehyde is assimilated to cell biomass through either via either the ribulose monophosphate (RuMP) cycle in the Type I methanotrophs or the serine cycle in the Type II methanotrophs (Anthony, 1982). Alternatively, formaldehyde is further oxidized using formaldehyde dehydrogenase into formate, which is then dissimilated, by formate dehydrogenase into CO_2 for ATP and reductant (NADH) production (Figure 1.3). Details about

carbon metabolic pathways in both types of methanotrophs are reviewed in Smith *et al.*, (2010). It is worth mentioning that some of the reducing equivalents that are produced during formation of formate are utilized by MMOs in mediating methane oxidation. Other alternative catabolic routes of formaldehyde have been reported in *Methylobacterium extorquens* (Vorholt, 2002). These routes are proposed to function in detoxifying formaldehyde and in producing ATP. In addition, it has been suggested that the methylene tetrahydromethanopterin dehydrogenase could oxidise formaldehyde in *Mc. capsulatus* (Adeosun *et al.*, 2004). Details about methane oxidation biochemistry can be found in Anthony (1982), Murrell *et al.*, (2000) and Semrau *et al.*, (2010).

1.8 Particulate methane monooxygenase (pMMO)

The particulate methane monooxygenase (pMMO) is a membrane-associated enzyme that was first described in the mid 1970s (Colby *et al.*, 1975; Ferenci *et al.*, 1975). This enzyme is found in the majority of methanotrophs and is expressed during growth when the ratios of copper to biomass are high. *Methylocella silvestris* (Dunfield *et al.*, 2003; Theisen *et al.*, 2005) and *Methyloferula stellata* (Vorobev *et al.*, 2010) lack pMMO. Copper is indispensable for pMMO expression (Nielsen *et al.*, 1996 and 1997; Choi *et al.*, 2003) and activity (Basu *et al.*, 2003; Yu *et al.*, 2003). In addition, copper enhances the formation of an intensive intracytoplasmic membrane (ICM) network in which pMMO is localized (Prior and Dalton, 1985b; Choi *et al.*, 2003). Compared to sMMO, pMMO is capable of oxidizing a narrow range of compounds including alkanes and alkenes up to five carbons in length. However, pMMO cannot oxidise aromatic compounds (*e.g.*, naphthalene) (Burrows *et al.*, 1984;

Hakemian and Rosenzweig, 2007). Differences between sMMO and pMMO are presented in Table 1.2.

Table 1.2 A summary comparing between sMMO and pMMO.

Character	pMMO	sMMO
Encoding genes	*pmoCAB*	*mmoXYBZDC*
Regulatory genes	Unknown	*mmoG, mmoR*
Promoter	σ^{70}	σ^{54}
Copy number	Multiple	Single
Location of enzyme	Particulate (membrane associated)	Cytoplasmic, soluble
Metal in active site	Copper and possibly iron	Iron
Expression conditions	High copper to biomass ratios	Low copper to biomass ratios
Substrate specificity	Narrow	Broad
Examples of substrates	Short chain alkanes and alkenes	Alkanes, alkenes, aromatic compounds
Naphthalene assay	Negative	Positive
Distribution	Most methanotrophs	Few methanotrophs

1.8.1 Biochemistry of pMMO

Particulate methane monooxygenase (pMMO) is a copper-containing enzyme, which catalyses the oxidation of methane to methanol. As pMMO is an integral membrane protein and thus more difficult to purify than sMMO, information on the structure of pMMO has until recently been very limited compared to sMMO.

pMMO consists of two components, a hydroxylase (pMMOH) and a reductase (pMMOR). Three subunits α (PmoB), β (PmoA) and γ (PmoC) form the hydroxylase (pMMOH) (Figure 1.4). These subunits have approximate masses of 47, 24, and 22 kDa respectively. The other component of pMMO is a reductase (pMMOR), which includes two proteins of 63 and 8 kDa (Zahn and DiSpirito, 1996; Basu *et al.*, 2003). Lieberman and Rosenzweig (2005) solved the crystal structure of pMMO from *Mc. capsulatus*. pMMO exists as a trimer in which the polypeptides are arranged in an

$\alpha_3\beta_3\gamma_3$ structure. Furthermore, three metal centres were identified in pMMO; two of them are copper centres (mononuclear and dinuclear) which reside in the soluble region of the pmoB subunit. The third metal centre was located within the membrane and contained zinc (Lieberman and Rosenzweig, 2005). These structural data about pMMO were consistent with those obtained in an independent study by Kitmitto and co-workers (2005). Although pMMO is a metalloenzyme, the nature of metal ions in the active centre and location of the active site have been controversial for many years. Recently, Balasubramanian *et al.* (2010) have attempted to resolve such a controversy by showing that the indispensible copper centre of pMMO activity is situated in the N-terminal soluble domain α-subunit and is a di-copper centre (Figure 1.4). The pMMO contains two metal centre located in the soluble domains of PmoB, mono- and di-copper centres. Mono-copper centre coordinated by two histidine residues (His 48 and His 72) and located in the soluble domain spmoBd2. Di-copper centre in which both copper atoms coordinated by three histidine residues (His 33, His137 and His139) and situated in spmoBd1 domain. In addition, a metal site that contained zinc from the crystallization buffer has been suggested to contain a di-iron centre. The proposed tri-copper coordinated by hydrophilic residues (Figure 1.4). The latter two metal centres are located in the transmembrane and are inactive (Balasubramanian *et al.*, 2010).

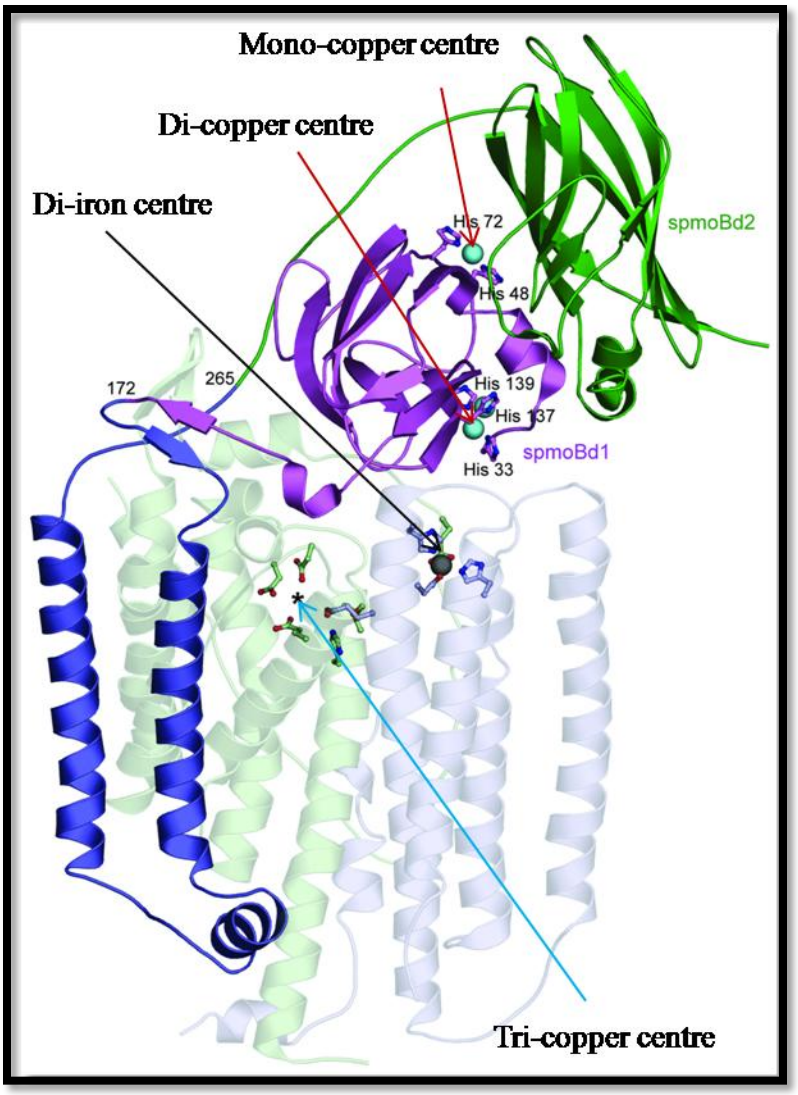

Figure 1.4 A pMMO protomer of *Mc. capsulatus* showing the different active centres. Faint light green is PmoA, faint light blue is PmoC and green, purple, and blue is PmoB. Taken from Balasubramanian *et al.* (2010).

1.8.2 Genetics of pMMO

The *pmoCAB* operon encodes the γ-subunit, β-subunit and α-subunit of the pMMO respectively, and is under the control of a σ^{70}-dependent promoter (Figure 1.5) (Semrau *et al.*, 1995; Nielsen *et al.*, 1997; Gilbert *et al.*, 2000; Stolyar *et al.*, 2001). Two separate but complete copies of pMMO gene cluster were sequenced in *Mc. capsulatus* (Bath), in *Ms. trichosporium* (OB3b) and in *Methylocystis* sp. Strain M. Comparative sequence analyses showed that the *pmoCAB* duplicate copies were almost identical (> 99% identity) (Stolyar *et al.*, 1999; Gilbert *et al.*, 2000).

Mutagenesis of each gene in both copies of *pmoCAB* revealed that both copies are functional and could complement one another (Stolyar *et al.*, 1999).

In addition, a third copy of *pmoC* (*pmoC3*) was identified only in *Mc. capsulatus* (Nguyen *et al.*, 1996). The *pmoC3* is situated in a putative operon, which might have a role in methane oxidation (Ward *et al.*, 2004).

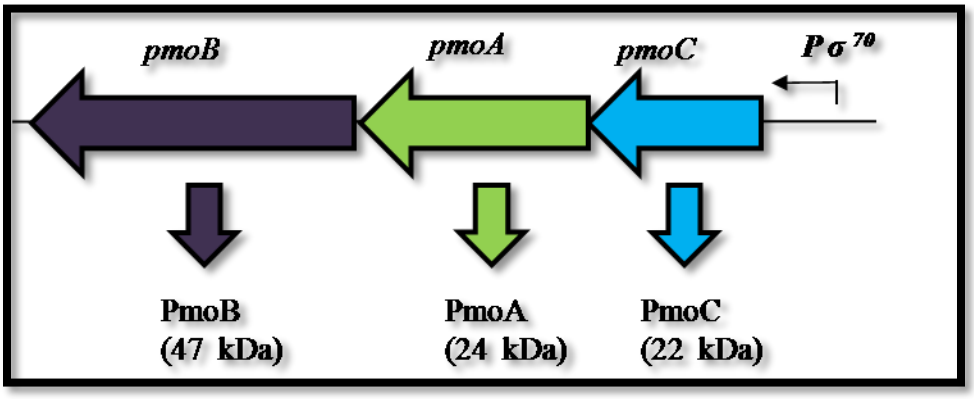

Figure 1.5 The structural gene organisation of pMMO operon in *Mc. capsulatus*. The *pmoCAB* operon encodes for the γ, β and α subunits of pMMO, respectively.

Duplication of pMMO-encoding gene clusters seems to be common in pMMO-containing methanotrophs (Auman *et al.*, 2000), however, it has been reported that the novel Type I methanotrophs *Methylovulum miyakonense* contains only one copy of the pMMO operon (Iguchi *et al.*, 2010).

It is clear that the sequences of *pmoA* are conserved and could be used as a phylogenetic marker in studying phylogeny of methanotrophs in natural habitats (Holmes *et al.*, 1995; McDonald and Murrell, 1997). Novel *pmoA*-like sequences have been discovered using such a strategy indicating, the presence of uncultured methanotrophs in rice field soils (Holmes *et al.*, 1995) and in marine ecosystems (Henckel *et al.*, 1999; Stoecker *et al.*, 2006).

1.9 Methanobactin (Mb)

Methanobactin (Mb) is a copper-binding, siderophore-like chromopeptide that is produced and excreted by a number of methanotrophs (Kim *et al.*, 2004; Choi *et al.*, 2005 and 2010; Yoon *et al.*, 2010; Bandow *et al.*, 2011; Yoon *et al.*, 2011). Mb is analogous to siderophores and can be called a chalkophore (sidero; Greek for iron, while chalko; Greek for copper).

The copper complex of Mb has a pyramid-like structure, with a single copper (I) ion coordinated by a N_2S_2 donor set at the base of the pyramid. The proposed structure for Mb is as follows: 1-(N- [mercapto-{5-oxo-2-(3-methylbutanoyl) oxazol-4-ylidene}methyl]-Gly1-Ser2-Cys3-Tyr4)pyrrolidin-2-yl-(mercapto-[5-oxo-oxazol-4-ylidene] methyl)- methyl)-Ser5-Cys6-Met7. (Kim *et al.*, 2004; Behling *et al.*, 2008; El Ghazouani *et al.*, 2011) (Figure 1.6).

Mb is believed to be a multi-functional compound. A large body of evidence suggests that Mb mediates copper uptake in Mb-producing methanotrophs. It has been reported that when *Mc. capsulatus* or *Ms. trichosporium* are grown in low-copper medium, Mb is detected in the supernatant and its level decreases upon copper addition (Zahn and DiSpirito, 1996; DiSpirito *et al.*, 1998). In addition, Mb is associated with pMMO and if dissociated from it, pMMO losses its activity. These observations led to the assumption that Mb has a role in pMMO activity, although the exact mechanism for this is still unclear (Choi *et al.*, 2003 and 2005). Furthermore, Mb protects the cells against oxidative stress. It has been shown that Mb from *Ms. trichosporium*, *Mc. capsulatus* and *Methylomicrobium album* exhibited activities of hydrogen peroxide reductase,

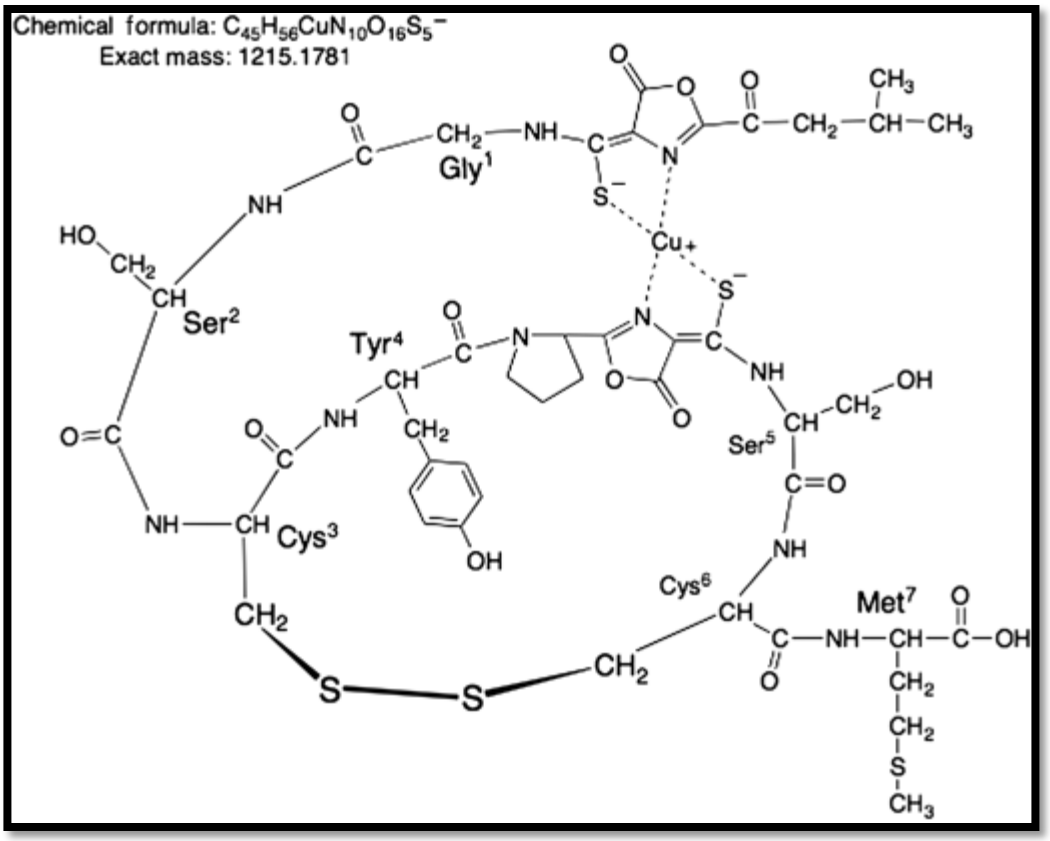

Figure 1.6 Structure of the copper (I) complex of Mb from *Ms. trichosporium*. The proposed structure for Mb is as follows: 1-(N- [mercapto-{5-oxo-2-(3 methylbutanoyl) oxazol-4-ylidene}methyl]-Gly1-Ser2-Cys3-Tyr4)pyrrolidin-2-yl-(mercapto-[5-oxo-oxazol-4-ylidene] methyl)- methyl)-Ser5-Cys6-Met7. The numbers indicate the order of the amino acid residues. Taken from Behling *et al.* (2008).

superoxide dismutase, and oxidase (Choi *et al*., 2008). An interesting recent review by Kenney and Rosenzweig (2011) summarizes the chemical and biological properties of Mb.

The genes involved in the synthesis of Mb have yet to be identified. It has been proposed that Mb is ribosomally synthesized in *Ms. trichosporium* (Krentz *et al.*, 2010). This possibility was investigated as part of the current study and the results are presented in Chapter 8. Alternatively, it is hypothesized that Mb may be synthesized by a non-ribosomal peptide synthase (NRPS) or polyketide synthetase (PKS), based on its similarity to siderophores (Balasubramanian and Rosenzweig, 2008;Ward *et al.*, 2004). Siderophores are small iron-chelating

compounds that mediate iron-uptake at low-iron conditions. Siderophores are generally synthesized by NRPS *e.g*., enterobactin in *Escherichia coli* (Ehmann *et al*., 2000) and pyochelin in *Pseudomonas aeruginosa* (Cox *et al*., 1981) or by PKS *e.g*. yersiniabactin in *Yersinia pestis* (Miller *et al*., 2002).

1.9.1 Polyketide synthases (PKS)

Polyketides are a group of secondary metabolites, which are produced by different organisms and perform various functions and may be used as therapeutic agents in medicine (*e.g*., antibiotics and antitumor agent). These bioactive compounds are synthesized by enzymes named polyketide synthases (PKS). PKS can be divided into three different groups according to product structure and enzyme features (Gao *et al*., 2010). It is noteworthy that, in the first two groups of PKS, the domains needed to accomplish one reaction cycle are a β-ketoacyl synthase (KS), an acyltransferase (AT), and a phosphopantethienylated acyl carrier protein (ACP). In addition, PKS contain domains that are involved in modifying the polyketide products such as ketoreductase (KR), dehydratase (DH) or cyclase (C) (Olano *et al*., 2010).

Type I PKS proteins can be variable in size (~ 3,000 kDa) as the many domains needed for the synthesis of a polyketide exist in a single polypeptide (Schirmer *et al*., 2005). Type I PKS are further divided into two subgroups. The first subgroup is designated modular, in which case PKS comprise several modules and each of these performs one full reaction cycle (adding one unit to the growing PK) (*e.g*. deoxyerythronolide B synthase (Donadio and Katz, 1992). The other subgroup is named iterative PKS. In this case, PKS is a single module (monomodular) which is composed of a single cluster of domains that catalyze the reaction cycles repeatedly, *e.g*. lovastatin nonaketide synthase (Kennedy *et al*., 1999).

The second group of PKS is known as Type II. In this group of PKS, the domains required for polyketide synthesis are distributed in different polypeptides as exemplified by aromatic polyketide **s**ynthases (McDaniel *et al*., 1993).

The last group is Type III PKS. The group accomplishes all the reaction cycles needed to produce PK using a single active site (Li and Müller, 2009). An example of this group is chalcone synthase which synthesizes chalcone, a small aromatic compound (Austin and Noel, 2003).

1.9.2 Non-ribosomal peptide synthetases (NRPS)

Non-ribosomal peptides are a group of secondary metabolites formed from simple monomers using enzymes called non-ribosomal peptide synthetases (NRPS). These enzymes are common in microorganisms, which synthesize peptides without the need for mRNA and ribosomes. Moreover, the building blocks that NRPS can use as substrates are all 20 proteinogenic amino acids (in both D and L forms) and other amino acids such as ornithine (Finking and Marahiel, 2004).

NRPS use a cluster of domains called a module for NRP peptide synthesis. A module comprises three domains, which add an amino acid to the growing NRP peptide. These domains are an adenylation (A), a thiolation (T) and a condensation (C) domain. Additionally, a thioesterase (TE) domain, which is involved in releasing the synthesized NRP may be present (Kohli *et al*., 2001).

NRPS can be divided into two groups based on the number of modules that they have. Group I, monomodular NRPS, is composed of a single module and Group II, multimodular NRPS, have several modules, which are involved in forming the peptide (Finking and Marahiel, 2004).

1.10 Soluble methane monooxygenase (sMMO)

The soluble methane monooxygenase (sMMO) is the other type of MMO which catalyses the conversion of methane to methanol, the first step in metabolism of methane in sMMO-containing methanotrophs. Unlike pMMO, the sMMO is a cytoplasmic enzyme and is expressed during growth when copper to biomass ratios are low. Some methanotrophs contain sMMO as well as pMMO *e.g.*, *Mc. capsulatus* and *Ms. trichosporium* (Murrell *et al.*, 2000). This feature might represent an ecological advantage for some species distributed in different habitats. However, as previously stated a few methanotrophs have only sMMO *e.g.*, *Methylocella silvestris* (Dunfield *et al.*, 2003; Theisen *et al.*, 2005) and *Methyloferula stellata* (Vorobev *et al.*, 2010).

sMMO can oxidize a broad range of substrates including aromatic compounds such as naphthalene, in addition to alkenes and alkanes. This interesting feature makes sMMO an excellent candidate for biotechnological exploitation and in developing novel synthetic catalysts (Sullivan *et al.*, 1998; Smith *et al.*, 2002; Lieberman and Rosenzweig, 2005; Borodina *et al.*, 2007; Smith *et al.*, 2010). The different substrates that sMMO can oxidises are discussed by Smith and Dalton (2004) and Jiang *et al.* (2010).

1.10.1 Biochemistry of sMMO

In contrast to pMMO, sMMO was relatively easily purified from many methanotrophs including *Mc. capsulatus* (Woodland and Dalton, 1984), *Ms. trichosporium* (OB3b) (Fox *et al.*, 1989) and *Methylocystis* sp. (Grosse *et al.*, 1999) due to both its stability and cytoplasmic location. Three components constitute the sMMO enzyme, a hydroxylase protein (MMOH), a reductase (MMOR) and a

coupling protein (MMOB), all of which are required for full enzyme activity (Colby *et al.*, 1977; Fox *et al.*, 1989).

The hydroxylase (MMOH) component of sMMO contains the α-subunit (MmoX), β-subunit (MmoY) and γ-subunit (MmoZ) with masses of 61, 45 and 20 kDa, respectively (Figure 1.7). MMOH exist in a dimeric form $(\alpha\beta\gamma)_2$. Furthermore, the active centre of sMMO is a di-iron site that is present in the α-subunit of the hydroxylase component (Fox *et al.*, 1989; Elango *et al.*, 1997; Rosenzweig *et al.*, 1993). The second component of sMMO is a reductase (MMOR) which is a 39-kDa protein (MmoC). This protein contains a [2Fe-2S] cluster and a flavin adenine dinucleaotide (FAD) co-factor. NAD(P)H is the source of the reducing equivalent to be transferred by MmoC to hydroxylase. The coupling protein (MmoB) is the last component of sMMO. MmoB has a mass of 16 kDa, contains no metals or prosthetic groups and is presumably a regulator of activity and selectivity of sMMO (Green *et al.*, 1985; Dalton, 2005; Froland *et al.*, 1992). The structures of the ligating amino acids of the diiron active sites are conserved between *Mc. capsulatus* (Bath) (Rosenzweig *et al.*, 1993) and *Ms. trichosporium* (OB3b) (Elango *et al.*, 1997).

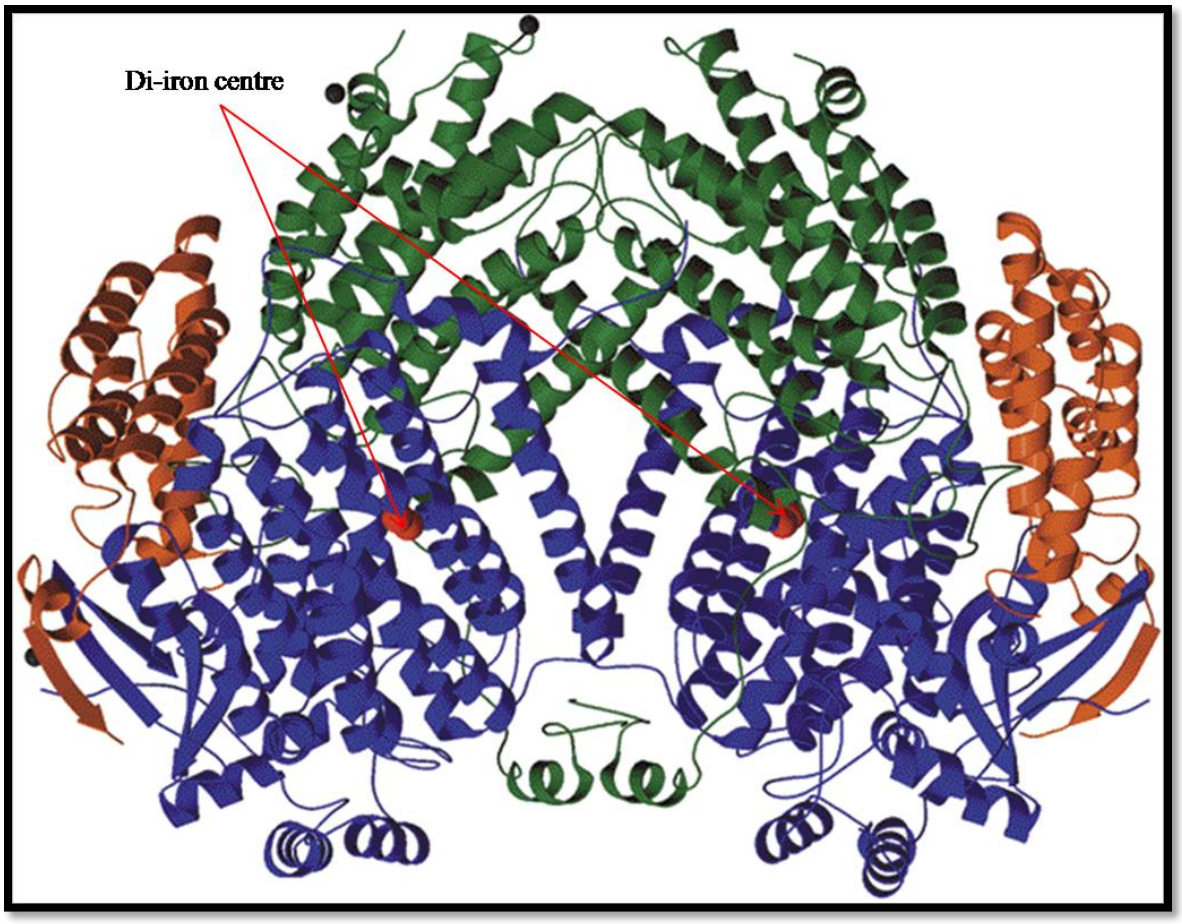

Figure 1.7 X-ray crystal structure of the sMMO hydroxylase of *Mc. capsulatus*. γ-, β- and α-subunit are in orange, green and blue, respectively. Taken from Rosenzweig *et al.* (1993).

Furthermore, the expression and activity of sMMO is suppressed by copper in *Mc. capsulatus* and *Ms. trichosporium* (Nielsen *et al.*, 1996 and 1997). In addition to the structural and biochemical aspects of sMMO systems, several aspects of the catalysis, including dioxygen activation and substrate hydroxylation at the active site have been studied extensively in *Mc. capsulatus* and *Ms. trichosporium*. This has been reviewed by several authors (Dalton, 2005; Tinberg and Lippard, 2009 and 2011).

It has been shown that copper ions are a potent inhibitor of MMOR and thus sMMO activity. Copper was found to exert its effect primarily at the iron-sulphur centre, which subsequently disrupts the protein structure, preventing the transfer of

electrons from NADH to the hydroxylase (Green *et al.*, 1985). It is noteworthy that in this experiment, 10 mM $CuSO_4$ was used in whole cells and 80 µM in MMO assay on cell extracts. In cell extracts, no activity was observed in the presence of copper, however, in whole cells, almost a quarter of the wild-type sMMO activity was observed, even in the presence of 10 mM $CuSO_4$ (Green *et al.*, 1985). This suggested that it might be possible to engineer a methanotroph capable of expressing sMMO constitutively and retain sMMO activity in copper-containing media.

1.10.2 Genetics of sMMO

Cloning and sequencing of the structural genes encoding sMMO have been carried out for a number of methanotrophs including *Mc. capsulatus* (Stainthorpe *et al.*, 1989 and 1990), *Ms. trichosporium* (Cardy and Murrell, 1990; Cardy *et al.*, 1991), *Methylomonas* (Shigematsu *et al.*, 1999) and *Methylocystis* sp. (McDonald *et al.*, 1997 and Grosse *et al.*, 1999). The order of arrangement of such structural genes is *mmoX*, *mmoY*, *mmoB*, *mmoZ*, *mmoD* and *mmoC* in all the above mentioned methanotrophs (Figure 1.8). These genes encode the hydroxylase α-subunit (MmoX) and β-subunit (MmoY), protein B (MmoB) the hydroxylase γ-subunit (MmoZ), MmoD and protein C (MmoC) units of sMMO respectively. Although the exact role of *mmoD* being unknown, it has been suggested that MmoD has an essential role in sMMO expression as *Ms. trichosporium* could not express sMMO in the absence of *mmoD* (Dumont, 2004). Transcription of the sMMO gene cluster is initiated from a σ^{54}-dependent promoter located 5' of *mmoX* (Csaki *et al.*, 2003; Stafford *et al.*, 2003). Another distinctive feature in all studied sMMO-producing methanotrophs is that the genes encoding sMMO exist as only one

copy, except for *Methylosinus sporium* where a duplicate copy of *mmoX* has been found (Ali, 2006).

mmoX is the most conserved gene (80% amino acid identity and 88% similarity) in the sMMO gene cluster in methanotrophs (McDonald *et al*., 1997; Leahy *et al*., 2003) and this is consistent with the fact that *mmoX* encodes for the active-centre containing subunit, MmoX (α-subunit of the hydroxylase) (Prior and Dalton, 1985a). Therefore, *mmoX* can be used as a functional gene marker in screening for methanotrophs in different ecosystems (Auman *et al*., 2000; McDonald *et al*., 1995; Cunliffe *et al*., 2008).

In addition to the structural genes, *mmoR* and *mmoG*, two regulatory genes have been identified downstream of the sMMO operon in some sMMO-expressing methanotrophs. However, the position of both genes varies from one methanotroph to another. For example, *mmoR* and *mmoG* are located upstream of the sMMO structural genes in *Ms. trichosporium* and *Ms. sporium*, while in *Mc. capsulatus* and *M. silvestris*, both genes are situated 3' of sMMO (Figure 1.8). *mmoR* encodes MmoR, a σ^{54}-dependent transcriptional activator, whereas *mmoG* encodes MmoG, a chaperonin GroEL homologue. Both genes are indispensible for sMMO expression (Csaki *et al*., 2003; Stafford *et al*., 2003; Scanlan *et al*., 2009) (Figure 1.8).

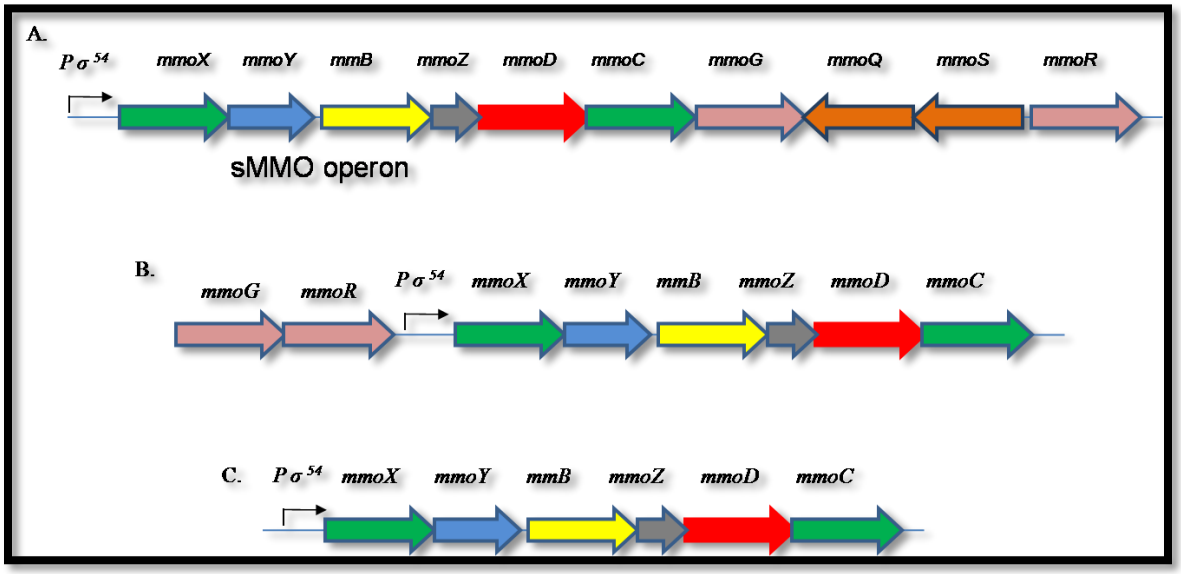

Figure 1.8 sMMO operon from different methanotrophs showing the location of the regulatory genes A. *Mc. capsulatus*: *mmoG mmoR mmoQ, mmoS* located downstream of the sMMO structural genes, B. *Ms. trichosporium*: *mmoG* and *mmoR* situated 5' of the sMMO operon and C. *Methylocystis* sp strain M: no regulatory genes identified.

mmoQ and *mmoS* are two additional genes that have been found in *Mc. capsulatus* located downstream of the sMMO operon (Figure 1.8). Both genes are positioned in the opposite direction to *mmoG* and *mmoR* and located between them. *mmoQ* and *mmoS* encode putative two-component (sensor-regulator) system signal transduction proteins, which are assumed to have a role in MMO regulation in *Mc. capsulatus* (Csaki *et al.*, 2003). It has been proposed that MmoS regulates sMMO transcription through interaction with MmoR depending on whether MmoS is present in the oxidised (FAD) form or reduced ($FADH_2$) form (Ukaegbu *et al.*, 2006). The crystal structure of MmoS suggested that it might act in detecting the environment changes via sensing the oxidation-reduction state in this way because it bound the FAD cofactor (Ukaegbu and Rosenzweig 2009). The expression levels of the structural and regulatory genes of sMMO under different growth conditions are described in Chapter 5.

1.11 Genetic systems for methanotrophs

Performing genetic manipulation of methanotrophs is challenging. There are many reasons contributing to this. These are firstly, limited growth substrates especially for the obligate methanotrophs, which grow only on methane. Secondly, a lack of appropriate cloning vectors and lastly, limited efficient systems for introducing vectors into methanotrophs. For more details in this respect, please refer to (Murrell, 1992 and 1994).

In 1995, Martin and Murrell introduced a marker-exchange mutagenesis technique to generate a stable mutant (mutant F) in *mmoX* in *Ms. trichosporium* (Martin and Murrell, 1995). In this technique, the gene of interest is mutated by using homologous recombination to remove (knock-out) an appropriate piece of the gene and replace it with an antibiotic-resistance cassette. *E. coli* S17.1λpir is the donor strain used to introduce the suicide vector construct into methanotroph cells via conjugation. One disadvantage of this method is it is time-consuming and involves many cloning steps. Nonetheless, this technique was used successfully to generate mutants in *Mc. capsulatus* and *Ms. trichosporium* during the current study.

An homologous expression system was developed for sMMO by Lloyd *et al.*, 1999b in which mutant F of *Ms. trichosporium* was complemented by a broad-host-range (BHR) plasmid that contained the sMMO encoding genes in addition to a wild-type promoter. The resulting transconjugants exhibited sMMO activity at high copper concentration (7.5 µM copper) (Lloyd *et al.*, 1999b). In the same year, successful heterologous expression attempts were made allowing the pMMO-containing methanotrophs, *Methylocystis parvus* OBBP and *Methylomicrobium album* BG8 to express active sMMO, which was negatively regulated by copper (Lloyd *et al.*, 1999a). In this approach, conjugations were carried out using *E. coli* S17.1 with

BHR plasmids containing sMMO genes and their natural promoter from *Ms. trichosporium* and *Mc. capsulatus* (Lloyd *et al.*, 1999a).

Smith *et al.* (2002) developed the homologous expression system for methanotrophs by introducing a new vector system, which relies on mutant F and enables one to generate mutants with engineered versions of *mmoX* (which encodes α-subunit of the sMMO hydroxylase). This system was validated by investigating the significance of two residues (Cys 151 and Thr 213) in the catalytic site of the sMMO hydroxylase via site-directed mutagenesis (Smith *et al.*, 2002). However, one the limitations of this system was that the other two subunits of the sMMO hydroxylase (β- and γ- subunits) could not be mutagenized. In order to mutate sites in *mmoX* that were outside the region deleted in mutant F, they designed a new system in which all genes encoding the sMMO were deleted (*mmoXYBZD* in addition to the first three codons of *mmoC*). The resulting mutant was designated *Ms. trichosporium* SMDM (SMDM_stands for sMMO Deletion Mutant) (Borodina *et al.*, 2007). Details of the methods used with the new system are given by Smith and Murrell (2011). This new system was used successfully in elucidating the significance of the 'leucine gate' in regioselectivity of the sMMO towards its substrates; 'leucine gate' refers to leucine residue (Leu 110), which was proposed to control the access of the substrates to the catalytic centre of the sMMO due to its position at the opening of the active site (Rosenzweig *et al.*, 1997; Borodina *et al.*, 2007). The ongoing studies on this system will provide further insights about the structure of sMMO in relation to the function and will provide an efficient tool in exploiting this enzyme in biotechnological applications (Smith *et al.*, 2010).

Recently, a new approach for genetic manipulating of methanotrophs was illustrated by deletion of the gene encoding for isocitrate lyase in *Methylocella*

silvestris BL2 by introducing linear DNA via electroporation (Crombie and Murrell, 2011). Another successful approach in generating mutants in *Methylocella silvestris* through unmarked gene deletion (no antibiotic cassette) was carried out using Cre-*loxP* recombinase systems (Crombie, 2011). However, obtaining electrocompetent cells in other methanotrophs is a challenge that has not yet been reliably overcome.

1.12 The Copper Switch

It is generally accepted that copper has a key role in regulation expression and activity of sMMO and pMMO in methanotrophs. As mentioned previously, pMMO is expressed during growth when the relative ratio between copper to cell biomass is high, whereas sMMO is expressed when such ratio is low (Stanley *et al.*, 1983).

The term 'copper switch' is given for methanotrophs that contain sMMO and pMMO and describes the expression shift to sMMO from pMMO at low-copper conditions. When copper –to-biomass ratio equals or exceeds 1 μmol g^{-1} dry weight of cells, the switch from sMMO to pMMO transcription occurs
(Theisen and Murrell, 2005; Semrau *et al.*, 2010; Fru 2011).

It has been reported that the regulation of sMMO by copper takes place at the transcriptional gene level (Nielsen *et al.*, 1996 and 1997). Choi *et al.* (2003) then confirmed these results. However, a discrepancy exists regarding the level at which pMMO is regulated. Some studies suggested that pMMO is regulated at the gene transcription level (Nielsen *et al.*, 1996 and 1997) while others proposed that pMMO is regulated at a different level of regulation; post-transcriptional level (Choi *et al.*, 2003). The reason for these contradictory theories is that results from different studies have differed as whether *pmoA* transcripts are detected under copper-limiting growth conditions, when sMMO is in fully (highly expressed). Nonetheless, there is

an agreement amongst these studies that pMMO transcription is induced by copper. A summary of what is experimentally proved about the copper switch is outlined below.

1- Transcription of the sMMO gene cluster is initiated from a σ^{54} –dependent promoter. The evidence for this was that mutants in the *rpoN* gene, which encodes for the σ^{54}-factor are unable to transcribe the sMMO gene cluster (Stafford *et al.,* 2003).

2- Transcription from the σ^{54}–dependent promoter is negatively regulated by copper. This was confirmed by Ali (2006) by constructing integrative suicide promoter probe vectors and selecting *Mc. capsulatu*s reporter strains carrying a chromosomal transcriptional fusion between a reporter gene *gfp* or *lacZ* and the sMMO σ^{54}–dependent promoter. The reporter gene activities were significantly very higher under low-copper growth conditions.

3- Furthermore, *mmoR* and *mmoG* of *Mc. capsulatus* and *Ms. trichosporium* have been proved to be essential for sMMO expression although the deduced amino acid sequences analysis of both genes revealed the absence of putative copper-binding motifs (Csaki *et al.*, 2003; Stafford *et al.*, 2003; Scanlan *et al.*, 2009). As mentioned previously, th*e mmoR* gene product is a putative σ^{54}–dependent transcriptional activator while the *mmoG* gene product is a putative GroEL-like chaperonin. Creation of knockout mutants in these genes by marker exchange mutagenesis resulted in complete loss of sMMO expression. This has led to the proposal that the MmoG might be a MmoR-specific chaperone that is required for the assembly of the complex responsible for the transcription of the sMMO gene cluster (Stafford *et al.*, 2003).

4- Additionally, *mmoQ* and *mmoS*, which are present in *Mc. capsulatus* alone and are situated downstream of the sMMO gene cluster, are proposed to be involved in MMO regulation (Csaki *et al.,* 2003). No copper-binding motif was identified in

MmoS, which acts as a redox sensor via reversible reactions FAD-$FADH_2$ (Ukaegbu *et al.*, 2006; Ukaegbu and Rosenzweig 2009).

5- Mb enhances pMMO activity and when copper is limiting, it is involved in copper uptake (Zahn and DiSpirito, 1996; DiSpirito *et al.*, 1998; Choi *et al.*, 2003 and 2005).

6- Transcription of pMMO is initiated from a σ^{70}-dependent promoter, which is likely to be partly constitutive, although it is induced by copper (Ali, 2006). Based on the above-mentioned facts, Ali (2006) proposed the following model (Figure 1.9) in an attempt to explain how copper regulates the copper switch between MMOs.

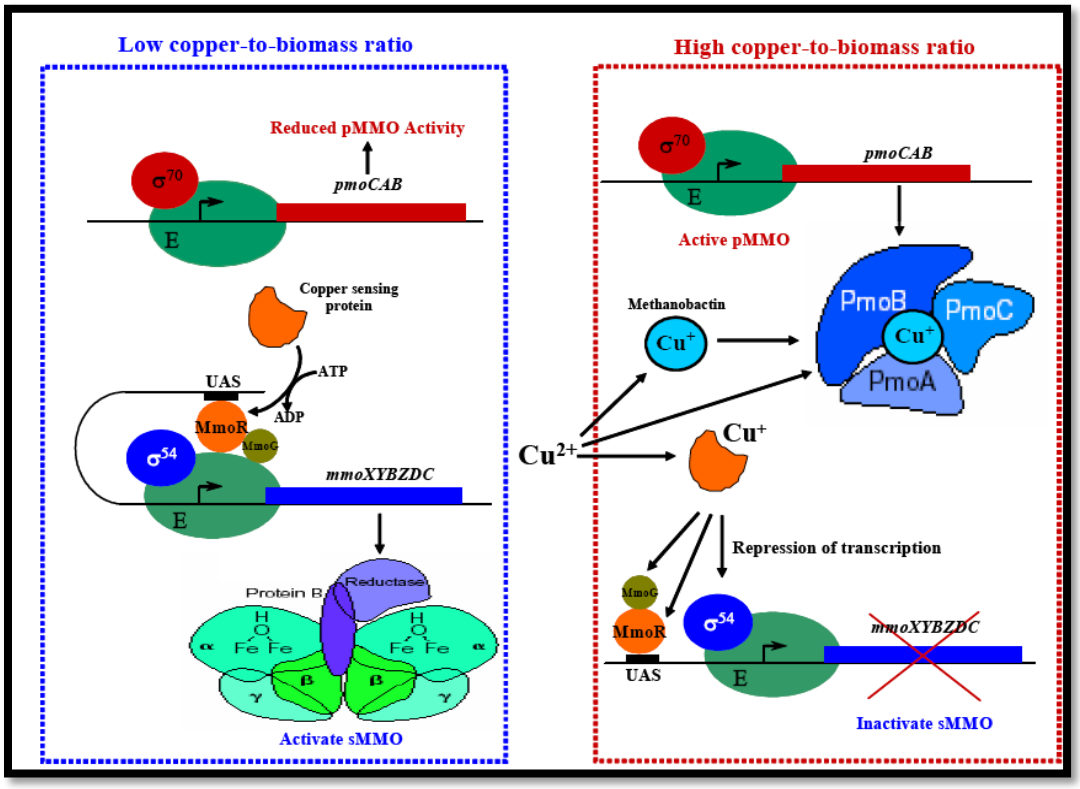

Figure 1.9 A schematic model for the mechanism of how copper regulates MMOs (Taken from Ali, 2006).

This model (Figure 1.9) can be summarized as follows:

sMMO is transcribed when the copper-to-biomass ratio is low. Transcription is started from the σ^{54} –dependent promoter. Both MmoR and MmoG are essential in

this process, although their exact role remains unknown (Scanlan *et al.*, 2009). pMMO is expressed at a basal level under these conditions (Ali, 2006).

pMMO is transcribed from σ^{70} promoter, which seems to be constitutive, although it is induced to a higher level of expression by copper (Ali, 2006). Excess copper relative to biomass repressed sMMO probably through a putative repressor, which was proposed to interact with MmoR and/or MmoG, thus preventing proper assembly of RNA polymerase- σ^{54}-MmoR-MmoG complex required to initiate sMMO expression. Therefore, no transcription of sMMO occurs under these conditions. However, based on the work done in this study and by other researchers this model is updated in Chapter 9.

1.13 Copper uptake in methanotrophs

Copper has a significant physiological role in methanotrophs and in particular those possessing sMMO and pMMO, such as *Mc. capsulatus* and *Ms. trichosporium* (Hanson and Hanson 1996; Semrau *et al.*, 2010; Fru, 2011). In addition to its role in the copper switch as described in the previous section, copper is needed for other vital processes. For instance, copper is the catalytic site metal of pMMO (Balasubramanian *et al.*, 2010) and copper-containing cytochrome oxidases (Zahn *et al.*, 1996), and enhances the synthesis of the intracytoplasmic membranes (Choi *et al.*, 2003).

Due to its pivotal role in the physiology of methanotrophs, these organisms seem to have specific transporters that mediate copper acquisition. Back in the 1990s, preliminary evidence about the first specific copper uptake system was obtained from the work done by Phelps *et al.* (1992) and Fitch *et al.* (1993). These workers generated mutants of *Ms. trichosporium* (OB3b), which were constitutive sMMO ($sMMO^c$),

pMMO deficient and copper resistant, and explained these phenotypes by defects in the copper-importing systems (Phelps *et al.*, 1992; Fitch *et al.*, 1993). It was reported that *Ms. trichosporium* or *Mc. capsulatus* growing under copper-limited growth conditions excreted small copper-binding compounds, which were later identified as methanobactin (Mb). The amount of Mb decreased in the spent media when copper was added to the culture (Zahn and DiSpirito, 1996; DiSpirito *et al.*, 1998). These findings stimulated the interest of researchers in such novel compounds and their possible role in copper uptake. It has been reported that Mb has a significant role in mineral weathering in the environment by enhancing dissolution of copper-bound minerals *e.g.*, glass (Knapp *et al.*, 2007; Kulczycki *et al.*, 2007 and 2010). Recently, Fru (2011) presented a comprehensive review about copper cycling by methanotrophs and the role of Mb in this context. The molecular properties of Mb are described earlier in this chapter and are discussed further in Chapters 4 and 8.

Evidence for another possible copper transporter was derived from the work done by Fjellbirkeland *et al.* (1997). In this study, they identified an outer membrane protein, MopE, which was induced by copper deficiency. In the same study, the maximum production of MopE was found to be under sMMO-expressing growth conditions in batch culture with shaking and decreased substantially within two days of addition of 4 µM copper. Within that time range, the cells switched from the iron-containing sMMO to the copper-containing pMMO. It has been reported that MopE, which is composed of 512 amino acids, was secreted in a truncated form, MopE*, which comprised only 336 aa residues (Karlsen *et al.*, 2003). Furthermore, the crystal structure of MopE* was obtained and revealed that the copper-binding site is composed of two histidine residues in addition to a kynurenine moiety, which is a product of oxidation of tryptophan (Helland *et al.*, 2008). The gene encoding MopE is

differentially up-regulated in *Mc. capsulatus* expressing sMMO and is discussed in Chapter 5.

Furthermore, a membrane protein, CorA (Copper repressible polypeptide A), was identified in *Methylomicrobium album* BG8 (Berson and Lidstrom, 1996) and was proposed to be involved copper acquisition (Berson and Lidstrom, 1997). This protein showed similarity to MopE in terms of amino acid sequences (Fjellbirkeland *et al.*, 2001).

In addition, other potential copper transporters, including copper-translocating P-type ATPase (CopA), are investigated in Chapter 3.

1.13.1 P-type ATPases

One group of the membrane transporters is P-type ATPases, which are found in all living cells, transporting various ions across membranes. The process by which P-type ATPases mediate transport of ions is an energy-requiring one *i.e.* they utilize the energy derived from the hydrolysis of ATP (Apell, 2004). P-type ATPases are divided into several subgroups, one of which comprises the P_{1B}-type ATPase heavy metal transporters (Argüello *et al.*, 2007). Copper is one substrate that P_{1B}-type ATPases can transport across membranes, therefore these transporters play a vital role in copper homeostasis (Argüello *et al.*, 2007).

In general, P_{1B}-type ATPases are composed of two main regions: 1) a transmembrane region and 2) a cytoplasmic region. The P_{1B}-type ATPases transmembrane region is distinguished by 6–8 transmembrane (TM) helices and a transmembrane metal binding site (TMMBS), which directly participate in recognizing and transporting metal ions across the membrane via a cysteine-proline (CPX) motif (Argüello *et al.*, 2007) (Figure 1.10).

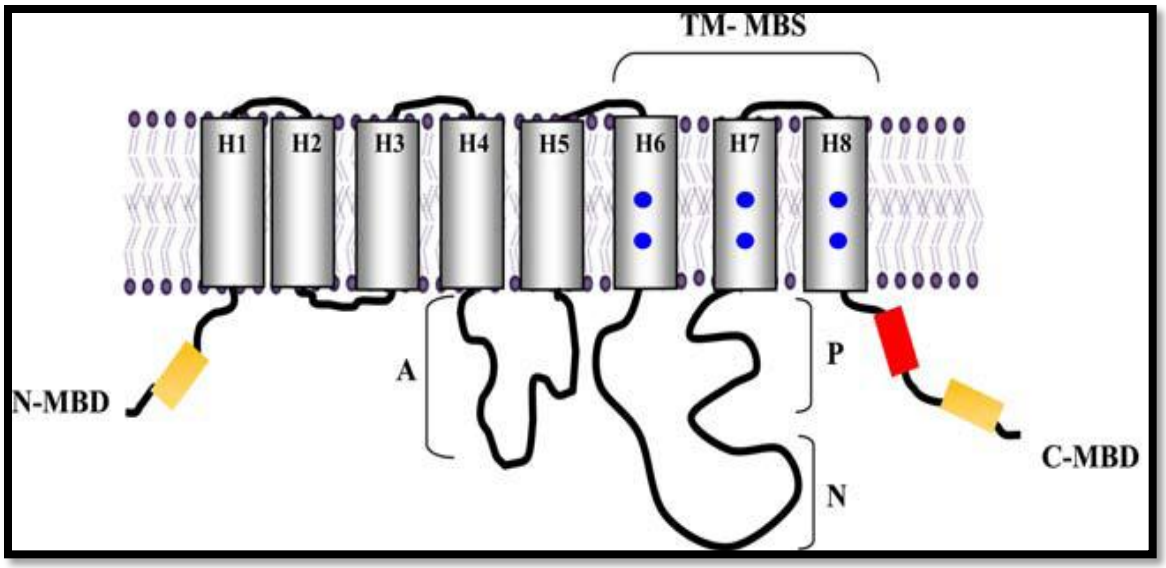

Figure 1.10 Schematic representation of the main domains present in P_{1B}-ATPases. H1 to H8, Transmembrane segments; A, actuator domain; P, Phosphorylation domain; N, Nucleotide-binding domains; TM-MBS, Transmembrane metal binding sites shown as blue circles; N-MBD, the C-terminal metal binding domains and C-MBD, the N-terminal metal binding domains (MBDs) (Taken from Argüello *et al.*, 2007).

The cytoplasmic region comprises three cytoplasmic domains. The cytoplasmic metal binding domain (MBD) is the first (and diverse) domain of the cytoplasmic region of P_{1B}-ATPases. The cytoplasmic MBD binds metal ions through either CXXC sequence motifs *e.g.*, Cu^{+}-ATPases (Voskoboinik *et al.*, 1999; Arnesano *et al.*, 2002; Lutsenko and Petris, 2003;), histidine-cysteine-rich MBD *e.g.*, *Arabidopsis thaliana* Zn^{+2}-ATPase HMA2 (Eren *et al.*, 2006) or histidine-rich MBD *e.g.*, *E. hirae* CopB (Bissig *et al.*, 2001). It has been proposed that the MBD in the cytoplasmic region plays a role in controlling the activity of the enzyme (Eren *et al.*, 2006; Argüello *et al.*, 2007). The second domain, called the energy transduction domain (A-domain), forms the small cytoplasmic loop (Figure 1.10). The third domain is the ATP binding domain (ATPBD). Two domains, a nucleotide binding domain (N-domain) and a phosphorylation domain (P-domain), form the ATPBD. Both domains represent a large cytoplasmic loop (Figure 1.10). It is worth mentioning a conserved

phosphorylation site (DKTGTL), which is essential for the phosphorylation step in the reaction cycle, is contained in the ATPBD.

P-type ATPases act like two-gated ion channels in which the presence of the occluded state ensures that one gate closes before the another opens (Artigas and Gadsby, 2003). This is probably to prevent the back-flow of ions and to achieve active transport of cations against an electrochemical gradient (Bublitz *et al.*, 2011). For more details about structure, function, topology and of phylogeny P-type ATPases please see the review by Chan *et al.* (2010).

1.14 DNA microarrays

The microarray technique is a high-throughput method that allows one to simultaneously measure the expression level of all active genes of a given organism under specified growth conditions (Hinton *et al.*, 2004; Kothapalli *et al.*, 2002), such as during growth with high or low copper concentrations. In this technology, oligonucleotide probes of between 25 and 75 bp in length (Rhodius *et al.*, 2002) corresponding to the genes under consideration are synthesized and immobilized in a known order on a glass microscope slide. Hybridization of these probes with labeled sequences (cDNA/cRNA) allows comparative gene expression profiling. The first paper introduced to the scientific community using microarray technology was the Science paper by Schena *et al.* (1995). Since then, many papers have been published using this technology. Microarrays were applied to examine genes induced during different life patterns (symbiosis versus free-living) as in *Azorhizobium caulinodans* (Tsukada *et al.*, 2009), to examine genes responding to different ecological stresses such as salt stress in *Bacillus subtilis* (Hahne *et al.*, 2010) and iron deficiency *Listeria monocytogenes* (Ledala *et al.*, 2010).

Microarray results, however, does not provide data about the post-transcriptional events; they reflect a snapshot of the whole transcriptome (Cook and Sayler, 2003). Microarrays have been used to study methylotrophs. For example, Okubo *et al.*, (2007) studied the comparative whole-genome transcriptome of *Methylobacterium extorquens* AM1 grown on methanol versus succinate. In order to use this technique with an obligate methanotroph, the whole-genome transcriptome of *Mc. capsulatus* growing under high- and low-copper medium was investigated and the results are presented in Chapter 5.

1.15 Project aims

The ultimate aim of this project was to elucidate the molecular basis of the role of copper in the regulation of methane oxidation in *Mc. capsulatus*. The specific aims of the project were to:

- Identify the genes involved in copper transport using targeted mutagenesis in *Mc. capsulatus*.
- Explore whether Mb is synthesized ribosomally or non-ribosomally using targeted mutagenesis.
- Study the global gene expression in *Mc. capsulatus* under high copper (pMMO) and low copper (sMMO) growth conditions to identify the genes involved in MMO regulation.
- Create mutants of *Mc. capsulatus* in these genes using antibiotic cassettes, plasmids, *E. coli* S17.1 and conjugation.
- Characterize these mutants and compare them with the wild-type organism.

Chapter 2

Materials and Methods

2.1 Chemicals

Chemicals used in this study were obtained from Sigma–Aldrich Corporation (St Louis, MO, USA), Melford Laboratories Ltd (Ipswich, UK), or Fisher Scientific UK (Loughborough, UK) unless otherwise indicated. Custom oligonucleotide primers were obtained from Invitrogen (Paisley, UK).

2.2 Antibiotics

Since antibiotics are heat-sensitive compounds, solutions of antibiotics were filter–sterilized with 0.22 µm filters (Sartorius Minisart, Göttingen, Germany) and stored at –20 °C until use. When needed, antibiotics were added aseptically to cooled medium to the specified concentrations: ampicillin 100 µg ml^{-1}; kanamycin, 25 µg ml^{-1} and gentamicin 5 µg ml^{-1}.

2.3 Bacterial growth media

All media and solutions were prepared using Milli–Q water, which was obtained using the SuperQ system (Millipore). For solid media, 2 % (w/v) Bacto (Difco) agar was added before autoclaving, which was carried out at 121 °C at 15 psi for 15 min.

2.3.1 Nitrate Mineral Salts medium (NMS)

Nitrate Mineral Salts (NMS) medium (Whittenbury *et al.*, 1970) was prepared from stock solutions with the following composition as indicated in Table 2.1.

Table 2.1 Composition of stock solutions of NMS medium

Ingredient	Quantity (g)	Preparation
Solution 1: Salt solution (10x stock)		
KNO_3	10	
$MgSO_4.7H_2O$	10	Dissolved in 1000 ml Milli–Q water
$CaCl_2.2H_2O$	2	
Solution 2: Iron EDTA solution (1000x stock)		
Fe-EDTA	0.38	Dissolved in 100 ml Milli–Q water
Solution 3: Molybdate solution (1000x stock)		
$NaMoO_4$	0.26	Dissolved in 1000 ml Milli–Q water
Solution 4: Trace elements solution (1000x stock)		
$FeSO_4$	0.5	
$ZnSO_4.7H_2O$	0.4	
H_3BO_3	0.015	
$CoCl_2.6H_2O$	0.05	Dissolved in 1000 ml Milli–Q water
Na–EDTA	0.25	
$MnCl_2.4H_2O$	0.02	
$NiCl_2.6H_2O$	0.01	
Solution 5*: Phosphate buffer solution (100x stock)		
$Na_2HPO_4.12H_2O$	71.6	Dissolved in 1000 ml Milli–Q water pH 6.8
KH_2PO_4	26	
Solution 6: Copper solution (1000x stock) 1mM		
$CuSO_4.5H_2O$	25	Dissolved in 100 ml

* Phosphate buffer was autoclaved separately in aliquots and added to the medium before use.

Mc. capsulatus (Bath) wild-type, *Ms. trichosporium* (OB3b) wild–type as well as the mutants generated in both strains were cultivated in 1 X NMS. To prepare 1 X NMS; 100 ml of solution 1, 1ml from each of solutions 2 - 4 were added to 887 ml water to give 990 ml. After autoclaving, 10 ml of sterilized solution 5 was added to the cooled medium to avoid phosphate precipitation. For "no–added copper" NMS medium, solution 6 was not included. Solution 6 was added to the necessary final copper concentration stated for each experiment. For liquid cultures, *Mc. capsulatus* or *Ms. trichosporium* were cultivated in 50 ml NMS medium in 250 ml Quickfit conical flasks which were sealed with suba–seals. The flasks were gassed with 20 % (v/v) methane. *Mc. capsulatus* was incubated at 45 ^{o}C,

while *Ms. trichosporium* was incubated at 30 ^{o}C on a shaking incubator (200 r.p.m min^{-1}) for 5 – 15 days. Growth was monitored by measuring the optical density (OD_{540}) using a Beckman DU–70 spectrophotometer. *Mc. capsulatus* or *Ms. trichosporium* grown on NMS agar plates were incubated in a methane/air atmosphere in a gas–tight container, at the relevant temperature. Methane was added every 2 - 3 day during incubation.

Mc. capsulatus was cultivated in 5 L fermentors (Inceltech LH Series 210) for large scale cultivation. The physical parameters of the fermentor were adjusted as follows: air flow (1 L min^{-1}), methane flow (140 ml min^{-1}), the dissolved oxygen level in the fermentor vessel (above 5 %) and pH (6.8 – 7.0). Oxygen limitation was avoided by adjusting the rate of airflow and agitation speed. pH of the culture was kept to the required value by automatic addition of 0.5 M NaOH or 0.5 M HCl. About 400 ml of late exponential phase *Mc. capsulatus* flask-grown culture was used as inoculum. Samples were taken regularly and OD_{540} was measured as a growth check and samples of the culture were tested for sMMO expression using the naphthalene oxidation assay. After harvesting, cultures were centrifuged (10,000 x *g* at 4º C for 10 min) and the cells were resuspended in a minimum volume of phosphate buffer (solution 5, Table 2.1) pH 6.8 and drop frozen in liquid nitrogen and stored at –80 ^{o}C. In the case of continuous culture, sterile NMS medium was added via a calibrated peristaltic pump and the outflow was collected in a sterile 25 L carboy.

2.3.2 Luria–Bertani (LB) medium

Luria–Bertani (LB) medium (Table 2.2) was used to cultivate *E. coli* strains (Sambrook *et al.*, 1989). LB agar plates were incubated at 37 ^{o}C while LB liquid cultures were incubated on a orbital shaker (200 rpm) at 37 ^{o}C.

Table 2.2 Composition of Luria–Bertani (LB) medium

Ingredient	Quantity (g l^{-1})	Preparation
Peptone	**10**	Dissolved in 1000 ml Milli–Q water
Yeast extract	**5**	
Sodium chloride	**5**	

2.2.3 Super optimal broth with catabolite repression (SOC)

The composition of super optimal broth with catabolite repression (SOC) medium was outlined in Table 2.3 (Hanahan, 1983). SOC medium was used initially to recover the transformed *E. coli* to get maximum efficiency of transformation.

Table 2.3 Composition of Super optimal broth with catabolite repression (SOC) medium

Ingredient	Quantity (g l^{-1})	Preparation
Bacto tryptone	20	Dissolved in 1000 ml Milli–Q water
Bacto yeast extract	5	
Sodium chloride	5	
NaCl	0.5	
KCl	0.19	
$MgCl_2$	0.95	
Glucose*	3.6	

*Glucose was prepared as a stock solution (1M), filter–sterilized and 20ml added to the cooled sterilized medium.

2.4 Bacterial strains

2.4.1 Bacterial strains and examination for purity

Bacterial strains were cultivated under aseptic conditions to avoid contamination. A list of all bacterial strains and plasmids used in this study is given

in Table 2.4. 16S ribosomal RNA genes of methanotrophs that were used in this study were amplified by PCR using primers 27F 5'-AGAGTTTGATCMTGGCTCAG-3' and 1492R 5'TACGGYTACCTTGTTACGACTT-3' and sequenced (refer to sections 2.8 and 2.10) . The sequences obtained were compared against the NCBI database to confirm the identity. Due to the obligate nature of methanotrophs studied during this work, cultures could be examined for contamination by streaking onto R2A plates and incubating at 37 ^{o}C. After incubation for 3–5 days, no growth on the R2A plates was taken to indicate no contamination. Methanotrophs were also examined using phase contrast microscopy under oil immersion.

2.4.2 Maintenance of bacterial strains

Methanotrophs were maintained by routinely streaking on NMS plates every 3 - 4 weeks. *E. coli* strains were preserved at -80 ^{o}C in the presence of 20 % (v/v) sterile glycerol.

2.4.3 Calculation of specific growth rate

Specific growth rate (μ) was determined using the following equation:

$$\text{Specific growth rate } (\mu)\ (h^{-1}) = \frac{\text{Natural logarithm of 2 (ln2)}}{\text{Doubling time } (t_D)\ (h)}$$

Microsoft Excel was used for estimate the specific growth rate and doubling time of each strain by plotting the natural logarithm of OD_{540} for five consecutive time points against time. The slope of the straight line, which represented the exponential growth phase, was taken as the specific growth rate, and then the doubling time was calculated using the above equation.

Table 2.4 Bacterial strains and plasmids used in this study

Strains/plasmids	Description	Source/reference
Strains		
***Ms. trichosporium* (OB3b)**	Wild–type strain	Warwick Culture Collection
Ms. trichosporium* Δ*mb	Δ*mb* strain, *Gm*^{R} (methanobactin mutant)	This study
***Mc. capsulatus* (Bath)**	Wild–type strain	Warwick Culture Collection
***Mc. capsulatus* ΔMCA1883 (Δ*nrpS–1*)**	ΔMCA1883 *(nrpS–1)* strain, *Gm*^{R}	(Ali, 2006)
***Mc. capsulatus* ΔMCA 2107 (Δ*nrpS–2*)**	ΔMCA 2107 *(ΔnrpS–2)* strain, *Km*^{R}	This study
***Mc. capsulatus* ΔMCA1238 (Δ*pkS*)**	ΔMCA1238 (Δ*pkS*) strain, *Km*^{R}, *Gm*^{R}	This study
***Mc. capsulatus* ΔMCA 0705 (Δ*copA1*)**	ΔMCA 0705 (Δ*copA1*) strain, *Km*^{R}, *Gm*^{R}	(Ali,2006)
***Mc. capsulatus* ΔMCA 0805 (Δ*copA2*)**	ΔMCA 0805 (Δ*copA2*) strain, *Km*^{R}, *Gm*^{R}	This study
***Mc. capsulatus* ΔMCA 2072 (Δ*copA3*)**	ΔMCA 2072 (Δ*copA3*) strain, *Km*^{R}, *Gm*^{R}	This study
***Mc. capsulatus* ΔMCA 1191(Δ*scO–1*)**	ΔMCA 1191(Δ*scO–1*) strain, *Gm*^{R}	This study
***E. coli* TOP10F**	Chemically-competent cells *recA*1 *thi pro hsdR*–2 RP4–2Tc ::Mu Km:: Tn7 λ*pir*	Invitrogen
E. coli* S17.1 λ*pir	*recA1 thi pro hsdR*$^-$ RP4–2Tc::Mu Km::Tn*7* λ*pir*	(Simon *et al.*, 1983)
Plasmids		
pAK111	pCR2.1–TOPO containing 1067 bp *pkS* fragment	This study
pAK222	pCR2.1–TOPO containing 1067 bp *copA2* fragment	This study
pAK444	pCR2.1–TOPO containing 1067 bp *copA3* fragment	This study
pK18mob	*Km*^{R}, RP4–mob, mobilizable cloning vector	(Schafer *et al.*, 1994)

pAK033	*Km*^{R}, pK18mob containing 981kbp *nrpS–2* fragment *Hin*dIII – *Pst*I	This study
p34S–Gm	Source of Gm^R cassette	(Dennis and Zylstra, 1998)
pK18mobs*ac*B	*Km*^{R}, RP4–mob, mobilizable cloning vector with *sac*B for positive selection	(Schafer *et al*., 1994)
pAK01	*Km*^{R} pK18mobs*ac*B with 1.067 bp *pkS* fragment *Sma*I – *Hin*dIII insert	This study
pAK011	*Gm*^{R}, *Km*^{R} pK18mobs*ac*B with 1,067 bp *pkS* fragment *Sma*I –*Hin*dIII insert	This study
pAK02	*Km*^{R}, pK18mobs*ac*B with 1,454 bp *copA2* fragment *Xba*I – *Hin*dIII insert	This study
pAK022	*Gm*^{R}, *Km*^{R} pK18mobs*ac*B with 1,454 bp *copA2* fragment *Xba*I –*Hin*dIII insert	This study
pAK04	*Km*^{R}, pK18mobs*ac*B with 1,513 bp *copA3* fragment *Eco*RI – *Hin*dIII insert	This study
pAK044	*Gm*^{R}, *Km*^{R} pK18mobs*ac*B with 1,513 bp *copA3* fragment *Eco*RI –*Hin*dIII insert	This study
pAK05	*Km*^{R}, pK18mobs*ac*B with 1,106 bp *scO-1* fragment *Xba*I – *Hin*dIII insert	This study
pAK055	*Gm*^{R}, *Km*^{R} pK18mobs*ac*B with 1,106 bp *scO-1* fragment *Xba*I –*Hin*dIII insert	This study
pAK06	*Km*^{R}, pK18mobs*ac*B with 1,239 bp *mb* fragment *Eco*RI – *Hin*dIII insert	This study
pAK066	*Gm*^{R}, pK06	This study

Abbreviations, *Gm*^{R}, gentamicin resistance; *Km*^{R}, kanamycin resistance; *Am*^{R}, ampicillin resistance

2.5 Nucleic acid extraction from methanotrophs

2.5.1 Extraction of genomic DNA from *Mc. capsulatus* and *Ms. trichosporium*

Genomic DNA was extracted from late exponential phase cultures (5 ml, OD_{540} 0.5) of *Mc. capsulatus* and *Ms. trichosporium*. Liquid cultures were centrifuged at 10,000 x *g* at 4º C for 10 min to obtain a cell pellet. The pellet was resuspended in 0.75 ml TE buffer and transferred to 15–ml Falcon tubes. Twenty µl of freshly prepared lysozyme (100 mg ml^{-1}, Sigma) were added and the tubes were incubated at room temperature for 10 min. Then, 40 µl of 10% (w/v) SDS and 8 µl of proteinase K (10 mg ml^{-1}) (Melford Laboratories) were added and mixed gently and tubes were incubated at 37 °C for 1 h. Following incubation, 100 µl of 5 M NaCl and 100 µl of warm cetyl–trimethylammonium bromide (CTAB) (10% in 0.7 M NaCl) were added and tubes incubated at 65 °C for 10 min. For removal of proteins, 0.5 ml of phenol/chloroform/isoamyl alcohol (25:24:1 v/v) was added and the contents of tubes were mixed gently. The tubes were centrifuged at 4,000 x *g* for 10 min at room temperature. The aqueous phase was carefully transferred to new tubes and 0.5 ml chloroform/isoamyl alcohol (24:1 v/v) was added for further extraction. Following centrifugation, the aqueous phase was transferred to new tubes and DNA was precipitated by adding 0.6 volumes of isopropanol and 30 min incubation at room temperature. DNA was pelleted by centrifugation (16,000 x *g*, 4 °C, 20 min), the supernatant was removed and the pellet washed in 200 µl of 70% v/v ethanol, air–dried and resuspended in 200 µl of nuclease-free water (Ambion).

2.5.2 Quantification and storage of DNA

DNA concentration was estimated by analysing 1.5 µl of DNA solution in a NanoDrop Spectrophotometer (ND–1000; NanoDrop™, USA) and measuring the absorbance at 260 nM. DNA was then stored at –20 °C until use.

2.5.3 Total RNA extraction from *Mc. capsulatus*

Due to RNA being easily degraded, appropriate precautions were taken during RNA extractions. All solutions, water and glassware used were treated with an effective inhibitor for RNases; diethylpyrocarbonate (DEPC) 0.1% v/v. The DEPC–treated items were left shaking overnight at 37 °C, then autoclaved. Tubes and tips were also RNase–free. The surface of the working area was wiped with RNaseZap (Fermentas). Total RNA was extracted from *Mc. capsulatus* cells expressing either sMMO or pMMO using the hot acid–phenol method (Gilbert *et al.*, 2000). One ml (OD_{540} 5) of fermentor cultures was immediately added to Stop Solution (95 % ethanol and 5 % phenol) to avoid RNA degradation by intracellular RNases. The bacterial culture was centrifuged at 16,000 x *g* for 10 min at 4 ºC. The pellets were resuspended in 200 µl of solution I (0.3 M sucrose and 0.01 M sodium acetate; pH 4.5) and 200 µl of solution II (2% sodium dodecyl sulfate and 0.01 M sodium acetate; pH 4.5). The contents of the tubes were transferred to a Ribolyser tube containing glass beads (Hybaid) in which 400 µl of phenol (saturated with 50 mM sodium acetate (pH 4.5)) was added. Cell lysis was carried out using a Hybaid Ribolyser (Hybaid) at speed 5 for 30 – 40 s. The cells were kept on ice during the extraction procedure. Tubes were centrifuged at 16,000 x *g* for 10 min at 4 ºC, and the aqueous phase was carefully transferred using RNase–free tips to a new

tube. Phenol (~ 400 µl) was added and the tubes were incubated for 4 min at 65 °C. Tubes were then placed in dry ice–ethanol for 10 – 20s then left to thaw at room temperature. Tubes were centrifuged at 16,000 x *g* for 10 min. and the aqueous phase was transferred to a new tube containing 400 µl of phenol–chloroform (50:50 v/v). Tubes were shaken vigorously for 30s before being centrifuged at 16,000 x *g* for 10 min. Again, the aqueous phase was carefully transferred to a new 1.5–ml tube. RNA was precipitated by adding 40 µl of 3M sodium acetate (pH 4.5) and 900 µl of 96% (v/v) ethanol and incubated at –20 °C for 60 min. Tubes were then centrifuged at 16,000 x *g* for 15 min at 4 ºC. Following centrifugation, 1ml of 70% (v/v) ethanol was added to wash the RNA pellet which was then air dried and resuspended in 87.5 µl of nuclease free water (Ambion). Finally, RNA was treated with Qiagen RNase–free DNase (4 units) for 30 min at 37 °C twice, each followed by purification using an RNeasy spin column (Qiagen, Crawley, UK) according to the manufacturer's instructions. PCR amplification of ribosomal RNA gene using primers 27f and 1492r (sequences of both primers are given in section 2.4.1) was carried out with 2 µl of RNA as a template to check RNA purity. Genomic DNA from Mc. capsulatus was used as a positive control. No PCR product was indicative that extracted RNA is free from DNA.

2.5.4 Estimation of RNA quality using Bioanalyzer

For accurate estimation of the quality and quantity of the RNA, RNA samples were submitted to the Molecular Biology Service, School of Life Sciences using a 2100 Bioanalyzer (Agilent Technologies, USA). Pure and intact RNA was stored at -80 °C until use.

2.5.5 Plasmid extraction from *E. coli* (mini-prep)

Plasmid extraction from late exponential phase *E. coli* cultures (3 ml) was carried out using the QIAprep Miniprep Kit (Qiagen) or GeneJET kit (Fermentas) following the manufacturer's instructions. The purified plasmid DNA was quantified using a NanoDrop Spectrophotometer (ND-1000; NanoDrop™, USA). Plasmids were stored at - 20 °C.

2.6 DNA manipulation techniques

2.6.1 DNA restriction digests

DNA restriction digestions were carried out with enzymes obtained from Fermentas or Invitrogen following the manufacturer's recommendations.

2.6.2 DNA purification from agarose gels

Following the enzymatic digestion reactions, DNA bands of interest were cut out of the TBE agarose gel using a scalpel blade and purified using the Gel Extraction Kit obtained from Nucleospin (Macherey-Nagel, Düren, Germany) or QIAquick (Qiagen) according to the manufacturer's instructions. PCR products were also purified using either of these kits.

2.6.3 Dephosphorylation

To enhance cloning efficiency, plasmid DNA that had been digested with restriction enzymes was dephosphorylated using Shrimp Alkaline Phosphatase (SAP) (Fermentas) following the manufacturer's instructions. SAP was inactivated by

heating at 65°C for 15 min. The dephosphorylation step was carried out before the ligation step.

2.6.4 DNA ligations

Ligation of the dephosphorylated plasmid DNA with DNA insert was performed using T4 DNA ligase (Fermentas) following the manufacturer's instructions.

2.6.5 Cloning PCR products

Cloning of PCR products into pCR2.1-TOPO (Invitrogen) or pGEM–T Easy (Promega, Madison, WI, USA) was conducted following the manufacturers' instructions.

2.6.6 Agarose gel electrophoresis

A horizontal Flowgen Minigel apparatus (Flowgen) was used to run DNA fragments in a 1% (w/v) agarose gel with 1 x TBE. Ethidium bromide (0.5 µg ml^{-1}) was added before gel casting. To estimate DNA band sizes, DNA 1 kbp ladder standard (Invitrogen) was loaded. Electrophoresis was conducted at 5 - 8V/cm for 30 min. After electrophoresis, DNA was visualized on a UV trans–illuminator (Syngene, UK). A UVP GD8000 gel documentation system (Ultra–Violet Products Ltd**)** was used for photographing gels.

2.7 Bacterial genetics

2.7.1 Transfer of plasmids into methanotrophs by conjugation

Conjugation of the desired plasmid from *E. coli* (donor strain) into *Mc. capsulatus* or *Ms. trichosporium* (recipient strain) was carried out according to the

method of Martin and Murrell (1995). An overnight *E. coli* S17.1 culture (10 ml) was centrifuged (6,000 x *g* for 10 min, 4 °C) and the pellet resuspended and washed twice with 30 ml sterile NMS. At the same time, 50 ml of *Mc. capsulatus* or *Ms. trichosporium* culture (OD_{540} ~ 0.5) was centrifuged (6,000 x *g* for 10 min, 4 °C), and the pellet resuspended and washed twice with a 50 ml sterile NMS. The pellets of the donor strain and the relevant recipient strain were suspended in 1 ml NMS and carefully placed on the centre of a sterile 0.2 µm pore–size nitrocellulose filter (Millipore, Billerica, MA, USA). This filter was initially placed on an NMS agar plate supplemented with 0.02 % (w/v) proteose peptone. The plates containing *Mc. capsulatus* were incubated at 37 ^{o}C while those containing *Ms. trichosporium* were incubated at 30 ^{o}C for 24 hours in the presence of methane and air. After incubation, the filter containing the cells was washed in 10 ml NMS and the cell suspension centrifuged (6,000 x *g* for 10 min, 4 °C). The pellet was resuspended in 1ml NMS medium and 100 µl aliquots were spread onto NMS plates supplemented with gentamicin (5 µg ml^{-1}) or kanamycin (15 µg ml^{-1}) (in case of *nrpS-2*). The plates were incubated aerobically at the relevant temperature for 2–3 weeks in the presence of methane as described in Section 2.3.1. To ensure complete removal of *E. coli* that might be present as background, colonies of the resultant transconjugants were streaked onto NMS agar plates containing nalidixic acid (10 µg ml^{-1}) and incubated for one week. The resulting transconjugants were then screened by growing them on NMS plates containing either gentamicin or kanamycin as appropriate. Mutants in which double homologous recombination occurred were then recognized as kanamycin sensitive and gentamicin resistant colonies.

The genotype identity of the mutants was confirmed by PCR, followed by analysis via agarose gel electrophoresis and sequencing.

2.7.2 Preparation and transformation of chemically-competent *Escherichia coli*

E. coli was made chemically competent by treatment with $CaCl_2$ according to the method of Sambrook and Russell (2001).

2.7.3 Transformation of chemically-competent *E. coli*

For transformation, 2 – 5 µl DNA solution (equivalent to 10 – 50 ng of plasmid DNA or ligation mix) were added to cells thawed on ice. Tubes were gently mixed and heat shocked at 42 °C for 45 s. Tubes were then chilled on ice for 2 min. About 900 µl of SOC medium was added to cells, which were then transferred to 15–ml sterile Falcon tubes and allowed to recover in a shaking incubator (200 rpm) at 37 °C for 50 – 60 min. For blue–white screening, 40 µl X-gal of (40 µg X-gal per ml DMSO) were spread onto LB plates containing the selective antibiotic and plates were incubated at 37 °C for 30 min. After spreading of aliquots, plates were incubated overnight at 37 °C. Successful vector–insert ligation was detected by the appearance of white colonies.

2.7.4 Preparation of electrocompetent *E. coli*

Preparation of electrocompetent *E. coli* was carried out according to the method of Sambrook and Russell (2001). Typically 500 ml of actively growing *E. coli* S17.1 culture was cooled on ice for 30 min and then collected by centrifugation at 4,000 x g for 15 min. The cell pellet was washed in 500 ml ice-chilled sterile water. This step was

repeated twice. Cells were resuspended in 10 ml of cold sterile glycerol (10 % v/v) and centrifuged at 4,000 x *g* for 15 min. Cells were again resuspended in 1 ml of cold sterile glycerol (10 % v/v). Finally, the cell suspension was divided into aliquots (40 µl) and frozen in liquid nitrogen and stored at –80 ^{o}C.

2.7.5 Transformation of electrocompetent *E. coli* by electroporation

For transformation of electrocompetent *E. coli* by electroporation, cells were thawed on ice. 2 µl of plasmid DNA solution (50 – 400 ng of DNA) was added. Tubes were gently mixed and incubated on ice for 2 min. The mixture was transferred to a 0.1 cm cooled electroporation cuvette (Plus BTX, Harvard Apparatus, and Holliston, MA, USA). Electroporation was carried out using a Bio–Rad GenePulser™ by applying an electric field of 1.8 kV at 25 µF and 200 Ω. Immediately after the electric pulse, 900 µl SOC medium was added to cells, which were then transferred to 15–ml sterile Falcon tubes. Tubes were incubated with shaking (200 rpm) at 37 ^{o}C for 50 – 60 min. Typically 75 µl aliquots of cells were spread onto plates of LB agar medium supplemented with the appropriate selective antibiotic and incubated overnight at 37 ^{o}C.

2.8 Polymerase chain reaction (PCR)

Amplification of DNA or cDNA samples using the Polymerase Chain Reaction (PCR) was carried out using a T3000 Thermal Cycling System 3000 (Biometra, Goettingen, Germany). The total volume of each reaction was 50 µl, which was composed of the reagents indicated in Table 2.5. dNTPs and *Taq* DNA

polymerase and were purchased from Fermentas. Primers were synthesized by Invitrogen. Amplification was carried out using the following program: 1) initial denaturation at 95 °C, 5 min, 2) denaturation at 95 °C, 1 min, 3) annealing (temperature varies according to primers), 30 s, 4) extension 72 °C for 1 min (1 min per 1kb), and 5) final extension at 72 °C, 10 min. Stages 2 – 4 were repeated for 30 cycles. Optimisation of PCR conditions was carried out by varying the concentration of primer and/or template, changing the temperature of the annealing stage or altering the time for the extension stage.

Table 2.5 Composition of a typical PCR reaction

Ingredient*	**volume (µl)**
PCR buffer (10X)	5
$MgCl_2$ (15 mM)	3
Forward primer (10 µM)	1
Reverse primer (10 µM)	1
dNTP mix (2.5 mM each)	0.5
BSA (20 mg ml^{-1})	1
DMSO (5% v/v)	2.5
Nuclease free water	to 47.5
***Taq* DNA polymerase (2.5 U)**	0.5
DNA (15–25 ng μl^{-1})	2

*All reagents were kept on ice during preparation and the concentrations given are for stocks.

DMSO and BSA were included in the PCR reactions when PCR amplifications were carried out with DNA extracted directly from bacterial colonies or from liquid cultures.

2.9 Reverse transcriptase PCR (RT–PCR)

According to the manufacturer's instructions, SuperScript II Reverse Transcriptase kit (Invitrogen) was used to generate cDNA for reverse transcriptase

PCR (RT–PCR). Negative control reactions were included where water was used instead of reverse transcriptase. From the generated cDNA, 2 µl was used as a template for subsequent amplification using PCR with the relevant primers. PCR reactions were made using 2 µl from the negative control tubes (tubes in which RT was omitted). Positive control tubes contained genomic DNA as template.

2.10 DNA sequencing and analysis

DNA samples were submitted to the Molecular Biology Facility at the University of Warwick for sequencing using a Dye terminator ready reaction Kit (Applied Biosciences, Warrington, UK) and ABI3100 capillary DNA sequencers. A typical 10 µl sequencing reaction was composed of 30 – 65 ng purified DNA and 5.5 pmol of the corresponding primer. Sequence data were analyzed using Chromas software (Technelysium Pty Ltd, Brisbane, Australia).

2.11 Biochemical analysis

2.11.1 Cell–free extract preparation

Samples of *Mc. capsulatus* growing on NMS with or without added copper were collected from a fermentor. Typically, 5 ml cultures of ~OD_{540} 5 were harvested by centrifugation at 10,000 x *g*, for 20 min at 4 °C. Pellets were washed in fresh NMS medium and resuspended in 3ml phosphate buffer (pH 6.8) containing 1 mM benzamidine to inactivate proteases. To break cells, cell suspensions were passed (three times) through a pre–cooled French pressure cell (American Instrument Company, Silver Spring, MD) at 110 MPa. Centrifugation (10,000 x *g*, 20 min, 4 °C)

was carried out to remove cell debris. The supernatant was carefully transferred to new tubes and considered as cell-free extract, which was then used for SDS–PAGE.

2.11.2 Estimation of protein concentration

Bio–Rad Protein Assay (Bio–Rad Laboratories Inc., Hercules, CA, USA) was used to estimate protein concentrations following the manufacturer's instructions. A standard curve was made using different concentrations of bovine serum albumin (BSA) (0– 100 µg).

2.11.3 Sodium dodecyl sulfate polyacrylamide gel electrophoresis analysis

Sodium dodecyl sulfate polyacrylamide gel electrophoresis (SDS–PAGE) analysis was carried out using an X–cell II Mini–Cell apparatus (Novex) to separate polypeptides. The composition of the stacking and the resolving gels is shown in Table 2.6.

Table 2.6 Composition of stacking and resolving gels used for SDS–PAGE

Solution/reagent	**4% Stacking gel (ml)**	**12.5% Separating gel (ml)**
(40% w/v) Acrylamide/bis (37.5:1)	1.0	6.25
Stacking buffer*	2.5	–
Resolving buffer**	–	2.5
SDS 10% (w/v)	0.1	0.2
Ammonium persulfate 10% (w/v)	0.05	0.15
TEMED ***	0.010	0.010
Water	6.3	10.9

* Stacking buffer (Tris 0.5 M pH 6.8),** Resolving buffer (Tris 3.0 M pH 8.8), *** TEMED (*N*, *N*, *N'*, *N'*–tetramethyl–ethane–1,2–diamine).

Sample loading buffer (1/4 volume of the sample) was added to cell–free extracts and the mixture was boiled for 10 min then centrifuged (10,000 x *g*, 15 min, 4 °C). The composition of sample loading buffer is given in Table 2.7. Typically 40 µg protein was loaded in each lane. Dalton Mark VII–L™ protein marker (Sigma) or PageRuler Plus prestained protein ladder (Fermentas) was used to determine the molecular masses of the protein bands. Running buffer (1 x) was added to the tank of X–cell II Mini–Cell apparatus and electrophoresis was performed.

Table 2.7 Composition of sample loading buffer used for SDS–PAGE

Solution/reagent	**Sample loading buffer (ml)**
Stacking buffer	0.25
SDS 10% (w/v)	1.2
Glycerol 100% (w/v)	0.2
Bromophenol blue 0.5 % (w/v)	0.08
β–mercaptoethanol 5 % (v/v)	0.010
Water	10.9

Table 2.8 Composition of running buffer used for SDS–PAGE

Solution/reagent	**Running buffer (5 X) (g l^{-1})**
Tris base	15
SDS	5
Glycine	72
Water	to 1 litre

The composition of the running buffer is given in Table 2.8. The voltage applied during separation of polypeptides through the stacking gel was 90V while 160V was applied during separation through the resolving gel. After electrophoresis, gels were carefully placed in Coomassie brilliant blue staining solution ((0.1 % (w/v) Coomassie brilliant

blue R–250 dissolved in 40 % methanol, 10 % acetic acid and 50 % water) and gently shaken overnight. Gels were then destained using destaining solution (40 % (v/v) methanol and 10 % (v/v) acetic acid).

2.11.4 Analysis of polypeptides using MS/MS

Bands containing polypeptides of interest were cut out from the SDS-PAGE gel with a clean scalpel blade. Each band was divided into 4 – 6 small cubes and transferred in known order into 96–well microtiter plate. After adding 200 µl de–ionized water to each sample, the plate was submitted to the Biological Mass Spectrometry and Proteomics Group at the University of Warwick. Samples were digested with trypsin and analyzed by Nano liquid chromatoghraphy electrospray ionization tandem mass spectrometry (nanoLC–ESI–MS/MS) using the NanoAcquity/Q–ToF Ultima Global instrumentation (Waters). The data were used to interrogate the *Mc. capsulatus* protein database using the Protein Lynx Global Server v2.4 and protein identities were assigned.

2.12 Enzyme Assays

2.12.1 Naphthalene oxidation assay for sMMO activity

Mc. capsulatus and *Ms. trichosporium* growing on plates or liquid cultures were tested for sMMO expression using a naphthalene oxidation assay (qualitative test) according to the method mentioned previously (Brusseau *et al*., 1990). Cells were incubated with few crystals of naphthalene for 30 min at the relevant temperature. A positive result was shown by a purple colour developing upon addition of a few drops

of a freshly prepared solution of the zinc complex tetrazotized *o*–dianisidine (10 mg ml^{-1}). This result was taken as evidence for sMMO expression.

2.12.2 Determination of whole-cell cytochrome oxidase activity

Whole cells cytochrome oxidase activity was assayed for according to the method of Frangipani and Haas (2009). Cells were grown in NMS liquid medium with the appropriate copper concentrations. Bacterial cultures were centrifuged (10,000 x *g*, 10 min, 4 °C) and the supernatant removed. Pellets were washed with 0.9% NaCl solution twice then and resuspended at OD_{600} ~1 in 1.4 ml of 50 mM 4–(2–hydroxyethyl)–1–piperazine ethanesulphonic acid (HEPES) and 200 mM NaCl, pH 7.0. Five µl of 0.54 M N, N, N′, N′–tetramethyl–p–phenylenediamine (TMPD) was added to start the reaction. The enzyme activity was followed by measuring the absorbance at A_{520} nm using an Ultrospec 3100pro UV/Visible Spectrophotometer (Amersham) fitted with an eight cuvette auto–changer, at room temperature. All reactions were carried out in triplicate in 1cm path–length disposable–plastic cuvettes and blank reactions with no TMPD and without cells were included. The molar extinction coefficient with a 1 cm path length for TMPD was 6.1 mM^{-1} cm^{-1} (Matsushita *et al.*, 1992). The activity was expressed in pmol TMPD oxidized min^{-1} $(mg\ dw)^{-1}$.

2.13 Methanobactin production assay

Mb production assay was carried out using a chrome azurol S – copper (Cu–CAS) agar, a qualitative assay developed by Yoon *et al.* (2010).

2.13.1 Preparation of chrome azurol S – copper (Cu–CAS) agar

Chrome azurol S – copper (Cu–CAS) agar was prepared as follows: Cu–CAS solution was prepared by adding 50 ml of CAS solution (0.42 mM) to 10 ml of $CuCl_2$ solution (5 mM). Sixty ml of Cu–CAS solution was added to 40 ml of hexadecyl trimethylammonium bromide (HDTMA) (0.525 mM) and mixed gently. This solution was autoclaved separately and 50 ml was added to 450 ml of warm NMS agar medium. Plates were left for 30 minutes; half of the solidified agar was carefully removed with the aid of a sterile blade. NMS agar medium was added to fill in the empty space. The plate appeared with a purple coloured half and a colourless half. *Mc. capsulatus* and *Ms. trichosporium*, as well as the putative Mb mutants, were streaked on the NMS (but not CAS) containing half of the CAS–plates and incubated at the relevant temperature for 2 – 4 weeks. Production of Mb was monitored visually by the change of the CAS–plates from blue to yellow over the incubation period. Plates which were not inoculated were used as a negative control.

2.14 Estimation of oxygen consumption rate using the oxygen electrode

The oxygen consumption rate of whole cells of *Mc. capsulatus* wild–type or a mutant grown on methane was estimated using a Clark oxygen electrode (Rank Brothers Ltd, Cambridge, UK). Initially, cells were grown on NMS liquid medium with no added copper or with 30 µM copper until they reached late exponential phase (OD_{540} ~ 0.5). The cells were harvested by centrifugation (6,000 x *g*, 20 min, 4 °C) and pellets were resuspended in 1 ml of fresh NMS medium. 100 µL of bacterial suspension (equivalent to 2 – 5.5 mg dry weight biomass) were added to 3 ml (40 mM (pH 6.8)) phosphate buffer

(solution 5 Table 2.1). The instrument cell was maintained at 45 °C using a circulating water bath (Churchill Co. Ltd, Perivale, UK). To ensure the buffer was oxygenated, the buffer was stirred in air for a few hours before use. Calibration of the Clark oxygen electrode was carried out by comparing with air-saturated water as mentioned previously (Green and Hill, 1984). Initially, the instrument was left until the endogenous oxygen consumption rate stabilized, then 15 µmol methane was added. The methane–induced rate was calculated by substracting the rate before (endogenous) from the rate after the methane was added. The oxygen consumption rate was expressed as nmol $(min^{-1}$ mg dry weight$)^{-1}$.

2.15 Statistical analysis

Differences between two means were tested using a t-test. Tests between more than two datasets used a one-way analysis of variance (ANOVA) with a Post-hoc Tukey's HSD test in Microsoft Excel using the ANALYSE-IT (Analyse-it, Leeds, UK) software package. All data tested to 95% significance value.

Chapter 3

Investigating potential copper transport systems by targeted mutagenesis in *Mc. capsulatus* (Bath)

3.1 Introduction

Copper is an essential element for both prokaryotic and eukaryotic organisms; it acts as a cofactor for enzymes that are involved in electron transfer. Copper becomes toxic at high concentrations (Kremer, 2006). For this reason, cells strictly control the uptake copper and the intracellular quota of this metal. An array of proteins, including transporters, chaperones and regulators, coordinates copper homeostasis and controls transport of copper to sub-cellular compartments and to enzymes that require copper (Solioz & Stoyanov, 2003).

Copper homeostatic systems are well understood in a number of organisms, such as *E. coli* and *Enterococcus hirae*. In these bacteria, CopA, a copper-translocating P-type ATPase, which encoded by a *copA*, has been identified to play a key role in copper trafficking into or out of the cells (Odermatt *et al.*, 1992; Rensing and Grass, 2003; Solioz and Stoyanov, 2003; Stoyanov *et al.*, 2001). P-type ATPases are membrane proteins that transport a broad variety of ions including copper and are found in eukaryotic and prokaryotic cells (Apell, 2004). They accomplish ion transport across the respective membranes by utilizing the energy released from ATP breakdown in an active transport process (Bublitz *et al.*, 2011).

Copper-to-biomass ratio is an important factor controlling the physiology and activity of methanotrophs that possess both sMMO and pMMO, such as *Mc. capsulatus* and *Ms. trichosporium*. In these organisms, the expression of the genes encoding sMMO and pMMO enzymes is regulated by the copper-to-biomass ratios, pMMO is up-regulated at high copper to-biomass ratios while sMMO is switched on when this ratio is low (Stanley *et al.*, 1983).

Phelps *et al.* (1992) have isolated mutants of *Ms. trichosporium* (OB3b), another model methanotroph, by random chemical mutagenesis. These mutants could tolerate high concentrations of copper compared to the wild-type, expressed sMMO constitutively (sMMO^{c}) and were deficient of pMMO. It has been postulated that the phenotype of these mutants was due to defects in copper uptake systems in *Ms. trichosporium*. However, the identification of the mutated genes was not possible due to the mutagenesis technique that they used. About a decade later, the sequencing of the genome of *Mc. capsulatus* revealed the presence of many putative P-type ATPase genes in this organism (Ward *et al.*, 2004). Among them, three copper translocating P-type ATPase homologues; MCA0705 (*copA1*), MCA0805 (*copA2*) and MCA 2072 (*copA3*) were identified. Due to the central role that copper has in MMO regulation, it was of interest to understand the copper transport systems in this methanotroph. Therefore, we hypothesized that the products of three *copA* genes are involved in copper transport (uptake) and in regulation of methane oxidation in *Mc. capsulatus*.

In order to test this hypothesis, a targeted mutagenesis approach was initiated to generate three mutants; *Mc. capsulatus* Δ*copA1*, Δ*copA2* and Δ*copA3*. These mutants were subsequently characterized (*e.g.*, testing sMMO expression and growth at different copper concentrations) and compared to the wild-type organism. Throughout the rest of this thesis, *copA* is used to refer to *copA1 copA2* and *copA3* genes, CopA to refer to CopA1, CopA2 and CopA3 proteins, and Δ*copA* is used to refer to Δ*copA1*, Δ*copA2* and Δ*copA3* mutant strains.

3.2 Features of CopA of *Mc. capsulatus*

The features of CopA of *Mc. capsulatus* are presented in Table 3.1. The putative function of these ATPases is copper transport in an active process, by using the energy released from the ATP hydrolysis to establish an electrochemical potential gradients for the transported ions across the *Mc. capsulatus* membranes.

Table 3.1 Features of *copA*1, *copA*2 and *copA*3 of *Mc. capsulatus* as indicated by the annotation of *Mc. capsulatus* genome.

Gene	***copA1***	***copA2***	***copA3***
Gene number	MCA0705	MCA0805	MCA2072
Length (bp/aa)	2340 /779	2496/831	2178/725
Strand	-	+	+
Number TMs*	8	8	8
Description	Copper-translocating P-type ATPase	Copper-translocating P-type ATPase	Copper-translocating P-type ATPase
Potential Function	Copper transport	Copper transport	Copper transport
Transporter type	ATP-dependent	ATP-dependent	ATP-dependent

***TMs; Transmembrane domains (predicted)

Analysis of amino acids sequence alignments showed that *Mc. capsulatus* CopA proteins had high homology to P-type ATPases from various bacterial species. The amino acid identities between CopA from *Mc. capsulatus* and known copper /silver ion-translocating ATPases; *E. coli* CopA (Rensing and Grass 2003), *Ent. hirae* CopA, *Ent. hirae* CopB (Solioz and Stoyanov 2003), *Synechococcus* sp. CtaA (Cavet *et al.*, 2003; Tottey *et al.*, 2004) *Synechococcus elongatus* PacS (Shcolnick and Keren 2006) ranged from 37 – 46%. As can be seen, (Figure 3.1), CopA1 and CopA2 from *Mc. capsulatus* seemed to be closely related to each other as both exhibited 52.8% sequence identity and were clustered together. *Synechococcus* sp. and CopA3. CopA3 was grouped with *E. coli*

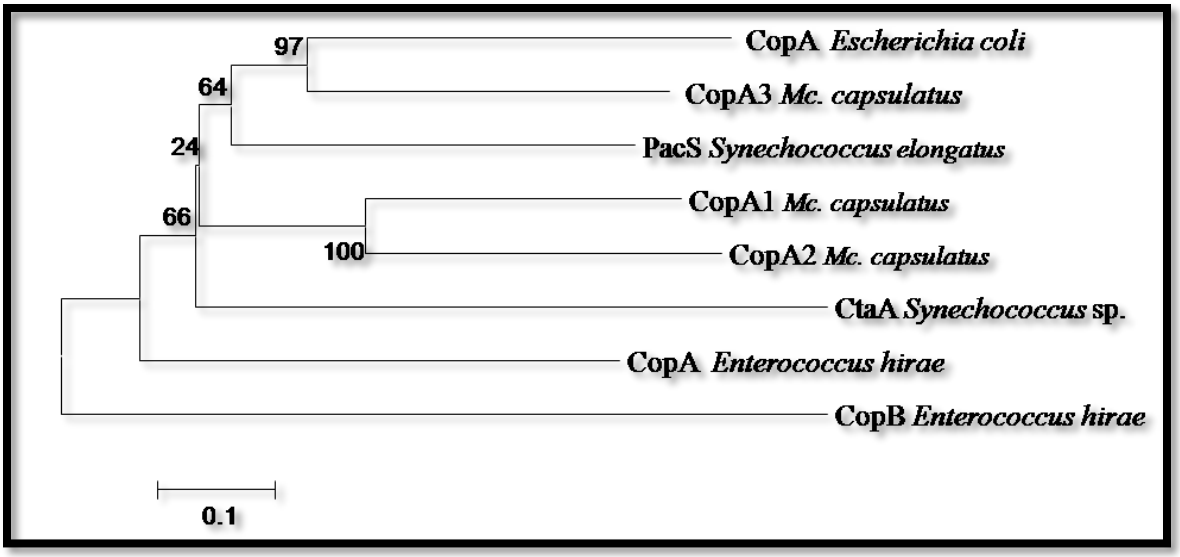

Figure 3.1 Phylogenetic tree showing the relationship between *Mc. capsulatus* CopA1(accession no. YP113215), CopA2 (accession no. YP113305) and CopA3 (accession no. YP114502), *E. coli* CopA (accession no. Q59385), *Ent. hirae* CopA (accession no. AAA61835) and CopB (accession no. AAA61836), *Synechococcus elongatus* PacS (accession no. BAA03907) and *Synechococcus* sp. CtaA proteins (accession no. AAB82020). MEGA5 software (Tamura *et al.*, 2011) based on the neighbour-joining method was used for phylogenetic comparison of the aligned amino acid sequences using Clustal. The bar scale indicates the number of substitutions per site.

(43.2% sequence identity) and with PacS from *Synechococcus elongates* (46.1 % sequence identity). CopA and CopB from *Ent. hirae* had relatively low sequence identities (37 – 38%) with the CopA from *Mc. capsulatus* and were outgrouped (Figure 3.1). Phylogenetic analysis of 216 proteobacterial P-type ATPases revealed that these bacteria were grouped according the ATPase family to which they belong. Extensive horizontal transfer of genes encoding P-type ATPases has been suggested to take place between bacteria (Chan *et al.*, 2010).

Furthermore, analysis of the protein sequences of the three CopA proteins of *Mc. capsulatus* revealed that these proteins contained highly conserved domains when comparing them with those of the well-characterized ATPases from different bacteria (Figure 3.2 and 3.3). *Mc. capsulatus* CopA proteins contains CXXC motif, a heavy-

metal-binding motif, in which the two cysteine are conserved (Figure 3.2A) and a cysteine-proline-cysteine (CPC) motif, a transmembrane metal-binding site (Figure 3.3A). *Ent. hirae* CopB contains a histidine-rich motif instead of cysteine. *Mc. capsulatus* CopA also contained the TGES motif in the phosphatase domain, although in CopA3 of *Mc. capsulatus* the serine residue is replaced by proline as in *E. coli* CopA (Figure 3.2B). In addition, *Mc. capsulatus* CopA had an invariant phosphorylation site (DKTGTL) in which the aspartate (K) residue is phosphorylated by ATP during the catalytic cycle (Figure 3.3B) and the ATP binding domain (GDGINDAP) (Figure 3.3C). Furthermore, eight membrane-spanning helices were predicted in *Mc. capsulatus* CopA1 (Figure 3.4A), CopA2 (Figure 3.4B) and CopA3 (Figure 3.4C). These results indicated that the three CopA proteins of *Mc. capsulatus* exhibited the characteristic features of P_{1B}-type ATPases, the heavy metal transporters (Argüello *et al.*, 2007) and might be members of this group transporters.

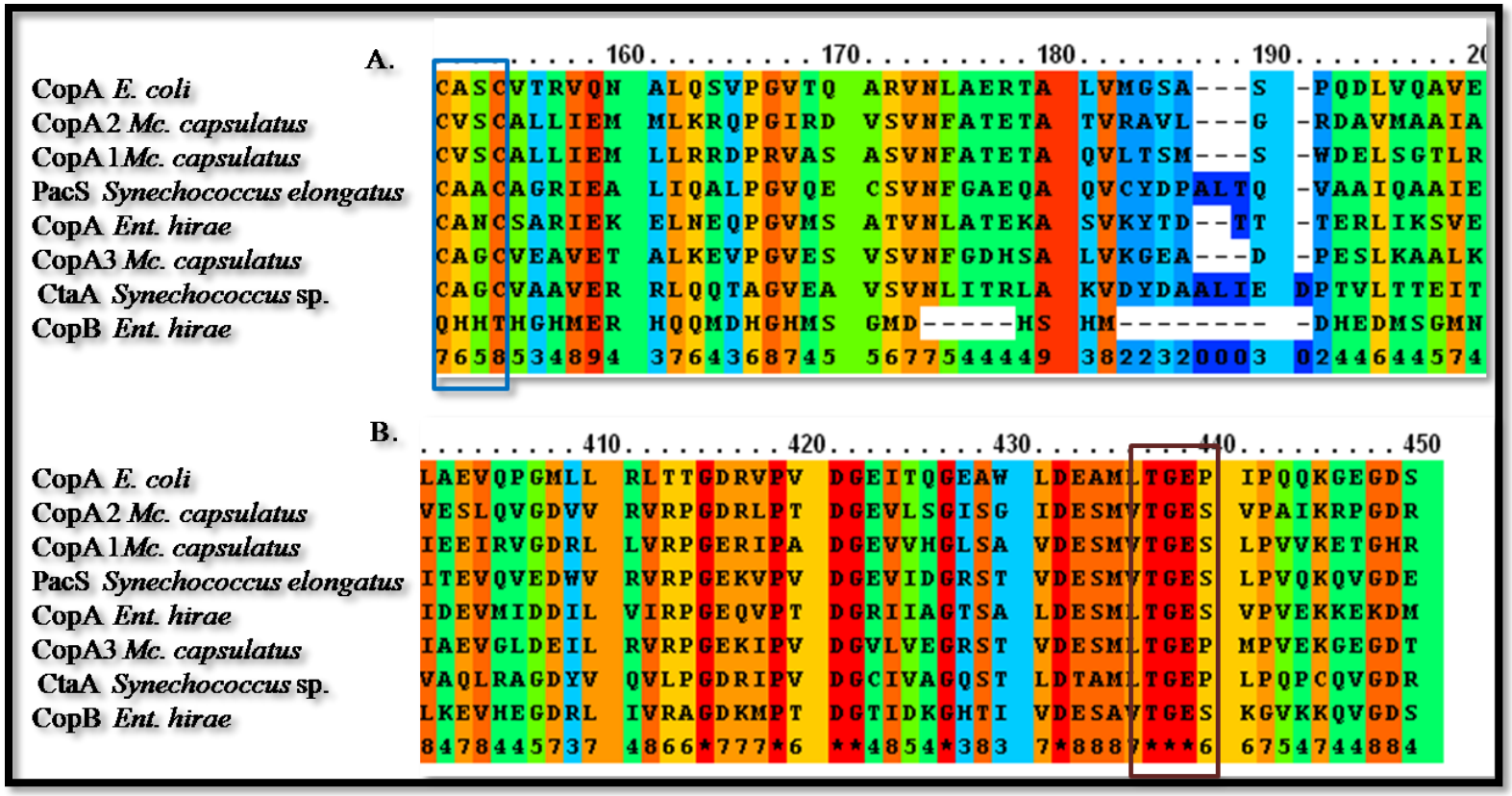

Figure 3.2 Sequence alignment of *Mc. capsulatus* CopA1 (accession no. YP113215), CopA2 (accession no. YP113305) and CopA3 (accession no. YP114502), *Ent. hirae* CopA (accession no. AAA61835) and CopB (accession no. AAA61836), *E. coli* CopA (accession no. Q59385) *Synechococcus elongatus* PacS (accession no. BAA03907) and *Synechococcus* sp. CtaA proteins (accession no. AAB8202), indicating: A, conserved CXXC motif in blue box; B and TGES motif brown box, (unconserved 0 1 2 3 4 5 6 7 8 9 10 conserved). Sequence alignments were carried out using the freely available PRALINE http://www.ibi.vu.nl/programs/pralinewww/ **(**Simossis and Heringa, 2005**).**

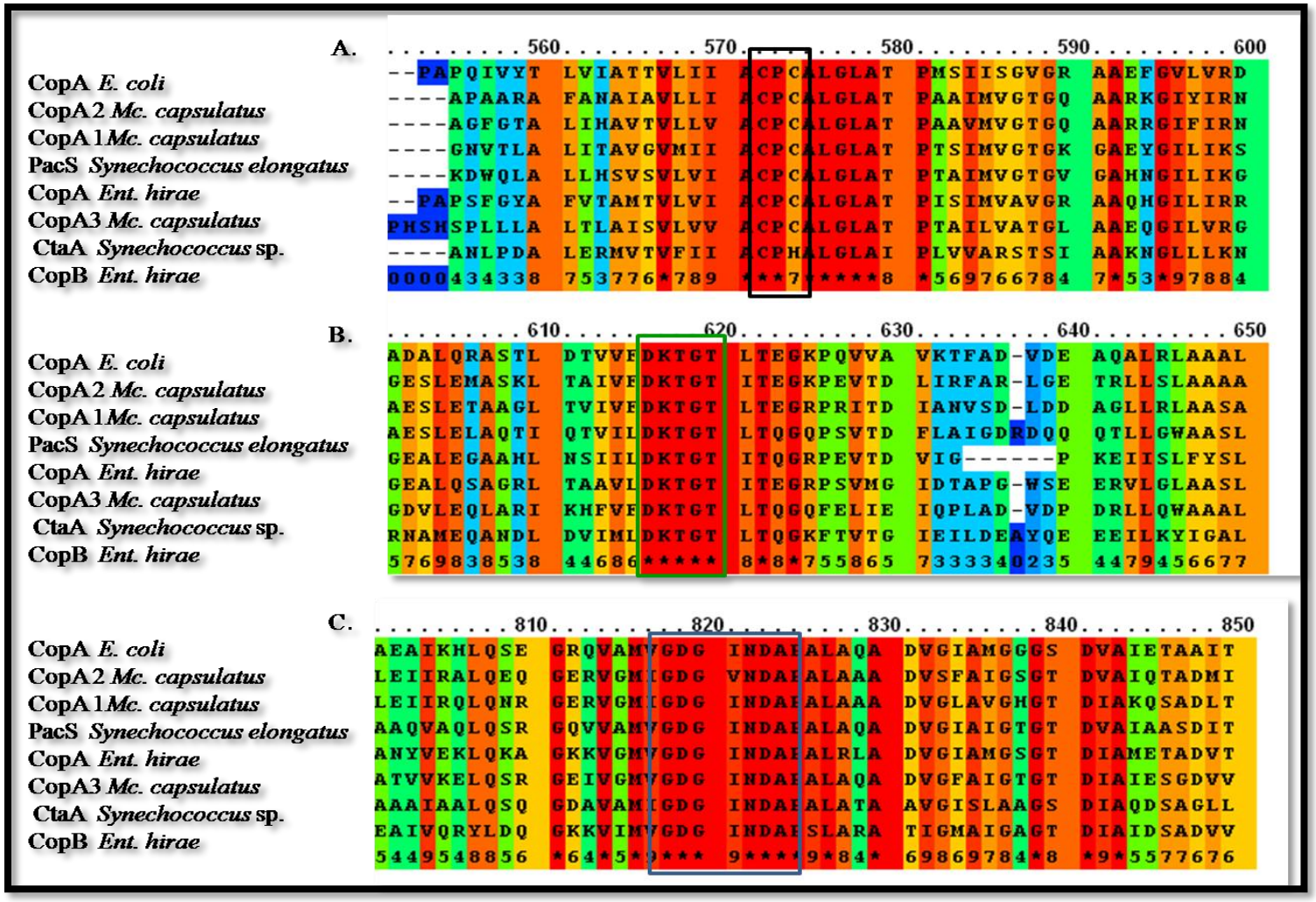

Figure 3.3 Sequence alignment of *Mc. capsulatus* CopA1, 2 and 3, *E. coli* CopA, *Synechococcus elongatus* PacS, *Ent. hirae* CopA, *Ent. hirae* CopB and *Synechococcus* sp. CtaA proteins indicating: A, CPC motif black box; conserved DKTGT motif green box and C, ATP binding domain (GDGINDAP) blue box .

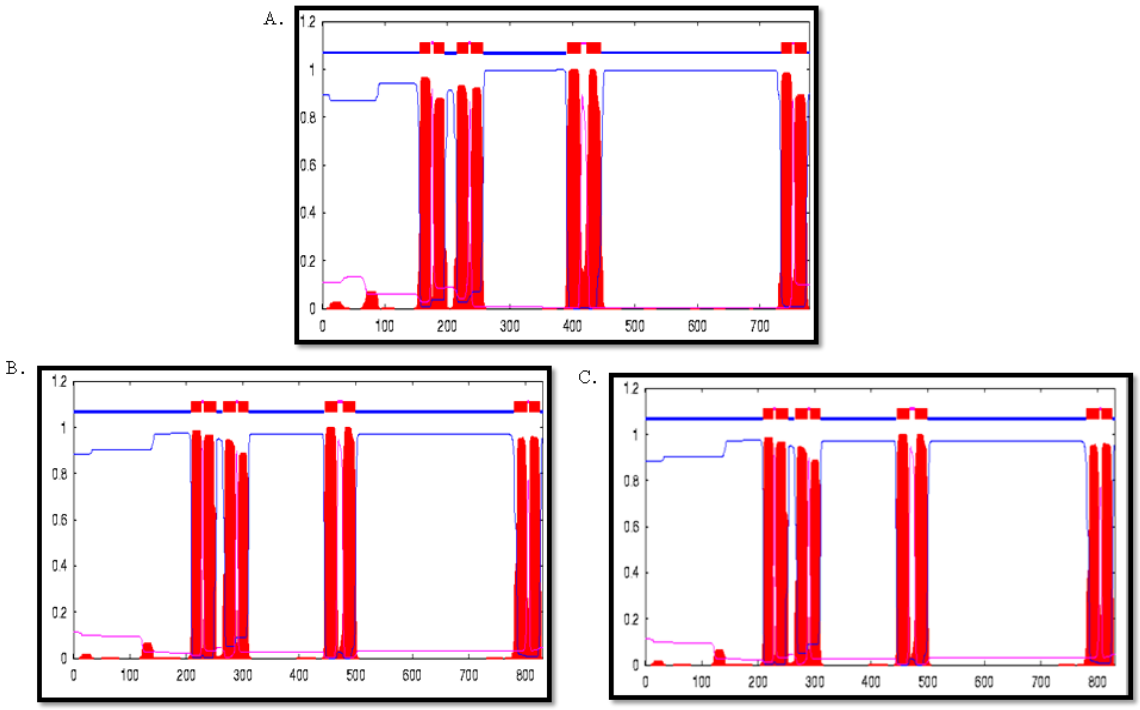

Figure 3.4 Topological predictions of the three copper translocating P-type ATPases using TMHMM (Krogh *et al.*, 2001). A, CopA1; B, CopA2 and CopA3. Transmembrane helices red bars, extracellular loops pink lines and intracellular loops blue lines.

The protein topology, the total number of the membrane helices and their in/out orientation relative to the membrane, was predicted using Tied Mixture Hidden Markov Model (TMHMM Server v. 2.0, http://www.cbs.dtu.dk/services/TMHMM/). All CopA-derived proteins were predicted to have eight membrane-spanning helices in pairs of two (Figure 3.4), indicating that they belong to the basic type I topology (Chan *et al.*, 2010). The putative transmembrane helices were each composed of 17 – 22 aa. The sixth transmembrane helix contained the copper-binding CPC motif, a distinctive feature of many copper ATPases (Fan and Rosen 2002). In addition, intracellular and extracellular loops were also predicted (Figure 3.4).

3.3 Inactivation of the *copA2* and *copA3* genes

An insertional inactivation mutagenesis technique was used to disrupt *copA2* and *copA3*, to determine the function of both genes (Table 3.1) was performed individually. *copA2* and *copA3* DNA fragments were amplified using the primers COPA2F506-*Xba*1 and COPA2R51959-*Hin*dIII, COPA3F635-*Eco*R1 and COPA3R2147-*Hin*dIII respectively (Table 3.2). The purified DNA fragments were cloned into pCR2.1-TOPO to give the constructs pAK222 and pAK444 respectively (Figures 3.5 and 3.8). Then, *copA2* and *copA3* DNA fragments were cloned to plasmid vector, pK18mob*sacB* via *Xba*1and *Hin*dIII and *Eco*R1 and *Hin*dIII restriction sites respectively, to give the constructs pAK011 and pAK02 (Figures 3.5 and 3.8). The gentamicin resistance cassette (Gm^R) was cloned via the *Pst*1 restriction site in the *copA2* and *copA3* DNA fragments the to give the final constructs, pAK022 and pAK044, which were electroporated into *E. coli* strain S17.1 λpir (Herrero *et al.*, 1990). Screening of the transconjugants was carried out by plating the resulting strains onto NMS plates supplemented with gentamicin. Then, PCR amplifications were performed using primers specific for gentamicin cassette and for the flanking regions of the target *copA2* and *copA3*. The existence of gentamicin and kanamycin resistance cassettes in the mutants was confirmed by PCR using specific primers (data not shown). Disruption of *copA2* was confirmed by PCR using the primer pair US_COPA2_F140 and GENR851, which targeted the region upstream from *copA2* and the gentamicin cassette respectively (lane 3, Figure 3.6). No PCR product of DNA from the wild-type in lane 2, Figure 3.6, as there is no specific binding sites of the gentamicin-specific primer. Likewise, inactivation of *copA3* was verified using PCR amplification with primers DS_COPA3_R2464 and GENF37, which were specific for the

3' region of this gene and for gentamicin cassette respectively (Figure 3.9). The PCR products were sequenced for further confirmation of the mutants. The primers used to confirm the genotype of the mutants are listed in Table 3.2. Mutants were designated as *Mc. capsulatus* ΔMCA0805 (Δ*copA2*) and *Mc. capsulatus* ΔMCA 2072 (Δ*copA3*). *Mc. capsulatus* ΔMCA0705 (Δ*copA1*) was made previously by Ali (2006).

It is noteworthy that, many attempts were made to obtain PCR products using *Pfu* DNA polymerase (Promega) or DreamTaq (Fermentas) with the primer pairs targeting the upstream and downstream regions of *copA2* and *copA3* from the mutants but all failed (lane 3 in both Figures 3.7 and 3.10). The reason for this was probably the large sizes of the target regions, which were about 7 kbp. In addition, many attempts were made to obtain double cross-overs by plating the single cross-over recombinants, which contained *sacB* on NMS supplemented with different concentrations of sucrose (up to 10%). The expression of *sacB* in the presence of sucrose has lethal effect on cells (Selbitschka *et al.*, 1993). Thus, double-cross over mutant would eliminate *sacB* from the chromosome. However, such attempts were not successful. This might due to the one arm of the target DNA being twice as long as the other arm; this made the chances of getting double cross-over recombinant very low. Even though the intended double-cross over mutants were not obtained, the desired genes were inactivated (truncated) in the single cross-over mutants via insertional inactivation. These drawbacks were avoided in the strategies that were used in generating subsequent mutants (*e.g.*, Δ*scO-1* in Chapter 6).

Table 3.2 Primers used to amplify PCR products of *copA2* and *copA3* and to confirm the genotype of the *Mc. capsulatus*Δ*copA2* and *Mc. capsulatus* Δ*copA3*. Restriction sites were introduced via the primers to facilitate cloning (restriction sites are highlighted in bold and underlined).

Primer *	**Sequence**
COPA2F506-*Xba*1	5'-**TCT AGA** ATGCAGTCATGGCGGCCATC 3'
COPA2R51959- *Hin*dIII	5' **AAGCTT**GAACACTGCCGCGAGCTTAC 3
US_COPA2_F140	5' CGGAGCGTTGTTACCTCTTG 3'
DS_COPA2_2363	5' CACGCCAGATTCTGATGGAC 3'
GENF37	5' GACATAAGCCTGTTCGGTTC 3'
GENR851	5' GCGGCGTTGTGACAATTTAC 3'
COPA3F635-*Eco*RI	5' **GAATTC**CCCTCGAACGCATGCAAATC 3'
COPA3R2147-*Hin*dIII	5' **AAGCTT**AAACCGCGTTGAAGGAGGTG 3'
US_COPA3_F13	5' TCGGTATGCTCAGGGTGTTG 3'
DS_COPA3_2464	5' GTGCCTTCTTCGAGCTTGAC 3'

*****The primers were used both in the construction of the mutants and subsequently for their analysis.

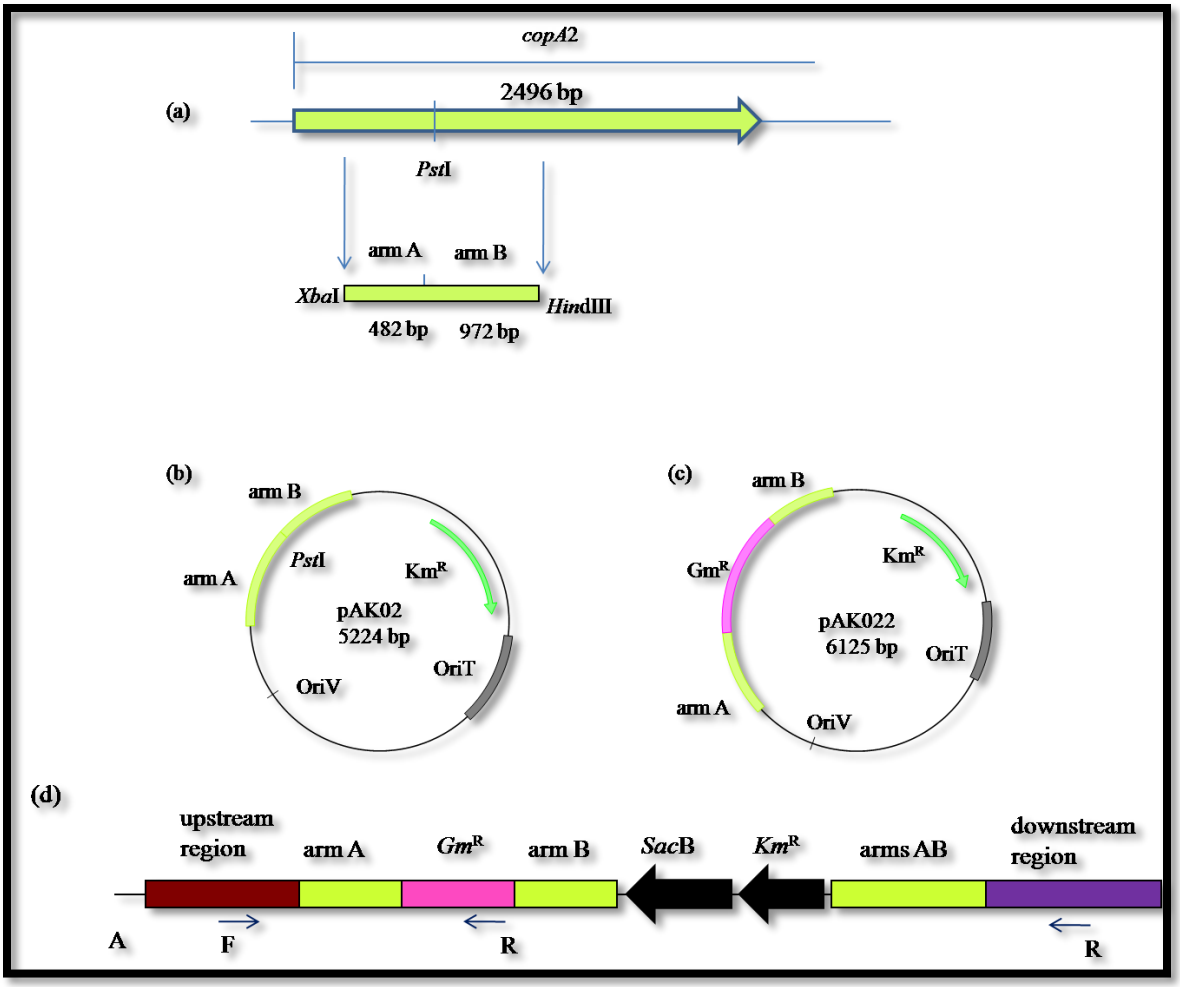

Figure 3.5 Schematic representation of the strategy of constructing *Mc. capsulatus* Δ*copA2* (a) the wild-type gene (*copA2*) and the target region was highlighted by arrows; (b) The intermediate plasmid construct pAK02 with *copA2* fragment, restriction sites *Xba*I and *Hin*dIII were introduced by PCR to facilitate cloning; (c) The plasmid construct pAK022 used to inactivate *copA2* and (d) *Mc. capsulatus* Δ*copA2* following single homologous recombination of pK18*mobsacB*. The primers used to check the genotype of the mutants indicated by small horizontal arrows.

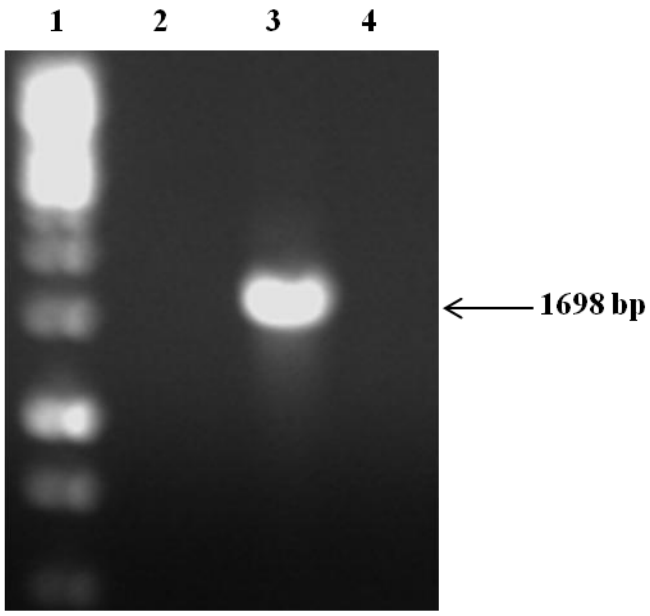

Figure 3.6 Confirmation of *Mc. capsulatus* Δ*copA2* genotype, via PCR using primers complementary to upstream DNA region F and gentamicin R. Lane 1, a 1 kb DNA ladder marker (Invitrogen); lane 2, genomic DNA extracted from wild-type of *Mc. capsulatus*; lane 3, *Mc. capsulatus* Δ*copA2* and lane 4, negative control.

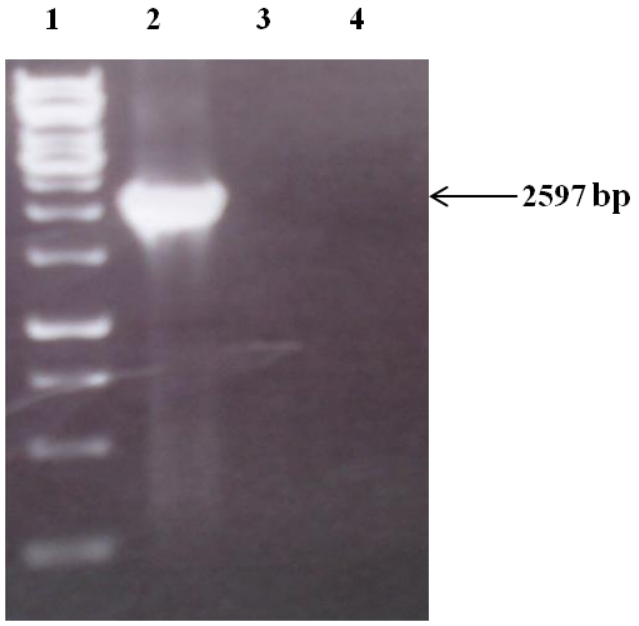

Figure 3.7 Confirmation of *Mc. capsulatus* Δ*copA2* genotype, via PCR using primers complementary to upstream and downstream the target DNA region. Lane 1, a 1 kb DNA ladder marker (Invitrogen); lane 2, genomic DNA extracted from wild-type of *Mc. capsulatus*; lane 3, *Mc. capsulatus* Δ*copA2* and lane 4, negative control.

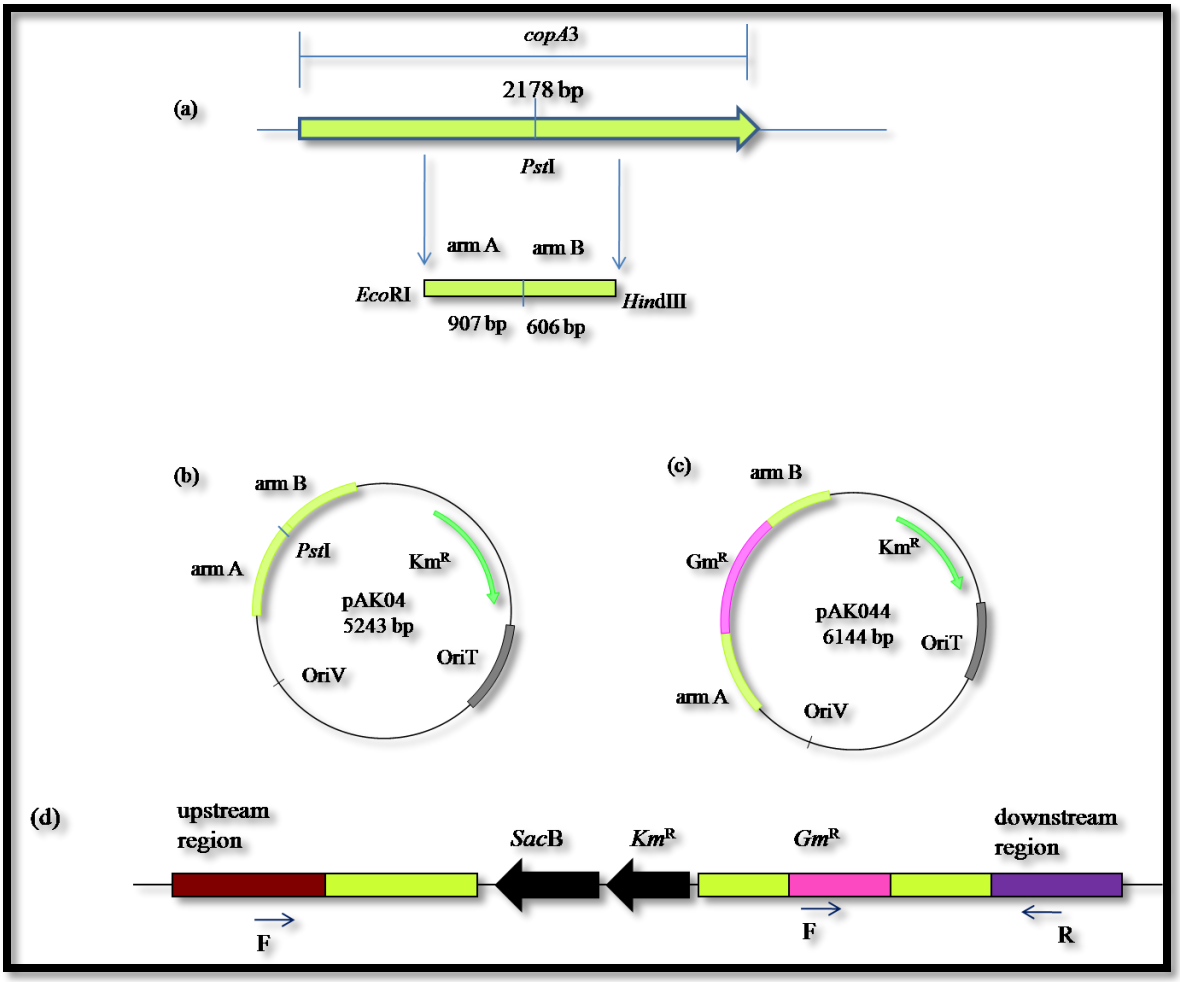

Figure 3.8 Schematic representation of the strategy for constructing *Mc. capsulatus*Δ*copA3* (a) the wild-type gene (*copA3*) and the target region is highlighted by arrows; (b) The intermediate plasmid construct pAK04 with *copA3* fragment, restriction sites *Eco*R1 and *Hin*dIII were introduced by PCR to facilitate cloning; (c) The suicide plasmid construct pAK044 used to inactivate *copA3* and (d) Δ*copA3* following single homologous recombination of pK18*mobsacB*. Small/horizontal arrows indicate the primers used to check the genotype of the mutants.

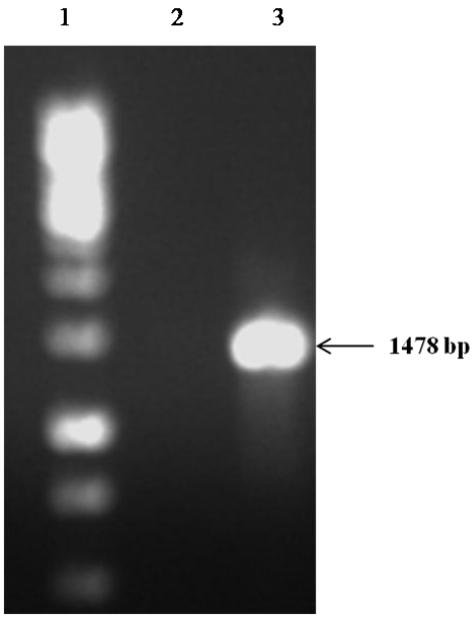

Figure 3.9 Confirmation of *Mc. capsulatus* Δ*copA3* genotype, via PCR using primers complementary to downstream DNA region R and gentamicin F. Lane 1, a 1 kb DNA ladder marker (Invitrogen); lane 2, genomic DNA extracted from wild-type of *Mc. capsulatus*; lane 3, *Mc. capsulatus* Δ*copA3*.

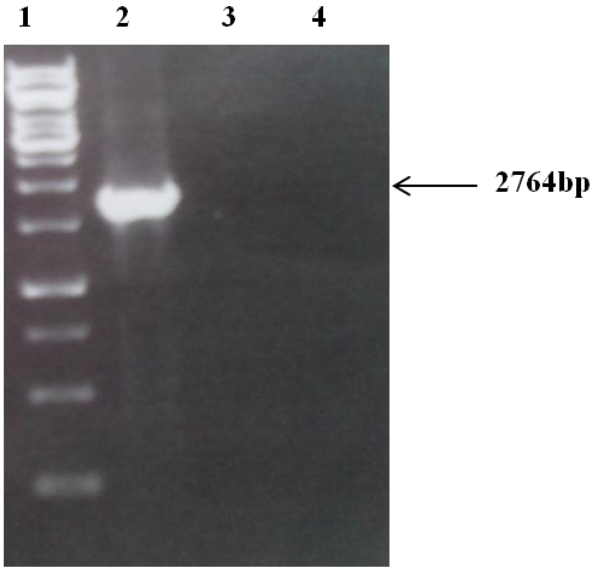

Figure 3.10 Confirmation of *Mc. capsulatus* Δ*copA3* genotype, via PCR using primers complementary to upstream and downstream of the target DNA region. Lane 1, a 1 kb DNA ladder marker (Invitrogen); lane 2, genomic DNA extracted from wild-type of *Mc. capsulatus*; lane 3, *Mc. capsulatus* Δ*copA3* and lane 4, negative control.

3.4 Characterizations of the *copA* mutants

3.4.1 Naphthalene assay:

Mc. capsulatus wild-type and the three *copA* mutants were tested for their ability to oxidise naphthalene as described in Materials and Methods. The qualitative assay was used to test for the sMMO expression (Brusseau *et al.*, 1990). The wild-type and the mutant strains were grown on NMS medium supplemented with either 0, 0.5, 1.0, 1.5, 2.0, 2.5, 3.0, 3.5, 4.0 and 5.0 µM copper (as copper sulfate).

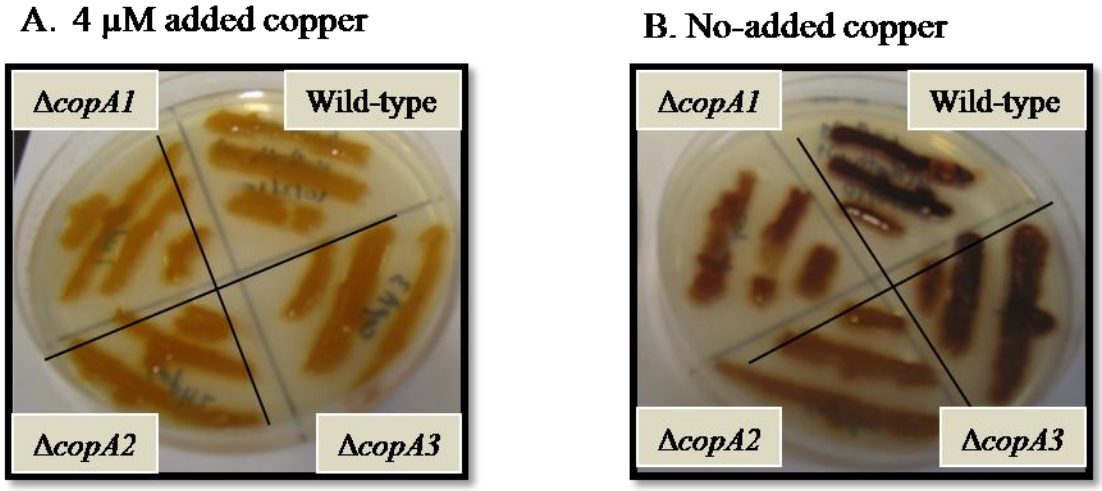

Figure 3.11 Naphthalene assay results A. under high copper concentration (4 µM added copper), B. under no added copper concentration for *Mc. capsulatus* wild-type, Δ*copA1*, Δ*copA2* and Δ*copA3* mutant strains.

There was no difference between *Mc. capsulatus* wild-type and the Δ*copA* strains in terms of sMMO activity using the naphthalene assay, as can be seen in Figure 3.11. Under low copper concentration growth conditions (less than 2.0 µM added copper) all strains gave a purple colour upon addition of the diazonium salt, indicating that they expressed the sMMO enzyme, which oxidized naphthalene to naphthol. On the other hand, none of the strains expressed sMMO during growth under high copper

concentrations (above 2.0 µM) as shown by no colour change with the naphthalene assay. These observations indicated that *copA* of *Mc. capsulatus* are not involved in MMO regulation and that the mutants expressed sMMO only when grown under low-copper growth conditions.

3.4.2 Determination of Minimum Inhibitory Concentrations (MIC) for copper

To look for a phenotypic difference between the *copA* mutant strains and the wild-type organism, all strains were tested for their ability to grow on NMS plates supplemented with different concentrations of copper (10, 20, 30, 40, 50, 60, 70, 80, 90, 100, 110, 120 and 150 µM). These experiments were done using physiologically similar strains and in triplicate. Late-exponential phase (OD_{540} ~ 0.5) cultures that were grown in copper-depleted NMS medium, were diluted 100 times in sterilized NMS and 20 µl of the strains compared were inoculated on NMS plates. The plates were incubated as described in Materials and Methods. The MIC of copper was taken as the lowest concentrations assessed at which no colony formation was recognized.

Both the wild-type and the mutant strains could grow on NMS plates supplemented with copper concentration up to 40 µM and neither of them grew at above 110 µM. Δ*copA1* and Δ*copA2* were in general more sensitive to copper than the wild-type organism was (Figure 3.12). Growth of Δ*copA1* and Δ*copA2* mutants was inhibited at copper concentrations of 50 and 65 µM respectively. On the other hand, the Δ*copA3* mutant strain was somewhat more resistant to elevated copper concentrations than

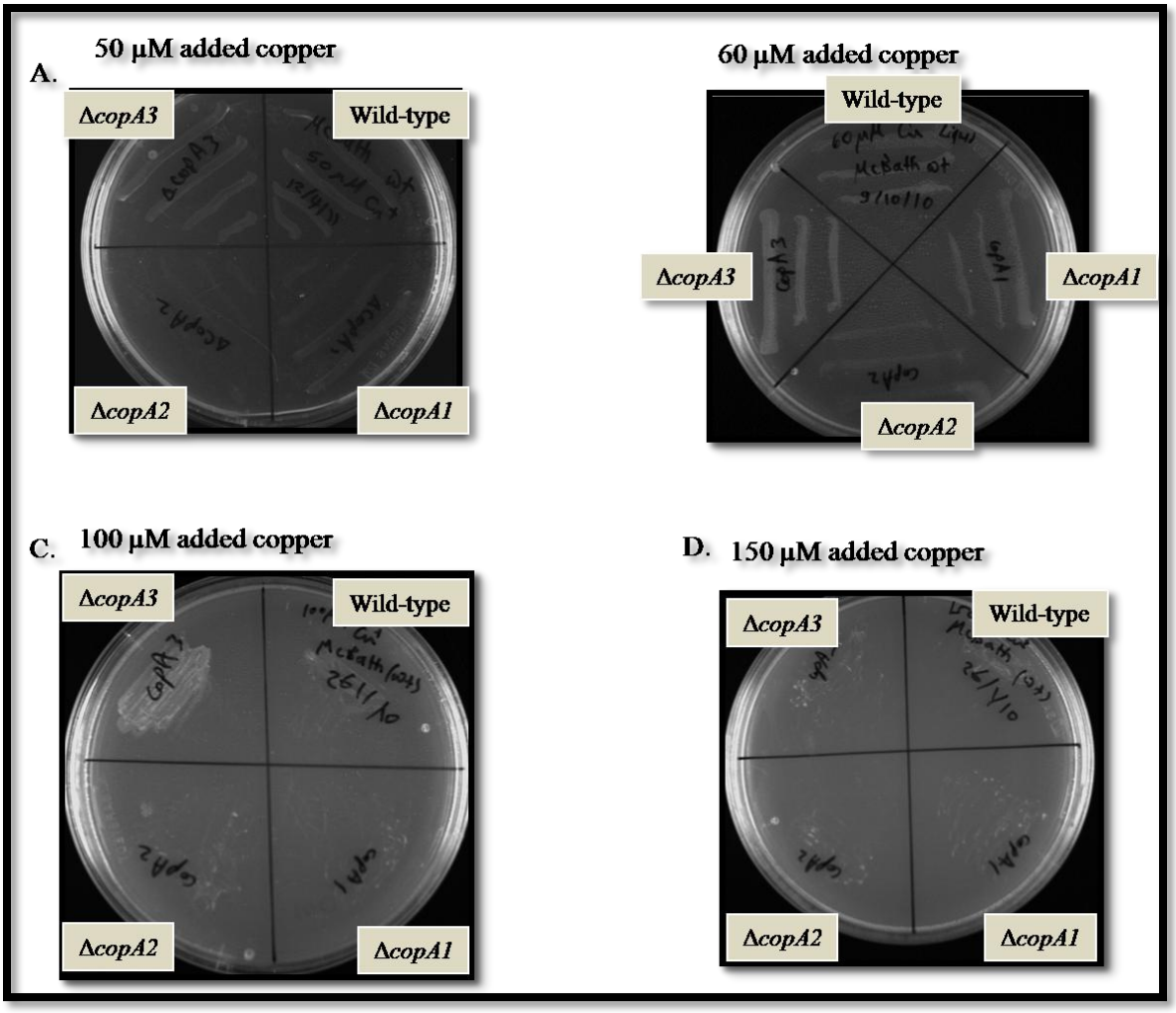

Figure 3.12 Growth of *Mc. capsulatus* wild-type and *copA* mutant strains on NMS with A, 50 µM; B, 60 µM; C, 100 µM and D. 150 µM added copper. These experiments were done in triplicate.

the wild-type. Δ*copA3* was found to grow at 100 µM, while the wild-type organism grew only at 80 µM added copper. These observations revealed that Δ*copA1* and Δ*copA2* were more sensitive to higher copper than the wild-type while Δ*copA3* was copper resistant. These results suggested that CopA of *Mc. capsulatus* might have potential roles in copper homeostasis in *Mc. capsulatus*.

3.4.3 Growth under different silver concentration

The Δ*copA*1, Δ*copA*2 and Δ*copA*3 mutants and the wild-type organism were tested for their ability to grow on NMS plates supplemented with different concentrations of silver (1-7 µM), silver was added as a filter-sterilized $AgNO_3$ solution.

The parental strain and putative *copA* mutants showed growth at silver concentration up to 4 µM and none of them could grow at 5 µM silver (Figure 3.13).

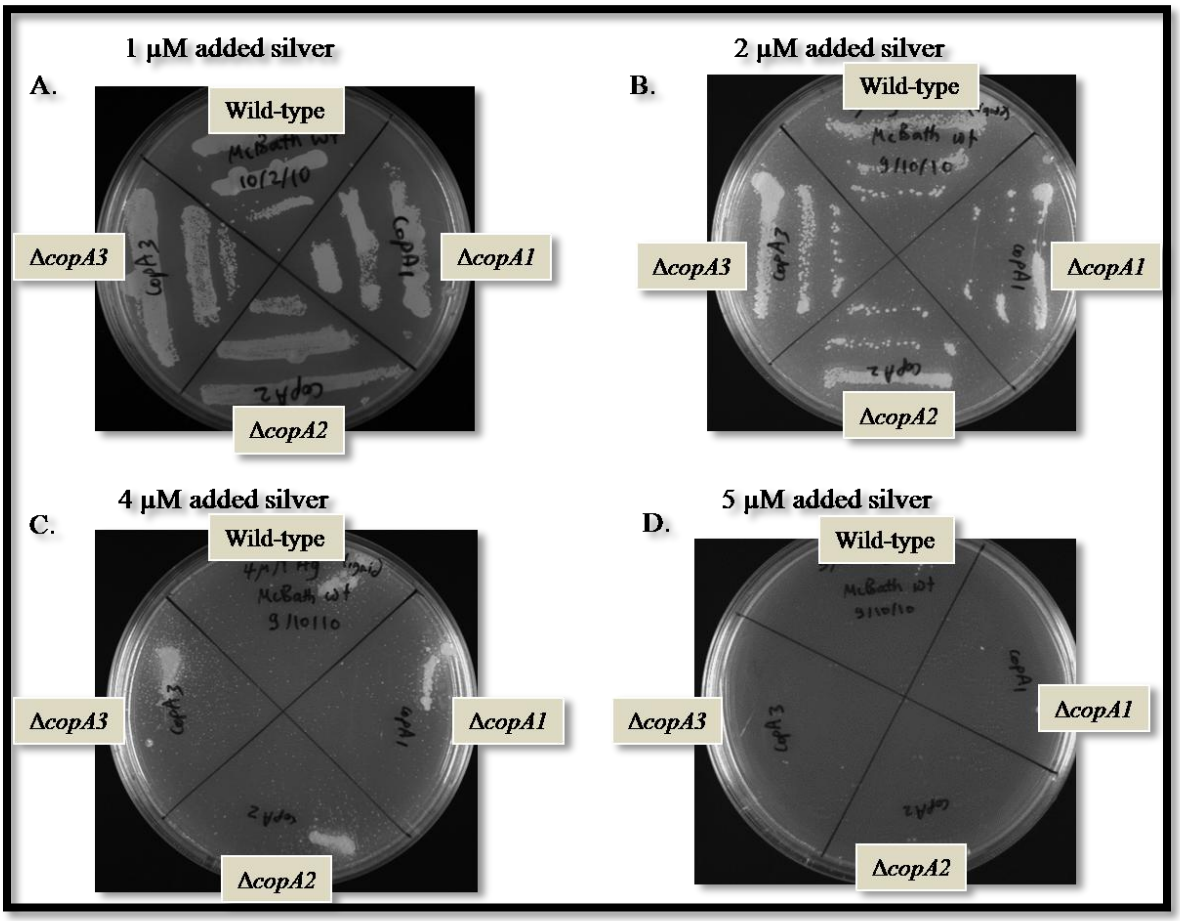

Figure 3.13 Growth of *Mc. capsulatus* wild-type and *copA* mutant strains on NMS with A, 1 µM; B, 2 µM; C, 4 µM and 5 µM added silver (as silver nitrate). These experiments were performed in triplicate.

Additionally, it was noticed that when the supplemented silver concentration increased, Δ*copA* strains and the wild-type showed a weak the growth. No obvious phenotypic difference between the strains was observed with different silver concentrations indicating that the mutagenesis of *copA1*, *copA2* and *copA3* of *Mc. capsulatus* had no effect on silver resistance or sensitivity.

3.4.4 Monitoring the growth of *Mc. capsulatus* and its Δ*copA* mutants at different copper concentrations

The effects of increasing copper concentrations on the growth patterns of Δ*copA* mutant strains, compared to the *Mc. capsulatus* wild-type, were investigated. All strains were tested on NMS liquid medium in flasks supplemented with 0, 10, 30 or 50 µM copper concentrations; copper was added as a filter-sterilized $CuSO_4.5H_2O$ solution. In general, it was noticed that as the copper concentration in NMS increased, the specific growth rates (µ) and the doubling times decreased (Table 3.3). Results showed no significant differences in growth patterns and growth rates between the *ΔcopA* mutants strains and wild-type at no-added copper (Figure 3.14A) and 10 µM added copper (Figure 3.14B). At 30 µM copper, *ΔcopA* strains exhibited significant differences in specific growth rates ($P < 0.001$) compared to the wild-type (Figure 3.14C). Δ*copA1* and Δ*copA2* strains exhibited growth patterns which differed markedly from Δ*copA3* and wild-type when grown at high copper concentrations. In contrast to Δ*copA1* and Δ*copA2* and to some extent to wild-type, Δ*copA3* seemed to grow relatively well at high copper concentrations (30 and 50 µM copper).

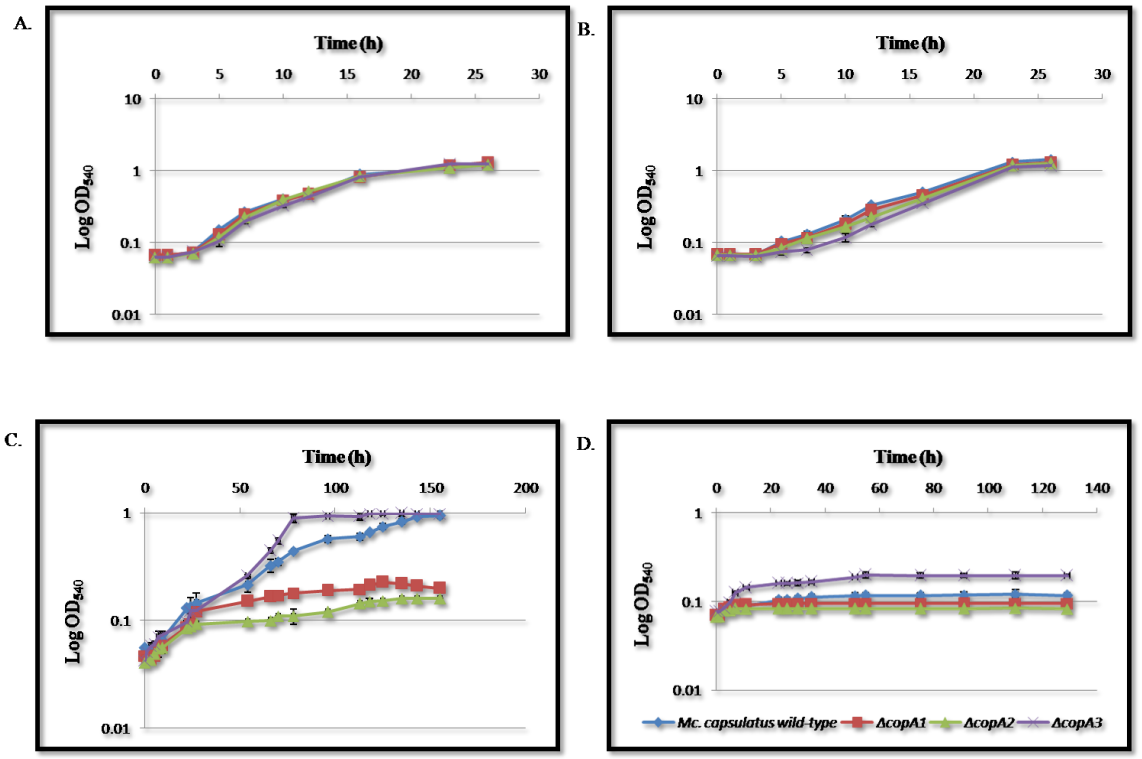

Figure 3.14 Growth of *Mc. capsulatus* wild-type and Δ*copA*1, Δ*copA*2 and Δ*copA*3 strains on 1x NMS supplemented with A, no-added copper; B, 10 µM; C, 30 µM and D, 50 µM added copper. The experiments were carried out in triplicate. All data points represent the mean of three replicates and error bars indicate the standard deviation.

Table 3.3 Specific growth rates of *Mc. capsulatus* wild-type and three Δ*copA* mutant strains on 1x NMS amended with different copper concentrations. Figures are the mean of three replicates ± standard deviation.

Copper (µM)	**Specific growth rate (h^{-1})**			
	0	**10**	**30**	**50**
Wild-type	0.15 ± 0.009	0.14 ±0.002	0.016 ± 0.0008	0.007 ± 0.0004
Δ*copA1*	0.16 ± 0.008	0.14 ±0.004	0.007 ± 0.0004	0.0007 ± 0.00005
Δ*copA2*	0.16 ± 0.006	0.14 ±0.007	0.005 ± 0.0005	0.0005 ± 0.00005
Δ*copA3*	0.16 ± 0.005	0.15 ±0.008	0.035 ± 0.005	0.005 ± 0.0006

This sensitivity of Δ*copA1* and Δ*copA2* and the resistance of Δ*copA3* were in general consistent with the MIC data.

3.4.5 Cytochrome oxidase

To investigate the role of CopA in the activity of cytochrome oxidase activity, cellular oxidase activity was tested in mutant and wild-type strains at two different copper regimes. Under no-added copper, Δ*copA1* strain exhibited significantly lower cellular oxidase activity, which was restored to some extent to that of the wild-type activity under 10 µM copper (Figure 3.15) ($P < 0.01$). There was no significant difference between Δ*copA2* and Δ*copA3* strains, and the wild-type oxidase activity under the copper conditions tested (no-added and 10 µM copper). These results indicated that inactivation of *copA*1 but not *copA*2 and *copA*3 of *Mc. capsulatus* might affect the cytochrome oxidase activity.

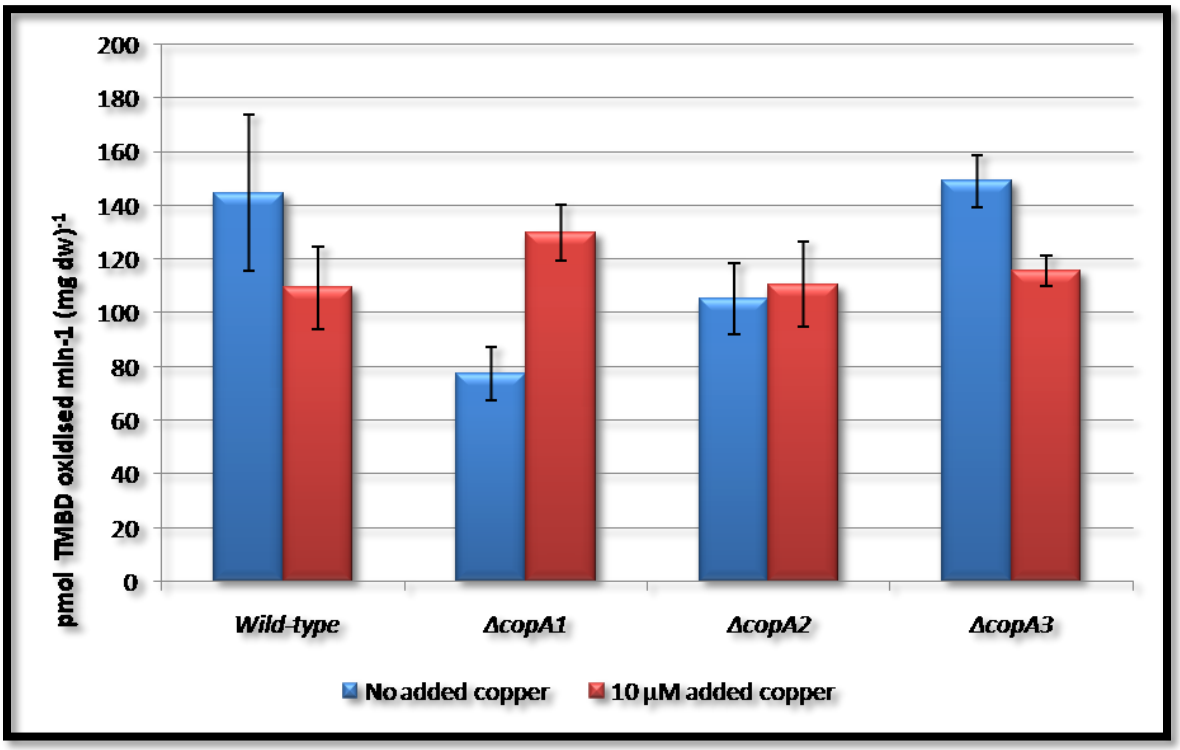

Figure 3.15 Cytochrome oxidase activity of whole cells of *Mc. capsulatus* Δ*copA1*, *Mc. capsulatus* Δ*copA2* and *Mc. capsulatus* Δ*copA3* compared to the wild-type at NMS with no added and with 10 µM copper. Error bars indicate the standard deviation of three replicate measurements.

3.4.6 Intracellular copper measurements

The distribution of copper was analyzed in late-exponential-phase cultures of wild-type and CopA mutant cells grown in NMS supplemented with 30 µM copper (Figure 3.16). Both Δ*copA1* and Δ*copA2* mutants accumulated about three-fold more copper than the wild-type ($P < 0.001$).

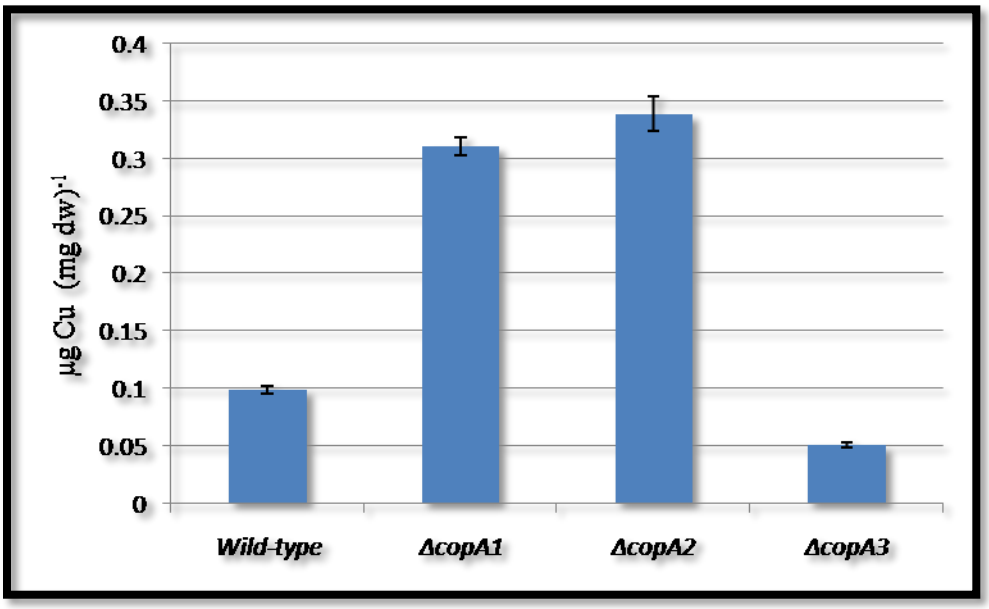

Figure 3.16 Copper measurements for the three mutants *Mc. capsulatus* Δ*copA1*, Δ*copA2* and Δ*copA3* and the *Mc. capsulatus* wild-type grown on NMS with 30 µM added copper. Error bars indicate the standard deviation of three replicate measurements.

Δ*copA3* mutant strain accumulated half the amount of copper (0.05 µg Cu (mg dw)$^{-1}$) when compared with the wild-type (Figure 3.16) ($P < 0.001$). In the NMS medium where no copper was supplemented, the background copper resulting from water or chemical compounds used in NMS was estimated (0.8 µM copper, data not shown). These results supported the proposal that *Mc, capsulatus* CopA might have potential roles in copper homeostasis in this organism.

3.5 Discussion

Amino acids sequence alignment analyses of *Mc. capsulatus* CopA1, CopA2 and CopA3, and the well-characterized CopA from different bacterial species, indicated that these transporters are more likely to belong to the heavy-metal transporting subgroup of ATPases (P_{1B}-type ATPases). This is because the three CopA of *Mc. capsulatus* are characterized by the distinctive features of P_{1B}-type ATPases such as N-terminal heavy-metal-binding motifs; an invariant phosphorylation site; ATP binding domain and eight transmembrane helices (Argüello *et al.*, 2007). Representatives of copper-importing and copper-exporting proteins were included in the alignment analyses to strengthen the conclusions. For instance, in the Gram-positive bacterium, *Ent. hirae* CopA is a copper importing ATPase while CopB is an exporter (Solioz and Stoyanov *et al.*, 2003). In the Gram-negative bacterium, *E. coli*, CopA is an exporter (Rensing and Grass, 2003), however, in *Ent. hirae* CopA is an importer (homologous to CtaA), (Solioz and Stoyanov *et al.*, 2003). CtaA imports copper from the periplasm to cytoplasm in the cyanobacterium, *Synechococcus* sp. and PacS, transports copper from the cytoplasm to the thylakoid, in *Synechococcus elongatus* (Cavet *et al.*, 2003; Totty *et al.*, 2004; Shcolnick and Keren, 2006).

The substrate of these ATPases is might be copper due to the presence of the predicted N-terminal heavy-metal-binding motifs and the experimental data that were obtained (see below). Redundancy in copper-ATPases was found to be uncommon in *Proteobacteria*. *Mc. capsulatus* and *Sinorhizobium meliloti* are the only two organisms in the *Proteobacteria* that have been reported previously to contain three copper-ATPase encoding genes in their genomes (Chan *et al.*, 2010). However, distinctive roles of the

two CopA copper ATPases that are found in *Pseudomonas aeruginosa* have been observed (González-Guerrero *et al.*, 2010).

copA of *Mc. capsulatus* were disrupted and the resulting Δ*copA* strains were characterized and compared to the wild-type. Δ*copA* mutant strains did not show a substantial difference in sMMO expression (Figure 3.11) this indicated that *copA*1, *copA*2 and *copA*3 are probably not involved to a significant extent in MMO regulation.

In addition, Δ*copA* mutant strains exhibited an alteration in copper susceptibility; Δ*copA1*, Δ*copA2* were found to be sensitive to higher copper than the wild-type. These observations were congruent with those obtained by Rensing *et al.* (2000) who generated an *E. coli* Δ*copA* mutant, which had a copper-sensitive phenotype (2.5 mM copper) compared to the parental strain (3.5 mM copper). Comparable results were obtained in other studies on different bacteria in which the *copA* homologues were disrupted such as in *Ent. hirae* CopB (Solioz and Odermatt, 1995) and in *Helicobacter pylori* (Bayle *et al.*, 1998; Ge *et al.*, 1995). In contrast to Δ*copA1* and Δ*copA2* mutants, *Mc. capsulatus* Δ*copA3* seemed to be a little more resistant to elevated copper concentration (100 µM) than the wild-type (80 µM). These results are in line with the results obtained for *Ent. hirae* CopA, which was assumed to import copper into the cells (Solioz and Odermatt, 1995). Although a null in CopA of *Ent. hirae* showed no change in copper resistance, unlike the wild-type, it could not grow after two generations in copper-limited growth conditions (Solioz and Odermatt, 1995). These results suggested that CopA of *Mc. capsulatus* might have potential roles in copper homeostasis in *Mc. capsulatus*.

Mc. capsulatus wild-type and Δ*copA* strains showed similar growth patterns when grown on NMS amended with different levels of silver. These results are parallel to those

achieved by Phung *et al.* (1994) who indicated that inactivation of *ctaA* in *Synechococcus* resulted in a copper-resistant mutant, which exhibited similar behaviour to silver in compared to the parental-strain. Furthermore, an *E. coli* Δ*copA* mutant strain showed a copper but not silver sensitivity (Franke *et al.*, 2001). Surprisingly, *E. coli*, CopA is regulated by CueR, which is induced by copper and silver (Outten *et al.*, 2000; Stoyanov *et al.*, 2001). These findings suggested that copper and silver are substrates for some P-type ATPases because both metals have resemblances in physical and chemical properties (Argüello, 2003). As in *Ent hirae* 5 µM silver completely inhibited cell growth of *Mc. capsulatus* (Figure 3.13D), confirming the toxicity of silver ions. Collectively, these observations showed that, the inactivation of genes encoding for P_{1B}-type ATPases (CopA1, CopA2 and CopA3) in *Mc. capsulatus* did not result in silver sensitivity or resistance.

The significant decrease in cytochrome oxidase activity observed in the Δ*copA1* is presumably due to the involvement of this P-type ATPases in assembly and/or function of cytochrome oxidase by unknown mechanism. These results are in accordance with those obtained in *P. aeruginosa* Δ*copA*2, which showed a reduced cytochrome oxidase activity phenotype (González-Guerrero *et al.*, 2010). They explained this phenotype by the suggestion that CopA2 of *P. aeruginosa* P-type ATPases could transfer copper to specific copper chaperones in the periplasm (González-Guerrero *et al.*, 2010), which then transfer it directly, or via another copper-binding protein, to cytochrome oxidase. Nevertheless, it has been found that periplasmic copper-binding proteins (SenC/SCO1) have a vital role in synthesis of bacterial cytochrome oxidases (Frangipani and Haas, 2009; Thompson *et al.*, 2010). Details about ScO-1 in *Mc. capsulatus* are given in

Chapter 6. Furthermore, disruption of *Rubrivivax gelatinosus ctpA*, a gene encoding a copper-translocating P1B-type ATPase, showed a drastic decrease in both cbb_3 and caa_3 oxidase activities but no copper-sensitive phenotype was obtained. This result indicated that *R. gelatinosus* the CtpA has a role in cytochrome oxidase assembly but is not essential for copper resistance (Hassani *et al.*, 2010). These findings suggest that *Mc. capsulatus* CopA1 but not CopA2 and CopA3 might have a role in cellular cytochrome oxidase assembly and/or activity.

In *Mc. capsulatus*, Δ*copA1* and Δ*copA2* strains accumulated significantly higher concentration of copper ions intracellularly compared to the parent-strain (Figure 3.16). This suggests that both CopA1 and CopA2 may function together to maintain a tolerable copper quota inside the cells. These observations are consistent with those previously obtained for inactivation of copper translocating P-type-ATPases that were shown to have a role in copper detoxification in *Salmonella typhimurium* (Osman and Cavet 2008), *P. aeruginosa* (Schwan *et al.*, 2005; Teitzel *et al.*, 2006; González-Guerrero *et al.*, 2010), *Staphylococcus aureus* (Sitthisak *et al.*, 2005) and in *Ent. hirae* (Solioz *et al.*, 2010). However, the exact mechanisms by which copper can kill the overloaded cells are still unknown. Nevertheless, a common theme in discussions of copper toxicity is that copper is involved in Fenton reactions, releasing highly reactive hydroxyl radicals that cause damage to biomolecules such as proteins and DNA (Gunther *et al.*, 1995; Gaetke and Chow, 2003). In addition, binding of copper to non-specific sites in biomolecules may cause alterations to their structure and function through displacement of original metal ions (Osman and Cavet, 2008). Both these

reasons could contribute to the susceptibility of Δ*copA1* and Δ*copA2* to higher copper concentrations than the wild-type.

Contrary to Δ*copA1* and Δ*copA2*, the Δ*copA3* mutant accumulated only half the copper concentration of the wild-type. This could be attributed to partial impairment of copper trafficking of the cells. These results are in harmony with those of growth patterns at elevated copper conditions. Cells of Δ*copA3* were more resistant to higher levels of copper than the wild-type. Similar results were obtained by Fitch *et al.* (1993) who noticed that *Ms. trichosporium* mutants accumulated lower intracellular copper levels than the wild-type. They explained the mutant phenotype by the possibility of defects in copper uptake (Phelps *et al.*, 1992). Furthermore, Lewinson *et al.* (2009) reported a copper-importing P-type ATPase, HmtA (heavy metal transporter A), in *P. aeruginosa* Q9I147 and confirmed their claim by many *in vivo* assays including, intracellular metal measurements. These results supported the proposal that *Mc. capsulatus* CopA have roles in copper homeostasis.

To date, two specific copper-uptake systems have observed; one is Mb-mediated (Zahn and DiSpirito, 1996; DiSpirito *et al.*, 1998). Further details about Mb of *Mc. capsulatus* and *Ms. trichosporium* are discussed in Chapters 4 and 8 respectively. A second system is MopE/CorA (Berson and Lidstrom, 1996; Fjellbirkeland *et al.*, 1997; Helland *et al.*, 2008; Semrau *et al.*, 2010). MopE is an outer membrane protein in *Mc. capsulatus*, while CorA is a membrane polypeptide in *Methylomicrobium album* BG8. These two proteins exhibit amino acid sequence homology to each other and are negatively regulated by copper (Berson and Lidstrom, 1996; Fjellbirkeland *et al.*, 1997; Helland *et al.*, 2008; Karlsen *et al.*, 2011). In addition,

porins in the outer membrane of the cells seems to be a non-specific copper uptake route. Recently, isotopic and fluorescent labeling studies have shown that the uptake of unchelated copper in *Ms. trichosporium* is through a porin dependent passive transport process (Balasubramanian *et al.*, 2011). Possibly, the presence of multiple copper transport systems in *Mc. capsulatus* indicates that they might operate under different copper conditions.

Mutagenesis of a single *copA* gene encoding putative copper transporter in *Mc. capsulatus* does not result in constitutive sMMO expression; indicating that if one system is disrupted others may compensate. For example inactivation of *mopE* in *Mc. capsulatus* did not result in distinctive phenotype in terms of tolerance to high copper or sMMO expression from the wild-type (Ali, 2006). It has been proposed that MopE/CorA can substitute or complement Mb in copper-uptake (Karlsen *et al.*, 2011) based on the assumption that the copper affinity of Mb of *Mc. capsulatus* was lower (10^{-15} M) (Choi *et al.*, 2010) than that of MopE* 10^{-20} M (Helland *et al.*, 2008). Therefore, it is possible that MopE, Mb and/or CopA of *Mc. capsulatus* can substitute or complement each other in copper transport. This raises the need for generation of copper uptake- related multiple mutants in order fully to investigate copper uptake in this organism.

One could speculate that both CopA1 and CopA2 ATPases of *Mc. capsulatus* are copper-efflux pumps while CopA3 might function as a copper-importing protein. In order to support this assumption more experiments need to be done for example determination of the direction of transport of *Mc. capsulatus* CopA whether into or out of the cells using everted vesicles from *E. coli* expressing such proteins (González-Guerrero *et al.*, 2010).

The results described in this chapter suggest that *Mc. capsulatus* CopA1 and CopA2 and CopA3 are not involved in MMO regulation. However, *Mc. capsulatus* CopA might have a role in copper homeostatic events, reflecting the vital role of copper in physiology, metabolism as well as regulation of both soluble and particulate methane monooxygenases of this obligate methanotroph. Inactivation of a single *copA* gene does not result in mutants, which exhibit constitutive sMMO expression, raising the need for construction of multiple mutants in more than one copper transporter. If multiple mutants were constructed, a role of CopA proteins in getting copper to the copper-sensor of the copper switch might be resolved.

Chapter 4

Investigating potential methanobactin biosynthesis by targeted mutagenesis in *Mc. capsulatus* (Bath)

4.1 Introduction

In the early 1990s, initial evidence for a specific copper acquisition system was highlighted from studies on *Ms. trichosporium* (OB3b) (Phelps *et al.*, 1992; Fitch *et al.*, 1993). In these investigations, results from Arnold's group showed that cells under copper starvation conditions excreted small copper-binding complexes, later identified as methanobactin (Mb) (Zahn and DiSpirito, 1996; DiSpirito, *et al.*, 1998). Mb is a siderophore-like, copper-binding, short peptide that is synthesized and excreted by some methanotrophs including *Mc. capsulatus* (Bath). Mb is believed to be a multi-purpose molecule. It has a role in copper uptake (Zahn and DiSpirito, 1996; DiSpirito *et al.*, 1998) and in pMMO activity (Zahn and DiSpirito, 1996; Choi *et al.*, 2003 and 2005). Furthermore, Mb is likely to act in protecting the cells against oxygen radicals and detoxifying the reactive compounds hydrogen peroxide and superoxide, which are produced during oxidative metabolism (Choi *et al.*, 2003 and 2005).

However, the gene products involved in biosynthesis of Mb are still unknown. Possibly, Mb is non-ribosomally-produced via polyketide synthase and/or non-ribosomal peptide synthetase megaenzymes. This assumption is based on the resemblance in both structure and function between Mb and the siderophores (Ward, *et al.*, 2004, Balasubramanian and Rosenzweig, 2008). Siderophores are low-molecular mass, small non-ribosomally synthesized peptides secreted by many organisms to mediate iron-acquisition when iron is limited. They are synthesized by non-ribosomal peptide synthetases (NRPS) or polyketide synthetases (PKS) (Yun *et al.*, 2000). Moreover, Mb is called a chalkophore because chalko is Greek for copper; sidero is Greek for iron. From the genome of *Mc. capsulatus*, two putative genes encoding putative non-ribosomal peptide synthetases (NRPS-1 and NRPS-2 respectively) and

one for polyketide synthase (PKS) were identified. Therefore, the purpose of the work described in this chapter was to explore whether NRPS and PKS are involved in biosynthesis of Mb and to investigate whether Mb acted as an extracellular copper-sequestering agent. In order to achieve these aims, a targeted mutagenesis approach was initiated to generate three mutants; *Mc. capsulatus* ΔMCA1883, ΔMCA 2107 and ΔMCA1238, which we have been designated; Δ*nrpS-1*, Δ*nrpS-2* and Δ*pkS* respectively. These mutants were characterized and compared to the wild-type organism.

4.2 Features of NRPS-1, NRPS-2 and PKS of *Mc. capsulatus*

From the genome of *Mc. capsulatus*, two genes were putatively annotated as non-ribosomal peptide synthetase (NRPS-1 and NRPS-2 respectively) and one for polyketide synthase (PKS) (Ward *et al.*, 2004). The three *orf*s, which are dispersed in the genome of *Mc. capsulatus*, *nrpS-1*, *nrpS-2* and *pkS*, encode proteins of 1314 aa, 1456 aa and 2888 aa respectively (Table 4.1).

The genome map of *Mc. capsulatus* revealed that the putative Mb genes are located near to putative membrane transporter protein genes. Blast searches using the MCA1884 aa sequence showed a similarity to an ABC transporter ATP-binding proteins. MCA2110 encodes a putative outer membrane efflux protein and is located downstream of *nrpS-2* (Figure 4.1). *pkS* is located between a sensory box protein-encoding gene MCA1237, and heavy metal efflux protein MCA1239. In addition, the genome of *Mc. capsulatus* contains a gene encoding for a putative phosphopantetheinyl transferase.

Phosphopantetheinyl transferase is essential for activation of NRPS and PKS (Copp and Neilan, 2006). Collectively, the genome context of operons of the putative Mb genes suggested that they are likely to be active.

Table 4.1 Putative genes that might be involved in Mb

Gene	*nrpS-1*	*nrpS-2*	*pkS*
Gene number	MCA1883	MCA2107	MCA1238
Accession no.	YP114319	YP114534	YP113701
Size (bp/aa)	3945 /1314	4371 /1456	8667 /2888
Strand	+	+	-
Description	Non-ribosomal peptide synthetase	Non-ribosomal peptide synthetase	Polyketide synthase
Potential Function	Biosynthesis of Mb	Biosynthesis of Mb	Biosynthesis of Mb

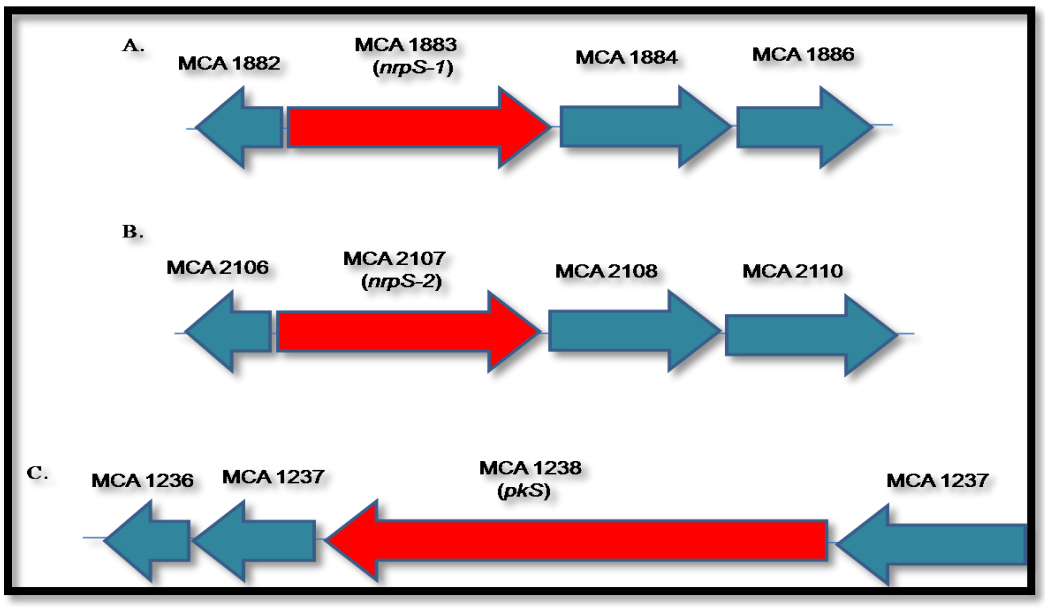

Figure 4.1 Genome map of the putative Mb genes *Mc. capsulatus*, A, *nrpS-1* (MCA1883); B, *nrpS*-2 (MCA2107) and C, *pkS* (MCA1238), highlighted with red arrows.

4.2.1 The domain organization of *Mc. capsulatus* NRPS and PKS

Taking advantage of the platform developed by Ansari *et al.* (2004) that includes well-characterized NRPS and PKS megaenzymes, the domain organization of *Mc. capsulatus* NRPS and PKS was predicted using NRPS-PKS web-based software, http://www.nii.res.in/nrps-pks.html (Ansari, *et al.*, 2004). NRPS-1 of *Mc. capsulatus* seemed to be monomodular, consisting of a single set of core domains (Figure 4.2a); 1- Adenylation (A) which identifies the substrate then adenylates it with ATP, 2- Thiolation (T) or a peptidyl carrier protein (PCP) domain which, forms a thioester linkage through which the adenylated substrate is linked to a 4'-phosphopantetheine (PP) cofactor and moves the substrate to a condensation domain, 3- condensation (C) domain, which links the two adjacent substrates via forming a peptide bond and 4- a thioesterase (TE) domain which terminates the peptide synthesis and liberates the peptide end product via internal cyclization or hydrolysis (Kohli *et al.*, 2001). NRPS-2 was found to be organized as n-terminal A-T c-terminal (Figure 4.2b) appear to be a somewhat a simpler monomodular NRPS.

The proposed domain arrangement of PKS is shown in Figure 4.3. From this figure, it is apparent that the PKS comprises a seven-domain structure. These are: (1) a ketoacyl synthase domain (KS) which accomplishes the decarboxylative condensation, (2) an acyltransferase domain (AT) which catalyses the transfer of the acyl unit to the acyl carrier protein, (3) an acyl carrier protein (ACP) which binds the acyl unit to KS, there are three ACP domains (4) a ketoreductase (KR) which reduces the ketone group during the chain growth and (5) a dehydratase (DH) which catalyses modification of the acyl unit after condensation by removal of water. However, no thioesterase domain (TE)

is detectable in the PKS of *Mc. capsulatus*, suggesting that the final product is likely to be released by the activity of another enzyme. It has been reported that the number of acyl units in the final PKS product often corresponds to the number of modules in the bacterial PKS (Staunton and Weissman, 2001). These bioinformatic predictions suggested that NRPS-1, NRPS-2 and PKS might be active.

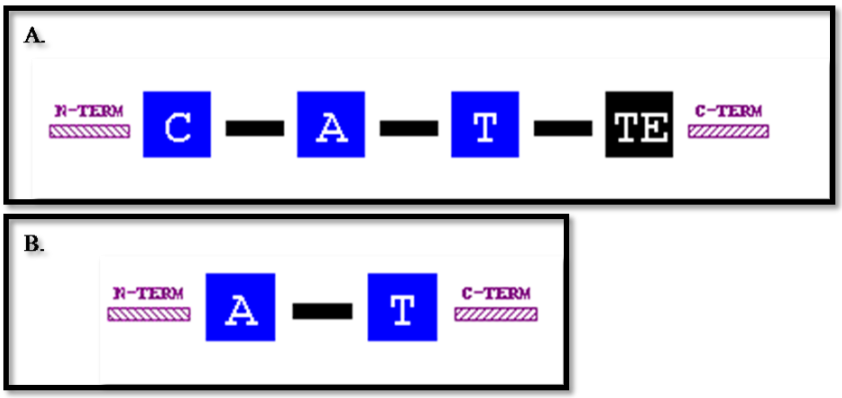

Figure 4.2 The domain organization of *Mc. capsulatus* non-ribosomal peptide synthetase A. NRPS-1 and B. NRPS-2, based on comparisons with well-characterized NRPS (Ansari *et al.*, 2004). (A), adenylation domain; (C), condensation domain; (T), thiolation and (TE), thioesterase domain.

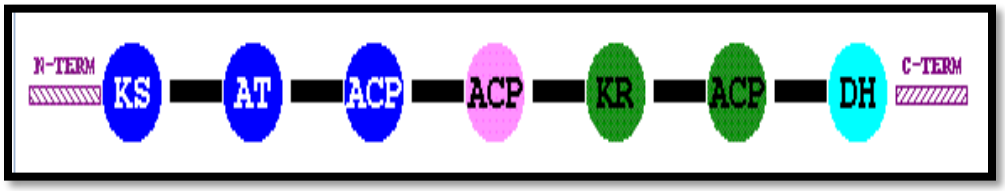

Figure 4.3 The domain organization of polyketide synthetase based on comparisons with other known PKSs (Ansari *et al.* 2004). (KS), β-ketoacyl synthase; (AT), acyltransferase; (ACP), phosphopantethienylated acyl carrier protein; (KR) ketoreductase; (DH), dehydratase.

4.2.2 Substrate specificity of the adenylation domain prediction *Mc. capsulatus* NRPS and PKS.

The substrate specificity-conferring amino acid in the adenylation domains was also determined by using both NRPS-PKS software and the NRPS predictor2 bioinformatics toolbox from University of Tübingen http://nrps.informatik.uni-tuebingen.de/ (Röttig *et al.*, 2011). The adenylation domain of NRPS-1 and NRPS-2 is probably recognizes lysine and pipecolic acid, respectively. Analysis of the residues in the AT domain of PKS indicated the substrate of *Mc. capsulatus* PKS is likely to be malonate. These bioinformatic predictions provide an indication about the building blocks of the compound that NRPS-1, NRPS-2 and PKS might produce.

4.3 Inactivation of the *nrpS-2* and *pkS* genes

To determine the function of the *nrpS-2* and *pkS*, insertional inactivation mutagenesis was performed. To interrupt these genes the chromosome of *Mc. capsulatus*, *nrpS-2* and *pkS* DNA fragment were amplified and cloned to the pK18mob via *Hin*dIII and *Pst*I and *Sma*I and *Hin*dIII restriction sites respectively, to give the constructs pAK033 and pAK01 (Figure 4.4 and Figure 4.7, respectively). The gentamicin resistance cassette (Gm^R) was cloned via *Bam*HI site into the middle of the *pkS* fragment in pAK01 to give the final construct, pAK011, which was then electroporated into *E. coli* S17.1 λpir strain (Herrero *et al.*, 1990). No gentamicin resistance cassette was inserted into *nrpS-2* in the pAK033 construct. Transconjugants were selected by plating onto NMS medium containing kanamycin (15 μg ml^{-1}) for *nrpS-2* and gentamicin (5 μg ml^{-1}) for *pkS*. Transconjugants were screened by PCR and

sequencing to verify disruption of the *nrpS-2* and *pkS* gene. Insertion of the gentamicin cassette into the *pkS* gene and the presence of the kanamycin cassette were verified using primer pairs specific to each antibiotic cassette (data not shown). The mutants were verified by PCR using combinations of primers specific to the antibiotic cassettes and to the regions of the *nrpS-2* and *pkS* fragments flanking the insertion sites, followed by sequencing of the correct size PCR product. A PCR product was obtained using the forward primer specific of the kanamycin cassette (KANF530) and the reverse primer specific to about 500-bp downstream of *nrpS-2* (500DS_NRPS-2R3770) (Figure 4.6). As expected no PCR product was obtained using DNA from the wild-type because there was no kanamycin-resistance cassette (lane 2, Figure 4.6). Similarly, as shown in lane 3 in Figure (4.8), the right size PCR product (1,805 bp) was obtained using the forward primer specific to 500 bp upstream of the *pkS* (US_PKS_F153) and the reverse primer specific to the gentamicin-resistance cassette (GENR851). Further confirmation was carried out by sequencing the PCR products obtained. The primers used to confirm the genotype of the mutants are listed in Table 4.2. Several attempts were made to obtain PCR product using the primers upstream and downstream of the target DNA of *nrpS-2* and *pkS* from the mutants. However, no product was obtained (lane 3 Figure 4.5 and Figure 4.9) and this might be due to the large sizes of the amplicon (about 6 - 7 kbp). Mutants were designated as *Mc. capsulatus* ΔMCA 2107 (Δ*nrpS-2*), *Mc. capsulatus* ΔMCA1238 (Δ*pkS*). *Mc. capsulatus* ΔMCA MCA1883 (Δ*nrpS-1*) was generated previously by Ali (2006).

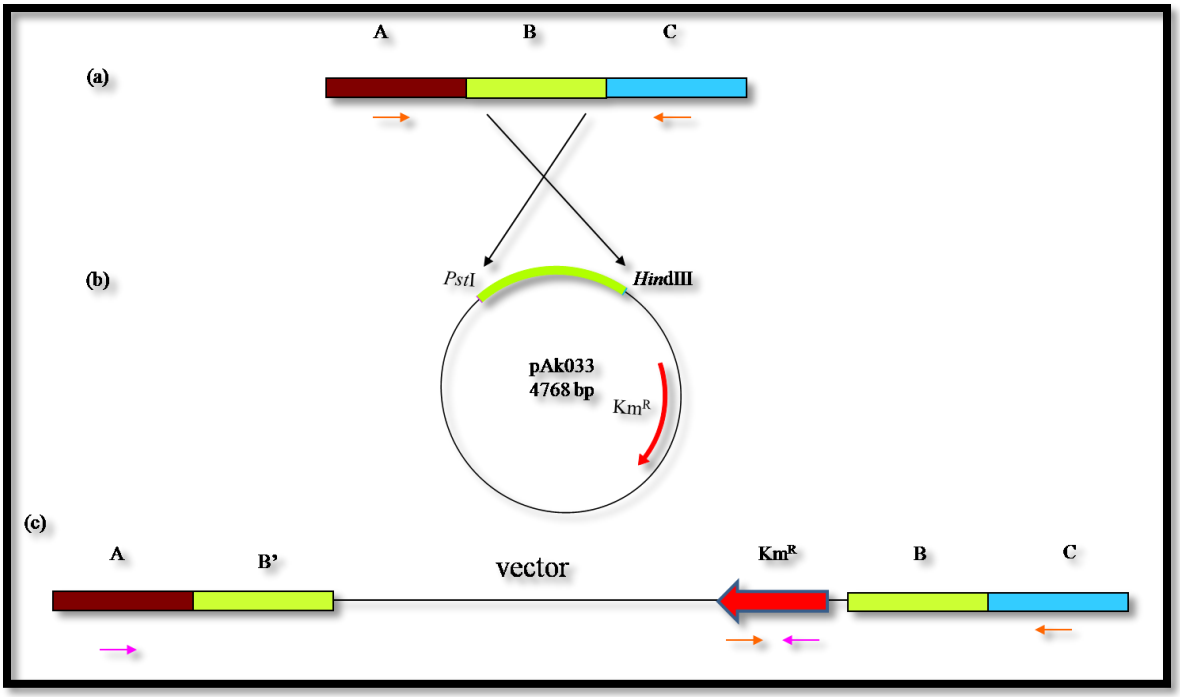

Figure 4.4 Schematic representation of the strategy for constructing *Mc. capsulatus* Δ*nrpS-2*, (a) the wild-type gene (*nrpS-2*) and the target region was highlighted in green. (b) The suicide plasmid construct pAK033 and pMHA501 used to inactivate *nrpS-2*. Restriction sites *Hin*dIII and *Pst*I were introduced by PCR to facilitate cloning. (c) The genotype of the *Mc. capsulatus* Δ*nrpS-2*. Primers used to confirm the genotype of the mutant are indicated by small red arrows.

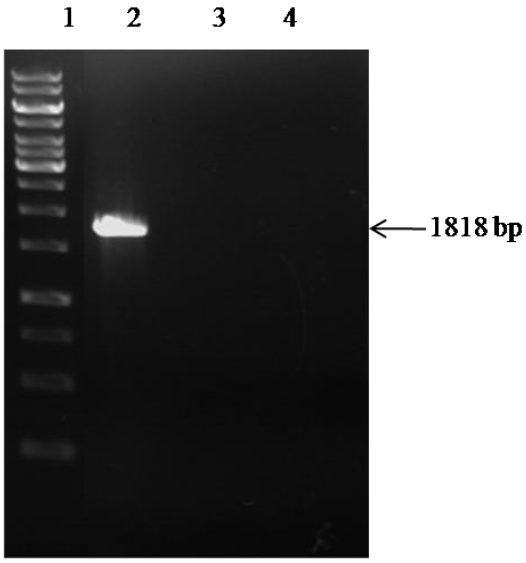

Figure 4.5 Confirmation of *Mc. capsulatus* Δ*nrpS-2* genotype, by PCR using primers upstream and downstream the target DNA region. Lane 1, a 1 kb DNA ladder marker (Invitrogen); lane 2 genomic DNA extracted from wild-type of *Mc. capsulatus*; lane 3 *Mc. capsulatus* Δ*nrpS-2* and lane 4, negative control. The expected size of the product is 1,818 bp.

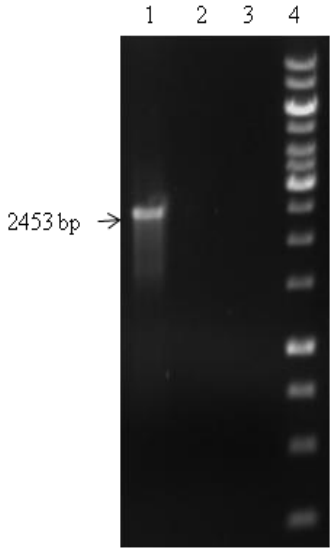

Figure 4.6 Confirmation of *Mc. capsulatus* Δ*nrpS-2* genotype, by PCR using the primers KANF530 and DS_NRPS-2R3770. Lane 1, *Mc. capsulatus* Δ*nrpS-2*; lane 2, genomic DNA extracted from wild-type of *Mc.capsulatus*; lane 3, negative control and lane 4, a 1 kb DNA ladder marker (Invitrogen). The expected size of the product is 2,453 bp.

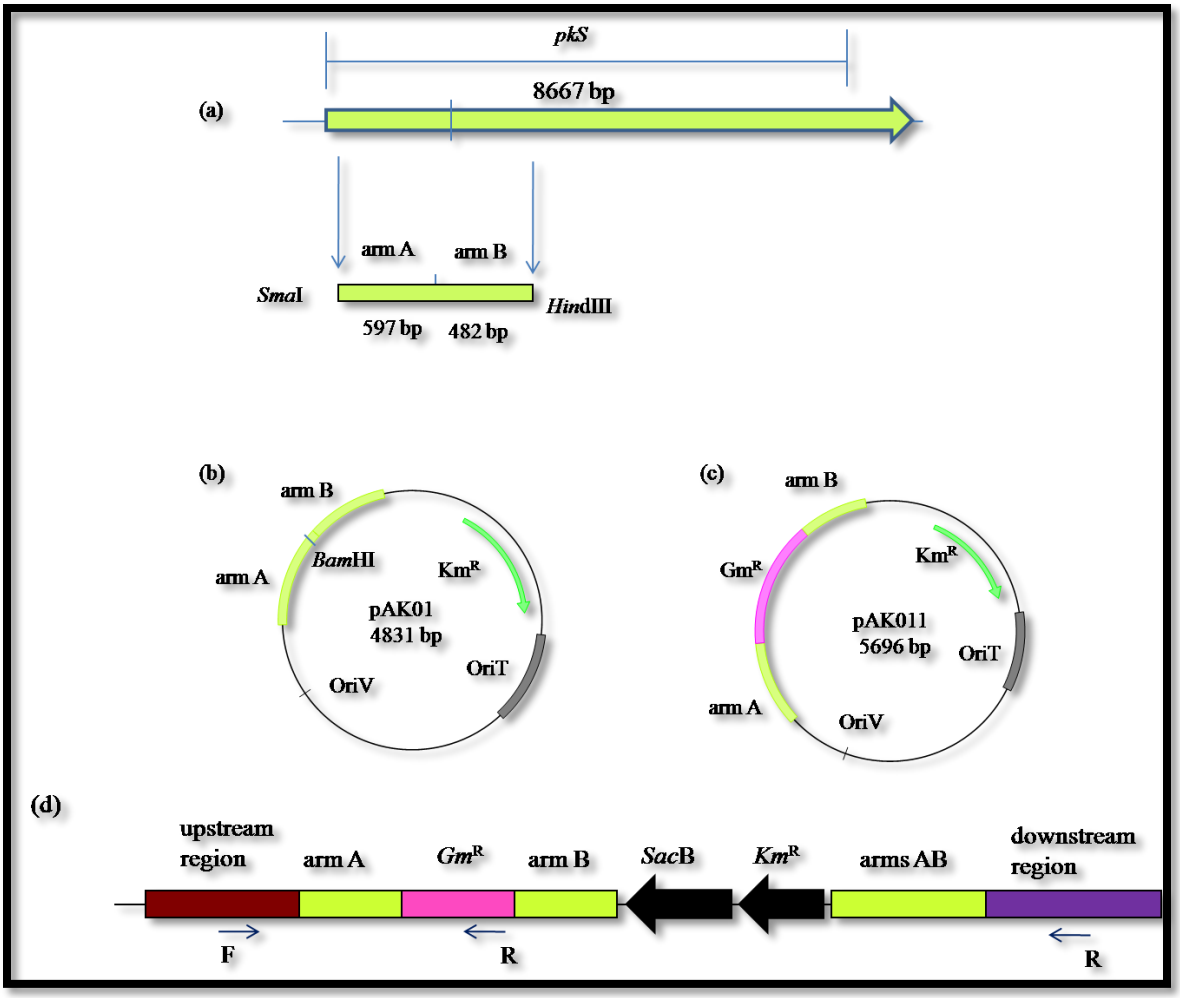

Figure 4.7 Schematic representation of the strategy for constructing *Mc. capsulatus* Δ*pkS* (a) the wild-type gene (*pkS*), the target region was highlighted in green. (b) The intermediate plasmid construct pAK01 with *pkS* fragment, restriction sites *Sma*I and *Hin*dIII were introduced by PCR to facilitate cloning (c) The suicide plasmid construct pAk011 used to inactivate *pkS*. (d) *Mc. capsulatus* Δ*pkS* following single homologous recombination of pK18*mobsacB*. The primers used to check the genotype of the mutants are indicated by black arrows.

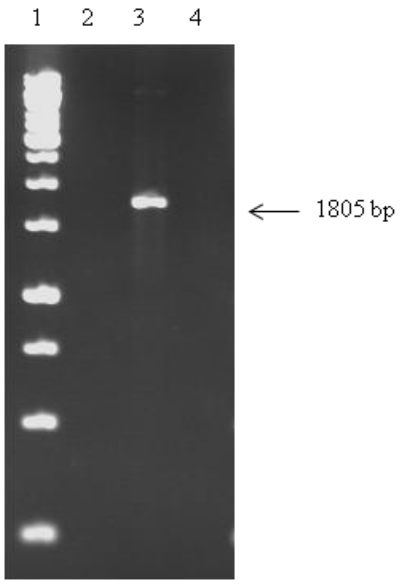

Figure 4.8 Confirmation of *Mc. capsulatus* Δ*pkS* genotype, by PCR using primers US_PKS_F153 and GENR851. Lane 1, a 1 kb DNA ladder marker (Invitrogen); lanes 2, genomic DNA extracted from wild-type of *Mc.capsulatus*; lanes 3, *Mc. capsulatus* Δ*pkS* and lane 4, negative control. The expected size of the product is 1,805 bp.

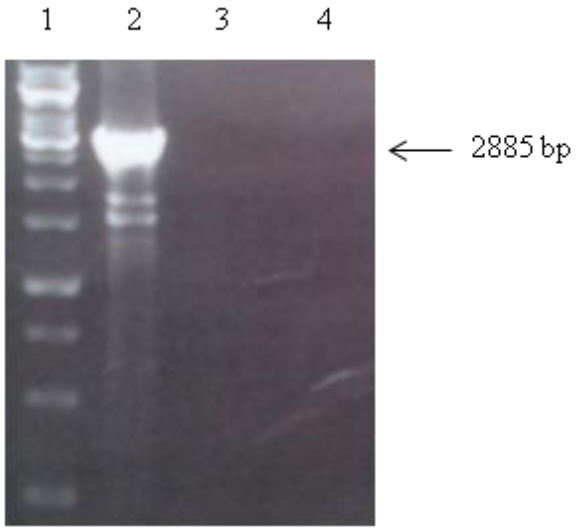

Figure 4.9 Confirmation of *Mc. capsulatus* Δ*pkS* genotype, by PCR using primers upstream and downstream the target DNA region. Lane 1, a 1 kb DNA ladder marker (Invitrogen); lane 2, genomic DNA extracted from wild-type of *Mc.capsulatus*; lane 3, *Mc. capsulatus* Δ*pkS* and lane 4, negative control. The expected size of the product is 2,885 bp.

Table 4.2 Primers used to amplify section of *nrpS-2* and *pkS* to construct the mutants and confirm the genotype of the *Mc. capsulatus* Δ*nrpS-2* and *Mc. capsulatus* Δ*pkS*. Restriction sites were introduced via the primers to facilitate cloning (restriction sites are highlighted in bold and underlined).

Primer	Sequence
NRPS-2F 2346-*Hin*d III	5-**AAGCTT**CGTATCCCGCATTACGACTT-3'
NRPS-2R1557- *Pst*I	5-**CTGCAG**AGCCATGGTGCCGTATAAAG-3'
US_NRPS-2_F1952	5'-GAGATCCCGATTACCAAGCA -3'
DS_NRPS-2R3770	5'-GAGCAGGCTGAAAACCAGAC-3'
KANF530	5'-GCCCTGAATGAACTCCAAGA -3'
KANR1017	5'-AGCCAACGCTATGTCCTGAT-3'
PKSF491- *Sma*I	5' -**CCCGGG**AGAGCGGTTCCAAGGAGTTC-3'
PKSR1557- *Hin*dIII	5 -**AAGCTT**GAAACCATGGCAACTCACAC-3'
US_PKS_F153	5' -ATTTGCCGCCGGGCAGTAAC-3'
DS_PKS_R1894	5' -AGAGCATGGTGCCGATCTCC-3'
GENF37	5' -GACATAAGCCTGTTCGGTTC-3'
GENR851	5' -GCGGCGTTGTGACAATTTAC-3'

4.4 Characterization of the methanobactin (Mb) mutants of *Mc. capsulatus*

4.4.1 Mb production assay

The aim of this experiment is to see if there are any differences between *Mc. capsulatus* wild-type and Δ*nrpS-1*, Δ*nrpS-2* and Δ*pkS* strains in terms of Mb production. A method described recently by Yoon *et al.*, 2010 for screening microbial production of chalkophore was used. According to this method, a colorimetric plate assay was used in which copper weakly binds to chrome azurol S (CAS) to form a blue complex (Cu-CAS) and Mb production was monitored when the colour changed from blue to yellow as the Mb sequestered copper from the Cu-CAS complex.

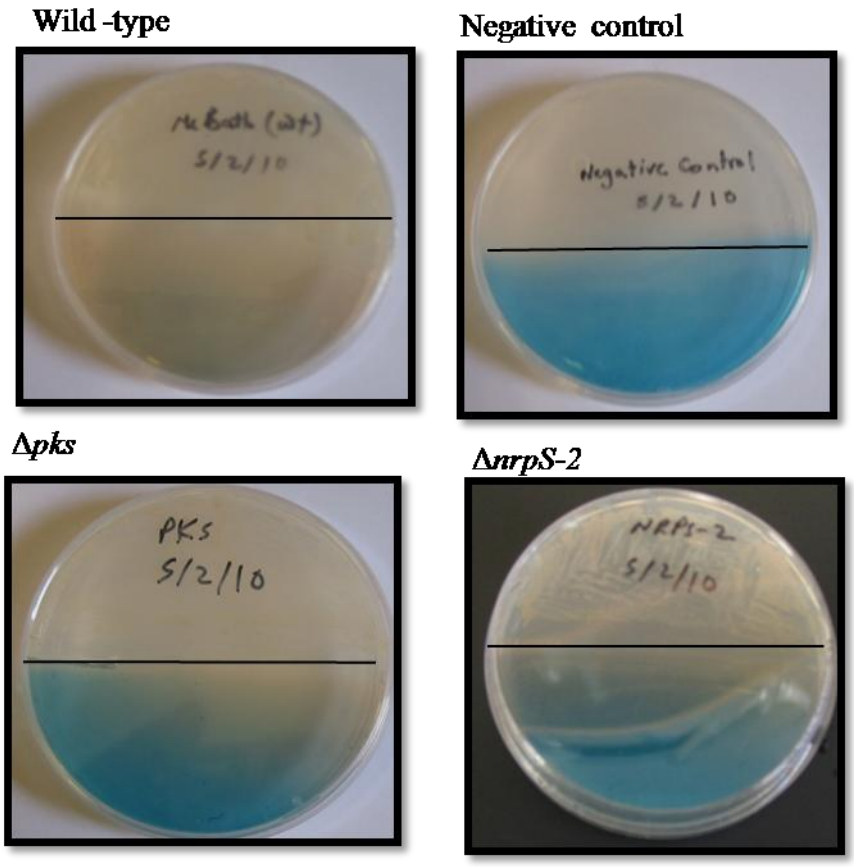

Figure 4.10 Mb assay using colorimetric plate assay in split NMS/Cu-CAS Plates.

As can be seen in Figure (4.10), *Mc. capsulatus* wild-type and Δ*pkS*, Δ*nrpS-1* and Δ*nrpS-2* strains showed growth on NMS agar with 1 µM copper close to 50 µM Cu-CAS agar. However, Δ*pkS* and Δ*nrpS-2*, showed no substantial shift in the coloration of the Cu-CAS agar within 10 days (Figure 4.10), while wild-type and Δ*nrpS-1* exhibited a complete colour shift from blue to yellow (data not shown). This indicated that Mb was produced and sequestered copper from the Cu-CAS plates. The negative control with no cells showed, as expected, no change in the blue colour. These results indicated that PKS and NRPS-2 but not NRPS-1 might be involved in production of Mb.

4.4.2 Naphthalene assay for sMMO activity

sMMO activity was determined using the naphthalene oxidation assay following the method of Brusseau *et al.* (1990). To determine the effects of different copper concentrations on the expression of sMMO, cells of *Mc. capsulatus* wild-type, Δ *nrpS-1*, Δ *nrpS-2* and Δ*pkS* were grown on NMS plates supplemented with either 0, 0.5, 1.0, 1.5, 2.0, 2.5, 3.0, 3.5, 4.0 or 5.0 µM copper (as copper sulfate), see Materials and Methods (section 2.12.1). None of the strains expressed sMMO under high copper concentration (4 µM added copper) growth conditions, as shown by the lack of colour

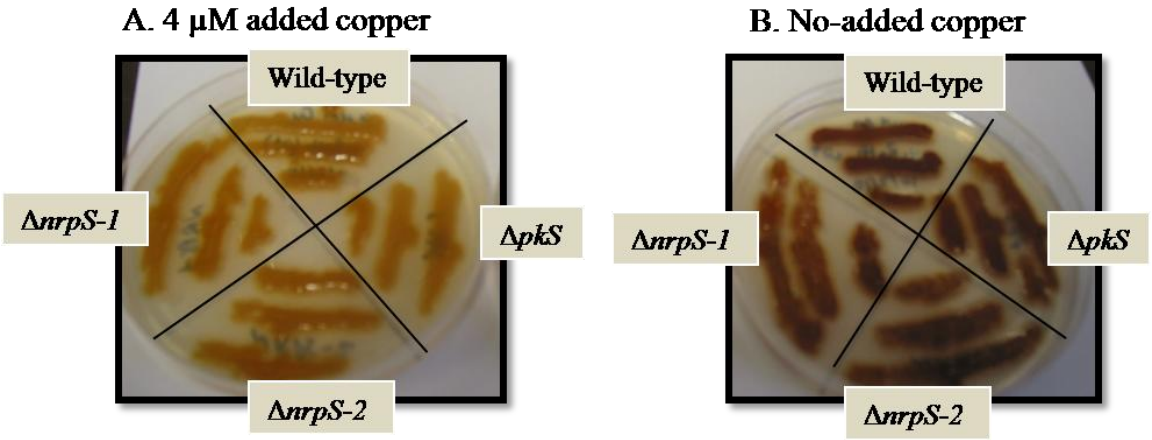

Figure 4.11 Naphthalene assay results A. under high copper concentration (4 µM added copper), B. under no added copper concentration. These experiments were performed in triplicate.

change in the zinc reagent (yellow) (Figure 4.11A). On the other hand under no-added copper growth conditions all strains gave purple colour upon addition of zinc complex, indicating that they expressed sMMO enzyme, which oxidized naphthalene to naphthol (Figure 4.11B). These observations highlighted that there was no difference between the wild-type and the mutant strains in terms of sMMO activity using the naphthalene assay.

These results suggested that the genes that encode for NRPS-1, NRPS-2 and PKS might be not involved in MMO regulation under these conditions.

4.4.3 Effect of decreasing strength of salt solution (solution I) of NMS on growth pattern of Δ*nrpS-1* compared to *Mc. capsulatus* wild-type

The purpose of this experiment was to monitor the growth behaviour of Δ*nrpS-1* mutant at different concentrations of the salt solution (solution I) of NMS medium compared to the *Mc. capsulatus* wild-type This solution is composed of KNO_3 10 g, $MgSO_4.7H_2O$ 10 g and $CaCl_2.2H_2O$ 2 g dissolved in 800 ml Milli-Q water and diluted to 1 litre to give a 10 x stock. For 1 X NMS, 100 ml from this solution is diluted to a litre. The reason for diluting only the salt solution of NMS is to minimize the copper contamination by salts, assuming the major source of the background copper is from solution I. The results obtained in Figure 4.12 showed that the wild-type grew well in all NMS formulations with specific growth rate ranging between 0.02 – 0.035 h^{-1} whereas Δ*nrpS-1* mutant grew only at 1 x solution I of NMS with and without copper with specific growth rate 0.004 and 0.024 h^{-1} respectively (Figure 4.12 A and 4.12 B). The growth rate of the Δ*nrpS-1* was slower than that of wild-type (Table 4.3). The Δ*nrpS-1* mutant could not grow in 0.1 x solution I of NMS, whereas the wild-type grew rather well (Figure 4.12C). Using 0.1 x solution I of NMS as a basal medium, copper was added as a filter-sterilized $CuSO_4.5H_2O$ solution. Adding 120 nM copper was found to be sufficient to restore the growth of Δ*nrpS-1* to a comparable rate (0.01 h^{-1}) to the wild-type (0.02 h^{-1}) (Figure 4.12 D and Table 4.3). It is worth mentioning that Δ*nrpS-2* and Δ*pkS* could not grow on 0.1x NMS but did grow when copper was added to the medium.

However, due to time limitations, these observations were not followed up. These observations speculated that NRPS-1, NRPS-2 and PKS might be involved in copper acquisition.

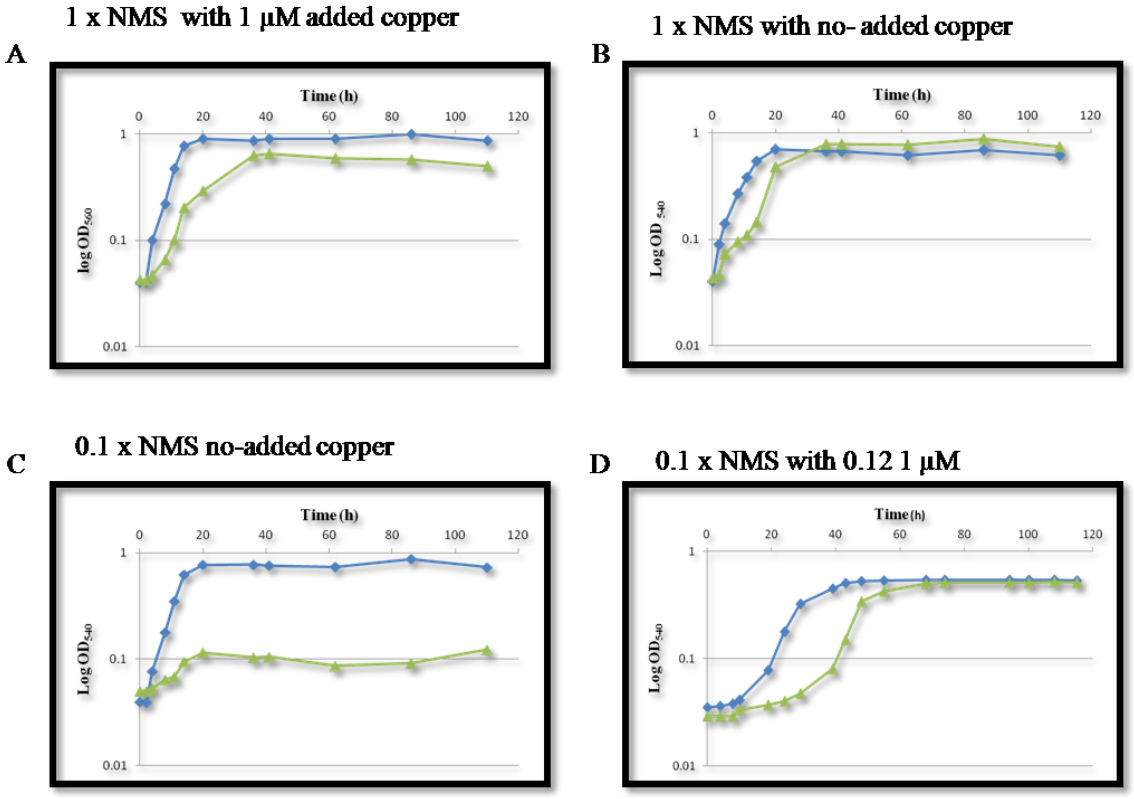

Figure 4.12 Growth of *Mc. capsulatus* wild-type and Δ*nrpS-1* mutant strain on A, 1x solution I of NMS with 1 µM copper; B, 1x solution I of NMS with no added copper; C, 0.1x solution I of NMS with no added copper and D, 0.1x solution I of NMS with 0.12 µM added copper. *Mc. capsulatus* wild-type represented by blue diamonds; Δ*nrpS-1* mutant strain represented by green triangles. These experiments done without replicates.

Table 4.3 Specific growth rates of Δ*nrpS-1*strain growing in flasks containing NMS with different copper concentrations compared to the wild-type

	Specific growth rate (h^{-1})			
Strength of solution I and copper concentration (µM)	**1x 1**	**1x 0**	**0.1x 0**	**0.1x 0.12**
Wild-type	0.03	0.035	0.05	0.02
Δ*nrpS-1*	0.004	0.024	0.0001	0.01

4.4.4 Growth under different silver concentration

The three putative Mb mutant strains and the wild-type were tested for their ability to grow on NMS plates supplemented with different concentrations of silver (1-7 µM), silver. The parental strain and putative Mb mutants showed growth at silver concentration up to 4 µM and none of them could grow at 5 µM silver (Figure 4.13). Furthermore, the growth of parental strain and the putative Mb mutants decreased, as the concentration of the added silver increased. No obvious phenotypic differences between the strains were observed at related silver concentration.

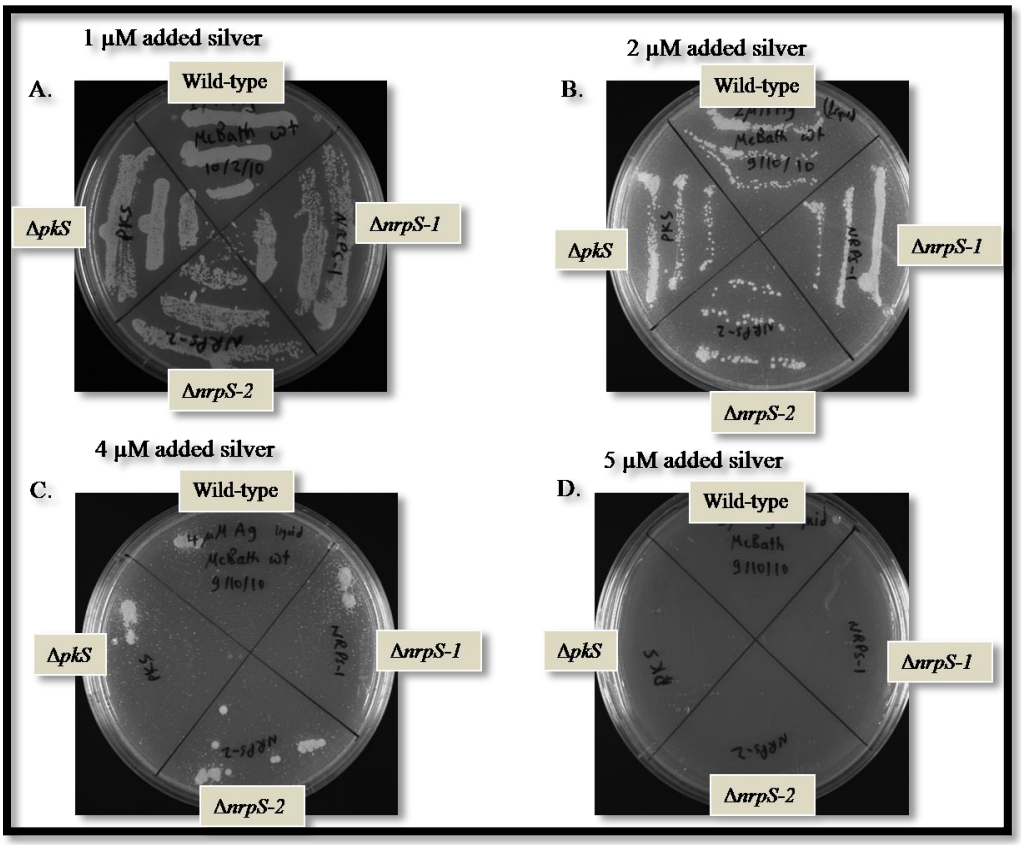

Figure 4.13 Growth of *Mc. capsulatus* wild-type and *copA* mutant strains on NMS with A, 1 µM; B, 2 µM; C, 4 µM and 5 µM added silver (as silver nitrate). These experiments were performed in triplicate.

4.4.5 Intracellular copper measurements

The intracellular copper concentration of late-exponential-phase cultures of wild-type and Δ*nrpS-1*, Δ*nrpS-2* and Δ*pkS* mutant strains grown in NMS with no-added copper was determined. (Figure 4.14). Copper content was expressed as (ng Cu (mg dw)$^{-1}$). The intracellular copper concentration of Δ*nrpS-1*, Δ*nrpS-2* and Δ*pkS* were significantly higher than that of the wild-type (Figure 4.14) ($P < 0.001$). However, the Δ*pkS* mutant accumulated about three-fold more (8.2 ng Cu (mg dw)$^{-1}$) than the wild-type (2.4 ng Cu (mg dw)$^{-1}$). The intracellular copper of Δ*nrpS-1* and *nrpS-2* was three- and two-times excess ($P < 0.001$) than that of the wild-type.

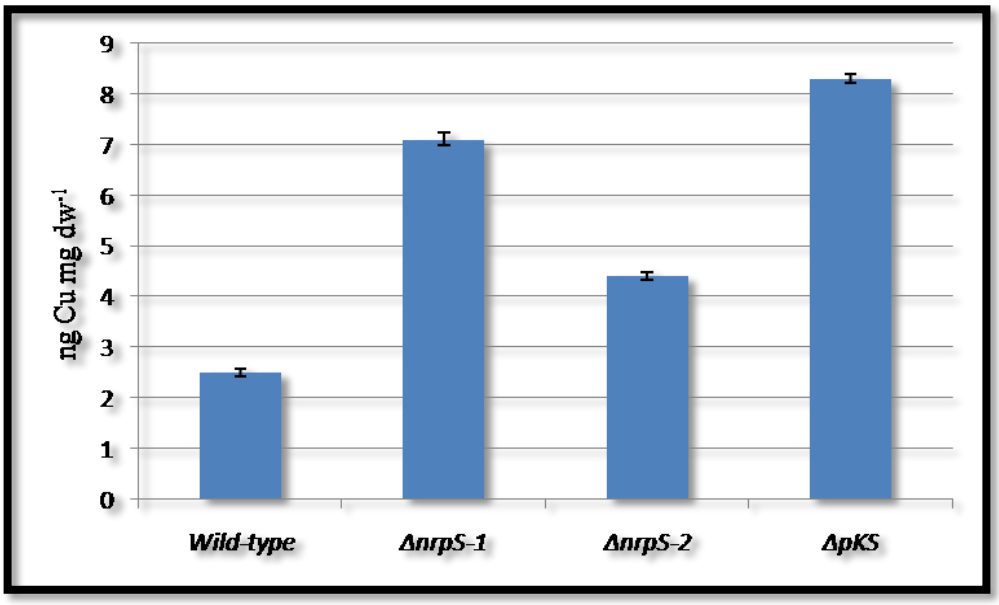

Figure 4.14 Intracellular copper measurements of the three putative Mb mutant strains *Mc. capsulatus* Δ*nrpS-1*, Δ*nrpS-2* and Δ*pkS* with *Mc. capsulatus* wild-type, all in NMS with no- added copper. Error bars indicate the standard deviation of three replicate measurements.

The data indicate that disruption of *nrpS-1*, *nrpS-2* and *pkS* altered the intracellular copper quota of the mutants highlighting the involvement of the product of these genes in copper transport in *Mc. capsulatus*. Intracellular copper concentration in late-

exponential-phase cultures of *Mc. capsulatus* Δ*nrpS-2* and *Mc. capsulatus* wild-type NMS with grown NMS with 30 µM added copper was analyzed (Figure 4.15). Δ*nrpS-2* accumulated significantly higher copper (0.4 µg Cu (mg dw)$^{-1}$) ($P < 0.001$) than the wild-type (~0.1 µg Cu (mg dw)$^{-1}$) (Figure 4.15). These results indicated that *nrpS-2* is involved in copper transport. However, the other mutants were not been analyzed at 30 µM copper due to lack of time.

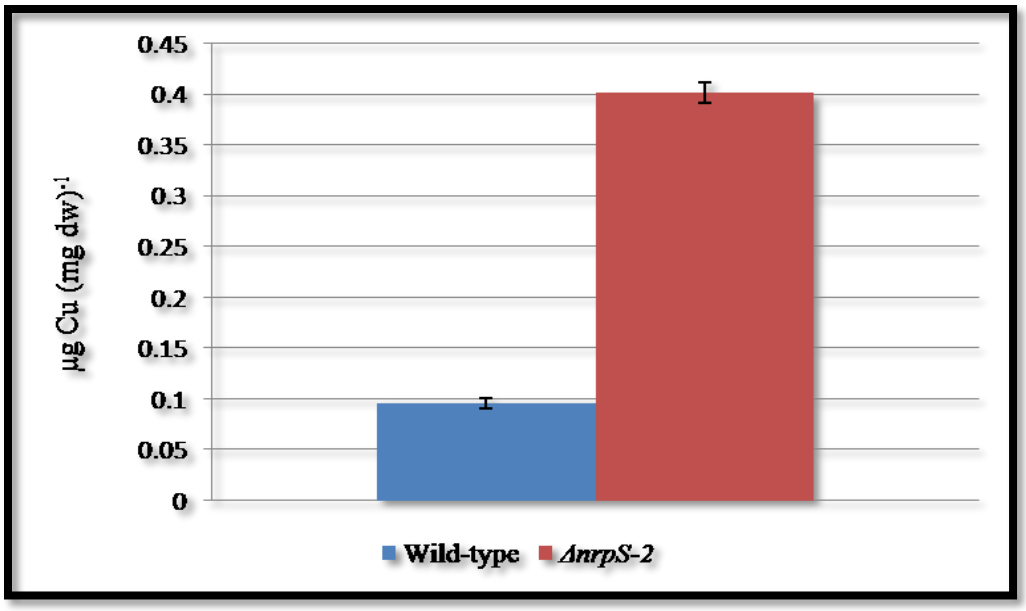

Figure 4.15 Intracellular copper measurements of *Mc. capsulatus* Δ*nrpS-2* and *Mc. capsulatus* wild-type NMS, grown in NMS with 30 µM added copper. Error bars indicate the standard deviation of three replicate measurements

4.4.6 Liquid chromatography–mass spectrometry (LC-MS)

To identify the compound (s) synthesized by the NRPS and/or PKS, comparative metabolite profiling of the wild-type and mutant strains was carried out using liquid chromatography–mass spectrometry (LC-MS). Initial analysis of supernatants of the putative Mb mutants and the wild-type grown on NMS with no-added copper revealed

that there was a metabolite (metabolite X) in the supernatant of the wild-type, which was absent in the supernatants of all the mutants strains (Figure 4.16). This peak corresponding to the metabolite X appeared at a retention time of 19 min and mass-to-charge ratio (m/z) = 212.4 (Figure 4.16). These results indicate that NRPS-1 and NRPS-2 and PKS are probably involved in the production of the metabolite X.

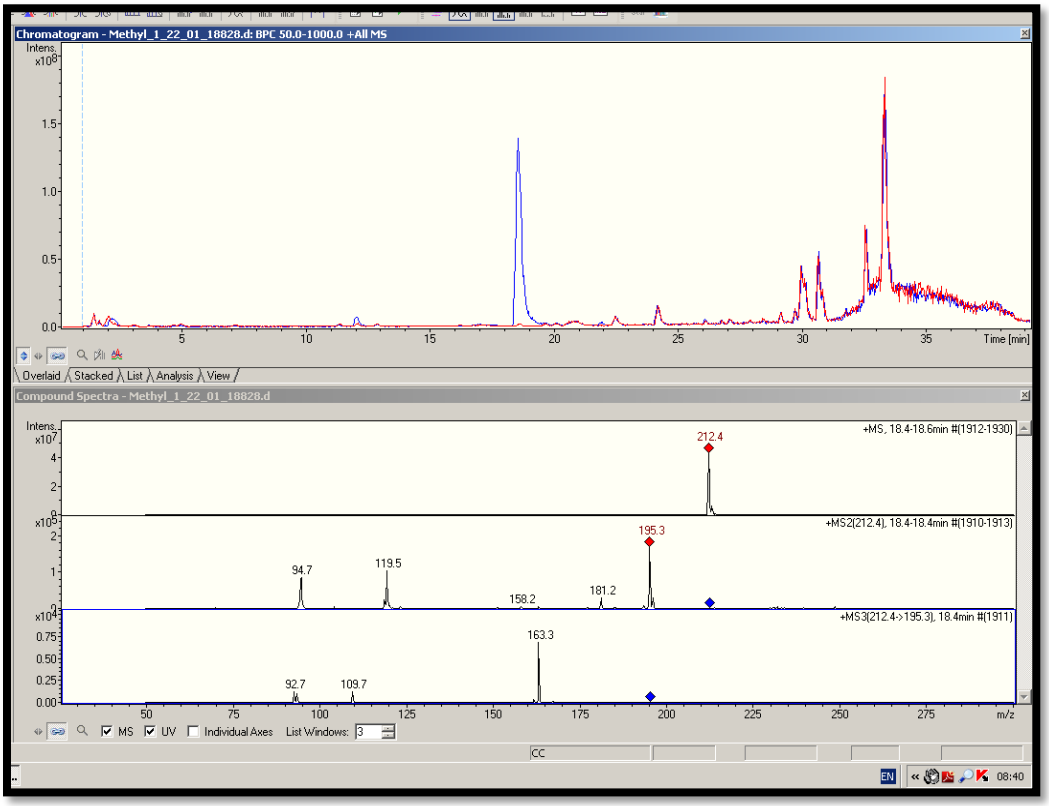

Figure 4.16 LC-MS analysis of supernatants of *Mc. capsulatus* wild-type (blue) and Δ*nrpS-1*, Δ*nrpS-2* and Δ*pkS* (red, orange and brown, respectively). Extracted ion chromatograms (EICs) at *m/z* = 212.4 (top of the graph) and measured mass spectrum of the compound with retention time of ~19 minutes (bottom of the graph).

Furthermore, LC-MS data showed that there was another metabolite (metabolite Y) with a retention time of 2.2 min and m/z 293 (Figure 4.17 – Figure 2.19). That compound was observed in the supernatants of putative Mb mutant strains as well as the wild-type but with varying level from sample to another. The concentration of the metabolite Y was

higher in the wild-type than that of the mutants, as indicated by peak heights. The lowest concentration of metabolite Y compared to that of the wild-type was observed in the supernatant of Δ*nrpS-2* (Figure 4.18). Δ*pkS* and Δ*nrpS-1* seemed to produce comparable quantities of compound Y but both still lower than that of the wild-type (Figure 4.17 and 4.19 respectively). The concentration of the metabolite Y was higher in both Δ*pkS* and Δ*nrpS-1* than that of the Δ*nrpS-2* mutant strain. These results highlighted that NRPS-1, NRPS-2 and PKS of *Mc. capsulatus* are probably either involved in controlling the quantity produced of the metabolite Y or integrated in its production.

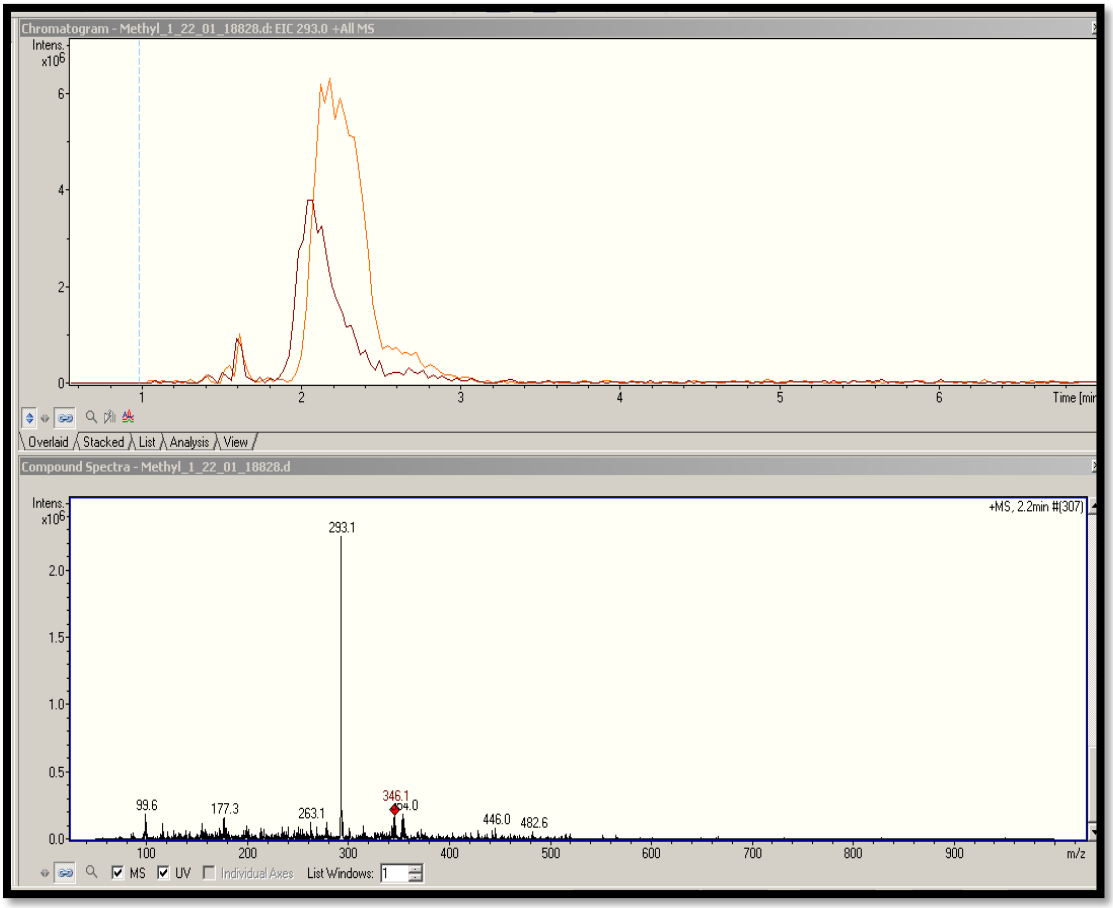

Figure 4.17 LC-MS analysis of supernatants of *Mc. capsulatus* wild-type (orange) and Δ*nrpS-1* (brown). Extracted ion chromatograms (EICs) at *m/z* = 212.4 (top part of the graph) and measured mass spectrum of the compound with retention time of ~ 2 minutes (bottom part of the graph).

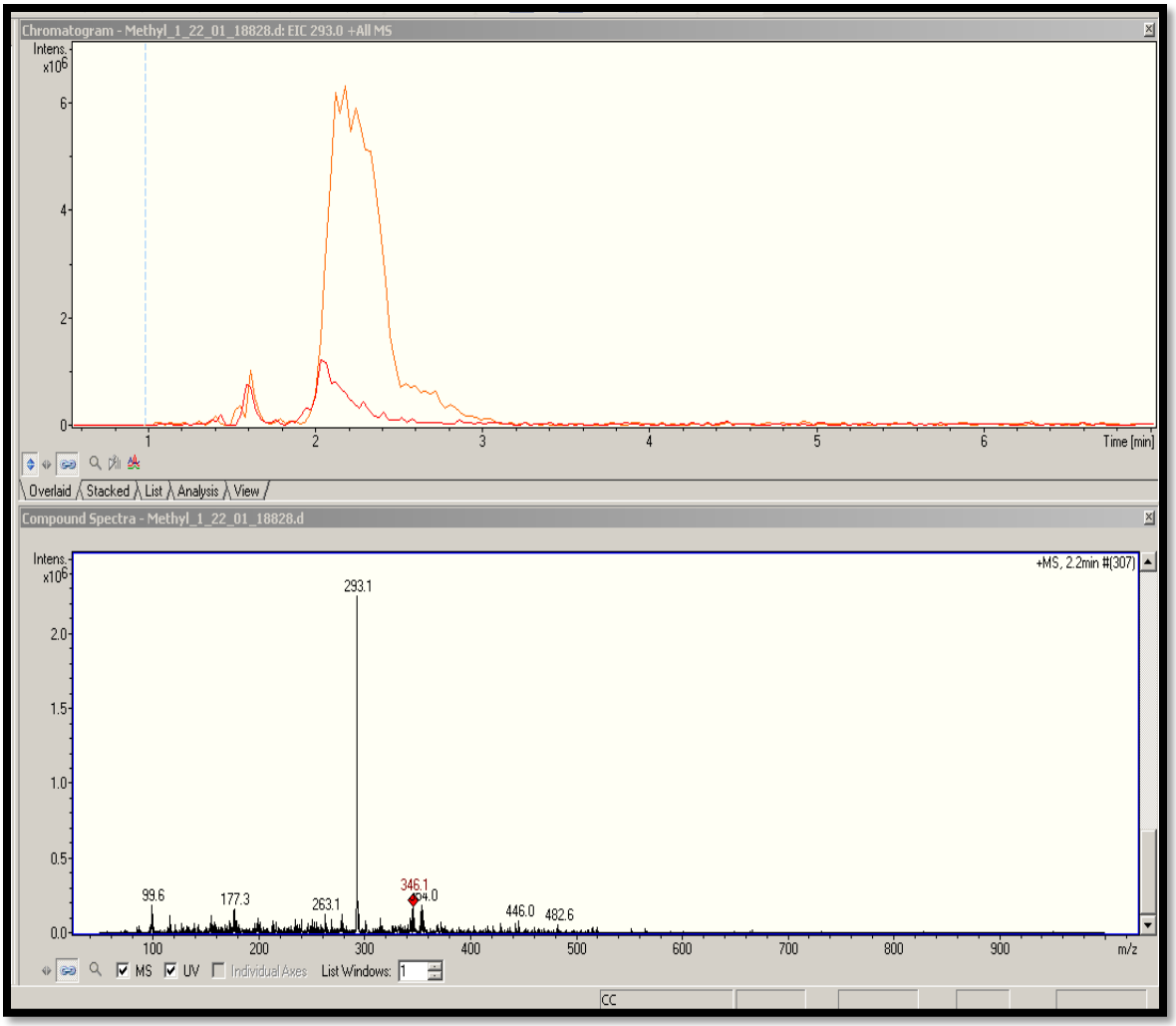

Figure 4.18 LC-MS analysis of supernatants of *Mc. capsulatus* wild-type (orange) and Δ*nrpS-2* (red). Extracted ion chromatograms (EICs) at *m/z* = 212.4 (top part of the graph) and measured mass spectrum of the compound with retention time of ~ 2 minutes (bottom part of the graph).

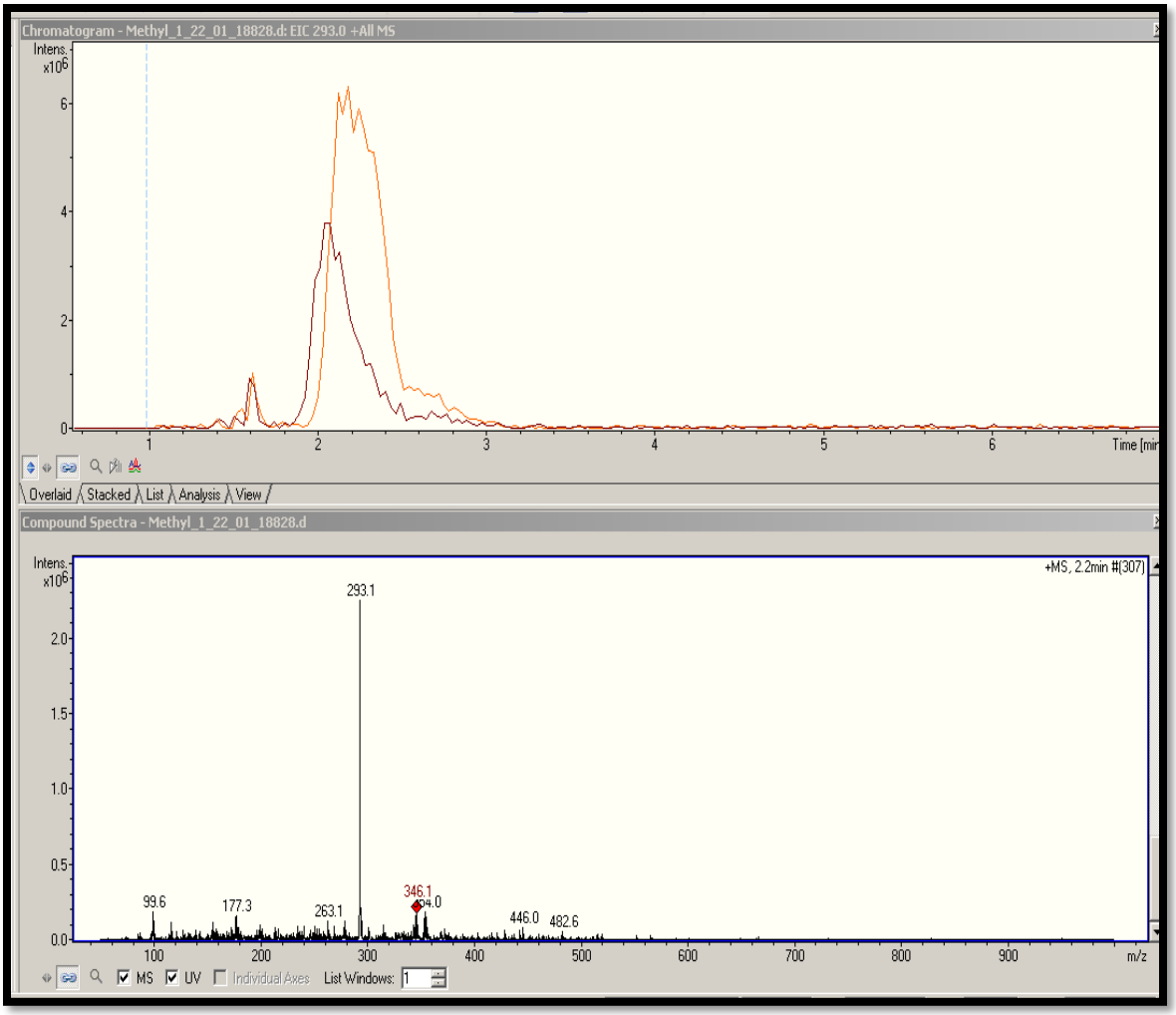

Figure 4.19 LC-MS analysis of supernatants of *Mc. capsulatus* wild-type (orange) and Δ*pkS* (brown). Extracted ion chromatograms (EICs) at *m/z* = 212.4 (top part of the graph and measured mass spectrum of the compound with retention time of ~ 2 minutes (bottom part of the graph).

4.5 Discussion

The genome of *Mc. capsulatus* contains two putative genes encoding for non-ribosomal peptide synthetase (NRPS-1 and NRPS-2 respectively) and one for polyketide synthase (PKS). Bioinformatic analyses of these proteins, when compared to the well-characterized NRPS and PKS, indicated that they have the main domains of

NRPS and PKS. Therefore, they are likely to be active ribosomal peptide synthetase and polyketide synthase respectively.

Disruption of the genes encoding for NRPS-1, NRPS-2 and PKS indicates that the genes may be involved in copper transport but not in MMO regulation. Two genes (*nrpS-2* and *pkS*) are probably involved in Mb production.

The resulting *Mc. capsulatus* Δ*nrpS-1* mutant was found to produce Mb based on the method described recently by Yoon *et al.* (2010) for screening microbial production of chalkophore. In this colorimetric plate assay, copper weakly binds to chrome azurol S (CAS) and Mb production is monitored when the colour changes from blue to yellow as it sequesters copper from Cu-CAS. The results of these experiments indicate that, based on this test, the Mb in *Mc. capsulatus* is not produced via NRPS-1. The other two mutant strains, Δ*nrpS-2*, Δ*pkS*, seem to be produce less Mb compared to the wild-type organism, therefore, NRPS-2 and PKS might affect (via unknown mechanism) the amount of Mb produced. To validate these results, the mutants have been sent to our collaborators, Prof. Alan DiSpirito at Iowa State University and Dr. Jeremy Semrau at University of Michigan, who have the expertise and equipment to quantify Mb and to investigate the metal binding properties. The initial results (not shown) that we received from them indicated that Δ*pkS* and Δ*nrpS-2* are producing as much Mb as the wild-type. If this is actually the case, one can suggest that NRPS-2 and PKS might be involved in production of a defective Mb that could not bind copper. To investigate this, determination of the chemical properties and in particular the copper-binding affinity of the produced Mb by Δ*pkS* and Δ*nrpS-2* could be done by our collaborators.

Unexpectedly, there was no observable difference between the wild-type and the mutants in terms of sMMO activity using the naphthalene assay (Figure 4.11). This indicated that there was no direct relationship between the mutated genes and MMO regulation. Further investigations need to be done on the mutant strains in the future work order to investigate the effect of these mutations on MMO expression. For example, quantitative RT-PCR studies of *mmoX* and *pmoA* transcripts in mutant strains and *Mc. capsulatus* wild-type cultures grown under varying copper concentrations are required. Further work is also needed to measure the sMMO and pMMO activities quantitatively *e.g.*, propylene oxidation using gas chromatography.

The poor growth of the mutants under copper-limited growth conditions and the restoration of growth when copper was added can be explained by the possibility that there is a defect in the copper acquisition systems. These findings are in agreement with those obtained by Rondon *et al.* (2004) who demonstrated that inactivation of a hybrid non-ribosomal peptide-polyketide encoding gene of *Agrobacterium tumefaciens* led to a mutant that grew more slowly than the parental strain on iron-deficient medium. This is an indicative that NRPSs and PKS might be involved in copper transport in *Mc. capsulatus*.

Δ*nrpS*-1, Δ*nrpS*-2 and Δ*pkS* mutant strains accumulated higher copper concentrations than that of the wild-type when grown on NMS with no-added copper indicating that these genes are more likely to be involved in copper trafficking in *Mc. capsulatus*. Under copper deficiency, *Mc. capsulatus* cells grow on methane using the alternative MMO enzyme: the iron-containing sMMO to sustain their growth. Under these conditions, cells are still in need of copper for copper requiring-enzymes such as

cytochrome oxidase. As mentioned previously in Chapter 3, there are multiple copper transport systems in methanotrophs. Knocking-out one system may trigger another system to substitute for the first. Thus, it is of interest for future study to investigate the comparative expression profiling of the genes encoding other copper-transporting protein (*e.g. mopE* and *copA*) for the Δ*nrpS*-1, Δ*nrpS*-2 and Δ*pkS* strains at different copper concentrations.

Under elevated copper conditions, Δ*nrpS*-2 accumulated high amounts of copper intracellularly, which caused cell-toxicity. Copper toxicity was outlined before (section 3.5). One possibility to explain this phenotype is the polar effect. If *nrpS-2* and a gene encoding a putative outer membrane efflux protein, which is located downstream of the *nrpS-2* are working as part of a copper homeostatic operon. Thus, knocking-out *nrpS-2* might prevent the transcription of the outer membrane efflux-encoding gene. Consequently, an accumulation of intracellular copper was observed in Δ*nrpS*-2 due to alteration in copper homeostasis. The copper contents of Δ*nrpS*-1 and Δ*pkS* growing under high copper concentration were not measured due to time constraints. However, more experiments need to be done to illustrate these phenotypes, including monitoring of the growth under different copper conditions, starting with the nanomolar range upwards, metal analysis at different time points and estimating the pMMO and sMMO activities. These points are already discussed with our collaborators in US and they are going to do these experiments since they have the required facilities.

The putative Mb mutant strains exhibited no obvious phenotypic difference compared to the *Mc. capsulatus* wild-type when testing their ability to grow in various silver growth conditions. This result highlighted that the inactivation of *nrpS-1*, *nrpS-2*

and *pkS of Mc. capsulatus* do not confer silver sensitivity or resistance. Silver is not an essential element for bacterial growth therefore, silver transport is probably fortuitous (Solioz and Odermatt, 1995). Likewise, as with *Ent. hirae*; 5 µM silver (Solioz and Odermatt, 1995) completely inhibited cell growth of *Mc. capsulatus*, confirming extreme silver toxicity. This toxicity might be through silver-mediated Fenton reactions.

As an attempt to compare the metabolite profiles of wild-type and mutant strains, initial LC/MS studies were conducted on the supernatants of the cultures. Analysis of supernatants of the putative Mb mutants and the wild-type grown on NMS with no-added copper revealed that there was a metabolite (X) in supernatant of the wild-type (retention time 19 min; m/z = 212.4) which was not observed in the supernatants of the putative Mb mutants (Figure 4.16). These results suggested that NRPS-1 and NRPS-2 and PKS are probably involved in the production of this metabolite. An attempt was made to identify this compound (X) but was not successful probably due to insufficient quantity. However, the compound with m/z = 212.4 could not be reproducibly observed in the samples prepared with copper and/or iron (data not shown) suggesting that the production of this compound is dependent of the growth conditions. Furthermore, LC-MS data showed that there was another metabolite (metabolite Y) with a retention time of 2.2 min, m/z 293. This compound was observed in Δ*nrpS-1*, Δ*nrpS-2* and Δ*pkS* as well as in the wild-type, but at varying levels from one sample to another. The concentration of the metabolite was higher in the wild-type than in the mutants as indicated by peak heights; wild-type is greater than that of Δ*nrpS-1* and Δ*pkS* which both were greater than Δ*nrpS-2*. One could speculate that NRPSs and PKS of *Mc. capsulatus* are involved in controlling the quantity produced of this metabolite. Alternatively, NRPSs and PKS

might integrate in production of metabolite Y. The results substrate specificity of these megaenzymes give insights about the residues that might constitute the metabolite that they synthesize. In-depth investigations are needed to identify metabolites X and Y using comparative metabolite profiling for mutants and the wild-type growing at different concentrations of copper and iron, samples should be taken at different growth phases. In addition, it is important to determine the expression levels of on *pkS* and *nrpsS* using real time PCR (RT-PCR) and to identify the metabolite produced.

The genome map of *Mc. capsulatus* revealed that the putative Mb genes were located near membrane transporter proteins. MCA2110, a gene encoding a putative outer membrane efflux protein, is located downstream from *nrpS-2* (Figure 4.1). *pkS* is located between a sensory box protein-encoding gene MCA1237, and heavy metal efflux protein gene MCA1239. MCA1237 is putatively involved in the synthesis of the secondary messenger molecules known as cyclic diguanylate cyclic (di-GMP). Signals are transmitted via synthesis or degradation of cyclic di-GMP, therefore, these molecules constitute a part of transduction signalling (D'Argenio and Miller, 2004, Jenal, 2004, Jenal and Malone, 2006). In support of this, cyclic-di-GMP was found to be involved in regulation of cellulose in *Gluconacetobacter xylinus* (Tal *et al.*, 1998), virulence and biofilm formation in *Vibrio cholerae* (Tischler and Camilli, 2004, Tischler and Camilli, 2005) and in certain strains of *Pseudomonas aeruginosa*, (Jenal, 2004; Hickman *et al.*, 2005). Therefore, PKS is likely to be part of a system dealing with a response to a change in metal (copper) concentrations. Collectively, the genome context of operons of the putative Mb genes indicated that they might be involved in transport.

The observations presented in this chapter consistent with multiple copper uptake systems exist in *Mc. capsulatus*. For example, MopE is a specific copper-importing protein (Fjellbirkeland, *et al.*, 1997; Helland, *et al.*, 2008). Whether the gene product of *pkS*, *nrpS-1* and/or *nrpS-2* interfere with MopE* in copper acquisition or it is a component of another specific copper uptake system, need further investigations.

To summarize of this chapter, these results indicate that PKS and NRPS-2 but not NRPS-1 might be involved in production of a defective Mb in *Mc. capsulatus*. It is crucial to determine the copper-binding affinities of the produced Mb from Δ*nrpS-2* and Δ*pkS*. The genes encoding these proteins might be involved in regulation of methane oxidation.

Recently, isotopic and fluorescent labeling studies have shown that intact copper-Mb complex was internalized by *Ms. trichosporium* through an active transport process (Balasubramanian *et al.*, 2011). This provided conclusive evidence that Mb mediates copper uptake. Despite the observation that Mb is being produced by several methanotrophs, only two Mb have been chemically characterized: one from *Ms. trichosporium* (OB3b) (Kim *et al.*, 2004) and the other from *Methylocystis* SB2 (Krentz *et al.*, 2010). Both types of Mb share similarities in metal binding affinities and spectral features, however, the peptide structure varies in terms of number and types of amino acid residues between them. The differences between the chemically characterized Mbs are outlined in Chapter 8. Additionally, two types of Mb have been isolated from *Ms. trichosporium*; one which has a methionine residue but the other has not, although both types bind copper in the typical arrangement (El Ghazouani, *et al.*, 2011). This confirms the notion that Mb is a structurally diverse group of metal chelators.

Therefore, another suggestion can be made which is that PKS and/or NRPS of *Mc. capsulatus* are probably involved in production in another form of Mb. Further investigations need to be carried out to address this possibility.

The gene for a ribosomally-produced peptide precursor for Mb of *Ms. trichosporium* (OB3b) has recently been predicted using bioinformatics tools (Krentz, *et al.*, 2010). Mutagenesis of this precursor gene has already been done and the mutant was characterized, details are given in Chapter 8.

Chapter 5

Transcriptome analysis using a *Mc. capsulatus* whole-genome microarray

5.1 Introduction

Not all bacterial genes are expressed simultaneously. Exceptions are housekeeping genes, encoding essential enzymes and other essential macromolecules, which are expressed at all times. Genes necessary for gene expression, DNA replication, respiration, energy production and other basic cellular functions fall under this category. As a strategy to save energy, bacteria tend to express a gene or a group of genes only when their function is required through gene regulation processes. Gene regulation is not a simple process and it involves complicated interactions between many proteins, signals and other elements in a well- coordinated network. Identification of regulatory genes, regulated proteins and their interactions provides insights in understanding the physiology of the cell and how the bacterium deals with different signals (Segal *et al.*, 2003). As an approach to estimate the level of gene expression, a microarray was used to understand the gene regulation networks in response to environmental signals and other metabolic pathways of the cell (Lorenz *et al.*, 2011).

Mc. capsulatus responds to levels of copper to switch between the two MMOs i.e. the cells express sMMO when copper is limited and express pMMO when more copper is available (Semrau *et al.*, 2010; Fru, 2011)).

It is of interest, therefore, to look at the differential expression patterns of whole-genome transcriptomics of *Mc. capsulatus* during growth on no-added copper (expressing sMMO) or high copper (expressing pMMO) taking advantage of the availability of microarray technology. The hypothesis of this chapter is that the key genes that are involved in MMO regulation are up- or down-regulated during growth on methane using the sMMO compared to the growth using the pMMO. Consequently, further insights

about the possible mechanisms of MMO regulation by copper in *Mc. capsulatus* will emerge.

5.2 Experimental workflow for transcriptome analysis of *Mc. capsulatus* using a whole-genome microarray

The experimental workflow for this microarray experiment comprised nine main stages: (1) microarray probe design; (2) chemostat work; (3) sampling from sMMO-expressing and pMMO-expressing cells; (4) checking sMMO activity by the naphthalene assay and polypeptide profiles of both MMO enzymes using SDS-PAGE of cell-free-extracts; (5) RNA extraction from samples; (6) labeling; (7) hybridization; (8) scanning and (9) data analysis. Details of each stage are given below. A schematic representation of the microarray experiment is outlined in Figure 5.1.

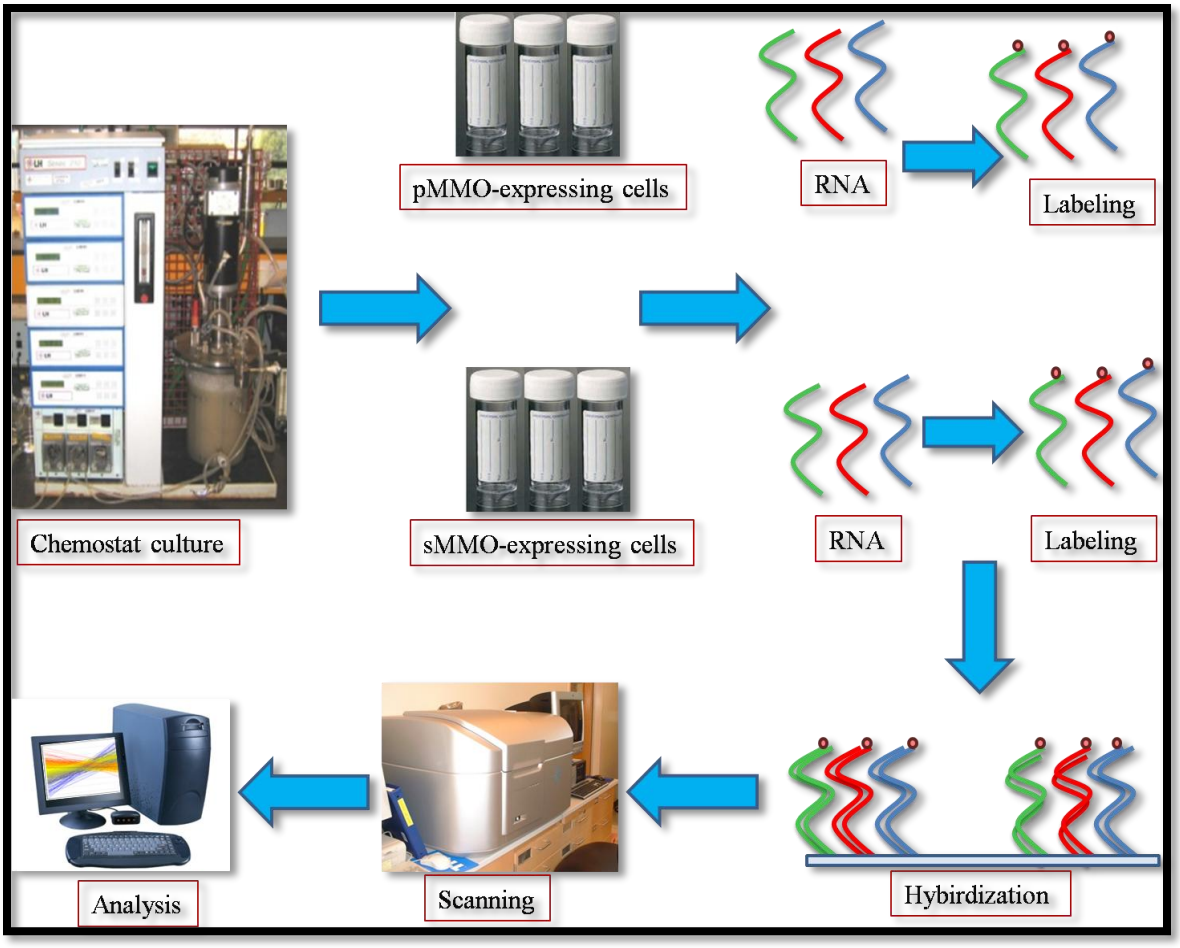

Figure 5.1 A schematic representation of the microarray-based comparative expression profiling of whole-genome transcriptomics analysis of *Mc. capsulatus* expressing sMMO versus pMMO.

5.2.1 Microarray technology and probes design

Comparative expression-profiling of whole-genome transcriptome of *Mc. capsulatus* was performed using a custom synthesized oligonucleotide microarray, using the 8X15K Agilent platform (Agilent Technologies, USA), https://earray.chem.agilent.com/earray. Four oligonucleotide probes were synthesized targeting each of 3,052 candidate genes that have been identified in the genome of *Mc. capsulatus* (Ward *et al.*, 2004) and based on the sequences available on NCBI. The

length of each probe was selected to be about 60 bases as recommended by Agilent technologies, to optimise sensitivity and efficiency in hybridization. A total of 11, 688 probes were printed on the biochip in known order. A one-colour platform was used in this experiment.

5.2.2 Growth of *Mc. capsulatus* in the chemostat

To ensure cells were grown in physiologically similar conditions, a chemostat was used to grow the *Mc. capsulatus* wild-type strain in continuous culture. Details about the chemostat growth conditions were described previously in Materials and Methods.

5.2.3 Sampling from sMMO-expressing and pMMO-expressing cells

Three biological replicates from three independent steady state continuous cultures of *Mc. capsulatus* for each experimental condition *i.e.*, expressing sMMO (no added copper) or expressing pMMO (4 µM added copper) were collected. Each sample was divided into three aliquots for naphthalene oxidation assay, SDS-PAGE and RNA extraction. Stop solution (95% ethanol and 5% phenol) was immediately added to the samples destined for RNA extraction to avoid any disturbance in the transcriptome.

5.2.4 Testing samples the naphthalene assay and SDS-PAGE

Each sample was checked for sMMO expression using the naphthalene oxidation assay and by using SDS-PAGE to obtain polypeptide profiles to slow the MMO of whole-cell extracts. The three samples taken from *Mc. capsulatus* cultures growing under no-added copper growth conditions showed a positive naphthalene assay as indicated by

a deep purple colour, indicating that sMMO was expressed and active. On the other hand, samples of cells growing with 4 µM copper exhibited a negative naphthalene assay, (since the pMMO does not oxidize naphthalene).

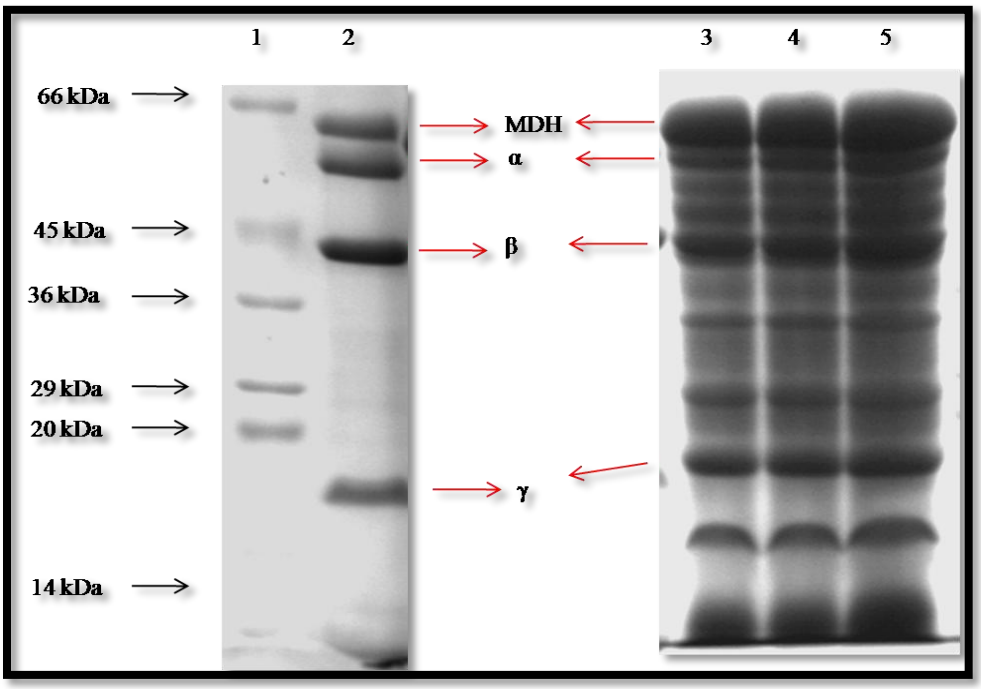

Figure 5.2 SDS-PAGE of cell-free extracts of *Mc. capsulatus* expressing sMMO. Lane 1, a Dalton VII molecular protein marker; lane 2, cell-free extract from *Methylocella silvestris* as control positive for sMMO and lanes 3 – 5 *Mc. capsulatus* expressing sMMO. The α, β and γ subunits of the sMMO hydroxylase and methanol dehydrogenase (MDH) are indicated by red arrows.

These results were further confirmed by observation of the polypeptide patterns specific for sMMO and pMMO using SDS-PAGE of whole-cell extracts. Whole-cell extracts were obtained using French press as described in Materials and Methods. The three hydroxylase subunits (α, β and γ), corresponding to MmoX (61 kDa), MmoY (45 kDa) and MmoZ (20 kDa) of sMMO were detected from *Mc. capsulatus* growing at no-added copper growth conditions (Figure 5.2). However, at 4 µM copper, three bands corresponding to the α–, β– and γ-subunits of the hydroxylase of pMMO were observed

(Figure 5.3). These bands corresponded to PmoB (47 kDa), PmoA (24 kDa) and PmoC (22 kDa) of pMMO respectively.

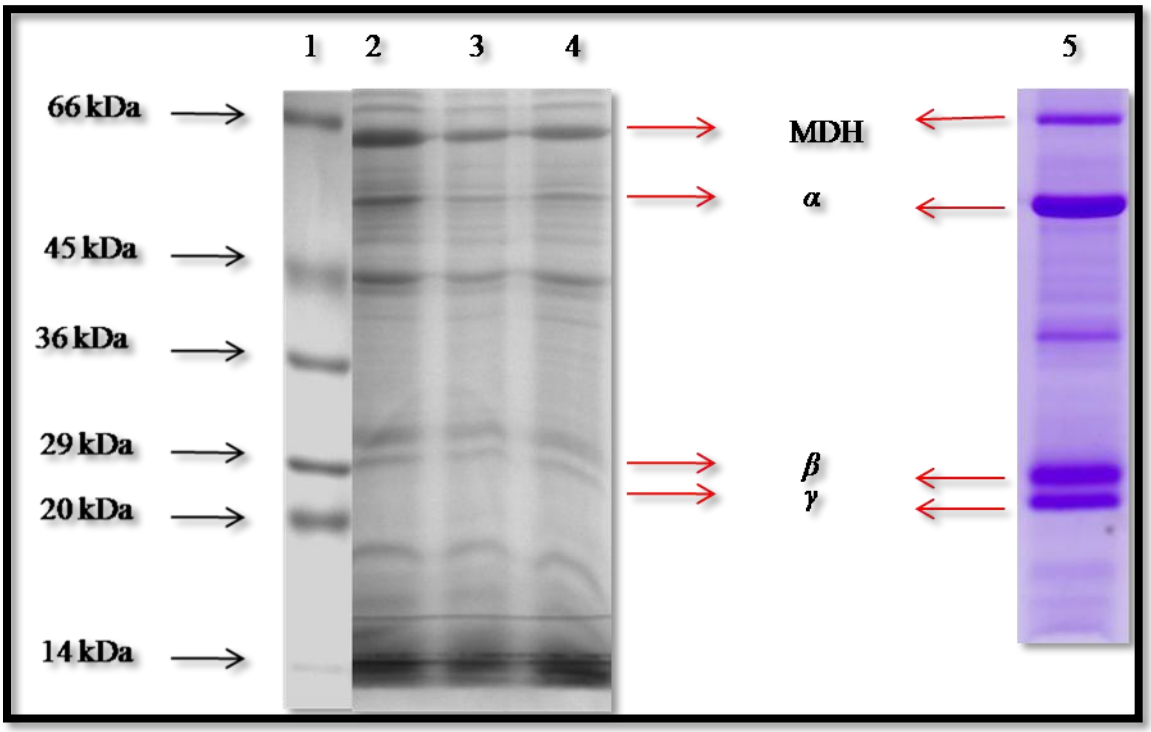

Figure 5.3 SDS-PAGE of cell free extracts of *Mc. capsulatus* expressing pMMO. Lane 1, a Dalton VII molecular protein marker; lanes 2 - 4, *Mc. capsulatus* expressing pMMO and lane 5, separate gel having purified pMMO from *Mc. capsulatus* photo kindly provided by Nataliia Myronova, The α, β and γ subunits of the pMMO hydroxylase, MDH, methanol dehydrogenase are indicated by red arrows.

5.2.5 RNA extraction

Extraction of total RNA from *Mc. capsulatus* expressing either sMMO or pMMO was carried out according to Gilbert *et al.*, (2000) as outlined in Materials and Methods. Purified RNA from sMMO-expressing cells was run in a 1% (w/v) agarose gel (Figure 5.4) and from pMMO-expressing cells (Figure 5.5) for a visual quality check**.** Purified RNA samples were submitted to the Molecular Biology Service of the School of Life Sciences for a quantitative quality check using the 2100 Bioanalyzer (Agilent

Technologies, USA). Representative electropherograms generated by the Bioanalyzer software of RNA samples are presented (Figures 5.6 and 5.7). False gel image was generated by the 2100 Bioanalyzer from three separate samples of each type of RNA extracted from sMMO-expressing cells or pMMo-expressing cells (Figure 5.8). Since accurate gene expression data are dependent initially on the purity and integrity of RNA, each sample was assessed for RNA integrity number (RIN). Good quality RNA samples, which showed a RIN of 6 and above, as suggested by Fleige and Pfaffl (2006), were then used for labeling and subsequent steps of the microarray experiments.

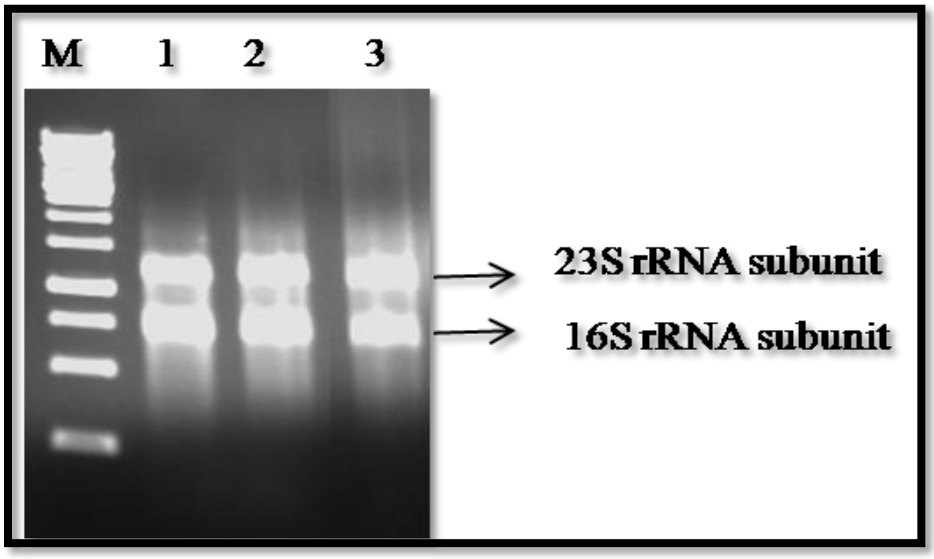

Figure 5.4 Total RNA extracted from *Mc. capsulatus* expressing sMMO M, DNA marker; 1, 2 and 3 biological replicates.

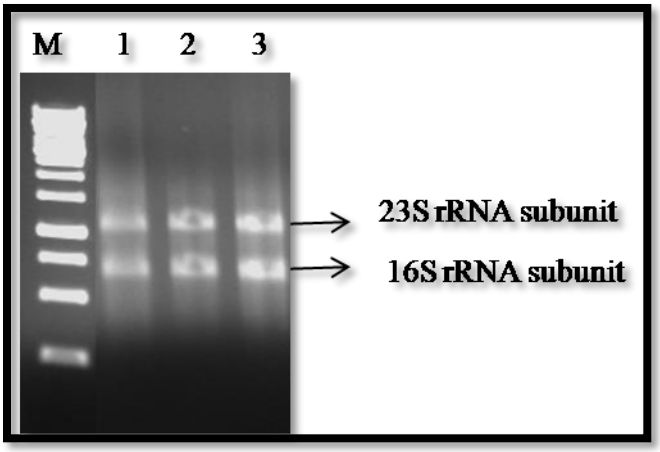

Figure 5.5 Total RNA extracted from *Mc. capsulatus* expressing pMMO M, DNA marker; 1, 2 and 3 biological replicates.

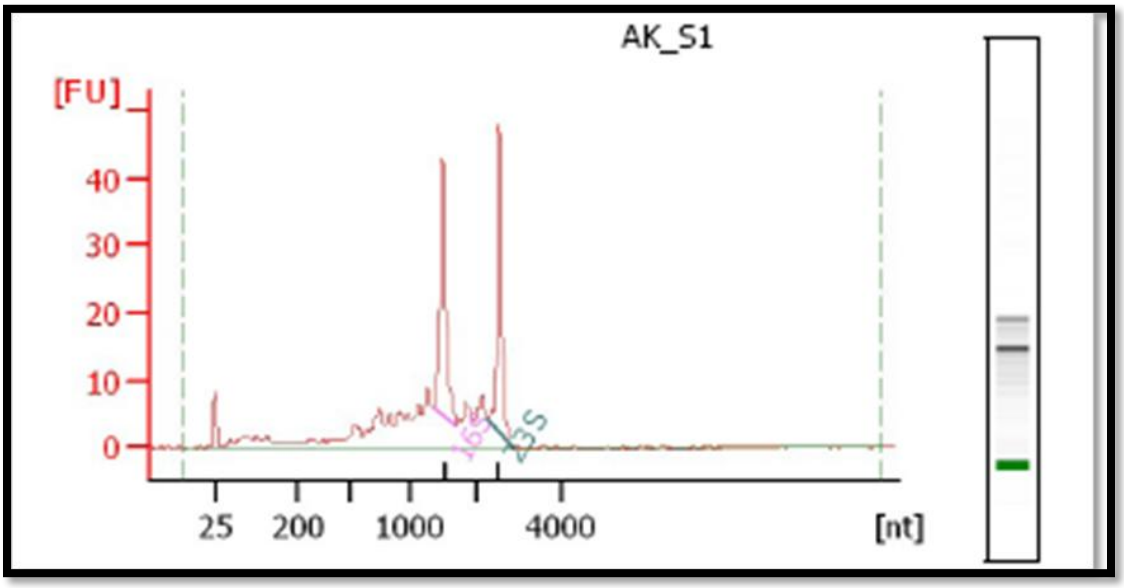

Figure 5.6 Bioanalyzer electropherogram of a representative *Mc. capsulatus* RNA sample (sMMO expressing cells). RNA area: 258, RNA concentration: 222 ng/µl. rRNA Ratio (23S/16S): 0.9, RIN: 7.2.

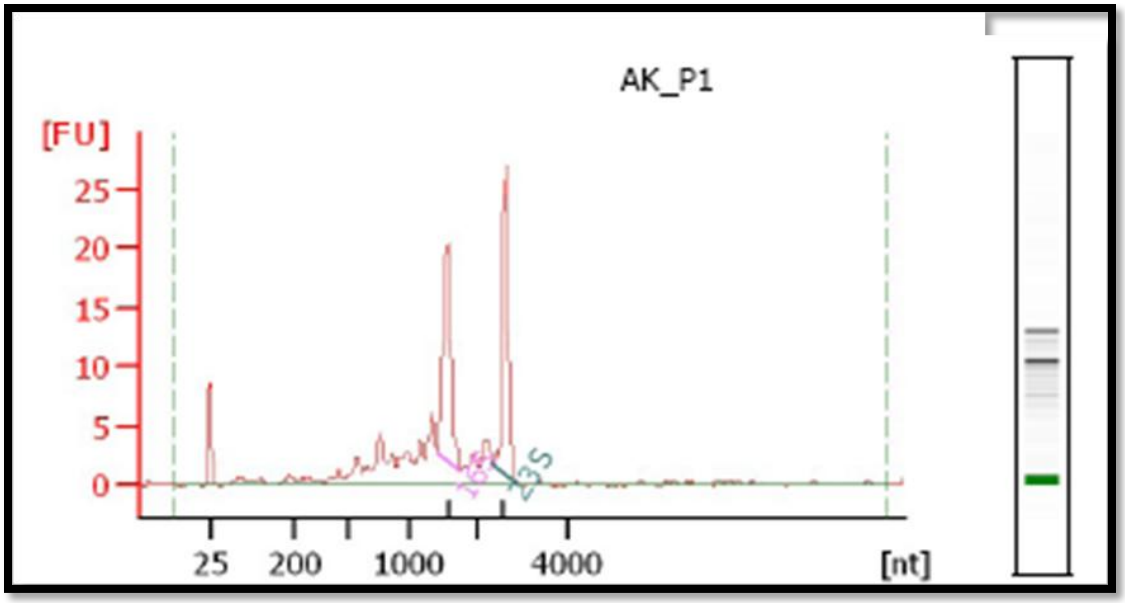

Figure 5.7 Bioanalyzer electropherogram of a representative *Mc. capsulatus* RNA sample (pMMO expressing cells). RNA area: 129.5, RNA concentration: 111 ng/µl. rRNA Ratio (23S/16S): 0.9, RIN: 7.4.

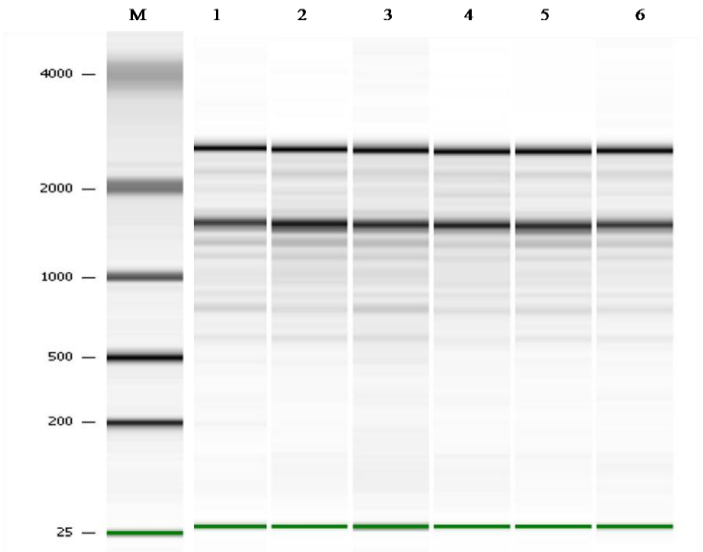

Figure 5.8 False gel image generated by the 2100 Bioanalyzer (Agilent Technologies, USA) with three RNA samples extracted from three separate sMMO expressing cells (Lane 1-3) or three separate pMMO expressing *Mc. capsulatus* (Lane 4-6). M, RNA ladder.

5.2.6 Labeling, hybridization and scanning

High quality RNA samples from three biological replicates of sMMO-expressing and pMMO-expressing cells were submitted to Molecular Biology Service, School of Life Science, the University of Warwick, for the subsequent labeling, hybridization and scanning. Fluorescent cRNA (complimentary) were generated from RNA samples, using T7 RNA polymerase for target amplification and incorporation of cyanine 3-labeled CTP, using Agilent's Quick Amp Labelling Kit according to the instructions of the manufacturer. Because the chip contains eight arrays, one sample for each tested condition was included as a technical replicate.

5.2.7 Data analysis

Analysis of the microarray data was carried out using GeneSpring X11 software (Agilent Analysis Technology, USA). Genes that had changes in expression levels of 2-fold or more were taken as a significant (Butcher, 2004) and therefore were recorded as up- or down-regulated in the analysis.

5.3 Differentially expressed genes

Analysis of the microarray data showed that out of a total of 3,052 genes, 25 genes appeared to be substantially up-regulated while 28 genes were down-regulated in *Mc. capsulatus* growing on no-added copper (sMMO-expressing cells) versus high copper concentration (pMMO-expressing cells). Details about these genes are given below.

5.3.1 Genes significantly differentially up-regulated in sMMO expressing *Mc. capsulatus*

Twenty-five genes appeared to be significantly up-regulated (≥ 2 fold changes) in *Mc. capsulatus* growing on added copper versus high copper concentration based on the microarray data analysis. A list of these up-regulated genes, their products, fold changes were presented in Table 5.1. The sMMO operon, in addition to a cluster of six genes upstream of it, was up-regulated under no added copper growth conditions. Some other genes dispersed in the *Mc. capsulatus* genome were also up-regulated. These genes encode proteins, which have putative functions associated with copper: 1) a multicopper oxidase enzyme that might have a role in copper resistance/transport, 2) TonB copper-dependent receptor that might play a role in signal transmission (copper sensory) or iron transport,

3) proteins involved in post-transcriptional modification. These genes and their products will be potential targets for future mutagenesis and proteomics as they may be involved in MMO regulation.

Table 5.1 List of genes significantly up-regulated, during growth in no-added copper compared to 4 µM copper, indicating gene product, putative function and average fold change. Figures are the mean of three replicates ± standard deviation.

Gene	Gene product/annotation	Putative function/common hint	Fold
MCA0440	TonB-dependent receptor, putative	Metal transport - Signal transmission	5±1
MCA0786	MxaC protein, putative	Contain metal ion-dependent Adhesion Site (MIDAS) – cell signaling	2±0
MCA1023	Antioxidant, AhpC/Tsa family protein	Post-translational modification - protein turnover, chaperones, thiol-specific Antioxidant (TSA) proteins	3±0
MCA1024	Hypothetical protein	Inorganic ion transport and metabolism	5±2
MCA1101	Multicopper oxidase family protein	Copper transport	6±2
MCA1188	Membrane-bound proton-translocating pyrophosphatase	Maintain a substantial proton motive force across membrane	9±3
MCA1189	Hypothetical protein	Ferritin-like superfamily of diiron-proteins	10±1
MCA1190	Hypothetical protein	Unknown function	11±5
MCA1191	SCO1/SenC family protein	SCO (Synthesis of Cytochrome c Oxidase) with Cu(I) binding site	6±3
MCA1192	Hypothetical protein	Unknown function	10±2
MCA1193	Hypothetical protein	*E. coli* Ras-like protein- with GTP/Mg^{2+} binding site	7±3
MCA1194	Methane monooxygenase, A subunit, alpha chain	α-subunit of sMMO hydroxylase (MmoX)	184±26

MCA1195	Methane monooxygenase, A subunit, beta chain	β- subunit of sMMO hydroxylase (MmoY)	122±11
MCA1196	Methane monooxygenase, B subunit	B subunit of sMMO (MmoB)	116±17
MCA1198	Methane monooxygenase, A subunit, gamma subunit	γ- subunit of sMMO hydroxylase (MmoZ)	20±2
MCA1199	Methane monooxygenase, D subunit	D-subunit a protein of unknown function of sMMO (MmoD)	29±8
MCA1200	Methane monooxygenase, C subunit	C-subunit a reductase of sMMO (MmoC)	62±21
MCA1201	Hypothetical protein	A σ^{54}-dependent transcriptional regulator (MmoR)	20±5
MCA1202	Chaperonin, 60 kDa subunit	Chaperonin GroEL (MmoG)	31±5
MCA1905	Hypothetical protein	Prefoldin – stability and correct folding of the synthesized polypeptides	13±2
MCA1907	Calcium/proton exchanger	Calcium/proton antiport	8±2
MCA2169	BNR repeat-containing protein	BNR: Bacterial neuraminidase repeat found in many glycosyl hydrolases and extracellular proteins of unknown function	22±6
MCA2477	Hypothetical protein	Posttranslational modification	4±1
MCA2589	Surface-associated protein precursor	MopE (copper uptake)	2±0.3
MCA2590	Cytochrome c peroxidase family protein, putative	Detoxifying of hydrogen peroxide	7±1

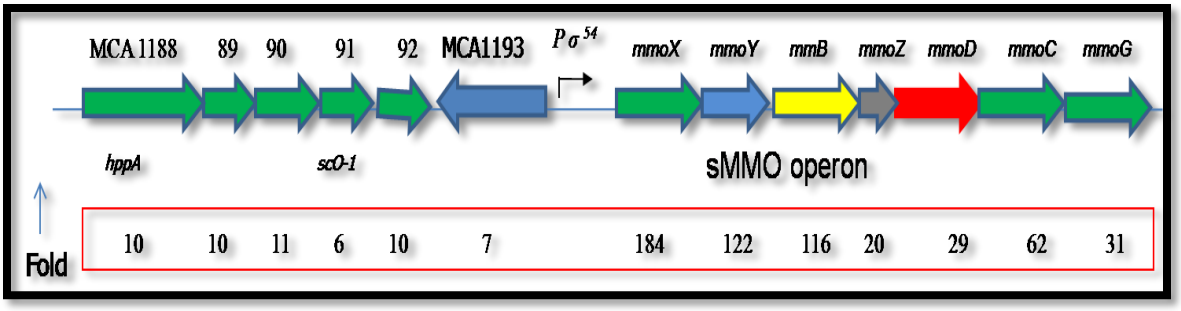

Figure 5.9 Up-regulation (fold) of sMMO operon and the upstream genes

As expected, the sMMO operon was up-regulated 20-150 fold (Figure 5.9). The genes encoding soluble methane monooxygenase, α-subunit, β-subunit and γ-subunit namely, MCA1194 (*mmoX*), MCA1195 (*mmoY*) and MCA1198 (*mmoZ*) showed substantial up-regulation with 184, 122 and 20 fold change respectively. These three subunits constitute the hydroxylase of sMMO. Furthermore, MCA1196 (*mmoB*) which encodes the coupling protein B, MCA1200 (*mmoC*) which, encodes a reductase and MCA1199 (*mmoD*) which encodes a protein of unknown function, were significantly up-regulated (116-, 62- and 29-fold respectively). In addition, the two regulatory genes MCA202 (*mmoG*) which encodes a putative GroEL; chaperonin 60 kDa subunit and MCA1201 (*mmoR*) which encodes a σ^{54} – dependent transcriptional activator were highly induced with 31 and 20 fold increases in expression respectively. Interestingly, the expression levels of six genes (MCA1188-MCA1193) located upstream of the sMMO operon were found to be high, with up-regulation from 6-11 fold (Figure 5.9). Five of these genes are organized in the same direction as the sMMO operon (Figure 1) while the sixth gene is oriented in the opposite direction. MCA1189, MCA1190, MCA1192 and MCA1193 were annotated as hypothetical proteins while MCA1188 and MCA1191 were annotated as a membrane-bound proton-translocating pyrophosphatase and a SCO1/SenC

family protein respectively. More details about ScO-1 protein are presented in Chapter 6. However, BLAST analysis of the proteins with unknown functions against NCBI protein databases identified the proteins listed in Table 5.1. These included an *E. coli* Ras-like protein with a GTP/Mg^{2+} binding site (MCA1193) and a member of the ferritin-like superfamily of di-iron-proteins (MCA1189), which might have a role such as iron-delivery to sMMO, considering sMMO is a di-iron containing enzyme.

Furthermore, the gene encoding a putative TonB-dependent outer membrane receptor protein, MCA0440, was up-regulated. The significance of this gene and its potential role in copper uptake mediated via Mb is presented in the discussion later in this chapter. The expression level of MCA1101 (6-fold increase), which was annotated as a multicopper oxidase family protein, suggests a possible role in copper homeostasis. Among the up-regulated genes, MCA1023 and MCA2477 seemed to be involved in post-translational modification. MCA1905 also exhibited a high level of expression. The gene product of MCA1905 appeared to play a role in proper stability and/or assembly of the newly produced polypeptides (Fink, 1999). In addition, the surface-associated protein precursor (MopE) gene (MCA2589) and a putative cytochrome c peroxidase (CCP) family protein encoding gene (MCA2590) were up-regulated. CCP is a di- haem protein involved in reduction of peroxide to water (Ellis *et al.*, 2011). A calcium/proton exchanger encoding gene (MCA1907) was also up-regulated. This protein is an integral membrane protein, which maintains the balance of the cellular calcium quota in relation to that of sodium (Barnes and Barnes,1980). The expression level of MCA2169 was high. This gene encoded a protein that contained Bacterial Neuraminidase Repeat (BNR). BNR

is a short invariant sequence (S-X-D-X-G-X-T-W) discriminating bacterial from influenza sialidases (neuraminidases) (Roggentin *et al.*, 1989).

5.3.2 Genes significantly differentially down-regulated in sMMO expressing *Mc. capsulatus*

Twenty-eight genes were significantly down-regulated (2-fold or greater) in sMMO-expressing versus pMMO-expressing *Mc. capsulatus* (Table 5.2). The products of some of these genes are hypothetical proteins with unknown function, while others have previously assigned functions.

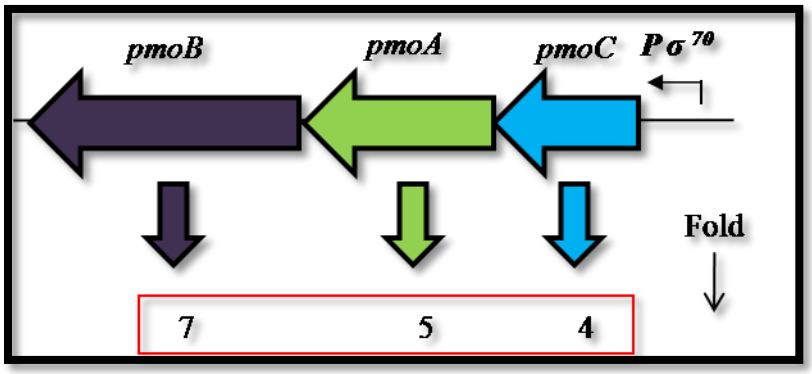

Figure 5.10 Down-regulation (fold) of the first copy of the genes encoding pMMO in *Mc. capsulatus*

Furthermore, the expression of the two copies of the genes encoding for the pMMO in *Mc. capsulatus* was down-regulated. MCA1796, MCA1797 and MCA1798 which encodes the β- subunit, γ- subunit and α-subunit of the first copy of pMMO hydroxylase were down-regulated (5-7 fold change) (Figure 5.10). Similarly, the expression levels of the genes encoding the three subunits (PmoA2, PmoC2 and PmoB2) of the hydroxylase of the second copy of pMMO was low, the change in expression level

was 5-, 4- and 7- fold respectively. The third copy *pmoC3* was also down-regulated (4-fold change) (Table 5.2). Interestingly, a gene (MCA0316) which encodes a TetR (transcriptional regulator) (Ramos *et al*., 2005) was down-regulated. MCA2866, which encodes formaldehyde-activating enzyme (Vorholt *et al*., 2000) was also down-regulated. The expression levels of three genes (MCA0392, MCA1310 and MCA0905) encoding for ribosomal proteins S16, S15 and S9 were very low. In addition, an MraZ protein encoding gene, MCA2437, was down-regulated. The MraZ protein is involved in synthesis of cell wall and cell division in *E. coli* (Adams *et al*., 2005). Similarly, MCA2432, which has a putative function in peptidoglycan biosynthesis, was down-regulated when copper is limited in the media. MCA2432 is annotated as a phospho-N-acetylmuramoyl-pentapeptide-transferase. MCA3040, which encodes a putative transketolase, was down-regulated. Transketolase is involved in the pentose phosphate pathway and in the biosynthesis of polyketides (Eisenreich *et al*., 1996). Four genes, MCA2030, MCA0160, MCA2245 MCA1738, were down-regulated. These genes encode proteins with hypothetical functions. MCA1739, which encodes a putative lyase, probably involved in the glyoxylate cycle (Meister *et al*., 2005), was down-regulated. The expression level of MCA2992 and MCA1011 was reduced under no-added copper growth conditions. MCA2992 is annotated as a GatB/Yqey domain-containing protein which has a role in tRNA metabolism, while MCA1011, is annotated as a DEAD-box ATP dependent DNA helicase and probably is involved in RNA unwinding (Pyle, 2008).

Furthermore, a sulfate adenylytransferase encoding gene (MCA2629), possibly involved in sulfate reduction (Speich and Trüper, 1988), was down-regulated by copper. However, MCA2079 and MCA2381, which are annotated as acetyl ornithine

aminotransferase and MxaD (polyketide cyclase), were down-regulated in copper deficient-media. Polyketide cyclase is involved in polyketide synthesis by closing ring of the product (Sultana *et al.*, 2004). The products of both genes are possibly involved in biosynthesis of secondary metabolism such as polyketides. MCA0302 was down-regulated by low bioavailable copper. The annotation of this gene is as a peptide chain release factor, which may be involved in termination of translation (Korostelev *et al.*, 2008). The peptidyl-prolyl *cis-trans* isomerase, FKBP-type encoding gene was down-regulated. FKBP is called FK506 binding protein and is probably involved in signal transduction and/or protein folding (Göthel and Marahiel, 1999). In addition, MCA2011, which encodes a multicopper oxidase family protein, was expressed at low level under copper-limiting growth conditions. Copper homeostasis and/or oxygen reduction may be the function of this protein (Rensing and Grass, 2003). MCA0160 was down-regulated. A BLAST search of the protein of MCA0160 with databases gave no hit, which indicates that it is likely to be a unique protein to *Mc. capsulatus*.

Table 5.2 List of genes significantly down-regulated, during growth with no-added copper compared to 4 µM copper, indicating gene product, putative function and average fold change. Figures are the mean of three replicates ± standard deviation.

Gene	Product	Putative function/common hint	Fold
MCA1796	Methane monooxygenase, B subunit	α-subunit of pMMO hydroxylase (PmoB1)	7±2
MCA1797	Methane monooxygenase, A subunit	β- subunit of pMMO hydroxylase (PmoA1)	5±1
MCA1798	Methane monooxygenase, C subunit	γ- subunit of pMMO hydroxylase (PmoC1)	4±1
MCA2853	Methane monooxygenase, B subunit	α-subunit of pMMO hydroxylase (PmoB2)	7±2
MCA2854	Methane monooxygenase, A subunit	β- subunit of pMMO hydroxylase (PmoA2)	5±1
MCA2855	Methane monooxygenase, C subunit	γ- subunit of pMMO hydroxylase (PmoC2)	4±1
MCA0295	Methane monooxygenase, C subunit	γ- subunit of pMMO hydroxylase (PmoC3)	4±1
MCA0081	Peptidyl-prolyl cis-trans isomerase, FKBP-type	Protein folding - signal transduction	2±0.3
MCA0160	Hypothetical protein	Unique protein (No hits from protein blast)	8±2
MCA0302	Peptide chain release factor 2	Termination of translation	2±0
MCA0316	TetR family transcriptional regulator	Transcriptional regulator	3±0.3
MCA0392	Ribosomal protein S16	Ribosome assembly	3±0
MCA0905	Ribosomal protein S9	Ribosome assembly	3±0

MCA1011	DEAD-box ATP dependent DNA helicase	A diverse family of proteins involved in ATP-dependent RNA unwinding	3±0.3
MCA1310	Ribosomal protein S15	Ribosome assembly	4±0.1
MCA1738	Hypothetical protein	No putative conserved domains detected - Outer membrane protein?	2±0
MCA1739	Citrate lyase, beta subunit, putative	Involved in glyoxylate cycle	4±0.7
MCA2011	Multicopper oxidase family protein	Copper homeostasis/Oxygen reduction	2±0
MCA2030	Hypothetical protein	Short Protein with unknown function (59 aa)	6±0.9
MCA2079	Acetylornithine aminotransferase	Arginine and proline metabolism - biosynthesis of secondary metabolites	3±0
MCA2245	Hypothetical protein	Unknown function	6±0.7
MCA2381	MxaD gene product	Polyketide cyclase (biosynthesis of polyketides)	4±0
MCA2432	Phospho-N-acetylmuramoyl-pentapeptide-transferase	Peptidoglycan biosynthesis	2±0
MCA2437	MraZ protein	Cell wall biosynthesis and cell division	4±0.6
MCA2629	Sulfate adenylyltransferase subunit 2	Catalyses sulfate reduction/sulfate metabolism	4±0.7
MCA2866	Formaldehyde-activating enzyme	Formaldehyde detoxification	3±0.3
MCA2992	GatB/Yqey domain-containing protein	Has a role in tRNA metabolism	3±0
MCA3040	Transketolase	Transketolase, an enzyme involved in the pentose phosphate pathway	3±0.7

5.4 An attempt to validate microarray results using reverse transcription quantitative PCR (RT-qPCR)

Quantitative PCR (RT-qPCR) with a SYBR® Green-based approach was used for validating the results of the microarray using the Applied Biosystems 7000 Real-Time PCR System (Applied Biosystems). Representatives of up-regulated and down-regulated

Table 5.3 List of primers used for quantitative RT-PCR

Primer	Sequences	Gene	Status
16s 2 F	5'-TGGGGAGCAAACAGGATTAG-3'	16s rRNA	housekeeping
16s 2 R	5'-TAGCTGCGCCACTAAAAGGT-3'		
RNAP F	5'-AACATCGGCCTGATCAACTC-3'	MCA1066	housekeeping
RNAP R	5'-GATACGGCGTCTCCAGAAAG-3'	(*rpoB*)	
MCA1191F	5'-GTCGCCGATTTCGTATTGAC-3'	MCA1191	up-regulated
MCA1191R	5'-GTGGGTATAGCCGACGAAGA-3'		
MCA1190F	5'-AACGGACGTTCATCGATTTC-3'	MCA1190	up-regulated
MCA1190R	5'-AGGACGTCGAACATCTCTGG-3'		
MCA1188F	5'-CTCGAAAAGTTTCGGTTTCG-3'	MCA1188	up-regulated
MCA1188R	5'-GGACCAACCGGTAGACTTCA-3'		
MCA1189F	5'-AACCAATCATCTCGCCTACG-3'	MCA1189	up-regulated
MCA1189R	5'-AGCGCATAGGATTTGAGCAT-3'		
MCA1194F	5'-GACGAAAGGCAGTTCGGTAG-3'	*mmoX*	up-regulated
MCA1194R	5'-TCCAGGAAGTTCGAAACCAC-3'		
MCA1796F	5'-TAGGTGGCGTCTTCCACTTT-3'	*pmoB*	down -regulated
MCA1796R	5'-ACAGCAAGTACCCGATCACC-3'		
MCA1797F	5'-ACAGTCGACGGTCTTTCCAG-3'	*pmoA*	down -regulated
MCA1797R	5'-TACCACATTCATGCCATGCT-3'		
MCA0316F	5'-TGCAGGCGTATTTCCATACA-3'	*tetR*	down -regulated
MCA0316R	5'-GACAGGTATCGCTGGTGTCC-3'		
MCA1192F	5'-GAATTCCATTCATTGGTGCAG-3'	MCA1192	up-regulated
MCA1192R	5'-CGACTTGATGACGAGCAGAC-3'		
MCA 0440F	5'-TCACCACCAACATGAACCTG-3'	*tonB*	up-regulated
MCA 0440R	5'-GAAACCCTGGTAGGGGATGT-3'		
MCA1101F	5'-TTCGAGCACCAAGGGTTACT-3'	*mucO*	up-regulated
MCA1101R	5'-GGTCATGAGGGTGATCTGCT-3'		

genes were selected for the RT-qPCR. Housekeeping genes were also selected as internal controls. Selected genes are listed in Table 5.3. However, no meaningful results were

obtained due to non-specific amplifications or primer dimer formation. Therefore, optimization of conditions for RT-qPCR is required but due to time limitations, further attempts were not made.

5.5 Validation of microarray results using reverse transcription PCR (RT-PCR)

An attempt to validate the results of microarray was carried out using reverse transcription (RT-PCR) for representative genes. cDNA was generated from RNA samples of sMMO- and pMMO-expressing *Mc. capsulatus* using the method described in Materials and Methods. To ensure that there was no DNA contaminations, RNA samples from sMMO- or pMMO-expressing cells were included as control in all RT-PCR experiments. In addition, a negative control using just water was also included.

scO-1 (MCA1191), which was found to be up-regulated under no-added copper growth conditions, was amplified from cDNA generated from sMMO and pMMO expressing cells. The primers used to amplify *scO-1* were MCA1191F7 and MCA 1191R603 (Table 5.4). As can be seen in Figure 5.11, the band in lane 4 from cDNA of sMMO was obviously more intense than that of pMMO expressing cells, lane 3. These results indicated that the relative abundance of *scO-1* transcripts was more in the RNA sample of sMMO cells than that of pMMO cells. As expected, a product was obtained from genomic DNA (lane 1) and a colony of *Mc. capsulatus* (lane 2) and nothing was obtained in the negative controls. These results gave indications that *scO-1* of *Mc. capsulatus* was up-regulated under low-copper growth conditions.

Table 5.4 A list of primers used for reverse transcription (RT-PCR)

Primer	Sequences	Genes	Size (bp)
MCA1191F7	5' –CGTACTACGCGGTTAGATCG-3	MCA 1191	597
MCA1191R603	5'-GAAAGGCGGGATCAGATAGC-3'	(*scO-1*)	
MCA1192F27	5'-AGCCTTGGCATGGTTCACTC-3'	MCA 1192	416
MCA1192R416	5'-TTCTCGACCGGCATCTTCAC-3'		
MCA1797F189	5'- GGNGACTGGGACTTCTGG -3	MCA 1189	493
MCA1797R682	5'- GAASGCNGAGAAGAASGC -3'	(*pmoA*)	

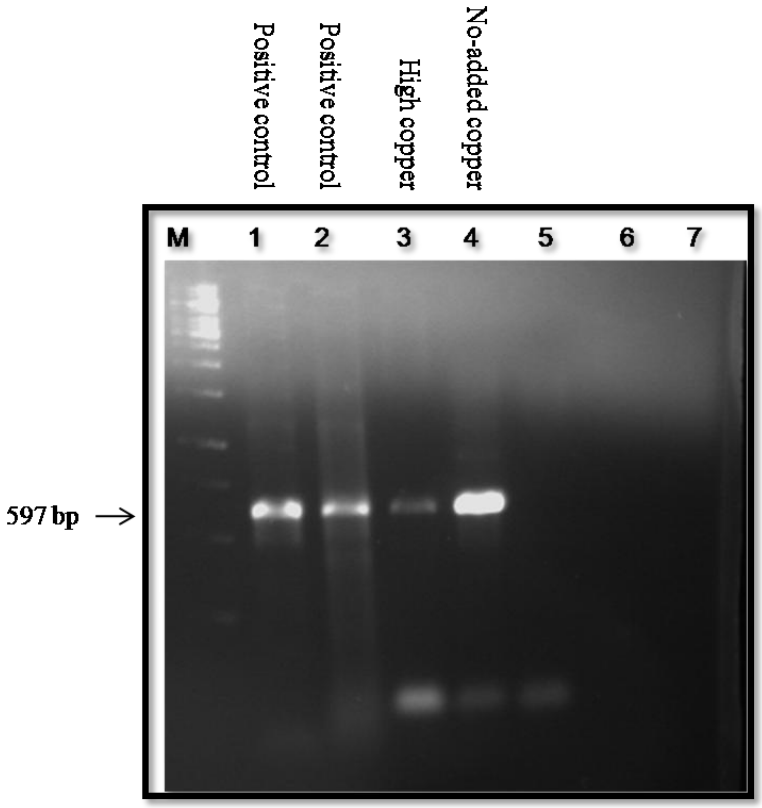

Figure 5.11 Agarose gel electrophoresis of RT-PCR of *scO-1* from *Mc. capsulatus*. Lanes 1 and 2 positive controls genomic DNA and DNA from a colony of *Mc. capsulatus*; lane 3, cDNA derived from RNA which was extracted from high copper grown cells; lane 4, cNDA derived from RNA which was extracted from no-added copper grown cells; lane 5, RNA extracted from high copper grown cells; lane 6, RNA extracted from no-added copper grown cells and lane 7, negative control. The expected size is approximately 597 bp. M, size marker (bp), 1 kb DNA ladder (Invitrogen).

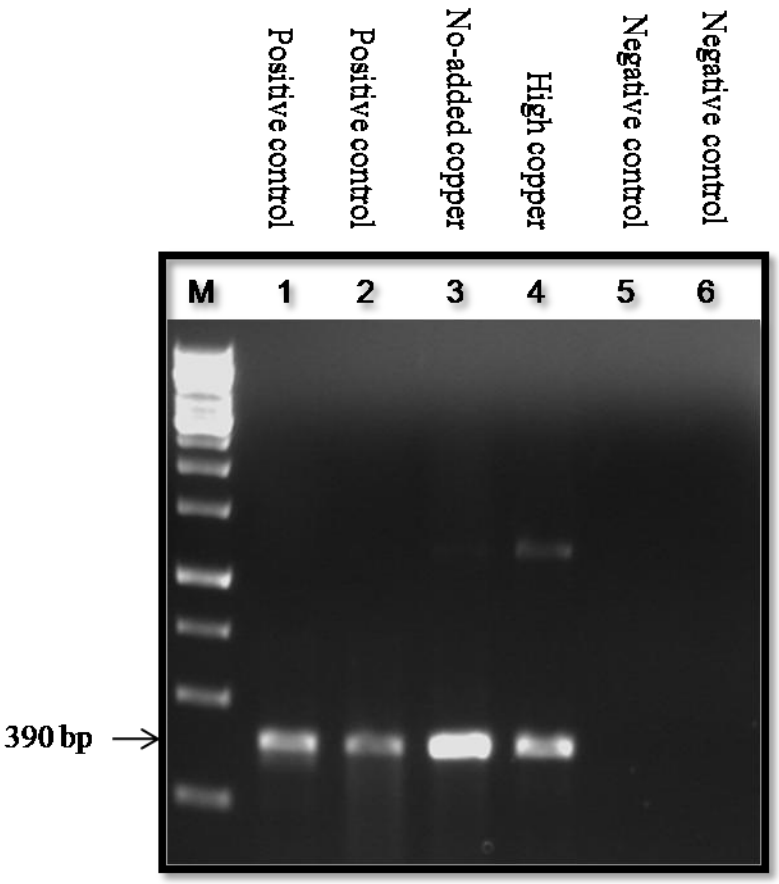

Figure 5.12 Agarose gel electrophoresis of RT-PCR of MCA1192 from *Mc. capsulatus*. Lanes 1 and 2 positive controls genomic DNA and DNA from a colony of *Mc. capsulatus*; lane 3, cDNA derived from RNA which was extracted from no-added copper grown cells; lane 4, cDNA derived from RNA which was extracted from high copper grown cells;; lane 5, RNA extracted from no-added copper grown cells; lane 6, RNA extracted from high copper grown cells and lane 7 negative control. The expected size is approximately 390 bp. M, size marker (bp), 1 kb DNA ladder (Invitrogen).

Likewise MCA1192 (also up-regulated gene under no-added copper growth conditions) was amplified using the primers (MCA1192F27 and MCA1192R416) from cDNA generated from sMMO and pMMO expressing cells. As can be seen in Figure 5.12, the band in lane 3 (expected size 390 bp) from cDNA of sMMO was obviously more intense than that of pMMO expressing cells in lane 4, highlighting the up-regulation of MCA1192 when *Mc. capsulatus* grown in copper-deficient medium.

The primers MCA1797F189 MCA1797R682 were used to amplify *pmoA1*, a down-regulated gene in the sMMO-expressing cells. PCR products were obtained from cells growing on no-added copper (lane 2, Figure 5.13) and added copper (lane 3, Figure 5.13) growth conditions. The band (493 bp) in lane 2 was relatively less intense than that in lane 3, indicating that *pmoA1* was transcribed in the presence and absence of copper.

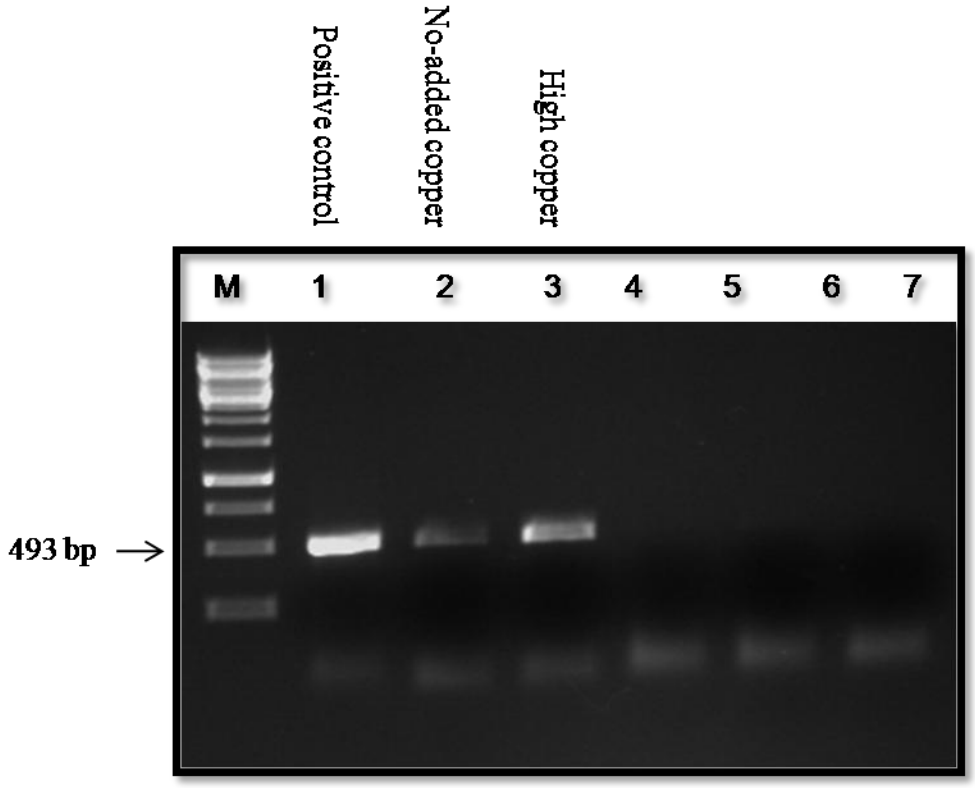

Figure 5.13 Agarose gel electrophoresis of RT-PCR of *pmoA* (189F/ 682R) from *Mc. capsulatus*. Lane 1 positive control genomic DNA from *Mc. capsulatus*; lane 2, cNDA derived from RNA which was extracted from no-added copper grown cells; lane 3, cDNA derived from RNA which was extracted from high copper grown cells; lane 4, RNA extracted from no-added copper grown cells; lane 5, RNA extracted from high copper grown cells and lane 6 negative control. The expected size is approximately 493 bp. M, size marker (bp), 1 kb DNA ladder (Invitrogen).

5.6 Transcriptional organization of the upstream genes of the sMMO operon

Checking the size of the intergenic spacer between the upstream genes of the sMMO operon revealed an overlap between the genes MCA1190 and MCA1191 and between MCA1191 and 1192, and 4 base pairs spacing between MCA1189 and MCA1190. These findings were encouraging to see if they are co-transcribed or not. To this end, total RNA was extracted from cells grown under no added copper (sMMO). Complementary DNA (cDNA) generated using Superscript II enzyme (Invitrogen) and gene-specific anti-sense primer (located at the end of MCA 1192(ER4859)), as described in Materials and Methods. Using cDNA as a template, the intergenic regions between each pair of adjacent genes (Figure 5.14) were amplified using specific primers using PCR. All primers used in this respect are listed in Table 5.5.

Table 5.5 A list of primers used for co-transcription

Primer	Sequences	Genes	Size (bp)
AF86	5' –CGGCGATGATGCCCAATACC-3	MCA 1187	630
AR715	5'-GCGATGTATTGCCGCTTGAG-3'	MCA 1188	
BF2133	5'-CATCGAGGATGGCATGTACG-3'	MCA 1188	396
BR2528	5'-CGAACATCAGGCCATGCTTG-3'	MCA 1189	
CF2889	5'-TGGCCGAGATCCGTGTCTAC-3	MCA 1189	370
CR3258 C	5'-ACAGGACCTCCTGCCAGAAC-3'	MCA 1190	
DF3847	5'-ATGGCTACGGTCGGGATCTG-3'	MCA 1190	330
DR4176	5'-CCGTCGTCACCGGTCAATAC-3'	MCA 1191	
EF4540	5'-GGTCCGTCTGGTTGGCTATC-3	MCA 1191	320
ER4859	5'-TCCCGCTGCACCAATGAATG-3'	MCA 1192	
FF31	5'-CCACCTCATGCTGCTGAAAC-3'	MCA 1192	810
FR840	5'- CCTGGATCAGGCATTGACTC-3'	MCA 1193	

As shown in Figure 5.14, PCR products with the expected sizes were obtained using primers spanning all inter-gene spaces MCA1188 to MCA1192. PCR products with sizes 369 (Figure 5.14b), 370 (Figure 5.14c), 330 (Figure 5.14d) and 320 (Figure 5.14e) bp

were obtained between each of the following pairs; MCA1188 and MCA1189; MCA1189 and MCA1190; MCA1190 and MCA1191 and MCA1191 and MCA1192 respectively. As expected, no PCR product was obtained using primers targeting the region between MCA1187 and MCA1188, because MCA1187 is predicted to be transcribed in the opposing direction. (Figure 5.14a). No PCR products were evident in the negative controls containing no RT, indicating no DNA contamination.

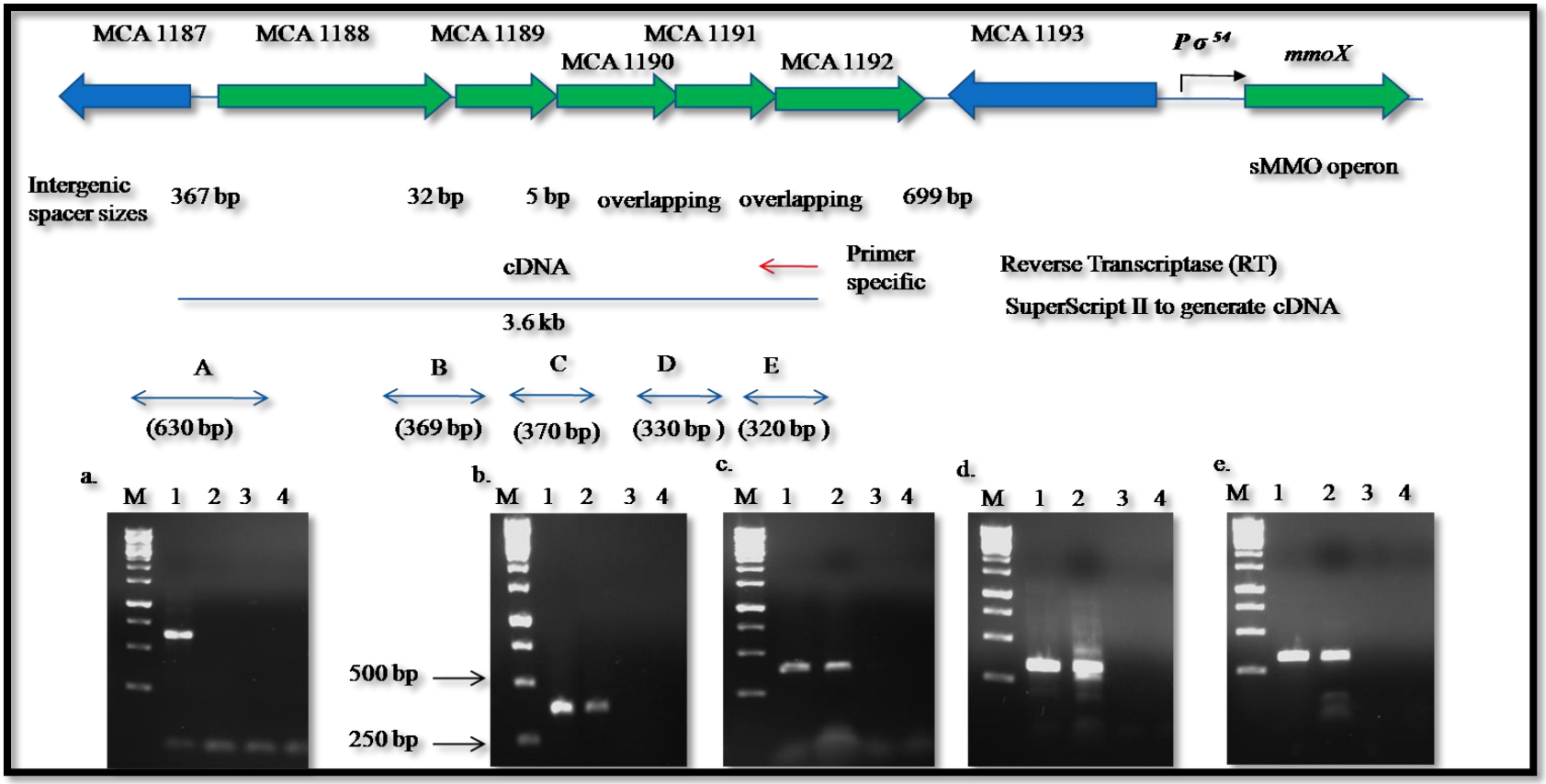

Figure 5.14 Co-transcription of the five genes (MCA 1188- MCA1192) upstream of the sMMO operon by reverse transcription PCR (RT PCR) of the intergenic regions between each pair of genes, A, MCA 1187 - MCA1188; B, MCA1188 - MCA1189; C, MCA1189 - MCA1190; D, MCA1190 - MCA1191 and E, MCA1191 - MCA1192. a, b, c, d and e corresponding agarose gels of the PCR targeting the regions of A, B, C, D and E respectively. Lane 1 genomic DNA from *Mc. capsulatus*; lane 2 cDNA from sMMO expressing cells; lane 3 RNA from sMMO expressing cells and lane 4 negative control. M, size marker (bp), 1 kb DNA ladder (Invitrogen).

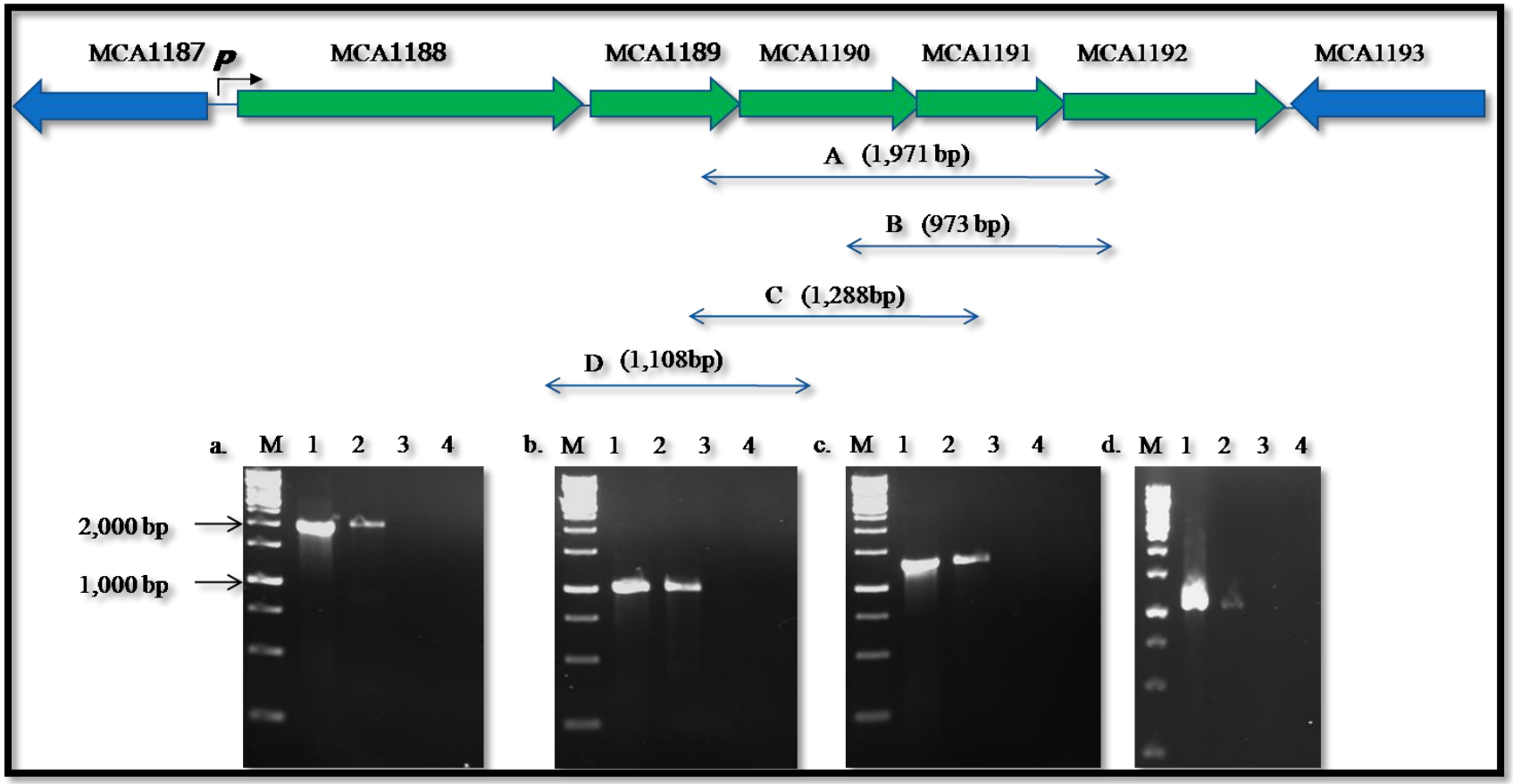

Figure 5.15 Co-transcription of the five genes (MCA 1188- MCA1192) upstream of the sMMO operon by reverse transcription PCR (RT PCR) of the DNA regions between each pair of genes, A, MCA 1189 - MCA1192; B, MCA1190 - MCA1192; C, MCA1189 - MCA1191 and D, MCA1188 - MCA1190. a, b, c and d agarose gels of the PCR targeting the corresponding regions of A (1, 971 bp), B (973 bp), C (1, 288 bp) and D (1, 108 bp) respectively. Lane 1 genomic DNA from *Mc. capsulatus*; lane 2 cDNA from sMMO expressing cells; lane 3 RNA from sMMO expressing cells and lane 4 negative control. M, size marker (bp), 1 kb DNA ladder (Invitrogen).

Furthermore, PCR products were obtained using primers targeting; MCA1189 and MCA1192; MCA1190 and MCA1192; MCA1189 and MCA1191 and MCA1188 and MCA1190. The sizes of these PCR products were 1,971 (Figure 5.15 a), 973 (Figure 5.15 b), 1,288 (Figure 5.15c) and 1,108 bp (Figure 5.15d) respectively. No PCR products were evident in the negative controls containing no RT, indicating no DNA contamination. These results indicated that MCA1188 to MCA1192 were co-transcribed and these genes are organized as an operon in *Mc. capsulatus*.

5.7 Promoter prediction

The organization of the five genes (MCA1188 to MCA1192) in one operon prompted investigation of the promoter region upstream of MCA1188 using free online prediction software. A promoter is defined as a regulatory DNA sequences located upstream of a gene, recognized by RNA polymerase, thus facilitating transcription.

-35 -10

-------TTGACA----------TATAAT----------

AGCTTGGTTCAGTACTATTGGTCAGAGTTATATGCATGGCTTATGA

CGATGGAATCAGGCGCCGCACCGGTGGCGGCGAGTCGTTGATATCAACCA

ACCAACAGGAGCGTATGGGATG

Figure 5.16 Predicted promoter sequences 5' of MCA1188 showing the transcription start site highlighted in red, start codon highlighted in green, possible -10 highlighted in yellow and -35 highlighted in blue. The underlined sequences are -10 and -35 consensus sequences σ^{70} promoter from *E. coli* (Harley and Reynolds, 1987).

Prediction of putative promoter sequences was carried out by examining about 400 bp sequences 5' of the predicted start codon of MCA1188 using BPROM-Prediction of

bacterial promoters online tool (http://www.softberry.com/). Putative promoter sequences were identified with transcription start sites; 131 bp (corresponding to -10 box) and 114 bp (corresponding to -35 box) upstream of the predicted start codon (Figure 5.16). However, experimental verification of the putative promoter sequences has yet to be carried out.

5.8 Discussion

This chapter describes *Mc. capsulatus* whole-genome transcriptomics experiments designed to identify genes transcribed differentially during growth on no-added copper (expressing sMMO) or high copper (expressing pMMO). The aim was to identify the key genes involved in MMO regulation assuming they will be up-regulated or down-regulated during growth using either sMMO or pMMO. Results of the microarray experiment revealed that 25 genes were found to be significantly up-regulated while 28 genes were down-regulated.

It was not surprising to note that the sMMO-encoding genes were among the twenty-five genes that were found to be highly up-regulated in *Mc. capsulatus* during growth on no- added copper versus high copper concentration growth conditions. It has been established from work done by many researchers that sMMO is expressed when copper is limited. For example, Choi *et al.*, (2003) found that the concentration of *mmoX* transcript was high as measured by quantitative RT-PCR, for cells growing in no-added copper medium. It is noteworthy that the regulatory gene, *mmoG* (MCA1202), which is annotated as a chaperonin, GroEL was up-regulated. It has been reported that *mmoG* is indispensible for sMMO expression (Csaki *et al.*, 2003) via initiation of transcription from the σ^{54} promoter (Ali, 2006). Similarly, the other regulatory gene *mmoR*, which encodes a σ^{54}-dependent transcriptional regulator, which is also essential for sMMO expression, was expressed above the 2-fold

threshold. These results confirm the essentiality of both *mmoG* and *mmoR* in sMMO expression. Nonetheless, *mmoS* and *mmoQ*, which are transcribed in the opposite direction to *mmoG*, were not up-regulated. *mmoS* and *mmoQ* encode a putative two component system (sensor-regulator) which was proposed to be involved in MMO regulation by sensing changes in copper levels and transfer the signals to MmoR (Csaki *et al.*, 2003). Contrary to this assumption, it has been shown that inactivation of *mmoQ* of *Mc. capsulatus*, using a transposon mutagenesis approach, resulted in a mutant that had no distinctive phenotype from the wild-type in terms of sMMO expression (Ali, 2006). Taking these results together with microarray results of *mmoQ*, it seems that this gene is unlikely to be involved in sMMO regulation.

It was interesting to find six up-regulated genes 5' of the sMMO operon, of which five (MCA1188 - MCA1192) were co-transcribed as an operon, indicating that they are organized in a polycistronic transcript. The first gene in this cluster is MCA1193, which is in close proximity to *mmoX*. However, BLAST analysis of the hypothetical protein product of this gene against the NCBI protein databases identified an *E. coli* Ras-like protein with a GTP/Mg^{2+} binding site. Looking at the literature, it was found that the *E. coli* Ras-like protein (Era) is loosely associated with the inner membrane and has GTPase activity. Furthermore, Era is likely to be essential for cell growth as inactivation of the *era* gene was lethal (March *et al.*, 1988). However, the exact function of Era of *E. coli* is unknown (Shimamoto and Inouye, 1996). The position of MCA1193 upstream of the sMMO operon and make this gene a candidate for further studies as it can be presumed that it has a role in sMMO regulation. MCA 1190 encodes a protein, which is likely to a member of the ferritin-like superfamily of di-iron-proteins. Ferritin is an iron-storage protein present in many living cells and is released in a controlled manner dependent upon the needs

of the cell (Halsey *et al.*, 2004). Whether MCA1190 is involved in expression, assembly or activity of the di-iron containing enzyme (sMMO) will require further studies to address this question. In addition, a synthesis of cytochrome c oxidase (ScO-1) encoding gene (MCA1191) was among these up-regulated genes. ScO-1 is predicted to have a copper-binding site (please see Chapter 6). MCA1192 is annotated as uncharacterized protein that is located 3' of the *scO-1*

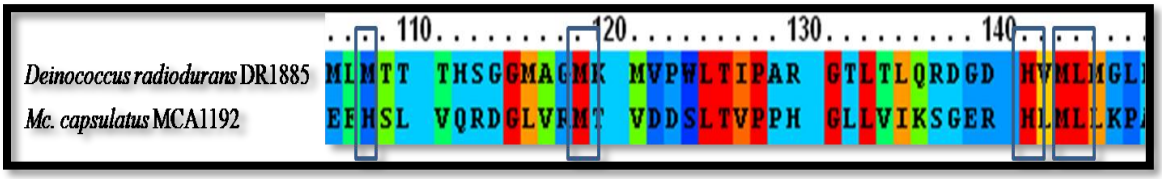

Figure 5.17 Partial sequence alignment of *Mc. capsulatus* MCA1192 (accession no. YP113657) and *Deinococcus radiodurans* DR1885 (accession no. NP295608) showing the metal-binding motif $H(M)X_{10}MX_{21}HXM$,the conserved residues are indicated in blue boxes, (unconserved 0 1 2 3 4 5 6 7 8 9 10 conserved).

Bioinformatic analyses of the genes close to the *sco-1* in many bacterial genomes identified, in a few species, an adjoining gene, which encodes a protein that is proposed to be a Cox17 homologue and has a metal binding motif (Banci *et al.*, 2005). The X-ray structure of one of these proteins, DR1885 from *Deinococcus radiodurans*, has been resolved and shown to bind copper via a metal binding motif (Banci *et al.*, 2005). Sequence alignments of DRA1885 and MCA1192 from *Mc. capsulatus* revealed that MCA1192 has the same metal binding motif $H(M)X_{10}MX_{21}HXM$ (Figure 5.17), indicating that this protein might bind copper. Taking together, the presence of predicted metal binding motifs in *scO-1* and MCA1192 and the juxtaposition of both genes upstream of the sMMO gene cluster indicate that these genes might be involved in MMO regulation in *Mc. capsulatus*. Therefore, the potential role of MCA1191 (*scO-1*) in MMO regulation in *Mc. capsulatus* is investigated in some details in Chapter 6. The fifth gene of the up-

regulated operon upstream of the sMMO gene cluster is MCA1988. This gene is annotated as a membrane-bound proton-translocating pyrophosphatase (PPases). The function of PPases is to utilize the energy released from pyrophosphate (PPi) hydrolysis to contribute to the electrochemical proton gradient of via translocating protons across the membranes (Maeshima, 2000). It has been reported that pyrophosphatase represents a complementary source of energy production for *Rhodospirillum rubrum* growing under insufficient energy conditions (*e.g.*, anoxia) (Garcia-Contreras *et al.*, 2004). One possible strategy of *Mc. capsulatus* to cope with the copper limiting growth conditions could be to over-express pyrophosphatases. It can be proposed that sMMO-expressing *Mc. capsulatus* requires more ATP for acquisition of metals (copper) essential for metabolic processes including those involving copper containing cytochrome oxidases.

Under low-copper growth conditions, the high expression level of gene (MCA0441) encoding a TonB copper-dependent receptor is indicative of its role in signal transmission (copper sensory) or iron transport. It has been proposed that copper-methanobactin (Cu-Mb) uptake is mediated via TonB receptors residing in the outer membrane then through TonB-ExbB-ExbD proteins and/or ABC transporters in the inner membrane (Figure 5.18) (Balasubramanian and Rosenzweig, 2008).

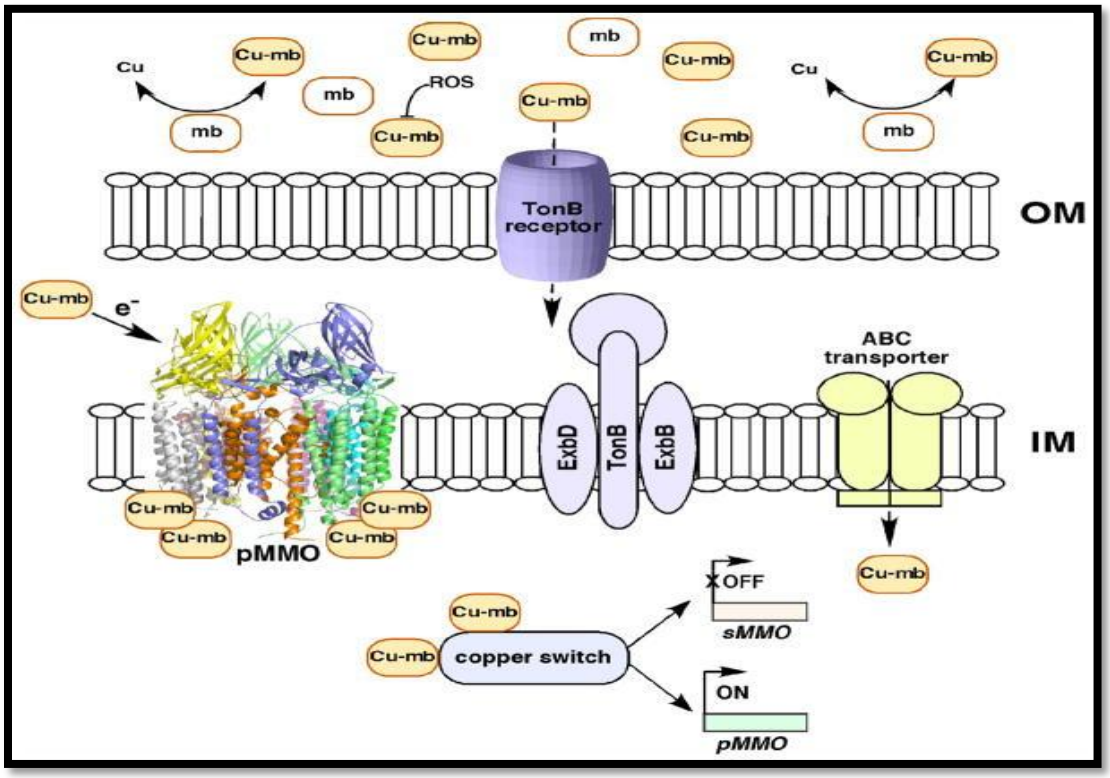

Figure 5.18 Schematic representation of proposed mechanism of copper uptake through the TonB receptor taken from Balasubramanian and Rosenzweig (2008).

It has been shown that TonB is used to import other metals, *e.g.*, nickel and iron (Schauer *et al.*, 2007). In *Helicobacter pylori*, a TonB/ExbB/ExbD dependent mechanism is used to import nickel across the outer membrane, while a permease is used to transport nickel through the inner membrane (Schauer *et al.*, 2007). It is of interest to explore in the future the possible role of MCA0441 in conjunction with the genes involved in Mb production. Among the up-regulated genes, some genes encode putative proteins that may be involved in post-transcriptional modification and cell signaling. These genes and their products will be potential targets for future mutagenesis and proteomics as they may be involved in MMO regulation.

Two different genes (MCA1101 and MCA2011) encoding for multicopper oxidase family proteins were differentially expressed; MCA1101 was up-regulated, while MCA2011 was down-regulated, indicating that each of them has a different

function in response to cellular copper levels. However, in general multicopper oxidases are involved in copper homeostasis. For example, multicopper oxidase was found to be essential in copper resistance in *E. coli* (Huffman *et al.*, 2002). These genes represent good candidates to be mutated for further insights about copper homeostasis and MMO regulation in *Mc. capsulatus*.

In addition, three up-regulated genes, MCA1023, MCA2477 and MCA1905 are probably involved in post-translational modification, proper stability and/or assembly of sMMO polypeptides.

The up-regulation of MCA2589 (*mopE*) is consistent with the results obtained by Karlsen *et al.* (2003) who indicated that *mopE* is induced when copper is limited and that MopE is a prominent surface protein of *Mc. capsulatus* (Karlsen *et al.*, 2008). Details about MopE are outlined in Section1.13, page 35. A gene (MCA2590) downstream (3') of *mopE* was also up-regulated. This finding is in accordance with that obtained by Karlsen *et al.*, (2005) who found both genes are co-transcribed and that a promoter is predicted upstream of MCA2590. MCA2589 is annotated as a cytochrome c peroxidase (CCP), which contains two haem groups each associated with a calcium binding motif. This protein was found to be a surface-associated protein which is a unique feature contrasting with the well-characterized CCP proteins that reside in the periplasm, therefore representing a novel group of CCPs (Karlsen *et al.*, 2005). Furthermore, MCA2590 showed sequence similarity to *mauG* which is involved in forming an indispensable prosthetic group (tryptophan-tryptophyl quinine) of methylamine dehydrogenase in many bacteria, for instance *Methylobacterium extorquens* AM1 (Chistoserdov *et al.*, 1994; Wang *et al.*, 2003; Pearson *et al.*, 2004). It has been suggested that *mopE* and MCA2590 are likely to have a correlated function; MCA2590 probably has a role in production of kynurenine

(product of tryptophan oxidation), which is involved in copper-binding in MopE (Karlsen *et al.*, 2011).

It is reasonable to find that both MCA2590 and the gene (MCA1907) encoding a calcium/proton transporter, were up-regulated. It is possible that both proteins are functionally linked. This is because cytochrome c peroxidase (CCP) has a calcium-binding motif in each of the two-haem groups, so it is likely to need the calcium. MCA1907 is probably involved in supplying the calcium requirement for CCP. This suggestion is strengthened by the work done on *Paracoccus denitrificans*, which showed that addition of calcium increased the activity of cytochrome c peroxidase (Prazeres *et al.*, 1995).

Furthermore, microarray results showed that 28 genes were down-regulated in *Mc. capsulatus* when comparing the transcriptome expression levels of cells expressing sMMO to those expressing pMMO. These included the two copies of the gene encoding pMMO and other genes scattered throughout the *Mc. capsulatus* genome. The products of some of these genes are hypothetical proteins with unknown functions, while others have some putative functions. Unlike sMMO, none of the down-regulated genes are in close proximity to the pMMO operon.

The genome of *Mc. capsulatus* has two complete sets of the genes (*pmoCAB*) encoding pMMO plus a third copy of *pmoC* (Stolyar *et al.*, 1999), both copies are under control of σ^{70} promoters (Stolyar *et al.*, 2001). Microarray results showed that the two copies were down-regulated during no-added growth conditions. There are conflicting reports about the transcription of the *pmoCAB* operons and whether they are constitutively expressed or they are induced by copper. However, results obtained by Ali (2006), who obtained consistent results from different molecular approaches, showed that the transcription from the pMMO σ^{70} promoter occurs regardless of the

absence or presence of copper in the growth medium of *Mc. capsulatus*. It can be concluded that the pMMO operon is transcribed at a low basal level when copper is absent and that in the presence of copper, the transcription of *pmoCAB* is significantly induced.

The gene (MCA2866) which encodes formaldehyde-activating enzyme, which has potential role in detoxifying formaldehyde (Vorholt *et al.*, 2000), was also down-regulated. This finding indicates that methane is metabolized into either cell biomass or energy production without accumulation of toxic levels of methanol and formaldehyde. However, it has been reported that inactivation of the gene (*fae*) encoding formaldehyde-activating enzyme of *Methylobacterium extorquens* resulted in a mutant which was unable to grow on methanol and was much more sensitive to methanol and formaldehyde (Vorholt *et al.*, 2000).

Another gene, which encodes TetR, was also down-regulated. TetR was originally identified as a regulatory protein that controls the expression of the gene encoding tetracycline resistance, but the description now covers a large family of transcriptional regulators that control many metabolic pathways (Ramos *et al.*, 2005). The down-regulation of this gene suggests that TetR may have a role either in the induction of transcription of the pMMO operon or in the repression of the sMMO operon via direct involvement in transcription/translation or through other proteins in cascade events.

The concomitant low expression of both MCA2079 and MCA2381, which encode acetylornithine aminotransferase and the MxaD, indicated that they might be involved in the biosynthesis of polyketides.

Three genes encoding different ribosomal proteins (S9, S15 and S16) which are small ribosomal proteins involved in the assembly of the ribosome were down-

regulated. It is well known that gene regulation takes place at different levels; one of which is the translational level in which a repressor protein binds mRNA thus blocking the translation process. Ribosomal proteins (*e.g.*, S15) are found to have regulatory roles during the early stage of translation via interactions with mRNA (Marzi *et al.*, 2007). Applying this scenario to MMO regulation in *Mc. capsulatus*, one can hypothesized that these ribosomal proteins may have a regulatory role in controlling pMMO production by inhibiting translation of the *pmoCAB* transcript into active protein when copper is limited. This assumption runs in parallel with the suggestion that pMMO is regulated at post-transcriptional level (Ali, 2006). It has been reported that microRNAs, small RNA molecules regulated by copper are involved in copper homeostasis (Burkhead *et al.*, 2009). If MMO regulation takes place with the involvement of microRNA, a new and exciting perspective will emerge in understanding of the mechanisms of the copper switch between sMMO and pMMO in *Mc. capsulatus*.

An attempt was made to validate the results of the microarray experiments using reverse transcription quantitative PCR (RT-qPCR). A selection of up-regulated and down-regulated genes and housekeeping genes were checked for their expression levels using RT-qPCR. However, results were inconclusive. This can be attributed to formation of primer dimers and amplifications occurring non-specifically. Therefore, it is important to optimize the conditions for RT-qPCR by trying different dilutions of the primers and targets, as well as by changing or optimizing primer sequences; however, no further attempts were made due to time limitations.

It is worth mentioning that although reverse transcription PCR is not used as an accurate quantitative approach for gene expression level studies, it provides an indication of the relative abundance of transcripts in the samples. Using ordinary

reverse transcription PCR, data for *scO-1* and MCA1192 were validated. These observations indicate that these two genes are highly induced in *Mc. capsulatus* expressing sMMO compared to cells-expressing pMMO.

Collectively, the data outlined in this chapter represent the first study, to our knowledge, exploring the whole-genome expression profiling of *Mc. capsulatus* transcriptomics growing on no-added copper (expressing sMMO) or high copper (expressing pMMO). Some interesting genes were differentially expressed; up-regulated (*e.g.*, *tonB*) or down-regulated (*e.g.*, *tetR*) under these conditions. These genes are proposed to be excellent candidate genes for further studies to give more insights for understanding the mechanisms of not only MMO regulation, but also copper homeostasis.

Chapter 6

Investigating the potential role of *scO-1* in regulation of methane monooxygenase in *Mc. capsulatus*

6.1 Introduction

Synthesis of Cytochrome c Oxidase (ScO) family proteins are ubiquitous in living cells, for instance, bacteria, yeast, plants and human. These proteins are composed of membrane-anchored region and a cytoplasmic soluble domain. They contain a metal binding motif CXXC and a conserved histidine ligand through which they bind copper and a transmembrane helix in the amino-terminal region (Banci *et al.*, 2007). ScO protein was first identified in yeast by Schulze and Rödel (1988) and was proposed to be essential for cytochrome c oxidase (COX) assembly through its function in copper delivery (Glerum *et al.*, 1996). It has been reported that inactivation of *scO* led to severe COX deficiency in humans (Valnot *et al.*, 2000), in *Bacillus subtilis* (Mattatall *et al.*, 2000) and in yeast (Glerum *et al.*, 1996). Recently, it has been suggested that ScO has additional roles such as signal transmission through oxidation-reduction reactions, delivers copper to the enzymes that require copper and protecting cells from oxidative stress (Banci *et al.*, 2011).

As described in Chapter 5, the microarray results of whole-genome transcriptome analysis of *Mc. capsulatus* indicated that a cluster of five genes upstream of the sMMO gene cluster was up-regulated under low copper (sMMO-expressing) growth conditions. One of these genes was MCA1191 (designated *scO-1*) which was annotated as a ScO family protein (ScO-1). Furthermore, the proximity of *scO-1* to the sMMO operon and the presence of a predicted copper-binding motif in *Mc. capsulatus* ScO-1 were two more reasons that prompted the investigation in detail of this gene and its possible role in MMO regulation.

The work in the chapter aimed at investigating whether or not *scO-1* has a role in the copper switch in *Mc. capsulatus*. To this end, a mutant in *Mc. capsulatus*

scO-1 was constructed using a marker-exchange mutagenesis technique and the resultant Δ*scO-1* mutant strain was then characterized.

6.2 Features of ScO-1 of *Mc. capsulatus*

scO-1 is a gene upstream of the sMMO gene cluster that was up-regulated based on the microarray results under low (sMMO-expressing) versus high (pMMO) growth conditions. This *orf* encoded a putative ScO-1 protein of 220 aa residues. Multiple amino acid sequences alignment analyses revealed high homology of *Mc. capsulatus* ScO-1 to the well-characterized ScO from human (Valnot *et al.*, 2000); yeast (Glerum *et al.*, 1996 and Abajian and Rosenzweig 2006); *Bacillus subtilis* (Mattatall *et al.*, 2000); (*Pseudomonas putida* (Banci *et al.*, 2011); *Agrobacterium tumefaciens* (Saenkham *et al.*, 2009) and *Rhodobacter capsulatus* SenC (Swem *et al.*, 2005). Furthermore, *Mc. capsulatus* ScO-1 appeared to be characterized by the following features: (1) presence of two conserved cysteines in a CXXC motif and a histidine residue which may be involved in copper binding; (2) presence of two invariant aspartates in a DXXXD motif which are likely to be indispensable for ScO-1 activity (Arnesano *et al.*, 2002); (3) presence of a YRVYF region which is proposed to be involved in protein-protein interactions with Cox2 (Figure 6.1) (Rigby *et al.*, 2008) and (4) presence of a predicted transmembrane helix length between 16 and 38 (Figure 6.2).

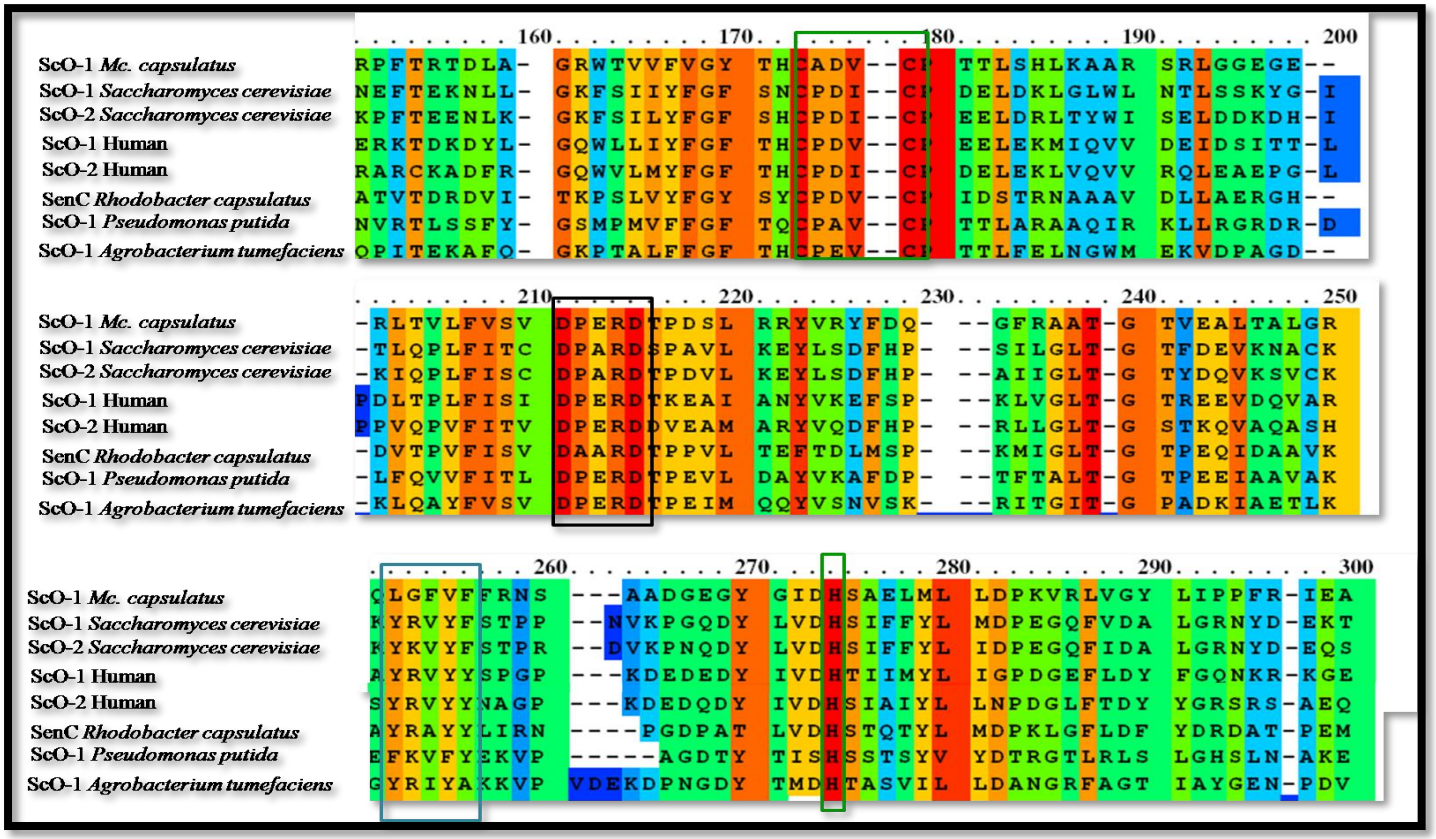

Figure 6.1 Partial multiple sequence alignment of *Mc. capsulatus* ScO-1 (accession no. YP113656), *Saccharomyces cerevisiae* ScO1 (accession no. P23833) and ScO2 (accession no. P38072), human ScO1 (accession no. O75880) and ScO2 (accession no. O43819), *Pseudomonas putida* ScO1 (accession no. NP744528), *Agrobacterium tumefaciens* ScO1 (accession no. NP_355038) and *Rhodobacter capsulatus* SenC (accession no. Q52720) amino acid sequences, showing the conserved CXXC motif and histidines (green box); DXXXD motif (black box) and YRVYF motif (blue box).

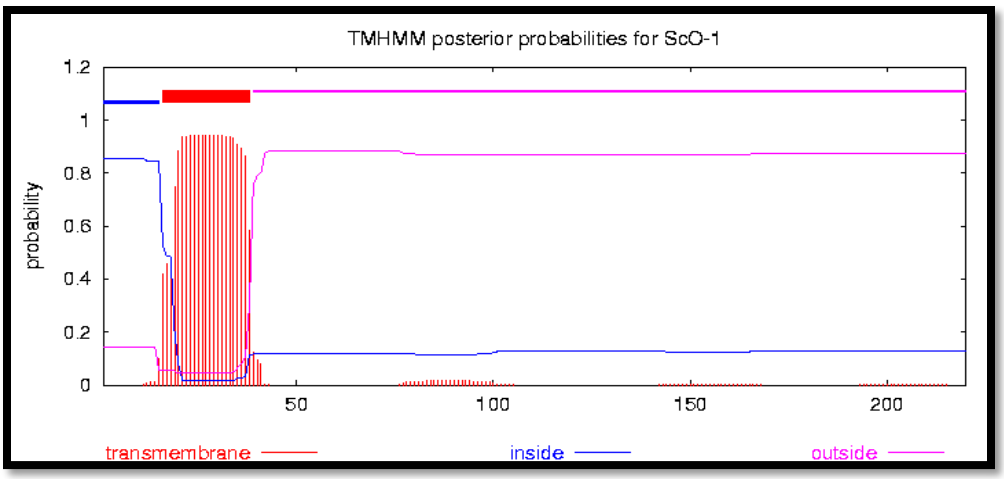

Figure 6.2 Transmembrane prediction in *Mc. capsulatus* ScO-1 using TMHMM (Krogh *et al.*, 2001). Transmembrane helices are shown as red bars, extracellular loops as pink lines and intracellular loops as blue lines.

6.3 Mutagenesis of *Mc. capsulatus scO-1*

A marker-exchange mutagenesis technique was used to create mutant in *Mc. capsulatus scO-1* to explore its potential function. A schematic diagram illustrating the strategy used for constructing *Mc. capsulatus* Δ*scO-1* is presented in Figure 6.3. Two DNA regions of *scO-1* were amplified by PCR and designated arm A and arm B, respectively (Figure 6.3a). The primer pair designated as SCO-1AF68-*Xba*I and SCO-1AR1557- *Sph*I were used to obtain arm A (542 bp) while arm B (565 bp) was obtained via SCO-1BR589-*Hin*dIII and SCO-1BF25- *Sph*I. Primers used to generate Δ*scO-1* are presented (Table 6.1). To enhance the ligation of the arms A and B into pK18mobs*acB*, the cloning vector, restriction sites were added upstream of the primers targeting the two arms, *i.e.* *Xba*I and *Sph*I to arm A and *Sph*I and *Hin*dIII to arm B. Arms A and B were cloned into pK18mobs*acB* to give the intermediate construct pAK05. The final construct pAK055A was obtained by cloning the gentamicin resistance cassette (913 bp *Sph*I fragment) into pAK05 (Figure 6.3c). *E. coli* S17.1 λ*pir* (Herrero *et al.*, 1990) was transformed with pAK055 via electroporation. Conjugation was carried as described by Martin and Murrell (1995).

NMS medium supplemented with a gentamicin concentration of 5 µg ml^{-1} was used for initial selection of single and double homologous transconjugants. To ensure complete removal of *E. coli* that might be present as background, colonies of the resultant *Mc. capsulatus* were streaked onto NMS agar plates containing nalidixic acid (10 µg ml^{-1}) and incubated at 45 °C in the presence of methane for one week. Double homologous recombinants were then identified by streaking on NMS plates with gentamicin (5 µg ml^{-1}) or kanamycin (15 µg ml^{-1}). Double homologous recombinants were identified as gentamicin resistant and kanamycin sensitive colonies, which had lost the vector backbone including the kanamycin resistance cassette. The genotype of resultant mutant, which named *Mc. capsulatus* Δ*scO-1* was proved by PCR using SCO-1USF, the forward primer and SCO-1DSR, the reverse primer. The PCR product with the right size was then sequenced for further confirmation. The resultant Δ*scO-1* mutant contained a deletion of 394 bp from *scO-1* and insertion the gentamicin resistance cassette (913 bp).

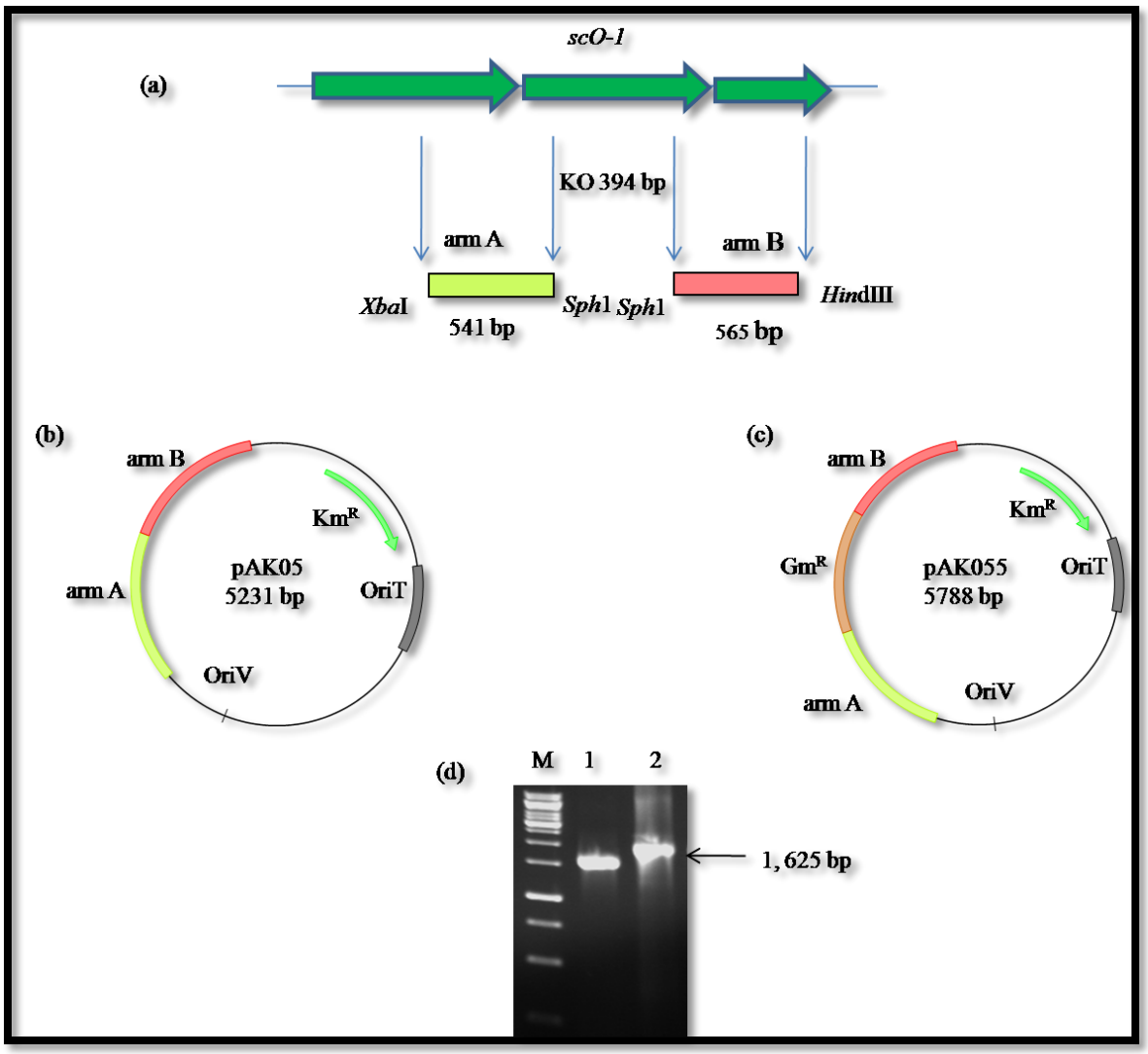

Figure 6.3 The strategy followed for constructing *Mc. capsulatus* Δ*scO-1*. (a) *scO-1* showing the two DNA target arms used for cloning. *Xba*I and *Sph*I and *Sph*I and *Hin*dIII restriction sites were incorporated via PCR to arm A and arm B respectively. (b) pAK05, the intermediate plasmid construct with arms A and B. (c) pAK055, the plasmid construct containing the with gentamicin cassette (brown) inserted in via *Sph*I restriction site between arms A and B. (d) Confirmation of *Mc. capsulatus* Δ*scO-1* strain. lane 1, PCR using DNA extracted from the wild-type strain; lane 2, *Mc. capsulatus* Δ*scO-1* mutant strain. The size of the PCR product obtained with primers (SCO-1USF and SCO-1DSR) using DNA wild-type (1,106 bp) is smaller than that of the double cross-over Δ*scO-1* mutant (1,625 bp).

Table 6.1 Primers used in the construction of *Mc. capsulatus* Δ*scO-1* and in confirmation of the genotype. Restriction sites that were added 5' of each primer are highlighted in bold and underlined

Primer name	Sequences	PCR product
SCO-1AF68-*Xba*I	5-**TCTAGA**TCCTGCCGCCAGAGATGTTC-3'	A
SCO-1AR1557-*Sph*I	5-**GCATGC**ACTAAGACCGAGGGCCAGAG-3'	
SCO-1BF25- *Sph*I	5'-**GCATGC**TCCGTCTGGTTGGCTATCTG-3'	B
SCO-1BR589-*Hin*dIII	5'-**AAGCTT**GATCCGCTGACACAAACCAC-3'	
SCO-1USF	5'-TCGCCGATTTCGTATTTGACC-3'	
SCO-1DSR	5'-TTCGGATCGAGCAACATCAG-3'	

6.4 Characterization of *Mc. capsulatus* Δ*scO-1*

6.4.1 Naphthalene oxidation assay

To investigate the effect of mutagenesis of *scO-1* on the expression of sMMO, the naphthalene oxidation assay was carried out. *Mc. capsulatus* wild-type and Δ*scO-1* were grown on NMS medium supplemented with copper at the following concentrations: 0, 0.5, 1.0, 1.5, 2.0, 2.2, 2.4 or 3.0 µM copper. This assay was performed as in Materials and Methods. Δ*scO-1* appeared to follow the same trend as the wild-type strain, based on sMMO activity using the naphthalene assay (Table 6.2). Under low copper concentration growth conditions (less than 2.0 µM added copper) both strains gave a purple colour upon addition of the reagent indicating that they both expressed the sMMO enzyme, which oxidized naphthalene into naphthol. However, none of the strains expressed sMMO when grown at 2.0 µM added copper or at any of the higher concentrations. In an attempt to find a phenotypic difference between the wild-type and Δ*scO-1* strain in terms of sMMO expression, a copper-specific chelator was added to NMS medium with no-added copper. Addition of 150

µM bathocuproine disulfonate (BCS) did not reveal any differences between the wild-type and Δ*scO-1* (data not shown). Both strains gave a purple colour indicating sMMO expression under the conditions tested.

Table 6.2 Results of naphthalene oxidation assay under different copper concentrations. These experiments were done in triplicate.

Copper (µM)	**0**	**0***	**0.5**	**1.0**	**1.5**	**2**	**2.2**	**2.4**	**3**
Wild-type	+	+	+	+	+	-	-	-	-
Δ*scO-1*	+	+	+	+	+	-	-	-	-

*No added copper plus 150 µM BCS

6.4.2 Growth under different copper concentrations

Further experiments were done to investigate if there was a distinctive phenotype between *Mc. capsulatus* wild-type and Δ*scO-1* strains. One of these experiments was to explore the response of the strains to high copper concentrations. To this end, Δ*scO-1* was compared to the wild-type for its ability to grow on NMS plates supplemented with different concentrations of added copper 10, 25, 50, 60, 75, 85, 100 and 125 µM.

Table 6.3 Results of growth of Δ*scO-1* and *Mc. capsulatus* wild-type strains on NMS agar with varying copper concentrations. These experiments were done in triplicate.

Copper (µM)	**10**	**25**	**50**	**60**	**75**	**85**	**100**	**110**	**125**
Wild-type	+	+	+	+	+	-	-	-	-
Δ*scO-1*	+	+	+	+	+	+	+	-	-

* + good growth
* - no growth

Both Δ*scO-1* and wild-type strains grew well at relatively low and moderate concentrations of copper (10, 25 or 50 µM) (Table 6.3). However, it seemed that Δ*scO-1* strain was more resistant to higher copper than the wild-type organism. Δ*scO-1* exhibited reasonable growth at a copper concentration of 85 or 100 µM (Figure 6.4)

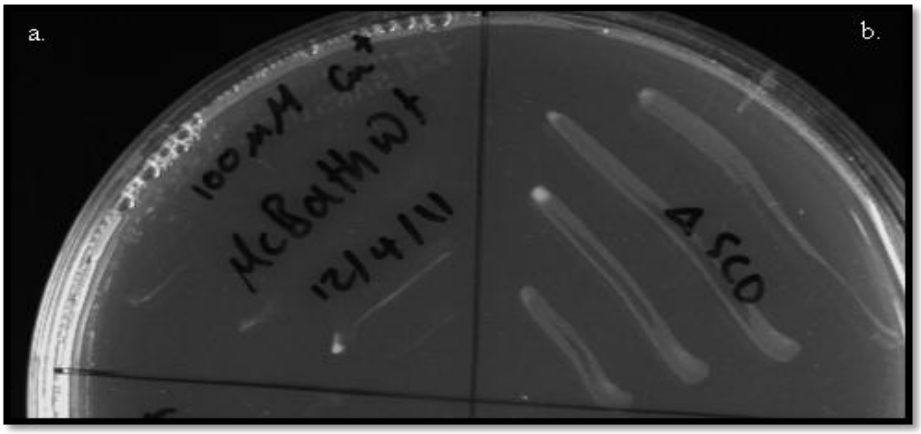

Figure 6.4 Growth of *Mc. capsulatus* wild-type (a) on NMS supplemented with 100 µM added copper compared to *Mc. capsulatus* Δ*scO-1* (b).

while the wild-type organism could only grow up to a copper concentration of 75 µM. The growth of Δ*scO-1* strain ceased at 110 µM copper (Table 6.3).

6.4.3 Growth patterns of Δ*scO-1* at different copper concentrations

The effects of increasing copper concentrations on the growth patterns of *Mc. capsulatus* Δ*scO-1* and wild-type were investigated in liquid culture. The growth of both strains was monitored on NMS medium amended with 0, 10 or 50 µM copper concentrations by recording the optical density (OD_{540}) (Figure 6.5). The findings in Table (6.4) showed that as the copper concentration of NMS increased, the specific growth rates (µ) decreased and the doubling times increased. No significant differences in specific growth rates between Δ*scO-1* strain and the wild-type were observed at no-added copper (Figure 6.5A) and with 10 µM added copper (Figure 6.5B) growth conditions. However, Δ*scO-1* grew significantly better at a high copper concentration (50 µM copper) (Figure 6.5C) with $\mu = 0.04\ h^{-1}$ ($P < 0.001$) than the wild-type, which struggled to grow at that concentration as indicated by a much slower growth rate and longer doubling time (Table 6.4).

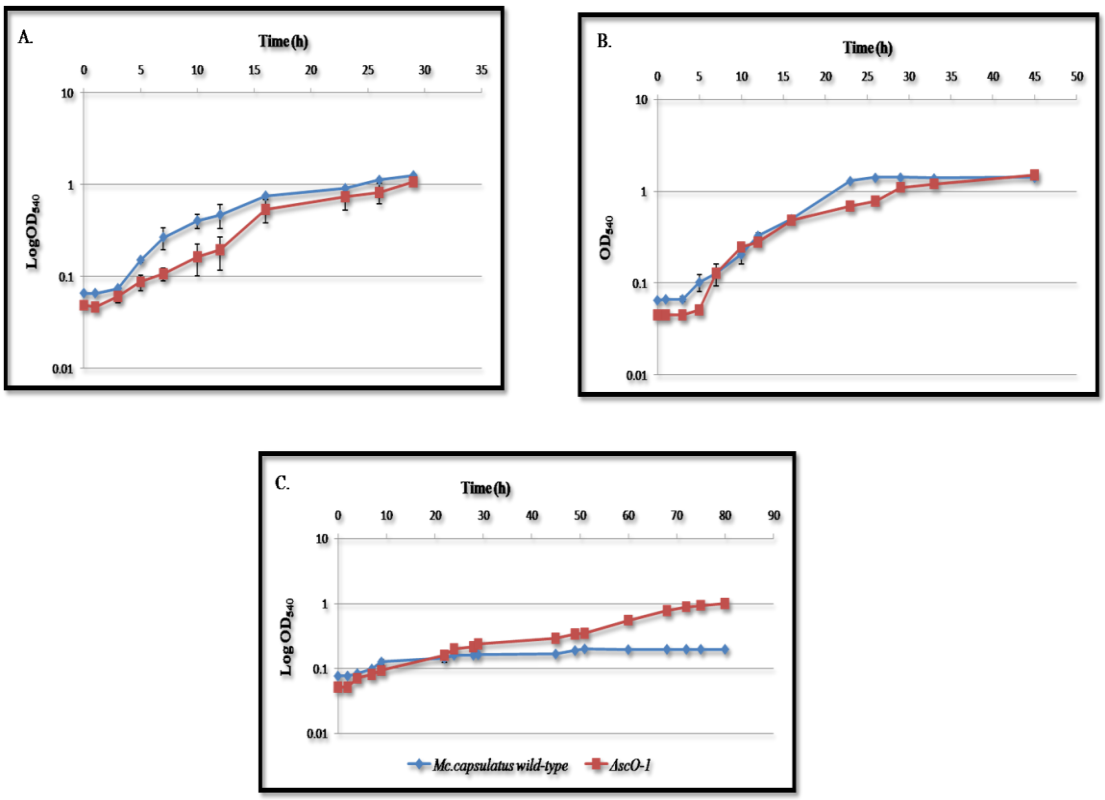

Figure 6.5 Growth of wild-type and Δ*scO-1* mutant *Mc. capsulatus* on NMS supplemented with no added copper (A), 10 µM (B) and, 50 µM added copper (C). All data points represent the mean of three replicates and error bars indicate the standard deviation.

Table 6.4 Specific growth rates and doubling times of *Mc. capsulatus* wild-type and Δ*scO-1* growing on NMS amended with different concentrations of copper. Figures are the mean of three replicates ± standard deviation.

	Specific growth rate (h^{-1})					Doubling time (h)		
Copper (µM)	**0**	**10**	**50**			**0**	**10**	**50**
Wild-type	0.16 ± 0.007	0.12 ± 0.005	0.003 ± 0.0008			4.1 ± 0.05	5.4 ± 0.07	177.7 ± 8
Δ*scO-1*	0.15 ± 0.008	0.11 ± 0.004	0.040 ± 0.006			4.4 ± 0.009	6.8 ± 0.06	16.5 ± 0.9

These results were in general congruent with MIC data, strengthening the conclusion that Δ*scO-1* is likely to be a copper-resistant mutant compared to the wild-type.

6.4.4 Mb production assay

To gain further insights into the copper resistance phenotype of Δ*scO-1* it was useful to assess Mb production by this mutant compared to the wild-type. The aim of this experiment was therefore to see if there were any differences between *Mc. capsulatus* wild-type and the Δ*scO-1* strain for the production of Mb. The assay was carried out as described in Chapter 4 and in Materials and Methods.

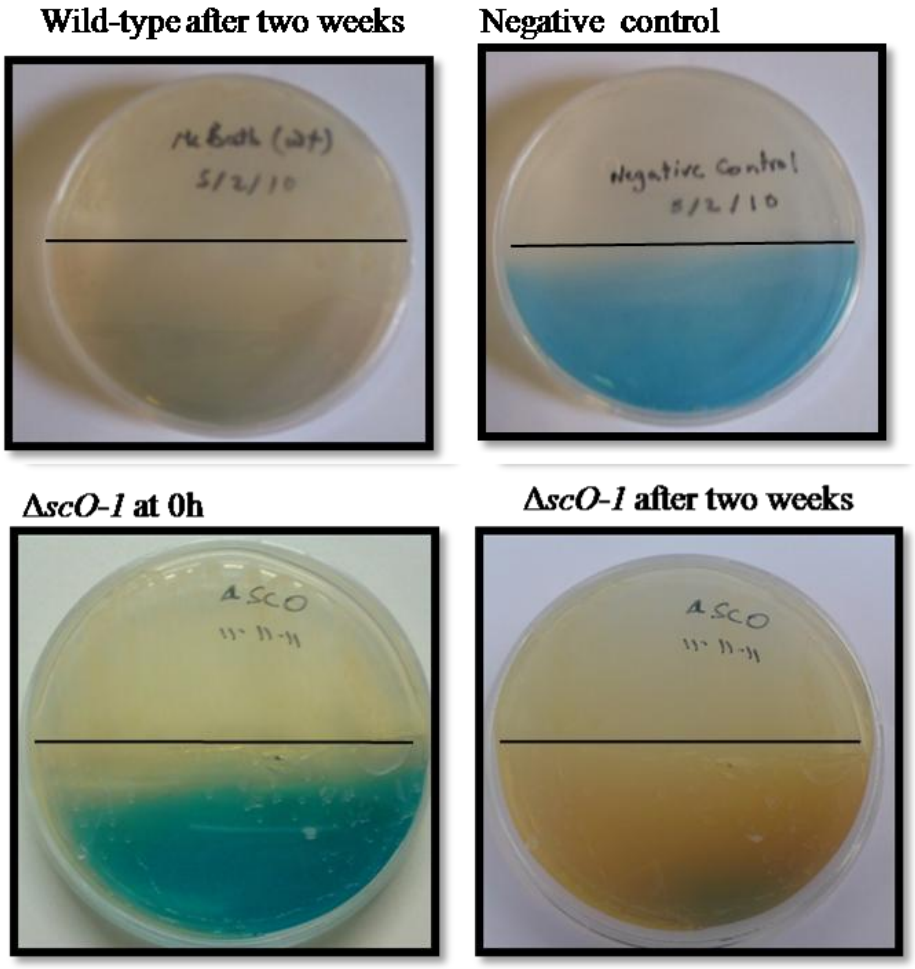

Figure 6.6 Results of Mb production using CAS-plates of *Mc. capsulatus* (wild-type) and the Δ*scO-1* incubated for two weeks. Negative control: where no bacteria were streaked, Δ*scO-1* 0h: Δ*scO-1* at the starting time. These experiments were done in triplicate.

The results obtained in Figure 6.6 showed that both wild-type and the Δ*scO-1* strains exhibited a complete colour shift from blue to yellow after 14 days incubation. As expected, no change in the blue colour was observed in the negative control plate

(Figure 6.6). This finding suggests that there is no involvement of ScO-1 in synthesis of Mb.

6.4.5 Intracellular copper measurements using inductively coupled plasma mass spectrometry (ICP-MS)

The intracellular copper measurements of the Δ*scO-1* and wild-type strains were carried out according to the method described Gonzalez-Guerrero *et al.* (2010b) with the modifications illustrated in Figure 6.7.

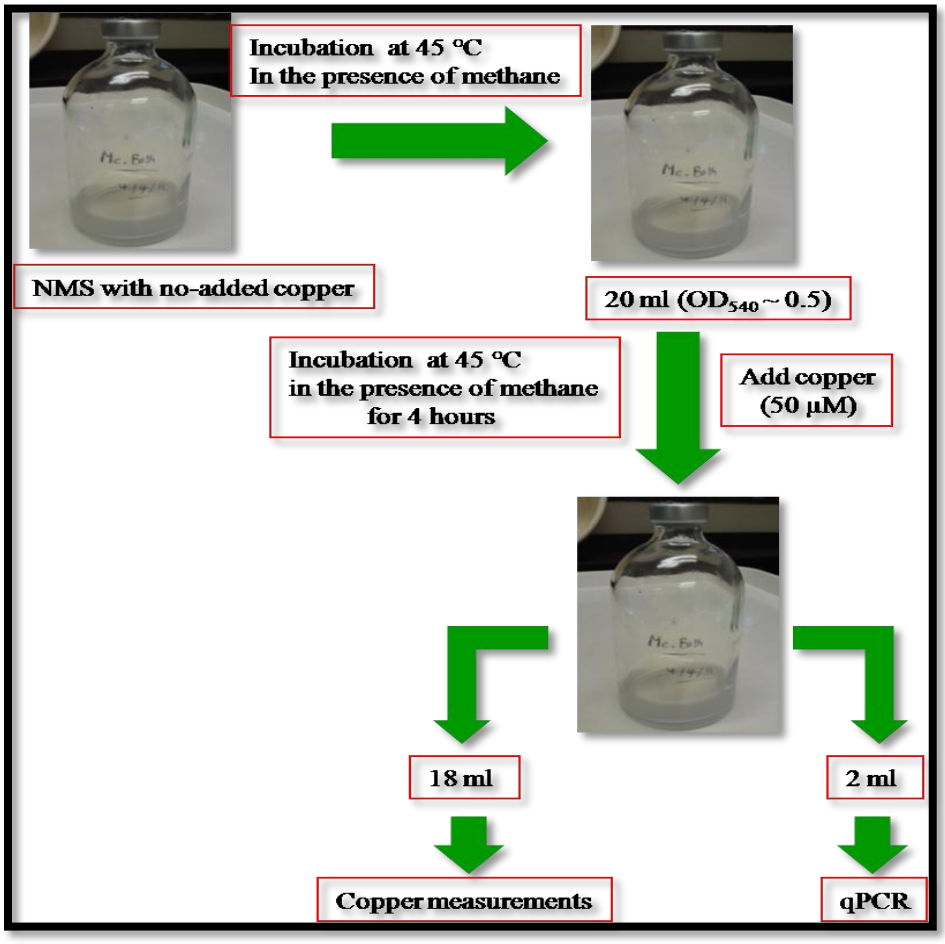

Figure 6.7 Strategy used for copper measurements of *Mc. capsulatus* (wild-type) and Δ*scO-1* strains. The experiment was performed in triplicate.

Twenty millilitres of wild-type and Δ*scO-1* cultures (OD_{540} ~ 0.5) were exposed to 50 µM copper and incubated for 4 hours in the presence of methane (10% v/v) (Figure 6.7). Sample preparation was carried out as described in Materials and Methods.

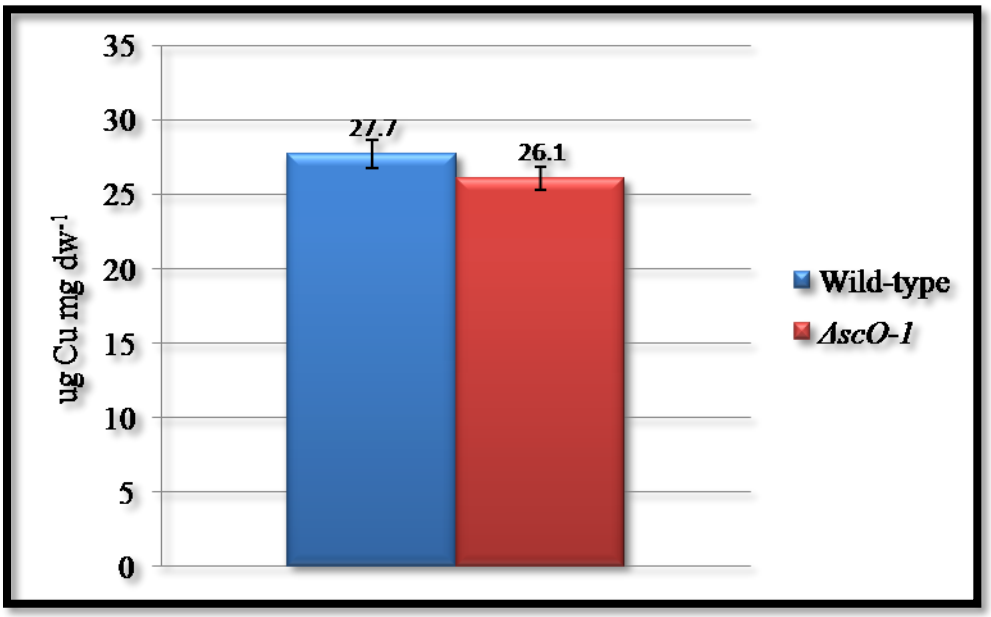

Figure 6.8 Intracellular copper measurements wild-type and Δ*scO-1* cultures exposed to 50 µM added copper for four hours. Figures are mean of three replicates and error bars indicate the standard deviation

The intracellular copper concentration of the wild-type and Δ*scO-1* cells was then quantified using ICP-MS, by Warwick Analytical Service. As can be seen in Figure 6.8, there was no significant difference between Δ*scO*-1 strain and the wild-type in terms of the intracellular copper concentration. It is worth mentioning that 2ml of the samples used for copper measurement was stored at -80 ºC for RNA extraction in order to study the expression level using quantitative PCR (qPCR) of some of the genes encoding for the copper transporters, however, due to lack of time, this experiment was abandoned.

6.4.6 Determination of methane oxidation rate by oxygen uptake using an oxygen electrode

The oxygen consumption rate of whole cells of *Mc. capsulatus* wild-type and Δ*scO-1* grown on methane was estimated using a Clark oxygen electrode (Rank Brothers Ltd, Cambridge, UK). Oxygen consumption was measured in response to addition of substrate. Initially, wild-type and Δ*scO-1* were grown on NMS liquid medium with no added-copper or with 30 µM copper until they reached late exponential phase (OD_{540}). Cells (2 – 5.5 mg dry weight) were used in the oxygen electrode and oxygen consumption measured in response to the addition of methane (15 nmol).

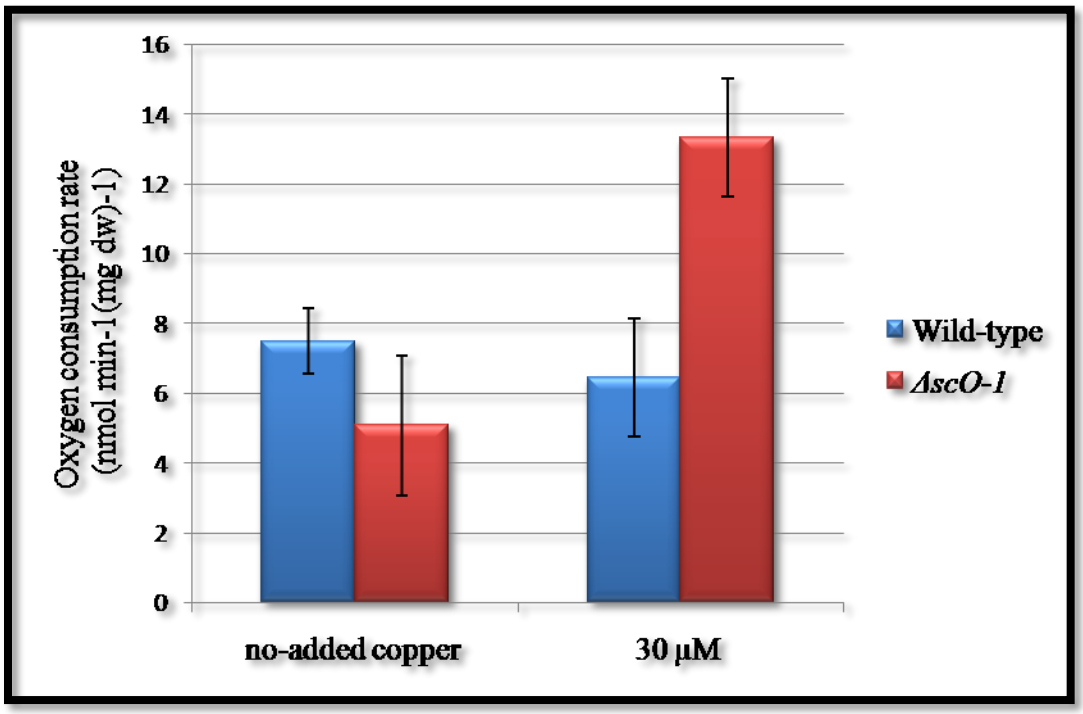

Figure 6.9 Oxygen consumption rate of *Mc. capsulatus* wild-type and Δ*scO-1* growing on no-added copper or with 30 µM added copper using Clark oxygen electrode. The rate is expressed in nmol O_2 min^{-1}(mg $dw)^{-1}$. Figures are mean of three replicates and error bars indicate the standard deviation.

As can be seen in Figure 6.9, under no added copper growth conditions, Δ*scO-1* showed no significant difference in the rate of oxygen consumption compared to the

wild-type strain. However, when cells were grown on NMS medium supplemented with 30 µM added copper, the Δ*scO-1* strain exhibited more than 2-fold higher oxygen consumption rate than the wild-type($P < 0.05$). These results were consistent with those for growth under different copper concentrations. The activity of the mutant is increased relative to the wild-type with the increase in added copper.

6.4.7 Cytochrome oxidase

To gain further insight into the possible function of *Mc. capsulatus scO-1*, cellular oxidase activity using N, N, N′, N′–tetramethyl–p–phenylenediamine (TMPD) as an artificial hydrogen donor was estimated in wild-type and Δ*scO-1* at no-added and 10 µM copper, as described in Materials and Methods. The results obtained showed no significant differences between Δ*scO-1* and wild-type (Figure 6.10) were observed at both concentrations of copper examined. These results suggested that inactivation of *scO-1* did not affect the cytochrome oxidase activity of *Mc. capsulatus* grown under the conditions tested.

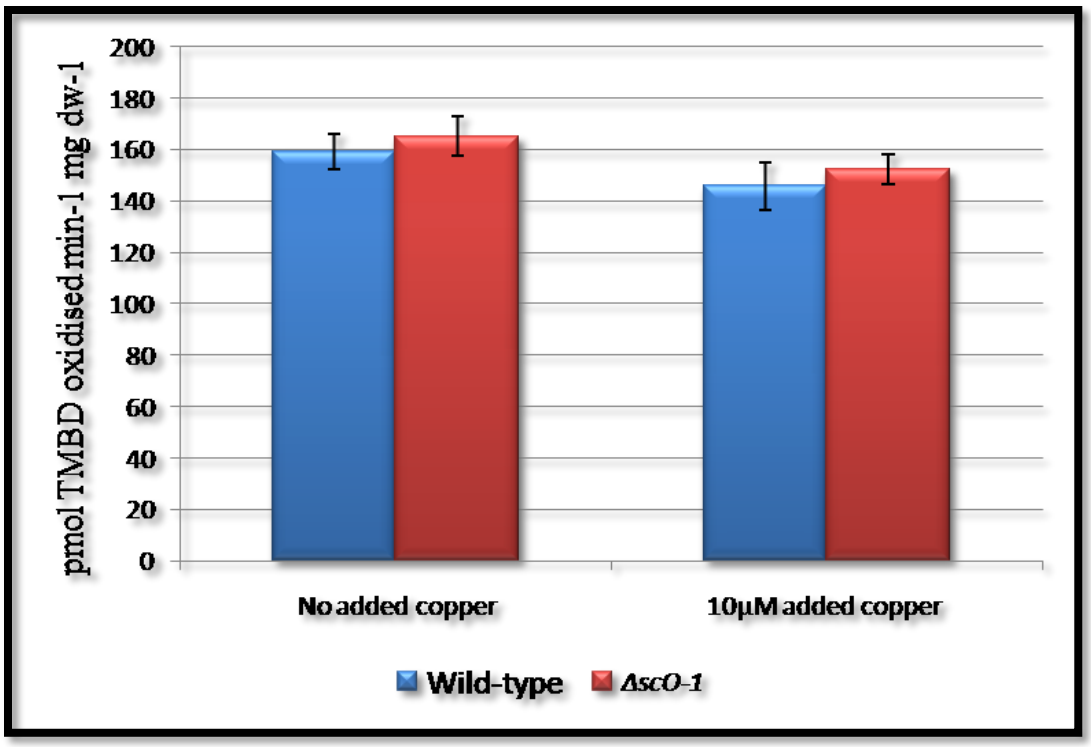

Figure 6.10 Cytochrome oxidase activity of whole cells of *Mc. capsulatus* Δ*scO-1* and *Mc. capsulatus* wild-type in NMS with no-added copper and with 10 µM added copper. Figures are mean of three replicates and error bars indicate the standard deviation

6.5 Discussion

To take advantage of the microarray results of whole-genome transcriptome analysis of *Mc. capsulatus* as described in Chapter 5, a representative of the up-regulated genes under no-added copper growth conditions was selected for further investigation. *Mc. capsulatus scO-1* was mutated to see whether or not it has a role in MMO regulation. The rational of selecting *scO-1* is the proximity of *scO-1* to the sMMO-encoding operon and the presence of the copper-binding motif.

Mc. capsulatus ScO-1 shared the common characteristics of the well-studied ScO from other organisms *e.g.*, human (Valnot *et al.*, 2000), yeast (Glerum *et al.*, 1996) and *Pseudomonas putida* (Banci *et al.*, 2011), as revealed by multiple amino acid sequence alignment analyses. This indicated that *Mc. capsulatus* MCA1191 is likely to be correctly annotated as ScO.

Contrary to our initial expectation, Δ*scO-1* showed no distinctive phenotype from the wild-type as indicated by the naphthalene oxidation assay which is a qualitative test for the expression of sMMO. These results show that *scO-1* is has no indispensable role in MMO regulation in *Mc. capsulatus*. However, it is of interest to determine the pMMO and sMMO activities under different copper regimes in future studies.

Successful attempts have been made to find a characteristic phenotypic difference between Δ*scO-1* and wild-type. Growth under various concentrations of copper formed the basis of these approaches. The Δ*scO-1* strain exhibited a more rapid specific growth rate (Figure 6.5C and Table 6.4) and a higher rate of methane-stimulated oxygen consumption (Figure 6.9) when grown at high copper levels compared to the wild-type. Similar results in growth pattern in response to added copper growth conditions were obtained in *scO* mutants in *Streptomyces*. *Streptomyces coelicolor* and *S. griseus* Δ*scoC* strains were found to produce about three-times more cell biomass when growing on medium supplemented with 10 µM copper compared to the wild-type strain (Fujimoto *et al.*, 2011). It is difficult to provide a clear-cut explanation for this phenotype due to lack of data regarding other potential factors that may interfere with ScO. For example, the activities of copper-requiring enzymes (particularly pMMO) and copper independent oxidases have yet to be determined. However, the following hypothesis is proposed in an attempt to explain the behaviour of that mutant. Inactivation of ScO-1 might lead to a cellular disorder in copper homeostasis in *Mc. capsulatus* and accordingly, the activities of the copper-containing enzymes are affected.

An interesting feature of *Mc. capsulatus* Δ*scO-1* is that the activity of the cytochrome oxidase of whole cells is not inhibited and this mutant exhibited good

growth in copper-limited medium. In contrast to these observations, it has been reported that the growth of *Bacillus subtilis* Δ*scO* (Mattatall *et al.*, 2000) and *Agrobacterium tumefaciens* Δ*scO* (Saenkham *et al.*, 2009) was impaired when grown at low copper due to the severe deficiency of cytochrome c oxidase activity. The phenotype of *Mc. capsulatus* Δ*scO-1* does not necessarily mean the COX activity is not affected because there are other genes encoding cytochrome c oxidase exist in the genome of this methanotroph, so if one gene is disrupted, others may compensate. This possibility raises the importance of the transcriptional analyses of such genes by qPCR. Furthermore, inactivation of Δ*scO-1* may induce the copper independent oxidases to compensate for the probable decrease in copper-dependent COX activity. The genome of *Mc. capsulatus* contains homologous to cytochrome *d* ubiquinol oxidase, which does not contain copper; MCA1105, MCA1106 and MCA1107 which encode cytochrome *d* ubiquinol oxidase subunit I, subunit II and subunit III respectively. Cytochrome *bd* oxidases are heme-iron containing enzymes and considered as an alternative pathway in the terminal respiratory chain. It has been reported that these genes are induced under stress conditions (*e.g.*, oxygen or iron deficiency) (Borisov *et al.*, 2011).

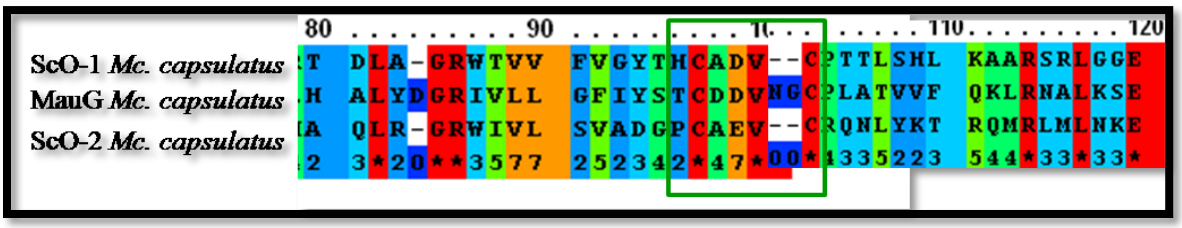

Figure 6.11 Sequence alignments of the three ScO proteins of *Mc. capsulatus*, ScO-1 (accession no. YP113656), ScO-2 (accession no. YP_112671) and MauG (accession no. YP112851) showing metal binding motif CXXXC (ScO-1 and ScO-2) and CXXXXXC (MauG) in the green box, (unconserved 0 1 2 3 4 5 6 7 8 9 10 conserved).

These oxidases can oxidize artificial electron donors like TMPD (Junemann, 1997). However, the heme-copper oxidases have a bioenergetic efficiency of two-times more than that of the cytochrome *bd* oxidases (Paulus and de Vries, 2011).

It is noteworthy that two other genes in *Mc. capsulatus* are SCO-like homologues: (1) MCA0132 which is annotated as hypothetical protein composed of 206 aa (ScO-2) and (2) MCA0318 (*mauG*), annotated as SCO1/SenC family protein/methylamine utilization protein MauG. MauG is significantly longer than ScO-1 as it is composed of 626 aa. Similarly to ScO-1, both proteins contain the metal-binding motif CXXXXXC for MauG and CXXXC for ScO-2 (Figure 6.11).

Checking the genome context of other *scO*-like genes, a gene (MCA0133) annotated as cytochrome oxidase assembly family protein was found downstream of *scO-2* suggesting that both genes are involved in proper assembly of cytochrome oxidase. However, no genes with putative functions related to cytochrome oxidase were found around *mauG*. Taking this difference with the absence of a conserved histidine (putatively involved in copper binding) in MauG, it is assumed that MauG is presumably not involved in cytochrome oxidation. Two genes (MCA1185 and MCA1167) annotated as cytochrome c family proteins are found near *scO-1*. A number of other genes in the genome of *Mc. capsulatus* encode potential cytochrome c oxidases. For example, MCA0880, MCA0879 and MCA0883 are annotated as cytochrome c oxidase subunit I, subunit II and subunit III respectively (Table 6.5). Taken together, it can be concluded that the presence of multiple *scO*-like homologues and multiple copies of cytochrome c oxidase encoding genes provides a safeguard for energy production and if one gene is knocked out, another may compensate, probably with more activity than the parent one. Another possible scenario is that the juxtaposed gene, MCA1192 may substitute the function of *scO*-

1, considering they both might bind copper. This raises the importance of detailed studies of these genes using comparative gene expression using real time PCR.

Interestingly, Δ*scO-1* seemed to be more resistant to higher copper than the wild-type. This finding indicates that ScO-1 protein might have a potential role in copper homeostasis in *Mc. capsulatus*. Prediction of a transmembrane helix (Figure 6.2) and a metal binding motif in ScO-1 (Figure 6.11) supports this assumption. Furthermore, it has been reported that ScO may be involved in copper transport based on analysis of 311 bacterial genomes (Banci *et al.*, 2007). However, the exact role of ScO-1 in copper transport has yet to be investigated. One possible explanation for the copper resistance phenotype is that ScO-1 acts as a copper signalling molecule via redox reactions that regulate the activity of copper transporters. Support for this proposal is found in the work of Leary *et al.*, (2007). In this study, human ScO appears to regulate copper

Table 6.5 Representatives of the putative cytochrome c oxidase encoding genes in *Mc. capsulatus* genome.

Gene number	Annotation
MCA0879	Cytochrome c oxidase subunit II
MCA0883	Cytochrome c oxidase subunit III
MCA0880	Cytochrome c oxidase subunit I
MCA2397	Cytochrome c oxidase subunit II
MCA2396	Cytochrome c oxidase subunit I
MCA2399	Cytochrome c oxidase, CbaD subunit
MCA0882	Cytochrome c oxidase assembly protein
MCA2394	Cytochrome c' ccp
MCA0338	Cytochrome c5530 family protein
MCA1187	Cytochrome c family protein
MCA2618	Cytochrome c-555
MCA1185	Cytochrome c family protein
MCA2259	Cytochrome c5530 family protein
MCA2160	Cytochrome c5530 family protein
MCA0426	Cytochrome c family protein
MCA0424	Cytochrome c family protein
MCA0421	Cytochrome c5530 family protein
MCA0948	Cytochrome c family protein

MCA2189	Cytochrome c family protein
MCA0423	Cytochrome c5530
MCA1799	Cytochrome c family protein
MCA2405	Cytochrome c family protein
MCA2603	Cytochrome c family protein
MCA0781	Cytochrome c family protein
MCA2395	Cytochrome c family protein
MCA1068	Cytochrome c family protein
MCA1775	Cytochrome c family protein
MCA0433	Cytochrome c (NHL domain) family protein
MCA2200	Cytochrome c' family protein

homeostasis of cells via generation of a signalling cascade which then affects the activity of copper transporters; CopA homologues (ATP7A or ATP7B) (Leary, 2010). The nature of this signal is highlighted by the work done by Chinenov (2000) who reported a similarity between ScO and thioredoxin in which redox reactions are mediated through thiol:disulfide exchange. *Mc. capsulatus* ScO-1 has a thioredoxin fold so it is likely to act as a sensor of the redox state of the membrane through the thiol:disulfide oxidoreductase activity and then transmit a signal to target destinations which are probably metal transporters. To get further knowledge about this a preliminary attempts to investigate the comparative gene expression of the *copA1*, *copA2* and *copA3* genes at high copper levels of *Mc. capsulatus* Δ*scO-1* were planned, but unfortunately due to lack of time these experiments were not completed.

Δ*scO-1* accumulates comparable amounts of intracellular copper to the wild-type. Contrary to these results, inactivation of human ScO led to lower intracellular copper, which was attributed to enhanced copper-exporting activity (Leary *et al.*, 2007). This, however, opens new areas for future studies, for example, the expression levels of the copper transporters (*e.g.*, CopA). It would be of interest to follow the level of copper at different time points but because of high cost of such study as well as the lack of suitable instrumentation on-site, these

experiments have not been done. Nevertheless, this was sent mutant to our collaborators Dr. Jeremy Semrau and Prof. Alan DiSpirito for time-course metal analysis and MMOs activity measurements at different concentrations of copper.

To investigate if inactivation of *scO-1* interferes with Mb in copper acquisition, CAS-Cu plates were used to answer this possibility. Investigating the production of Mb revealed that Δ*scO-1* strain produces as much Mb as the wild-type. These observations suggest that ScO-1 is not involved in the biosynthetic pathway of this chalkophore. In addition, it seems that there is no specific copper delivery between ScO-1 and Mb in *Mc. capsulatus*. Another approach should be tackled in the future to see if there is a link between ScO-1 and the other copper transporters (*e.g.*, MopE).

In summary, the results of this chapter indicate that *Mc. capsulatus* ScO-1 appears not to have a role in copper-mediated regulation of sMMO and pMMO. ScO-1 is might be involved in copper homeostasis through its potential role in regulating the activity of copper transporters via signalling in *Mc. capsulatus*. Although ScO proteins are widespread in living organisms and share common features, they appear to perform different functions in different organisms. In future studies, other candidate genes will be selected from the microarray results in order to decipher the regulation mechanisms of MMO by copper in *Mc. capsulatus*.

Chapter 7

Some physiological features during the copper switch in *Mc. capsulatus*

7.1 Introduction

One advantage of the use of microarray techniques is that it could lead to the identification of the genes that have important roles in regulatory mechanisms or metabolic routes. This is based on the assumption that the up-regulation of a particular mRNA transcript under defined growth conditions suggests that the resultant gene-product is likely to be involved in regulation or metabolism under those conditions. In other words, transcription of a gene occurs only when its function is needed (Dorrell *et al*., 2001; Chalabi *et al*., 2007; Borneman *et al*., 2010).

Chapter 5 outlined a comparative transcriptome analysis using a *Mc. capsulatus* whole-genome microarray in cells expressing sMMO and expressing pMMO to identify the potential genes involved in regulation MMO. However, nothing is known about the change in the transcriptome profile of *Mc. capsulatus* during the transition state from growth in cells fully expressing sMMO to those fully expressing pMMO. One can predict that the regulatory genes and the regulated proteins involved in the copper switch from growth using sMMO to pMMO upon addition of copper would be apparent during that transition state. In addition, to take advantage of the spare chip that had been obtained from Agilent Company plus the valid licence of the GeneSpring X11, another microarray experiment was initiated. Therefore, the aim of this work was to study the change in the global gene expression of *Mc. capsulatus* under no added copper (expressing sMMO) with gradual addition of copper until the copper switch occurred (expressing pMMO) to identify the genes involved in MMO regulation. Furthermore, it was of interest to link this change in transcriptome with the copper content of the cells.

7.2 Experimental design

The different stages of the of the time course experiment are outlined in the schematic representation in Figure 7.1.

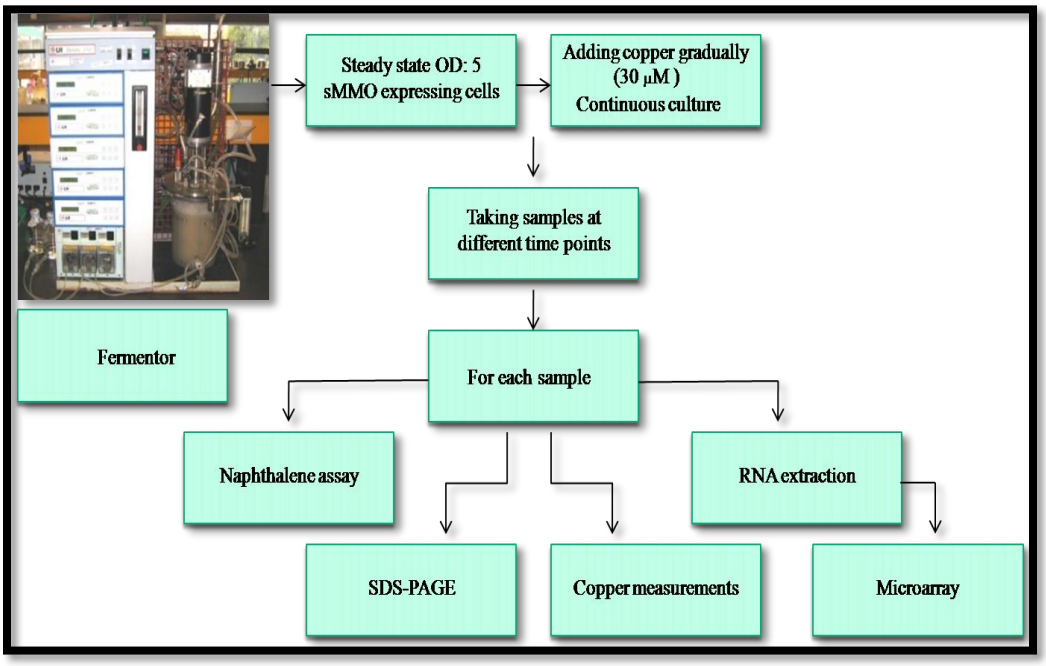

Figure 7.1 Schematic representation of the experimental design of the time course microarray experiment.

There were four main stages. These include (1) chemostat work which comprised of growth of *Mc. capsulatus* in batch then continuous mode (the steady state) and addition of copper gradually; (2) sampling which involved taking samples out of the chemostat at different time points before and after addition of copper; (3) sample analysis which involved three different analyses for each sample: (a) naphthalene oxidation assay, (b) SDS-PAGE of cell-free extracts and (c) copper measurements of three different fractions: intracellular, biomass-associated and residual copper in the spent media, and (4) RNA extraction then different stages of microarray strategy as shown in Chapter 5.

7.2.1 Microarray technology and probes design

As described previously in Chapter 5, section 5.2.

7.2.2 Growth of *Mc. capsulatus* in fermentor

Mc. capsulatus (wild-type) strain was grown on NMS medium with no-added copper in a fermentor as described in Materials and Methods. When cells expressed sMMO (OD_{540} ~ 5), as indicated by a positive naphthalene assay, the fermentor was switched to continuous mode, fresh NMS medium with 30 µM copper was added at a dilution rate of 3.3 ml min^{-1} and maintained at steady state. Just before adding NMS medium, a sample (20 ml) was taken and considered as t= 0h. At this stage cells were expressing sMMO i.e. before copper switch. Then different samples were taken at different time points; 0.12, 0.25, 0.5, 1, 2, 3, 4, 5, 6, 7, 8, 19 and 40h. Each sample was divided into different tubes for subsequent measurements; naphthalene assay, SDS-PAGE of total cell protein, copper measurements and RNA extraction. Details about each experiment are given below.

7.2.3 Naphthalene assay to check sMMO

To check for sMMO expression, all *Mc. capsulatus* samples were tested using the naphthalene oxidation assay as described previously in Materials and Methods. The results showed a gradual decrease in the intensity of the purple colour (positive naphthalene test) with gradual addition of copper over the time course tested (Figure 7.2). However, the first eight samples exhibited positive results for naphthalene oxidation, while samples taken after 4h showed no purple colour appearance when zinc reagent was added, which indicated that sMMO had become inactive. As expected, the two negative controls showed no change in colour (yellow); one tube had culture with no naphthalene

added and the other was no-cells control. The positive control in which *Methylocella silvestris* was added, showed a positive result (a purple colour) (Figure 7.2). *Methylocella silvestris* possesses only sMMO and does not contain pMMO.

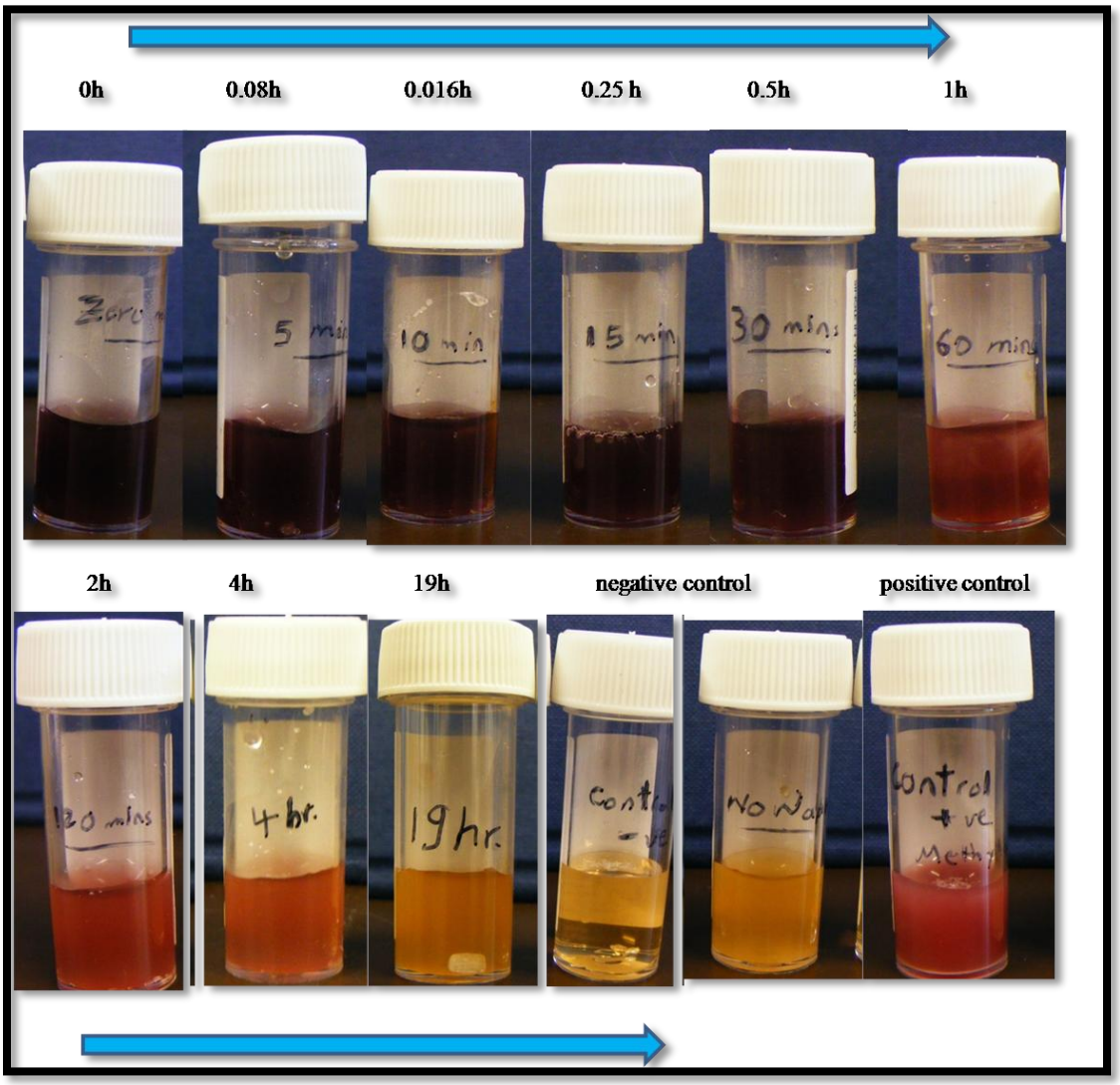

Figure 7.2 Results of naphthalene oxidation assay at representative time points, the arrows indicate the gradual decrease in the intensity of the purple from deep at 0h to pale purple at 4h then yellow colour after 4h. Purple colour: positive result (sMMO expressed), yellow colour: negative result (pMMO expressed).

These results indicated that the copper switch from sMMO to pMMO is likely to occur between 2 - 5 h based on the results of naphthalene test (Figure 7.2). In addition, these observations confirm that copper negatively regulates sMMO activity in *Mc. capsulatus*.

7.2.4 SDS-PAGE

To identify the different patterns of polypeptides of both sMMO and pMMO SDS-PAGE analysis was carried out as described previously in Materials and Methods.

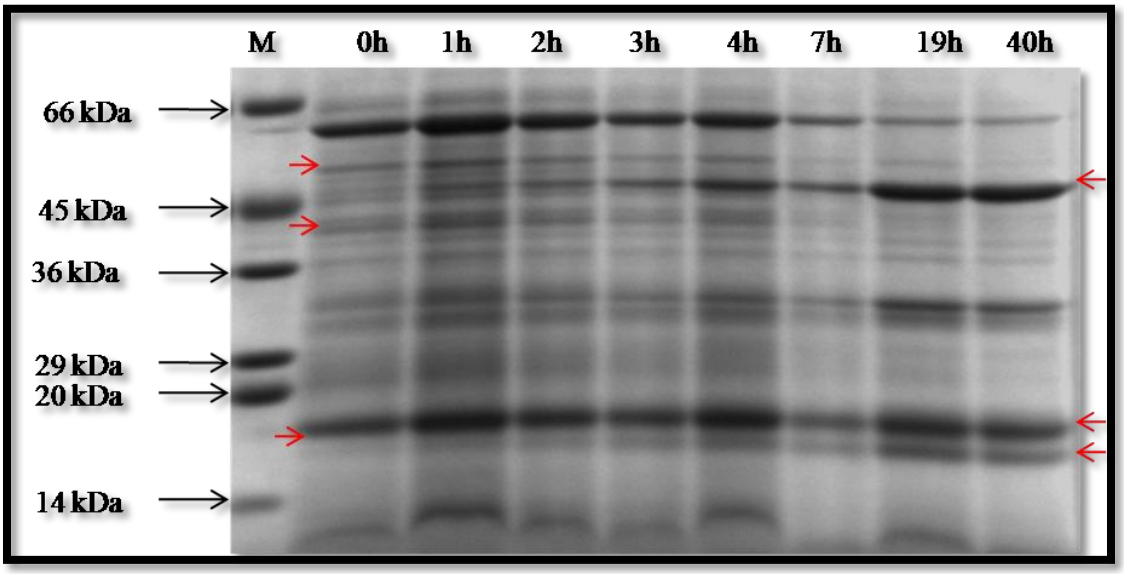

Figure 7.3 A Coomassie-stained 12.5 % SDS-PAGE gel of cell-free extracts from *Mc. capsulatus*. The red arrows on the left point to the three subunits of the hydroxylase component; α−, β− and γ-subunits of the sMMO and the right the three subunits of the pMMO. M, a Dalton VII molecular marker was used on the left of the samples and the sizes are indicated on the side. Time points after initial addition of copper-containing NMS medium were indicated in hours at the top of each lane.

Cell-free extracts from *Mc. capsulatus* samples collected at the indicated different time points were obtained by boiling the pellets of 2ml culture of OD_{540} = 5 in sample buffer for 20 min. The extracts were separated by loading 40 µg proteins from each sample on a 12.5 % (w/v) SDS-PAGE gel. As can be shown in (Figure 7.3), the α− and β−subunits of

the hydroxylase of the sMMO were detected and their intensities gradually decreased with time. These bands correspond to the MmoX (61 kDa), MmoY (45 kDa) and MmoZ (20 kDa) of sMMO On the other hand, the intensities of the bands corresponding to α−, β− and γ-subunits, which correspond to PmoB (47 kDa), PmoA (24 kDa) and PmoC (22 kDa), of the hydroxylase of pMMO, increased with time in a gradual manner. The top band at approximately 63 kDa visibly detected in lanes from all samples was methanol dehydrogenase (MDH). MDH became less abundant with addition of copper over the time course. The results are in general agreement with those obtained with the naphthalene oxidation assay. Furthermore, the results revealed that copper-switch from sMMO to pMMO seemed to take place at about 4h.

7.2.5 Analysis of polypeptides using MS/MS

In order to confirm the identity of polypeptides of both sMMO and pMMO, eleven bands (Figure 7.4) were cut out from the SDS-PAGE gel and submitted to the Biological Mass Spectrometry and Proteomics Facility at the University of Warwick, for analysis by LC/ECI-MS/MS. These bands were prominent in lanes 2 (at 0h, sMMO-expressing cells) and 9 (at 40h, pMMO-expressing cells). The results showed that 128 proteins were identified from 792 polypeptides detected from the eleven bands analysed. Typically, 506 polypeptides from sMMO-expressing cells (corresponding to 87 proteins) (Table 7.1) and 236 from pMMO-expressing cells (corresponding to 41) (Table 7.2) were identified. The most five abundant proteins in each band were presented in Tables 7.1 and 7.2. It was apparent that the major subunits of the hydroxylase of the sMMO were identified in the no-added copper growth conditions, while those of the pMMO were detected after adding of copper by 40 hours (Tables 7.2). Under no-added copper growth conditions, MmoX,

MmoY in addition to the MmoG were identified, while PmoB, PmoA and PmoC were detected in the added copper growth conditions.

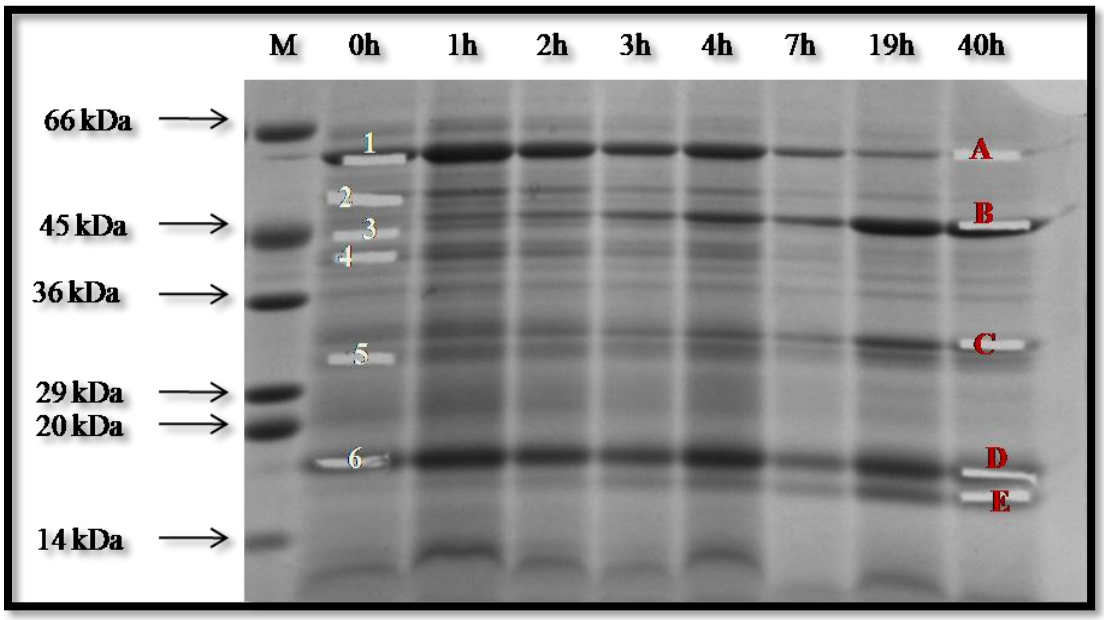

Figure 7.4 A Coomassie stained 12.5 % SDS-PAGE gel shown in Figure 7.3 indicating the bands, which were selected for mass-spectrometric analysis. The numbers and letters identify bands, which were analyzed from cell-free extracts of samples collected at 0h and 40h respectively. Band-identifying numbers and letters refer to Table 7.1 and 7.2 respectively.

Methanol dehydrogenase (MDH) was also detected in all bands of both lanes 2 and 9 and represented 20% of the total polypeptide identified. However, the abundance of MDH was much higher in no-added copper (lane 2 (137 polypeptides)) than that in high-copper growth conditions (lane 9 (43 polypeptides)). Inorganic H^+ translocating pyrophosphatase and surface associated protein MopE were also detected in a relatively high abundance, 13 and 20 polypeptides respectively (Tables 7.1 and 7.2). These data are in general consistent with those obtained from the transcriptome analysis (Please see

Chapter 5). These results indicated sMMO is expressed under low-copper-to-biomass ratio while pMMO is expressed under high-copper-to-biomass ratio growth conditions.

Table 7.1 Polypeptides identified by MS/MS. Cells were grown in no-added copper growth conditions. Band-identifying numbers refer to (Figure 7.4, lane 0h). MW: molecular weight (kDa), MDH: methanol dehydrogenase protein, MMO: methane monooxygenase. The five most abundant polypeptides in each lane are shown.

Band no.	Accession no.	Locus tag	Description	Total no. of proteins	MW (kDa)	Peptides	Total no. of peptides	Coverage (%)
1	Q60AR6	MCA0779	MDH large subunit (MxaF)		66.3	38		51.9
	Q607Q3	MCA1704	60 kDa chaperonin 2 (GroEL2)		57.4	23		52.4
	Q60AY0	MCA0707	60 kDa chaperonin 1 (GroEL1)		57.1	10		20.7
	Q9AIP9	MCA2589	Surface associated protein (MopE)		57.6	8		18
	Q7WZ32	MCA1202	60 kDa chaperonin 3 (GroEL3, MmoG)		59.4	7		13.8
				11			102	
2	Q60AR6	MCA0779	MDH large subunit (MxaF)		66.3	24		40.6
	Q605W9	MCA2155	Sulfide quinone reductase (SqR)		46.9	18		26.2
	Q602I7	MCA3076	Putative uncharacterized protein		48.5	13		28.4
	Q607Q3	MCA1704	60 kDa chaperonin 2 (GroEL2)		57.4	9		20.7
	P22869	MCA1194	MMO component A α-chain (MmoX)		60.6	3		6.5
				21			124	
3	Q60AR6	MCA0779	MDH large subunit (MxaF)		66.3	14		2 4.6
	Q9AIP9	MCA2589	Surface associated protein (MopE)		57.6	7		14.6
	Q60AY0	MCA0707	60 kDa chaperonin 1 (GroEL1)		57.1	7		16
	Q607Q3	MCA1704	60 kDa chaperonin 2 (GroEL2)		57.4	6		13.7
	Q609P4	MCA1188	Inorganic H^+ translocating pyrophosphatase		63.2	5		12.8
				15			66	
4	Q60AR6	MCA0779	MDH large subunit (MxaF)		66.3	26		44.3
	Q607W0	MCA1643	Peptidyl prolyl cis trans isomerase family protein		35	10		40.9
	P18798	MCA1195	MMO component A β-chain (MmoY)		45.1	8		16.5
	Q60CK1	MCA0105	D alanyl D alanine carboxypeptidase		43.9	7		18.6

	P22869	MCA1194	MMO component A α-chain (MmoX)		60.6	4		7.8
				15			78	
5	Q60AR6	MCA0779	MDH large subunit (MxaF)		66.3	19		34.8
	Q49104	MCA1796	MMO subunit B2 (PmoB)		46	9		21.7
	Q60AR5	MCA0780	MxaJ protein		21.3	8		34.2
	Q60CR4	MCA0012	ATP synthase β-subunit (AtpD)		50.1	6		12
	Q60CR6	MCA0010	ATP synthase α-subunit (AtpA1)		55.4	6		7.8
				16			85	
6	Q60AR6	MCA0779	MDH large subunit (MxaF)		66.3	16		26.8
	Q607M1	MCA1738	Putative uncharacterized protein		33.1	12		19.2
	Q60A48	MCA1023	Antioxidant AhpC Tsa family protein		22	8		40.3
	Q605B3	MCA2371	50S ribosomal protein L4		22.1	3		15.6
	Q60AR2	MCA0783	MoxR protein		38.2	3		7.7
				9			51	
Total				87			506	

Table 7.2 Polypeptides identified by MS/MS. Cells were grown in added copper growth conditions. Band-identifying letters refer to (Figure 7.4, lane 40h). MW: molecular weight (kDa), MDH: methanol dehydrogenase protein and MMO: methane monooxygenase. The five most abundant polypeptides in each lane are shown.

Band	Accession	Locus tag	Description	Total no. of proteins	MW (kDa)	Peptides	Total no. of peptides	Coverage (%)
A	Q60AR6	MCA0779	MDH large subunit (MxaF)		66.3	26		43.4
	Q607Q3	MCA1704	60 kDa chaperonin 2 (GroEL2)		57.4	17		34.1
	Q60AY0	MCA0707	60 kDa chaperonin 1 (GroEL1)		57.1	9		23.1
	Q49104	MCA1796	MMO subunit B2 (PmoB)		46	5		14.5

	Q607G3	MCA1797	MMO subunit A2 (PmoA)		28.4	2		7.3
				9			76	
B	Q49104	MCA1796	MMO subunit B2 (PmoB)		46	21		47.6
	Q60AR6	MCA0779	MDH large subunit (MxaF)		66.3	3		5.3
	Q607M1	MCA1738	Putative uncharacterized protein		33.1	3		3.9
	Q608D0	MCA1564	Putative uncharacterized protein		42	2		6.5
	Q9AIP9	MCA2589	Surface associated protein (MopE)		57.6	2		4.3
				7			35	
C	Q49104	MCA1796	MMO subunit B2 (PmoB)		46	19		36.7
	Q9ZID6	MCA3103	MopB		38.3	12		42.8
	Q60AR6	MCA0779	MDH large subunit (MxaF)		66.3	4		7.8
	Q607M1	MCA1738	Putative uncharacterized protein		33.1	4		7.8
	Q608D1	MCA1563	Putative uncharacterized protein		68.1	2		3.9
				5			41	
D	Q60A48	MCA1023	Antioxidant AhpC Tsa family protein		22	9		43.8
	Q607M1	MCA1738	Putative uncharacterized protein		33.1	7		11.4
	Q60AR6	MCA0779	MDH large subunit (MxaF)		66.3	7		11.6
	Q49104	MCA1796	MMO subunit B2 (PmoB)		46	7		16.2
	Q60C16	MCA0295	MMO C subunit (PmoC3)		29.6	3		6.3
				9			42	
E	Q49104	MCA1796	MMO subunit B2 (PmoB)		46	11		25.8
	Q607M1	MCA1738	Putative uncharacterized protein		33.1	7		15
	Q60A48	MCA1023	Antioxidant AhpC Tsa family protein		22	6		28.4
	Q60AR6	MCA0779	MDH large subunit (MxaF)		66.3	3		6
	Q60A86	MCA0982	Heat shock protein Hsp20 family		19.9	3		11.9
				11			42	
Total				41			136	

7.2.6 Copper measurements

Intracellular, extracellular and copper associated with biomass was measured and as expected the copper concentrations is increased with time. To ensure no copper contamination, all glassware was acid-washed then rinsed in deionised water several times. The cultures were centrifuged at 12,000 x *g* for 10 min and the supernatant stored at -80 ºC. Cell pellets were resuspended in 0.1% NaCl and centrifuged. This supernatant was considered to represent biomass-associated copper. Cell pellets were dried then dissolved in 5ml of nitric acid (70%). The copper in this fraction was considered as intracellular copper. Samples were diluted to 3 ml in 0.1 M trace metal grade nitric acid obtained from Sigma. All samples were measured using an atomic absorption spectrophotometer.

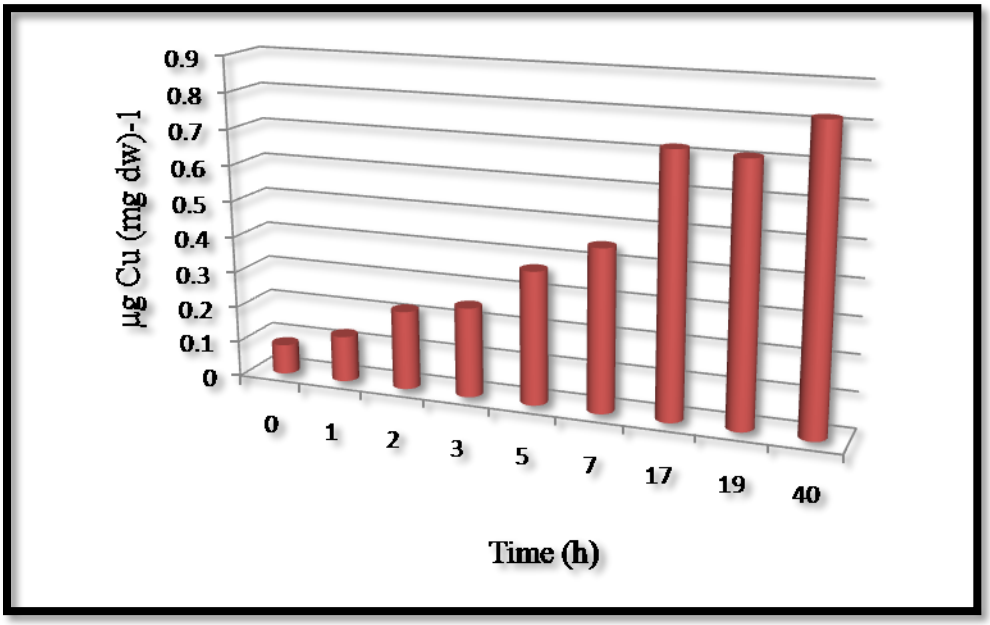

Figure 7.5 Measurements of intracellular copper concentrations

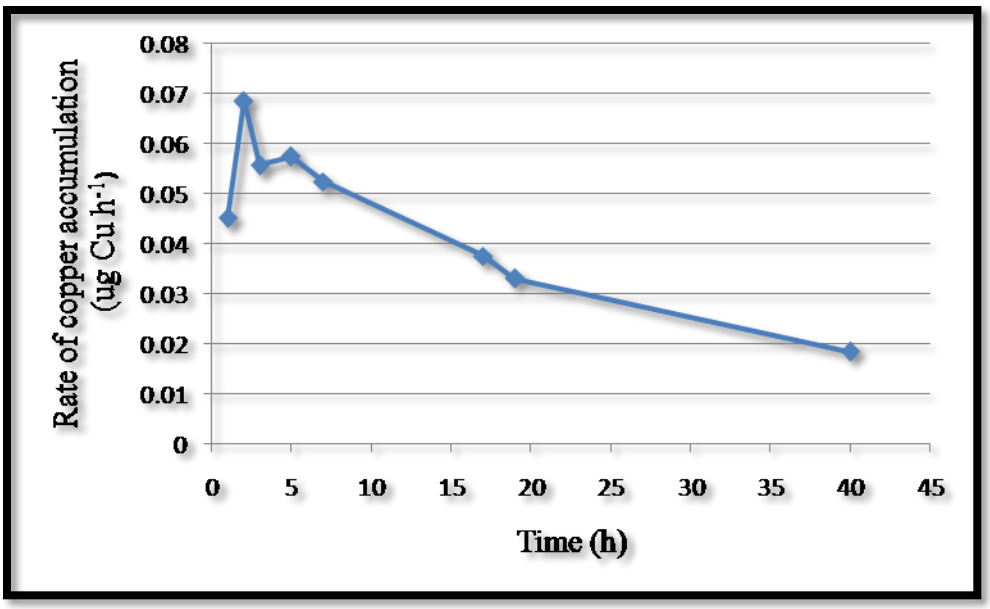

Figure 7.6 Rate of copper accumulation inside *Mc. capsulatus*. The rate is expressed as ug Cu h^{-1}

The data illustrated in Figure 7.5 showed that, the intracellular copper concentration of *Mc. capsulatus* increased with the gradual addition of copper to the medium over the time course applied. At 0h (no added copper), the cells accumulated 0.083 µg Cu (mg dw)$^{-1}$, (note that the background copper resulted from copper contamination in the medium is about 0.8 µM. The accumulation rate of the intracellular copper of *Mc. capsulatus* is presented in Figure 7.6. The cells seemed to take up copper more rapidly during the first seven hours than afterwards (Figure 7.6). At 17h and 19h the cells exhibited comparable rate of accumulation of copper. The slowest rate of copper accumulation and the highest copper content recorded was at 40h. These data indicated that the copper-starved cells of *Mc. capsulatus* accumulated more copper intracellularly at a high rate during the early hours of addition of copper to the growth medium. Then, cells decreased the rate at which copper is accumulated. This copper could be used to produce active pMMO and copper-containing cytochrome oxidases as well as copper-containing enzymes.

The results of measurements of biomass-associated copper for all tested samples are presented in Figure 7.7. The copper associated with the cell biomass appeared to be low over the first seventeen hours with an average concentration about 0.04 µg Cu (mg dw)$^{-1}$. The amount of copper retained outside the cells increased at 19h and at 40; 0.4 and 0.63 µg Cu (mg dw)$^{-1}$respectively. Unexpectedly, a tiny amount of copper was detected on the surface of cells growing at no-added copper, 0.02 µg Cu (mg dw)$^{-1}$. These results showed that most of copper was taken up by *Mc. capsulatus* growing on low-copper medium until a certain point at which less copper was needed to sustain metabolic processes inside the cells. Then, any excess copper was retained, associated with biomass.

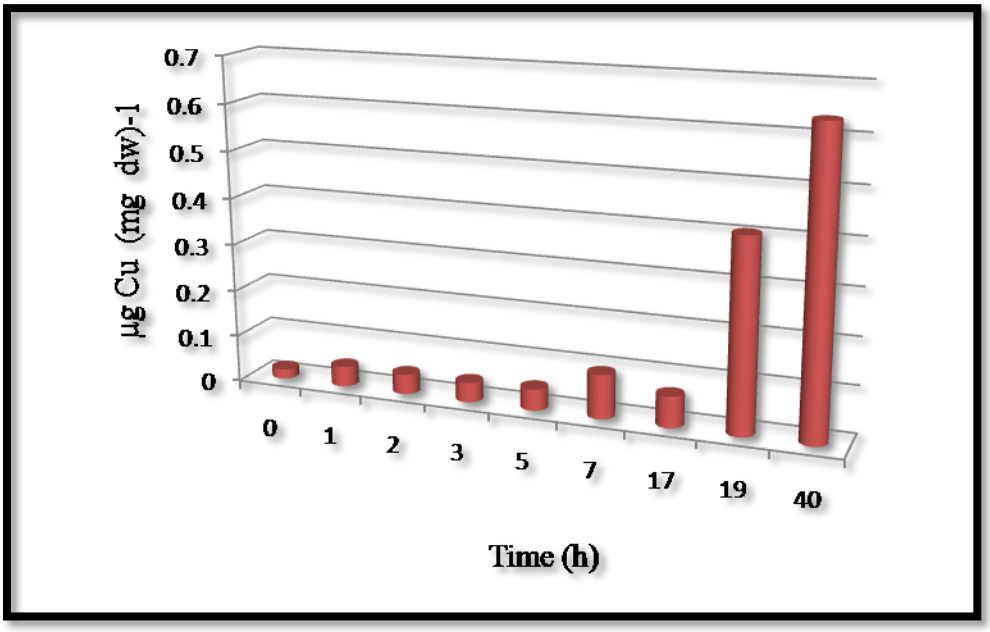

Figure 7.7 Biomass-associated copper concentrations.

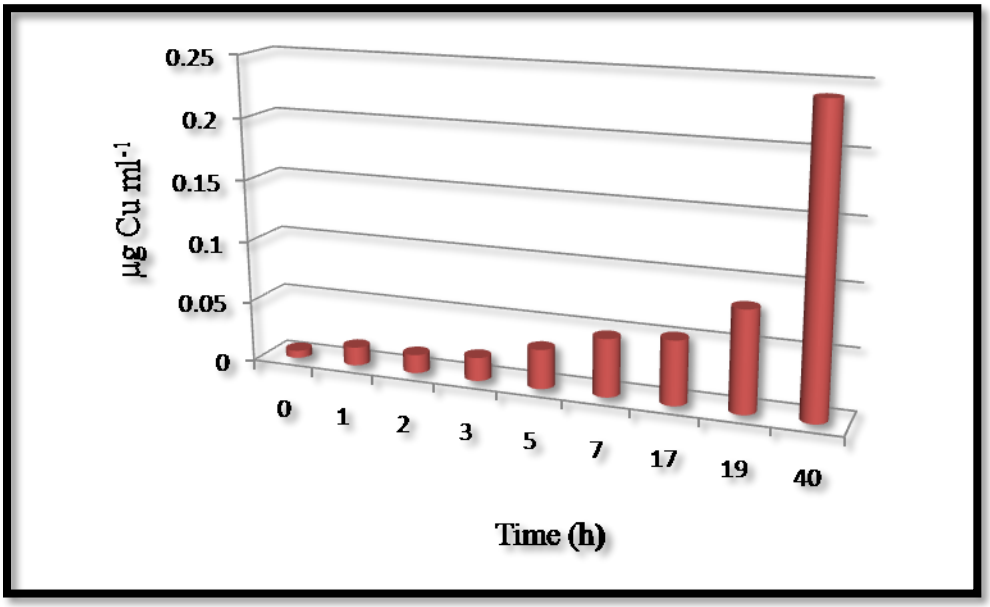

Figure 7.8 Residual (supernatant) copper concentrations.

Figure 7.8 shows that the residual copper in the spent NMS media was found to gradually increase with time. Likewise with the copper associated with biomass, the residual copper was small (less than 0.05 µg Cu ml^{-1}) at the first seven time points tested (0h-17h). At the last two time points (19h and 40h), the residual copper was found to increase to 0.08 and 0.24 µg Cu ml^{-1}. These data confirmed the conclusions drawn from the measurements of copper associated with biomass. Cells tend to satisfy their needs of copper before decreasing the uptake levels of this metal, which is being toxic at high levels.

7.2.7 RNA extraction and assessment of RNA quality

To ensure no change in the transcriptome profile, stop solution was immediately added to samples for RNA extraction. RNA was extracted from all *Mc. capsulatus* samples at different time points as described earlier (Gilbert *et al.*, 2000). For details, please see Chapter 2 (Materials and Methods). Quality of purified RNA samples was checked using the Bioanalyzer (Table 7.1).

Table 7.3 RNA concentration and RIN number of the different samples.

Sample/Time (h)	RNA concentration ng. μl^{-1}	RIN number*
0	7.0	6.5
1	4.6	6.3
2	3.6	6.2
3	2.0	5.9
5	3.7	6.3
7	5.0	6.1
17	10.2	6.1
19	10.2	6.1
40	0.3	6.0

*RNA integrity number (RIN)

The quality of RNA samples were generally good as indicated by the RIN which was 6 or above (Table 7.3) except for sample 3h which showed a RIN which was slightly less than the 6-threshold. Labeling of the RNA samples was poor. This is probably due to the quantity of RNA, which was insufficient to do hybridization. Due to limited time, this experiment was not finished.

7.3 Discussion

The work done in this chapter describes an attempt to investigate *Mc. capsulatus* whole-genome transcriptomics experiments designed to identify genes transcribed differentially during growth on no-added copper (expressing sMMO) or high copper (expressing pMMO). The hypothesis is that the key genes involved in MMO regulation will be up-regulated or down-regulated during growth on methane using either sMMO or pMMO. Although this hypothesis was the same for the other microarray experiment described in Chapter 5, the advantage of the current experiment is the expression shift of particular genes will be identified during the switching from sMMO to pMMO. It was assumed that many critical changes related to the regulatory mechanisms would happen during such a transition state. Such information was not obtained from the work done in Chapter 5 where the transcriptomes were compared before and after copper switch. In addition,

measurements of the copper distribution of each sample are another advantage of the current experiment. This is because it would be possible to relate the changes in the transcriptome to certain concentration of copper.

Due to the limited number of arrays (8) on the chip, eight different time points were chosen rather than using biological replicates. Furthermore, the data of the other microarray in which biological replicates were used (Chapter 5) could be combined with the data of this experiment during analysis. To provide more robustness, monitoring the copper distribution, checking the polypeptide profiles of whole-cell extracts in SDS-PAGE and testing sMMO expression via the naphthalene assay were also carried out. Together this could provide better insights and stronger conclusions about the key genes involved in MMO regulation. Two important factors were considered in this experiment; which copper concentration to use and at which sampling time intervals. Selecting which copper concentration that could be added and time points that could be taken built on the work done by Nielsen *et al.*, (1996). In their study, no sMMO transcripts were detected after 20 minutes of addition of 50 µM copper as a final concentration indicating significant suppression of sMMO transcription. Therefore, our approach is to explore what was happening in those 20 minutes in terms of regulation of sMMO, which took place within that period. Because the addition of such a high copper concentration to *Mc. capsulatus* is likely to induce stress-response genes, some modifications were introduced. Choosing a moderate copper concentration (30 µM), adding copper gradually, and taking samples in a narrow range (minutes initially) are probably the most effective way to detect the changes of regulatory proteins during the copper switch from sMMO to pMMO.

The activity of sMMO enzyme was assessed using a colorimetric test introduced by (Brusseau *et al.*, 1990). This test is based on the ability of the cell to

oxidize naphthalene into naphthol and as pMMO does not have this ability, the test is sMMO-specific. The gradual decrease in the purple colour intensity upon gradual copper addition over indicates that sMMO activity diminished until it became fully inactive after 4 hours of adding copper. However, the switch from sMMO to pMMO seemed to take place between 2 - 4h. These results are consistent with those obtained by Nielsen *et al.* (1996), who reported that sMMO activity was decreased to 50 % after one hour of addition of 50 μM copper and was completely inhibited after two hours.

To check the polypeptides profile of sMMO and pMMO, SDS-PAGE of whole-cell extract was carried out. As expected, the three subunits of the sMMO hydroxylase were detected with a gradual decrease in the band intensities from 0-4h indicating the expression of polypeptide has ceased and a possible turnover of these polypeptides took place. On the other hand, the α-, β- and γ-subunits of the hydroxylase of pMMO were also identified with increased band intensity with time. These findings are in agreement with what is known about pMMO; pMMO is expressed as a basal level even at no-added copper, however, its abundance and activity increased in response to added copper (Choi *et al.*, 2003). The time point at which the shift from sMMO to pMMO -at the level of polypeptides- appeared to happen at about 4h. These observations are congruent with those obtained from the naphthalene assay. It would be of interest to investigate the activity of sMMO and pMMO of protein extracts but due to the lack of time, these experiments were not done.

With the exception of the γ-subunit (MmoZ) of the sMMO hydroxylase, mass spectrometry analysis of the selected bands of *Mc. capsulatus* of cell-free extract in the no-added copper or added copper growth conditions identified the α-, β-, and γ-

subunits of the hydroxylase of sMMO or pMMO. It is unclear why the MmoZ was not identified, although the activity of sMMO was high as indicated by results of the naphthalene assay (the deep purple colour (Figure 7.2)). However, the possible reason was that the corresponding polypeptides to the MmoZ was not cut out of the gel by the gel-cutting tip because the band (band 6, lane 0h, Figure 7.4) was thicker than the width of the tip. In addition, it is unlikely that MmoZ was degraded during cell-free extract preparation by boiling but this is still a possibility. Many other proteins with unknown functions were also detected. Most abundant proteins in each band is differentially regulated during the copper switch.

It is worth mentioning that not every single protein identified by mass spectrometry, had a corresponding transcript detected by the transcriptome analysis in Chapter 5. There are two main reasons for this; firstly, not all the proteome of *Mc. capsulatus* was investigated, while the genome-wide transcriptome was analyzed. The other reason is that the threshold of 2-fold or more that was used in the analysis of microarray data but not polypeptides analysis. In addition, the concentration of copper that was used in the transcriptome analysis (4 µM copper) is much lower than that in the partial proteome analysis (30 µM copper).

Copper distribution of all the samples was measured. In general, the intracellular, extracellular and copper associated with biomass increased by adding copper over the time tested. The detection of copper in the sample at 0h where no copper was added is not surprising because copper contamination of the chemical ingredients of NMS medium and water accounts for about 0.8 µM copper (data not shown). The cells tend to take up copper more rapidly during the early hours of addition of copper, reflecting their need for this essential element, not only for pMMO expression and activity but also for other copper-requiring enzymes such as

cytochrome oxidases. Cells satisfy their need from copper before they restrict the uptake of this metal because it is toxic at high concentrations. The time needed to accomplish this is more likely to be 17 h after which excess copper is retained on the biomass or in the spent medium. The switch point from sMMO to pMMO seems to take place at 4h at which the intracellular copper concentration is 0.37 µg Cu (mg dw)$^{-1}$. It has been reported that the copper switch point in *Ms. trichosporium* was above 0.9 nmol of Cu (mg protein)$^{-1}$ (about 0.11 µg Cu (mg dw)$^{-1}$) (Lontoh and Semrau, 1998).

Mc. capsulatus samples from eight selected time points to cover all the possible changes during the course of the copper switch from sMMO-expressing to pMMO-expressing growth conditions, were subject to RNA extraction. The quality of the samples was rather good based on the bioanalyser analysis. An attempt has been made to label RNA but the labeling was poor. Further attempts to extract more RNA have not been made due to the restricted period, therefore these experiments was abandoned.

In summary, the data outlined in this chapter confirm the negative regulation of sMMO and the induction of pMMO by bioavailability of copper through the sMMO-specific naphthalene assay, SDS-PAGE and copper measurements. An initial attempt to investigate the change in the transcriptome during switching from sMMO to pMMO has been made. Despite not being finished, this promising experiment is worth following up in future work to establish how MMO is regulated.

Chapter 8

Methanobactin of *Methylosinus trichosporium* (OB3b)

8.1 Introduction

Methanobactin (Mb) received increased interest from researchers working in the field of methanotrophs due to the significance (outlined in Chapter 4) of this novel compound. However, the genes involved in synthesis of Mb are still unknown. In Chapter 3, the possibility that Mb is non-ribosomally-produced in *Mc. capsulatus* was explored. Here, a different possibility that Mb is produced via mRNA and ribosomes was investigated in *Ms. trichosporium* (OB3b).

The rationale of selecting *Ms. trichosporium* was that the chemical structure and properties of Mb produced by this methanotroph were available. (Kim *et al.*, 2004; Behling *et al.*, 2008). In addition, the genome sequence of *Ms. trichosporium* was available (Stein *et al.*, 2010). These provided a blueprint for prediction of a Mb biosynthetic pathway and the putative genes involved in Mb production. Recently, the gene for a ribosomally produced peptide precursor for Mb of *Ms. trichosporium* has been predicted using bioinformatics tools (Krentz, *et al.*, 2010). Stephane Vuilleumier, University of Strasbourg, France, provided the sequences of the putative precursor (operon) for the Mb. Taking advantage of the availability of these sequences, it was exciting to investigate whether or not this putative precursor is actually involved in biosynthesis of Mb in *Ms. trichosporium* (OB3b). To this end, a marker-exchange mutagenesis approach was used to inactivate this coding sequence, which was designated as *mb*. The resulting mutant *Ms. trichosporium* Δ*mb* was then characterized and compared to the wild-type organism.

8.2 Mutagenesis of *Ms. trichosporium mb*

To explore its potential function in production of Mb, *Ms. trichosporium mb* was disrupted by a marker-exchange mutagenesis technique as previously described in

Chapter 6. An illustration of the strategy followed to generate *Ms. trichosporium* Δ*mb* is presented in Figure 8.1 and the sequences of the primers are found in Table 8.1.

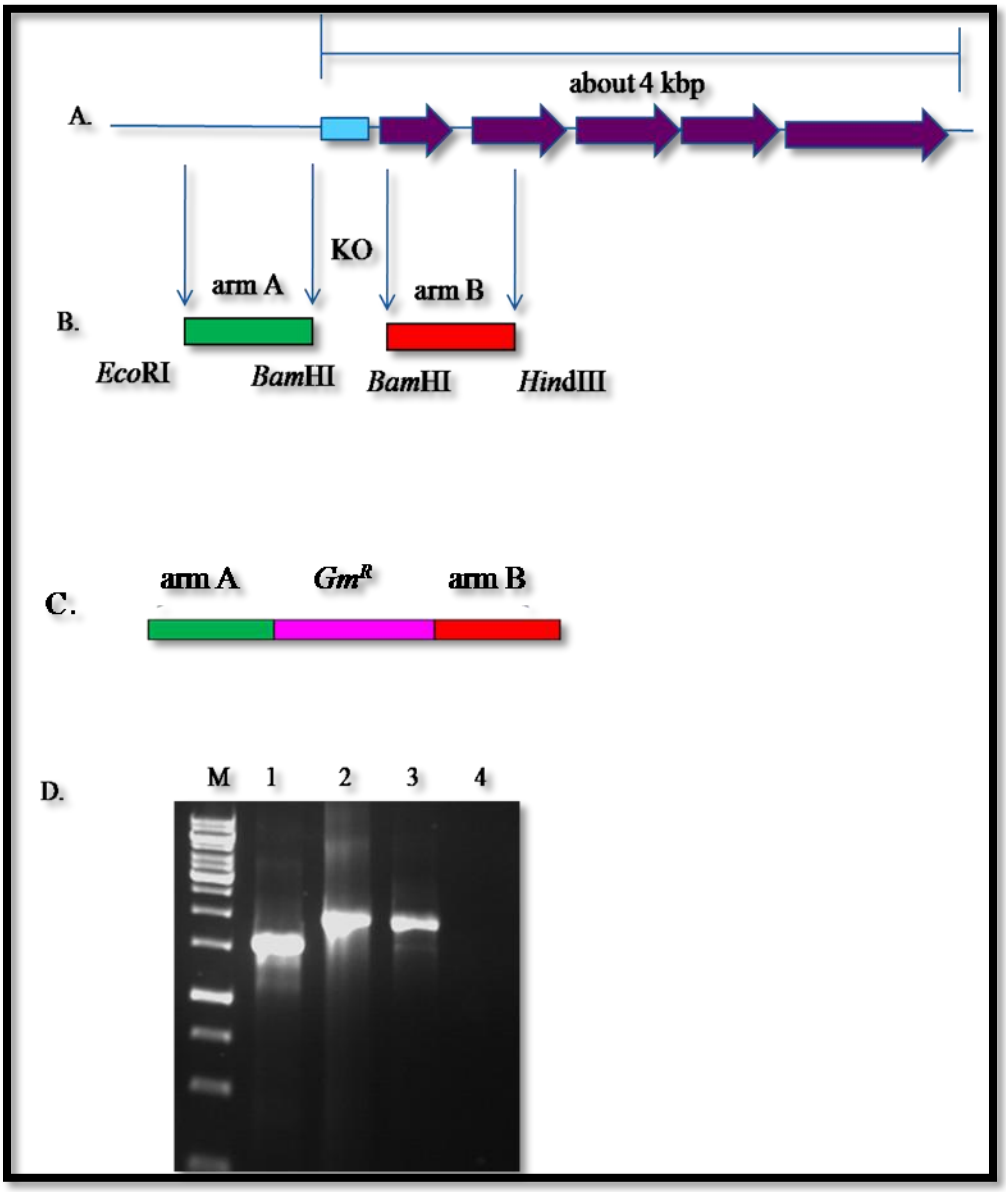

Figure 8.1 Strategy used for constructing *Ms. trichosporium* Δ*mb*. A. putative Mb precursor (blue box). B. indicating the DNA target fragments arm A and arm B used for cloning, KO: knockout region. *Eco*RI and *Bam*HI and *Bam*HI and *Hin*dIII restriction sites were introduced by PCR to facilitate cloning of arm A and arm B respectively. C. Gm^R was inserted between arms A and B via *Bam*HI restriction site. D. Confirmation of genotype of the *Ms. trichosporium* Δ*mb* strain, lane 1, PCR with primers (MBUSF176 and MBDS D569) from wild-type strain; lanes 2-3, *Ms. trichosporium* Δ*mb* and lane 4, negative control.

Table 8.1 Primers used in generating *Ms. trichosporium* Δ*mb* and in confirming its genotype. Restriction sites are highlighted in bold and underlined.

Primer	Sequence
MBAF-AF68-*Eco*RI	5-ACCATA**GAATTC**GGAATGTGTCGCTTCTATCG-3'
MBAR -AR1557-*Bam*HI	**5**ACCACA**GGATCC**ACCGGAAGGACTTTCTTCTG3'
MMBF25- *Bam*HI	5'-ACACAC**GGATCC**GGCGATTCTGGCCGTATTCC-3'
MBAF -BR589-*Hin*dIII	5'-ACACCC**AAGCTT**CGGGCTTGTCGAAAGACGTG-3'
MBUSF176	5'-GGAATGTGTCGCTTCTATCG-3'
MBDS D569	5'-CGGGCTTGTCGAAAGACGTG-3'

Two DNA regions 3' and 5' of the *mb* were amplified by PCR and named arm A and arm B, respectively (Figure 8.1 B). Restriction sites were introduced into the primers to enhance cloning of these PCR products. Products A and B were cut with *Bam*HI separately, which were then purified according to the method described in Materials and Methods. The two arms were then ligated and the ligation product was used as a template for PCR amplification to give the AB DNA fragment (Figure 8.1C). The fragment AB was cloned into pK18mob*sacB* to give the construct pAK06. The plasmid p34S-Gm was cut with *Bam*HI to produce a DNA fragment of an 865 bp, which contained the gentamicin resistance (Gm^R) gene. Gm^R gene was cloned via the *Bam*HI site between product A and B, to give the final targeting construct pAK066, which was used to transform *E. coli* S17.1 λ*pir* (Herrero *et al.*, 1990) by electroporation. Conjugation between the donor (*E. coli* S17.1 containing the pAK066 construct) and the recipient (*Ms. trichosporium*) strains was carried out according to the method of Martin and Murrell (1995). The resulting transconjugants were selected by plating onto NMS medium containing gentamicin. To ensure that no cells of *E. coli* remained as a background, colonies of the resultant *Ms. trichosporium*

were cultured in flasks containing NMS medium supplemented with nalidixic acid (10 μg ml^{-1}). The incubation conditions, screening the resultant transconjugants, identifying the double homologous recombinants and proving the genotype of the cross-over mutant were carried out as described previously in Materials and Methods. The mutant was designated as *Ms. trichosporium* Δ*mb* which was characterized by a slight transparent appearance compared to the wild-type.

8.3 Characterization of *Ms. trichosporium* Δ*mb*

8.3.1 Mb production assay

To assess whether *Ms. trichosporium* Δ*mb* produce methanobactin compared to the wild-type, CAS-Cu plate method was used as described previously in Materials and Methods. *Ms. trichosporium* wild-type exhibited a complete colour shift from blue to yellow indicating that cells sequestered copper from the Cu-CAS complex over the three weeks at 30 ºC in presence of methane (Figure 8.2A). *Ms. trichosporium* Δ*mb* strain showed no colour shift; the blue colour remained suggesting that no copper was removed from the plates (Figure 8.2B). As expected, no change in blue colour occurred in the negative control plate (not shown). These results strongly suggested this coding sequence, *mb*, is likely to be involved in Mb production in *Ms. trichosporium*.

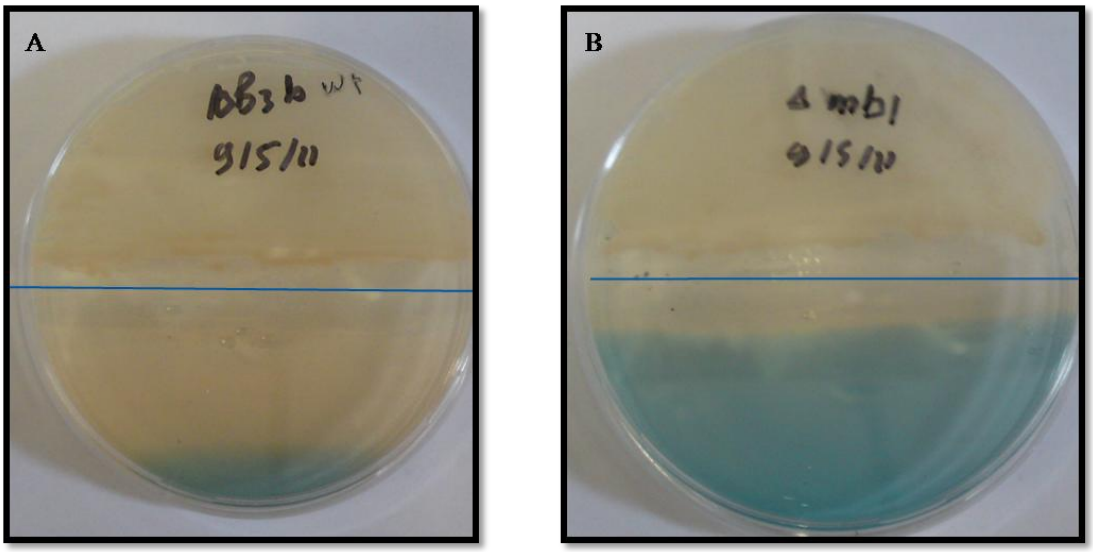

Figure 8.2 Mb assay using colorimetric plate assay in split NMS/Cu-CAS plates of A. *Ms. trichosporium wild-type*; B. *Ms. trichosporium* Δ*mb*. After three weeks of incubation at 30 ºC in presence of methane. This experiment was done in triplicates.

8.3.2 Naphthalene assay for sMMO activity

To determine the ability of *Ms. trichosporium* Δ*mb* to express sMMO, the naphthalene oxidation assay was carried out. Strains of the wild-type and mutant were grown on NMS plates containing increasing copper concentrations: 0, 0.5, 1.0, 1.5, 2.0, 2.5, 3.0, 3.5, 4.0 or 5.0 µM copper.

Table 8.2 Results of the naphthalene oxidation assay for *Ms. trichosporium* Δ*mb*.

µM copper	Wild-type	*Ms. trichosporium* Δ*mb*
No added copper	**+***	**-****
0.5	+	-
1	+	-
1.5	+	-
2	+	-
2.5	+	-
3	-	-
4	-	-
5	-	-

*: positive naphthalene assay (sMMO expressed), **: negative naphthalene assay (sMMO not expressed).

The resulting colonies were tested for sMMO expression following the method mentioned previously (Chapter 2). The results of sMMO activity as measured by the naphthalene oxidation assay are presented in Table 8.2 and Figures 8.3 - 8.5. The results showed that the *Ms. trichosporium* Δ*mb* mutant strain was unable to oxidise naphthalene as indicated by the lack of a change in the yellow colour of the reagent; a negative naphthalene assay was obtained with all concentrations of copper tested (Figure 8.3A, 8.4B, 8.5B 8.6B). Nevertheless, *Ms. trichosporium* wild-type gave a purple colour (positive naphthalene assay) upon addition of zinc complex at or below a copper concentration of 2.5 µM (Figure 8.3B, 8.4A and 8.5A). At concentration above 2.5 µM, the wild-type gave a negative naphthalene assay result. These observations revealed that in contrast to the wild-type, *Ms. trichosporium* Δ*mb* did not express sMMO (sMMO$^-$) and hence did not show a copper switch in response to copper concentration.

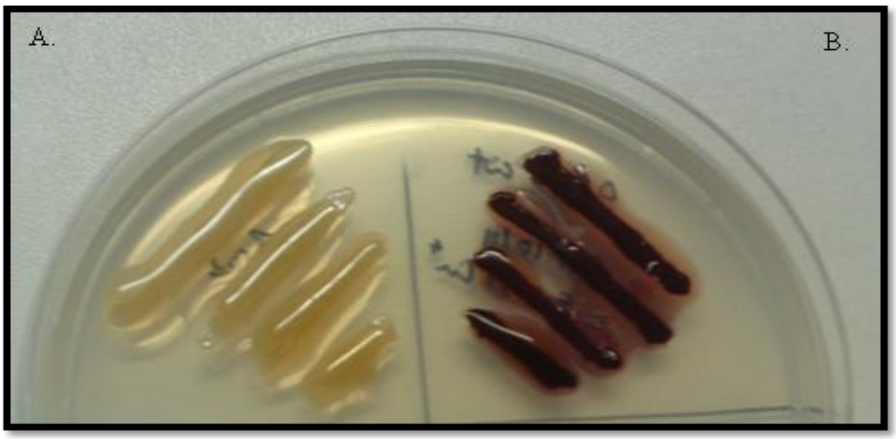

Figure 8.3 Naphthalene assay results under no-added copper concentration. A. *Ms. trichosporium* Δ*mb* (yellow colour, sMMO not expressed) and B. *Ms. trichosporium* wild-type (purple colour, sMMO expressed).

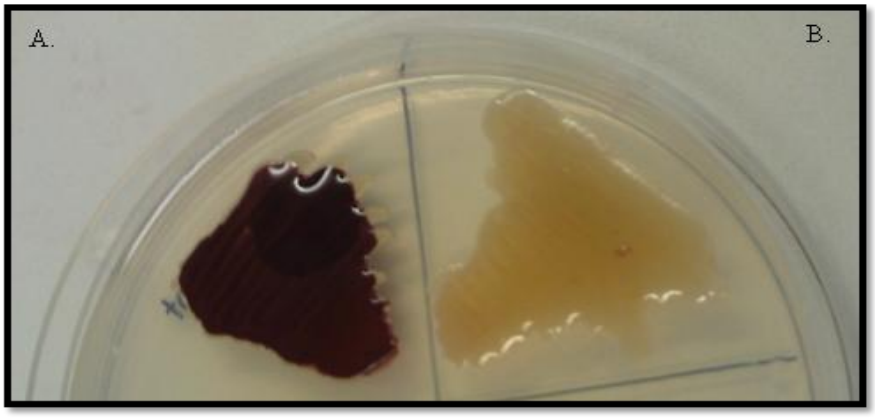

Figure 8.4 Results naphthalene assay growing at NMS supplemented with 1 µM copper. A. *Ms. trichosporium* wild-type and B. *Ms. trichosporium* Δ*mb*.

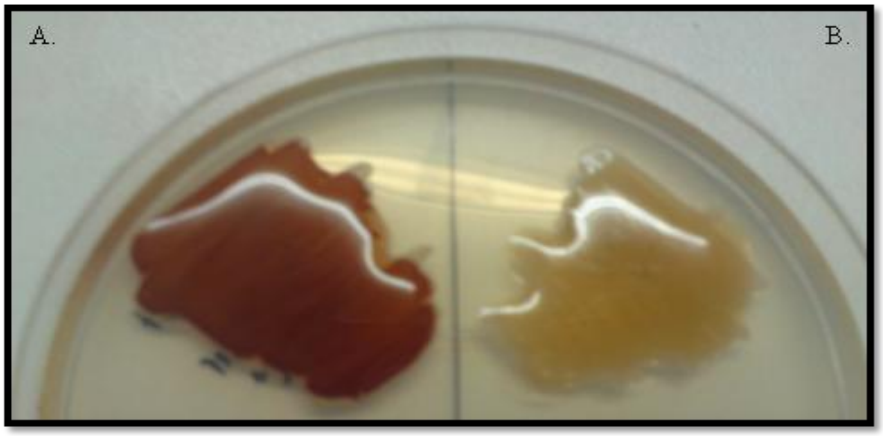

Figure 8.5 Results naphthalene assay growing at NMS supplemented 2 µM copper. A. *Ms. trichosporium* wild-type and B. *Ms. trichosporium* Δ*mb*.

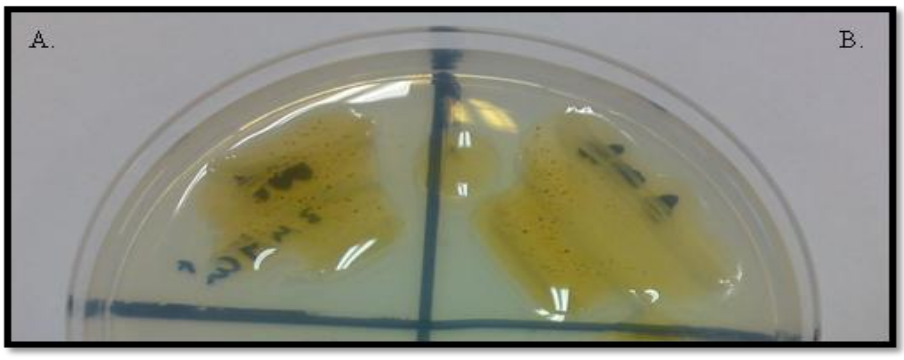

Figure 8.6 Naphthalene assay results under high copper concentration (3 µM copper). A. *Ms. trichosporium* Δ*mb* and B. *Ms. trichosporium* wild-type.

8.3.3 Growth under different copper concentration

Ms. trichosporium Δ*mb* and wild-type strains were investigated for their ability to grow on NMS plates supplemented with increasing concentrations of copper (5, 10, 15, 20, 30 and 40 µM). Both *Ms. trichosporium* wild-type and Δ*mb* strains grew well under concentration of copper up to 15 µM but they could not grow at 40 µM copper (Table 8.3). The wild-type strain showed no growth at 20 µM concentration of copper while the Δ*mb* strain could grow up to 30 µM of copper. These results indicated that Δ*mb* seem to be copper resistant compared to the wild-type.

Table 8.3 Growth under different copper concentration.

Copper concentration (µM)	Wild-type	*Ms. trichosporium* Δ*mb*
No added copper	+*	+
5	+	+
10	+	+
15	+	+
2 0	-**	+
30	-	Weak growth
40	-	-

* + : good growth and **- : no growth

8.4 Discussion

It was of interest to answer the question: is the coding sequence (*mb*) identified by Krentz *et al.*, (2010) involved in production of methanobactin in *Ms. trichosporium*? To provide the answer, marker-exchange mutagenesis was used to inactivate *mb* and interestingly, the resulting *Ms. trichosporium* Δ*mb* had three distinctive phenotypes. These are: *Ms. trichosporium* Δ*mb* (1) does not produce methanobactin (Mb^-); (2) does not express sMMO ($sMMO^-$) under copper-limiting growth conditions and (3) exhibits copper resistance. These phenotypes are

indications of a pleiotropic role of the Mb-encoding sequence in the metabolism and physiology of *Ms. trichosporium*.

Based on the CAS- Cu plates, a qualitative assay for Mb described previously by Yoon *et al.* (2010), *Ms. trichosporium* Δ*mb* does not produce Mb. This result signifies that the precursor is more likely to be involved in synthesis of Mb and validates the bioinformatic predictions made by Krentz *et al.*, (2010). The authors compared the amino acid sequence (LXGSCYPXSCM) which was predicted from the chemical composition of Mb of *Ms. trichosporium* against the whole-genome sequence of this organism and obtained the precursor gene (peptide) which appeared in the genome sequence of *Ms. trichosporium* the accession number is ZP_07840071.1 (Stein *et al.*, 2010). Also, this result supports the suggested mechanism of Mb biosynthesis which involves a series of post-transcriptional modifications (Behling et al., 2008).

Furthermore, *Ms. trichosporium* Δ*mb* does not express sMMO as indicated by the results of the naphthalene assay. This is an unexpected because there has been evidence that Mb is found to be associated with purified pMMO and that it enhanced pMMO activity (Zahn and DiSpirito 1996; Choi *et al.*, 2003). The exact explanation of the $sMMO^-$ phenotype is not clear, it might be that Mb has a role in regulating sMMO expression. One possible scenario suggests a mechanism in which Mb is acting as a specific copper sensor (or part of the copper-signaling system) through redox reactions that transfer the signal either on/off to a regulatory element (may be a repressor) for the transcription of sMMO. Consequently, in the absence of Mb as in *Ms. trichosporium* Δ*mb* the repressor remains active at all times even with no-added copper which means no expression of sMMO. Therefore, Mb is may be essential in sMMO expression and in the copper switch.

From the above mentioned phenotype, one can conclude another phenotype, which is that the pMMO is induced to the level it sustains the growth of *Ms. trichosporium* Δ*mb* at no-added copper growth conditions. This expectation is based on the facts that *Ms. trichosporium* wild-type is an obligate methanotroph, which possesses both pMMO and sMMO. The expression and activity of these enzymes are regulated by the available copper ions and MMOs are indispensible for growth. However, experimental evidence is needed to prove this assumption by measuring the activity of pMMO and the expression level of *pmoA* under such conditions. Moreover, the $sMMO^-$ and Mb^- phenotypes of Δ*mb* mutant strain are indirect evidence that Mb is less likely to be essential for pMMO expression although it enhances pMMO activity at the post-transcription level. In addition, Mb might have a role in sMMO-expressing cells, which is different from that in pMMO-expressing cells.

Ms. trichosporium Δ*mb* exhibited higher copper resistance compared to the wild-type. These results were consistent with the function of Mb in copper-uptake (Zahn and DiSpirito 1996; DiSpirito *et al.*, 1998). This is because Δ*mb*, which is unable to produce Mb, is likely to take up less copper compared to the wild-type. Therefore, the mutant tolerates more copper. These data are congruent with those obtained by Phelps *et al.* (1992) and Fitch *et al.* (1993), who generated *Ms. trichosporium* mutants that constitutively expressed sMMO, even at high copper concentration and were also found to be copper resistant. Later on, these mutants were found to produce copper-binding ligand (now known as methanobactin). A possible explanation of the phenotype is that there was a defect in copper uptake system (Tellez *et al.*, 1998) apparently not involving Mb. Results in this work confirm that methanotrophs harbour multiple routes of copper acquisition (please

see detail in Chapter 3). Furthermore, Mb is presumably involved in copper homeostasis in *Ms. trichosporium*, however, the other components (*e.g.*, CopA) involved in this process and the possible interaction amongst them represent an interesting topic to be explored in the future.

It is worth mentioning that "blasting" the amino acid sequences of Mb precursor of *Ms. trichosporium* against the genome sequence of *Mc. capsulatus* does not reveal similar peptides with significant similarities. Nonetheless, *Azospirillum* sp. B510, a nitrogen-fixer and rice-associative bacterium, was found to have a similar peptide precursor of Mb of *Ms. trichosporium* (Krentz *et al.*, 2010). Amino acid sequence alignment analysis revealed that both coding sequences share 66% identity (Figure 8.7) and contained the Cys-Gly-Ser motif (Figure 8.7).

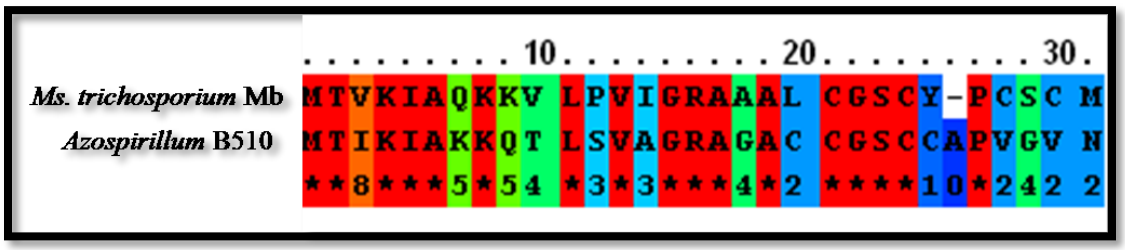

Figure 8.7 Sequence alignment of Mb coding sequence from *Ms. trichosporium* and that of *Azospirillum* B510, the conserved amino acids are highlighted with red. (unconserved 0 1 2 3 4 5 6 7 8 9 10 conserved). Sequences were aligned using PRALINEPSI strategy of the freely available PRALINE http://www.ibi.vu.nl/programs/pralinewww/ **(**Simossis and Heringa, 2005**).**

Mb production by *Azospirillum* sp. B510 is not documented, yet its genome contains a few genes that encode TonB-dependent proteins, which mediate iron-siderophore uptake under low-iron growth conditions (Kaneko *et al.*, 2010). In addition, certain *Azospirillum* species have been reported as siderophore-producers. For example, two phenolic siderophores with lysine and leucine as conjugates were produced by *Azospirillum lipoferurn* under iron-starvation (Saxena *et al.*, 1986 and

Shah *et al.*, 1992). It would be of interest to investigate *Azospirillum* sp. B510 for Mb production in comparison with *Ms. trichosporium* in future studies. Mb production might not be restricted to methanotrophs.

Furthermore, another Mb, which is chemically defined, is found in the facultative methanotroph, *Methylocystis* SB2. A comparison between both characterized Mb from *Ms. trichosporium* (OB3b) and *Methylocystis* SB2 is illustrated in Table 8.4. The significant differences between both Mbs confirm the diversity of Mb in methanotrophs. It has been assumed that *Methylocystis* SB2 Mb is also produced via ribosomes but the genome sequence of this methanotroph is not available yet (Krentz *et al.*, 2010). In addition, uptake of Mb-Cu complex by *Ms. trichosporium* under copper deficiency growth conditions has recently been proved by Balasubramanian *et al.* (2011).

More experiments need to be carried out on the *Ms. trichosporium* Δ*mb* strain, for example measuring pMMO activity and quantifying the expression level of the *pmoA* transcripts and copper content at different copper concentrations. However due to time constraints these experiments were not done. Therefore, *Ms. trichosporium* Δ*mb* and the wild-type were sent to our collaborator Prof. Alan DiSpirito Iowa State University and Dr. Jeremy Semrau, and Michigan University, USA for further studies. The initial results indicated that Δ*mb* produced a siderophore but not methanobactin as shown by analysis of the spent media using LC-MS. Identification of the siderophore is ongoing. In addition, Δ*mb* did not express sMMO as revealed from SDS-PAGE. The mutant was copper-resistant. Therefore, the basic phenotypes of the Δ*mb* was reproduced in other laboratories, providing more robustness to the findings reported in this chapter.

Table 8.4 A comparison between Mb from *Ms. trichosporium* (OB3b) and from *Methylocystis* SB2

	OB3b-Mb	**SB2-Mb**
Producing organism	*Ms. trichosporium*	*Methylocystis* SB2
MMO	pMMO and sMMO	pMMO
Methanotrophic nature	Obligate methanotroph	Facultative methanotroph
Phylogeny group	*Alphaproteobacteria*	*Alphaproteobacteria*
Molecular mass	1215.1781 Da	815.34 Da
Residue number	Seven	Four
Residue type	Glycine, serine, cysteine, tryptophan, serine, cysteine and methionine	Alanine, serine, alanine, alanine
Copper-binding site	Two oxazolone (5-membered heterocylic rings) each attached with enethiol	One oxazolone and one imidazolone each attached with enethiol
Sulfate group	Absent	Present
Affinity to copper	High	Relatively high
Other metals	Can bind many other metals (*e.g.*, Au(III), Fe(II) and Zn(II)	Not determined

References: Behling *et al.* (2008), Krentz *et al.* (2010), Choi *et al.* (2006) and Choi *et al.* (2010).

A future task is to clone the gene encoding for Mb into an appropriate expression system to overproduce this exciting compound. If these experiments succeed, then research can be directed towards production of Mb on an industrial scale for different applications *e.g.*, treating diseases like Wilson's disease. In support of that, it has been reported that Mb can be used for treating the rat model of Wilson's disease, a disease characterized by accumulation of copper in certain tissues (*e.g.*, liver and brain) (Summer *et al.*, 2011). A notable reduction of copper in the liver was observed upon treating with Mb. Although these exciting results were obtained on experimental animals, Mb represents a pivotal active constituent of a potential novel drug that can be used as an initial option in treating Wilson's disease (Summer *et al.*, 2011).

In brief, the data outlined in this chapter show that the precursor gene candidate proposed by Krentz *et al.* (2010), is involved in the synthesis of Mb in *Ms. trichosporium*. Mutagenesis of this precursor resulted in a mutant which is unable to produce Mb or express sMMO and resist high concentrations of copper, highlighting the pleiotropic role of that precursor in physiology of *Ms. trichosporium*. To our knowledge, this is the first study, which provides experimental proof that Mb is ribosomally synthesized in a methanotroph.

Chapter 9

General discussions, conclusions and future perspectives

9.1 General discussions and conclusions

Mc. capsulatus is an obligate methanotroph that gains its needs of carbon and energy via oxidation of methane, a potent greenhouse gas, thus reducing of the amount of methane released to the Earth's atmosphere. This bacterium oxidises methane into methanol using a membrane-bound particulate methane monooxygenase (pMMO) and a soluble cytoplasmic enzyme (sMMO). The expression and activity of both enzymes is significantly affected by the bioavailability of copper. Under high copper-biomass ratios, the biosynthesis of pMMO is switched on while sMMO is up-regulated during growth at low copper-to biomass ratios. Despite *Mc. capsulatus* being one of the most intensively studied methanotroph, the exact mechanisms by which copper regulates MMO is unclear. Therefore, the main aim of this study was to shed new light on the copper switch between pMMO and sMMO using the available genome sequence of this organism, together with mutagenesis and transcriptional regulation studies. The work presented in this study is considered a step forward towards understanding the copper switch in *Mc. capsulatus* as it tackled three main potential factors based on the work of previous researchers.

The first factor was copper transport and in particular copper translocating P-type ATPases. Choosing this factor was based on the work done previously on the *Ms. trichosporium* by Phelps *et al.* (1992) and Fitch *et al.*(1993) when they used a random mutagenesis technique to generate a mutant that expressed sMMO constitutively. This phenotype was explained by suggesting a possible defect in copper uptake. In the genome of *Mc. capsulatus*, three copper translocating P-type ATPases homologues are identified (Ward *et al.*, 2004) which putatively function in copper transport. A mutant in one of the three genes (Δ*copA1*) was generated by Ali

(2006) and in this study two mutants in the other two genes (*copA2* and *copA3*) were constructed. Inactivation of these genes did not result in constitutive sMMO expression. CopA of *Mc. capsulatus* might have roles in copper homeostasis.

The second factor was Mb, which is a copper-chelating small peptide that provides another route for copper uptake in *Mc. capsulatus* (Zahn and DiSpirito 1996; DiSpirito *et al.*, 1998). However, the enzymes involved in the biosynthetic pathway of this molecule are unknown and the genome of *Mc. capsulatus* lacks any corresponding *orf* that may be identified with this function. It has been suggested that Mb is produced non-ribosomally via NRPS, based on the similarity of Mb to siderophores (Balasubramanian and Rosenzweig 2008). Looking at the *Mc. capsulatus* genome, two NRPS homologues in addition to one for PKS were identified (Ward *et al.*, 2004). Ali (2006) inactivated one of the two genes encoding NRPS, while the other copy (*nrpS-2*) in addition to the gene encoding PKS was disrupted in this study. Again, these genes seemed not to regulate MMO in *Mc. capsulatus*. The distinctive phenotypes of the mutants indicated that they might be involved in the synthesis of defective Mb.

Another suggestion about the genes involved in Mb formation has been made by Krentz *et al.* (2010) when they assumed that this small peptide may be produced ribosomally and they predicted a putative peptide for this role. In this study, a mutant in this coding sequence was made and characterized. Surprisingly, the mutant not only did not synthesize Mb but also did not express sMMO. In addition, copper resistance was another phenotype of this mutant. These novel and interesting findings will widen our perception about the copper switch and the possible biotechnological application of Mb (*e.g.*, treating Wilson's disease). In

addition, the coding sequence for Mb has a pleiotropic role in *Ms. trichosporium* physiology.

The third factor was using microarray technology in studying whole-genome transcriptome of *Mc. capsulatus* expressing sMMO versus pMMO, and to our knowledge, this was the first study in this regard. The results revealed interesting genes that were up-regulated or down-regulated under conditions that would be important not only in MMO regulation but also in copper homeostasis. Another attempt was made in this study to study the gradual changes in the transcriptome of *Mc. capsulatus* as a function of time while copper was added stepwise. This experiment was not finished due to lack of time. This approach will provide deeper and detailed information about the potential genes involved in the copper switch from sMMO to pMMO, if followed up.

A summary of the results and conclusions of each chapter followed by the future prospects are described below.

9.2 Copper transport in *Mc. capsulatus*

In Chapter 3, two copper translocating P-type ATPase homologues; MCA0805 (*copA2*) and MCA 2072 (*copA3*) were generated. Both mutants in addition to the third one MCA0705 (*copA1*) (Ali, 2006) were characterized using naphthalene oxidation assay, growth at different copper or silver concentrations, cytochrome oxidase and intracellular copper measurements. The results obtained highlighted that the three genes are not involved in MMO regulation as indicated by the same response to an sMMO assay. Generation of a constitutively expressing sMMO mutant needs inactivation of more than one copper transporter. However, CopA might have a role in copper homeostasis in this obligate methanotroph.

9.3 Methanobactin of *Mc. capsulatus*

The work described in Chapter 4 was attempted to identify which genes are involved in the production of methanobactin (Mb) in *Mc. capsulatus*. Two mutants in genes encoding for non-ribosomal peptide synthetase (*nrpS-2* and polyketide synthase (*pkS*) were obtained. A third mutant Δ*nrpS-1* (Ali, 2006) was included in the characterization using a qualitative Mb assay (CAS-Cu plates) and other tests. According to the results of CAS-Cu plates assay, NRPS-1 seemed to not be involved in Mb synthesis while PKS and/or NRPS-2 may be involved in the production of a functional metal-chelating compound. Based on the initial results received from our collaborators; Prof. Alan DiSpirito Iowa State University and Dr. Jeremy Semrau, Michigan University, Inactivation of NRPS-2 and PKS does not affect Mb production. These seemingly contradictory finding suggest a possible role for PKS and NRPS-2 in the post-translational modification of Mb. Furthermore, it seemed that regulation of MMO by copper in *Mc. capsulatus* is independent of these genes; *nrpS-1*, *nrpS-2* and *pkS* although they might interfere with copper transport.

9.4 Transcriptome analysis of *Mc. capsulatus*

Chapter 5 outlined an attempt to identify the genes that are probably involved in regulation of MMO by copper using microarray technology. A comparative study of the differential expression profiling of whole-genome transcriptomics of *Mc. capsulatus* expressing sMMO versus pMMO was carried out in three biological replicates. A whole-genome microarray identified 53 genes which were differentially expressed; 28 genes were significantly down-regulated while 25 genes were substantially up-regulated. Among these genes, some genes seem promising in MMO regulation, *e.g.*, *tetR* which was down-regulated, and in Mb transport *e.g.*, *tonB* was

up-regulated. Furthermore, the cluster of five genes 5' of sMMO, which were up-regulated, were shown to be co-transcribed by RT-PCR and promoter 5' were predicted. Many of these genes are promising candidates in future studies dealing with both MMO regulation and copper homeostasis.

9.5 *Mc. capsulatus* MCA1191 (*scO-1*)

The work conducted in Chapter 6 aimed at investigating the potential role of MCA1191 (*scO-1*), one of the up-regulated genes in the operon upstream of the sMMO, in MMO regulation. *scO-1* was inactivated by a marker-exchange mutagenesis technique and the resulting *Mc. capsulatus* Δ*scO-1* was characterized and compared to the wild-type. No significant difference between the mutant and the wild-type was obtained in respect to expression of sMMO according to the naphthalene test. Therefore, the function ScO-1 seemed to be not linked with the regulatory systems of MMO by copper. Nevertheless, Δ*scO-1* appeared to be a copper resistant mutant indicating that ScO-1 is involved in copper homeostatic mechanisms presumably via signal transfer controlling the rate of the copper translocating protein. Furthermore, the results confirmed that ScO proteins are multi-functional and perform various functions in various organisms.

9.6 Physiological features during the "copper switch"

The initial purpose of the work in Chapter 7 was to explore the gradual changes in the transcriptome of *Mc. capsulatus* that initially expressed sMMO, in response to the gradual addition of copper in order to get an in-depth snapshot of the transcriptome during the switch from sMMO to pMMO. In addition to this, the other aim was to link what is happening in the transcriptome with both the copper

distribution of the cells (extracellular, intracellular and associated with biomass) and the proteomics by comparing the sMMO and pMMO polypeptides. Despite the first aim not being achieved, due to insufficient RNA extracted and the lack of time to repeat the experiment and extract more RNA, the other aim was fulfilled. *Mc. capsulatus* was grown on NMS medium in a chemostat (continuous steady state) then copper was added gradually. Samples were collected at different time points and assayed for sMMO expression using the naphthalene assay, SDS-PAGE of total cell protein, copper measurements and RNA extraction. The results confirmed that copper negatively regulates sMMO and induces pMMO. Although this experiment is not completed, it is worth following up.

9.7 Methanobactin of *Ms. trichosporium* (OB3b)

Results in Chapter 8 were intriguing in the whole thesis. Although the work performed was on another model methanotroph, *Ms. trichosporium* (OB3b), the results achieved a very exciting and promising. Initially the aim was to inactivate a putative ribosomally-located gene, which was predicted using bioinformatics to be involved in the synthesis of Mb (Krentz *et al.*, 2010). One of our collaborators: Stephane Vuilleumier, Strasbourg University, France, kindly sent us the putative Mb precursor sequences and a mutant was constructed by marker-exchange mutagenesis. Subsequently, the resulting mutant *Ms. trichosporium* Δ*mb* was characterized using the CAS-Cu plates, the naphthalene oxidation test and by testing the ability to grow at different copper concentrations. Interestingly, the results reported with the CAS-Cu plate assay indicated that *Ms. trichosporium* Δ*mb* was unable to produce Mb. Furthermore, the mutant could not express sMMO even when tested at no-added copper growth conditions, which represented an unexpected but

exciting result. A third phenotypic feature of the mutant was copper resistance compared to the wild-type in addition to a difference in the colony appearance; the mutant being more transparent than the wild-type. Collectively, the findings described in this chapter showed that Mb of *Ms. trichosporium* is ribosomally-synthesized via the coding sequence predicted by Krentz *et al.* (2010). In addition, Mb is involved in sMMO regulation presumably via signalling events, which will provide further insights in understanding the copper switch in *Ms. trichosporium*. In addition, Mb seemed to have a role in copper homeostasis. This mutant was also sent to Prof. Alan DiSpirito and Dr. Jeremy Semrau for further studies.

Based on the work done in this study and in other studies the following model is proposed (Figure 9.1).

sMMO expression

When the cells grow under low-copper growth conditions, copper-uptake is mediated through MopE, Mb or CopA3. Cu-Mb complex is internalized as such by the cells where it is proposed to interact directly or indirectly with a putative sMMO repressor through a coupled redox reaction therefore, the repressor become inactivated, allowing sMMO transcription to take place. At the same time pMMO is expressed but at a basal level.

pMMO expression

When excess copper is available, cells take up copper through energy-saving routes such porins and may be other transporters such as CopA3 with low rate. No Mb is secreted outside the cells. Under these conditions, Mb is proposed to enhance the activity of pMMO rather than inactivate sMMO. The repressor became activated, preventing the transcription of sMMO by a mechanism yet to be identified.

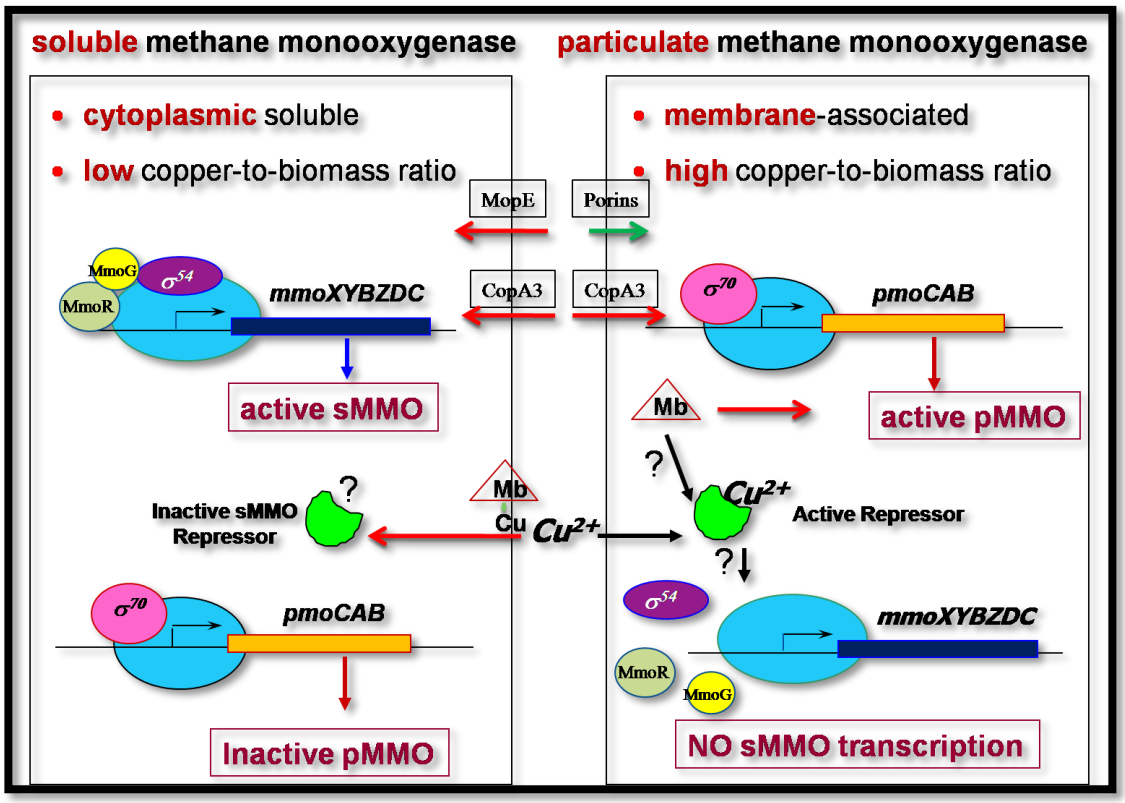

Figure 9.1 Proposed model for the copper switch of the two MMOs.

Two important points need to be addressed in the context of the copper switch. The first point is that *mmoQ* and *mmoS* are identified in *Mc. capsulatus* only, and if both genes are involved in the copper switch, one can assume that the mechanism of MMO regulation by copper in this methanotrophs is unique. However, both *mmoQ* and *mmoS* are overlapped by one codon indicated they might be co-transcribed implying they might integrate in performing their specific function. Furthermore, inactivation of *mmoQ* did not affect sMMO expression and these genes and not regulated themselves by copper based on the microarray data (Chapter 5). Therefore, *mmoQ* and *mmoS* are less likely to be involved in the copper switch in *Mc. capsulatus*.

The other point is that *mmoG* and *mmoR* are not proved to be indispensable for sMMO transcription, although no copper-binding motifs has been predicted in MmoG nor MmoR (Csaki *et al.*, 2003; Stafford *et al.*, 2003; Scanlan *et al.*, 2009).

This does not absolutely mean that they cannot bind copper unless experimentally proved, which has not been done yet. MmoG and/or MmoR might bind copper via novel copper-binding motif. For example, kynurenine, which was a previously unknown compound to be involved in copper-binding in any protein, has been shown to do this job in MopE (Helland *et al.*, 2008). In addition, *mmoR* was shown to be co-transcribed with the structural genes of the sMMO operon: all under control of the *mmoX* promoter (Iguchi *et al.*, 2010). These observations indicate that the exact mechanisms of regulation of MMO by copper in methanotrophs seem to be a species-specific although the general architecture of the MMO is conserved.

9.8 Future perspectives

The work described herein presents the basis for three main lines of future investigations in order to gain in-depth knowledge about 1) how copper represses sMMO or activates pMMO the molecular level; 2) how methanotrophs deal with copper stress or copper deficiency; and 3) if there are links between such copper homeostatic mechanisms and the copper switching between both forms of MMO.

The first line of research will be based on the work conducted in Chapter 3, copper transporters. For instance, comparative gene expression of *mmoX* and *pmoA* transcripts using real time (RT-PCR) Δ*copA1*, Δ*copA2* and Δ*copA3* growing at various copper concentration compare to the wild-type will provide a better idea about the possible integration in performing certain functions. In parallel with these experiments, estimating the activity of sMMO and pMMO from the same samples using *e.g.*, propylene oxidation assay will link the gene, transcript and the function. Because the copper switch process is very copper sensitive, it is of significant

importance to minimise the background copper in the NMS medium by adding specific copper chelator *e.g.*, BCS.

Furthermore, exploring the possibility to generate a constitutive sMMO mutant via inactivation of multiple copper uptake systems. This could also resolve the potential role of CopA proteins in getting copper to the copper-sensor of the copper switch in *Mc. capsulatus*. A different strategy from marker-exchange mutagenesis technique should be followed to overcome the problems of selecting double or triple mutants. For example, *Cre-Lox* recombination technology, which has been successfully used in another methanotroph, *Methylocella silvestris* (Crombie, 2011) will help in this respect. The possible role of Mb in regulating the rate of copper-translocating P-type ATPases is needs to be addressed.

Additionally, detailed studies can be carried out considering the roles of *copA1 copA2* and *copA3* in copper homeostasis by estimating the activity of copper transporters; inactivation some of the flanking genes in each of operon and looking at different proteins or chaperonins that might interact with the transporters. In addition, attempts to identify the other components (such as sensor or regulator) that integrate in function to deal with copper level changes are critical.

The second line of research will be based on the observations shown in Chapter 5 and Chapter 8 regarding the Mb from both methanotrophic models; *Mc. capsulatus* and *Ms. trichosporium*. Regarding *Mc. capsulatus* Mb, the results reveal that PKS and/or NRPS-2 but not NRPS-1 is probably involved Mb production. Quantification of Mb produced by these mutants and different copper concentrations is needed to draw solid conclusions about the roles of these proteins in Mb. However, the mutants have been sent to Alan DiSpirito and Jeremy Semrau and the initial results showed that, the mutants produced as much Mb as the wild-type. These

findings raised other question: does the produced Mb by PKS and NRPS-2 bind copper with the same affinity as the wild-type. Comparing the quantity and the quality of different metabolites that the relevant mutants secrete in the spent media when grow at varying copper and/or iron concentrations metabolic profiling are worth exploring using LC-MS. In addition, monitoring the metabolite profiling over the different growth phases is vital. As this is the first study to our knowledge that investigates NRPS or PKS from methanotrophs, therefore the possibility to find a new metal chelator is rather high priority if there are distinctive copper-sensitive phenotypes obtained from the relevant mutants. Furthermore, similar work on copA mutants is worth doing for the Δ*nrpS-1*, Δ*nrpS-2* Δ*pkS*.

Regarding *Ms. trichosporium* Mb, Δ*mb* exhibited exciting phenotypes; inability to produce Mb, inability to express sMMO and copper resistance. Further investigations are needed: for example, estimating SDS-PAGE of pMMO and sMMO polypeptides, analysis of metal content and real time PCR of *pmoA* and *mmoX*. However, these observations open the door to other more promising experiments *e.g.*, over-expression of Mb using an appropriate expression system then exploring the possibility of producing Mb on a large scale for possible biotechnological applications. Mb was proved to be useful in treating Wilson's disease in experimental animals and this might lead to developing a novel drug in which Mb is the active compound. Subsequently, this drug will represent an alternative option in treating human Wilson disease (Summer *et al.*, 2011). Also, taking advantage of the genome of *Ms. trichosporium* that has been sequenced, putative copper transporters and other proteins that have roles in copper homeostasis or sMMO regulation can be studied in conjunction with Mb. It will be of interest to

propose an updated model suggesting how the copper switch occurs in the light of the new role of Mb.

The third line of future work will depend upon the results of the comparative gene expression of the whole transcriptome of *Mc. capsulatus* growing at sMMO or pMMO expressing conditions. The findings that 53 gene were differentially expressed under both conditions stimulate the close investigation of every single gene after validating them by optimised qPCR. However, from the Blast results of the annotations of these genes, one can pick a few genes to be the priority for future studies dealing with MMO regulation. One of these genes is *tetR*, a gene encoding a putative transcriptional regulator, which was down-regulated in sMMO expressing conditions. Another candidate is *TonB*, an up-regulated gene, which encodes for a protein that is proposed to be a part of membrane transporter. This gene is proposed to be involved in the copper Mb uptake system. In addition, a gene, which is just upstream of sMMO and oriented in the opposite direction; MCA1193 needs to be inactivated and its phenotype examined.

Furthermore, the initial experiment in Chapter 7, which aimed at looking at the gradual change in the transcriptome with supplying of copper, is of high importance to be followed up. In addition, including biological replicates will strengthen the results obtained. Taking these experiments, together with the results of the other microarray experiment in Chapter 5, will provide a clearer picture about switching from sMMO to pMMO.

The last future research line will emerge from the results reported in Chapter7 about the ScO-1 protein in *Mc. capsulatus*. Despite *scO-1* seeming to be involved in function independent of MMO regulation, it has a role in copper homeostasis. As the genome of *Mc. capsulatus* contains another two ScO-like homologues, measuring the

expression levels of both genes in the mutant compared to the wild-type at different copper concentrations will reveal if one or both are over-expressed to compensate for the mutated one. In addition, estimation of the gene expression of the copper transporters encoding genes will provide explanations of the copper resistant phenotype. This is because copper resistance may be due to a high rate of copper exporting proteins or slow rate of copper importing ones. A third group of genes that is worth examining at the expression level are the genes encoding cytochrome c oxidases and in particular both genes downstream of *scO-1*(MCA1191).

References

References

Abajian, C. and Rosenzweig, A. C. (2006). Crystal structure of yeast ScO1. *J. Biol. Inorg .Chem*. **11**, 459-66.

Adams, M. A., Udell, C. M., Pal, G. P. and Jia, Z. (2005). MraZ from *Escherichia coli*: cloning, purification, crystallization and preliminary X-ray analysis. *Acta. Crystallogr. Sect. F. Struct. Biol. Cryst. Commun*. **1**, 378-80.

Adeosun, E. K, Smith, T. J., Hoberg, A. M., Velarde, G., Ford, R. and Dalton, H. (2004). Formaldehyde dehydrogenase preparations from *Methylococcus capsulatus* (Bath) comprise methanol dehydrogenase and methylene tetrahydromethanopterin dehydrogenase. *Microbiology* **150**, 707–713.

Ali, H. (2006). Development of genetic tools in methanotrophs and the molecular regulation of methane monooxygenase. PhD thesis submitted to the Department of Biological Sciences, University of Warwick.

Amaral, J. A. and Knowles, R. (1995). Growth of methanotrophs in methane and oxygen counter gradients. *FEMS Microbiol. Lett*. **126**, 215-220.

Ansari, M. Z., Yadav, G., Gokhale, R. S. and Mohanty, D. (2004). NRPS-PKS: a knowledge-based resource for analysis of NRPS/PKS megasynthases. *Nucleic Acids Res*. **32**, W405-413.

Anthony, C. (1982). The biochemistry of the methylotrophs, pp. 1-41, New York, NY: Academic Press.

Anthony, C. (2004). The quinoprotein dehydrogenases for methanol and glucose. *Arch. Biochem. Biophys*. **428**, 2-9.

Apell, H., J. (2004). How do P-Type ATPases transport ions? *Bioelectrochem*istry **63**, 149-156.

Argüello, J., M. (2003). Identification of ion-selectivity determinants in heavy-metal transport P1B-type ATPases. *J. Membr. Biol*. **195**, 93–108.

Argüello, J. M, Eren, E. and Gonzalz-Guerrero, M. (2007). The structure and function of heavy metal transport P_{1B}-ATPases. *Biometals* **20**, 233-248.

Arnesano, F., Banci, L., Bertini, I., Ciofi-Baffoni, S., Molteni, E., Huffman, D. L. and O'Halloran, T. V. (2002). Metallochaperones and metal-transporting ATPases, a comparative analysis of sequences and structures. *Genome Res*. **12**, 255-271.

Artigas, P. and Gadsby, D., C. (2003). Na^+/K^+-pump ligands modulate gating of palytoxin-induced ion channels. *Proc. Natl. Acad. Sci. USA* **100**, 501-505.

Auman, A. J., Stolyar, S., Costello, A. M. and Lidstrom, M. E. (2000). Molecular characterization of methanotrophic isolates from freshwater lake sediment. *Appl. Environ. Microbiol*. **66**, 5259-5266.

Austin, M. B. and Noel, J. P. (2003). The chalcone synthase superfamily of type III polyketide synthases. *Nat. Prod. Rep.* **20**, 79-110.

Balasubramanian, R. and Rosenzweig, A. C. (2008). Copper methanobactin: a molecule whose time has come. *Curr. Opin. Chem. Biol.* **12**, 245-249.

Balasubramanian, R., Kenney, G. E. and Rosenzweig, A. C. (2011). Dual pathways for copper uptake by methanotrophic bacteria. *J. Biol. Chem.* **286**, 37313-37319.

Balasubramanian, R., Smith, S. M., Rawat, S., Yatsunyk, L. A., Stemmler, T. L. and Rosenzweig, A. C. (2010). Oxidation of methane by a biological dicopper centre. *Nature* **465**, 115-119.

Banci, L., Bertini, I., Ciofi-Baffoni, S., Katsari, E., Katsaros, N., Kubicek, K. and Mangani, S. (2005). A copper (I) protein possibly involved in the assembly of CuA center of bacterial cytochrome c oxidase. *Proc. Natl. Acad. Sci. USA*, **102,** 3994-3999.

Banci L, Bertini I, Cavallaro G, and Rosato A (2007). The functions of ScO proteins from genome-based analysis. *J. Proteome Res.* **6**, 1568–1579.

Banci, L, Bertini, I., Ciofi-Baffoni, S., Kozyreva, T., Mori, M. and Wang, S. (2011). ScO proteins are involved in electron transfer processes. *J. Biol. Inorg. Chem.* **16**, 391-403.

Bandow, N. L., Gallager, W. H., Behling, L., Choi, D. W., Semrau, J. D., Hartsel, S. C., Gilles, V. S. and DiSpirito, A. A. (2011). Isolation of methanobactin from the spent media of methane oxidizing bacteria. *Meth. Enzymol.* **495**, 248 - 259.

Barnes J., Barnes, E. M. (1980). Proton-coupled calcium transport by intact cells of *Azotobacter vinelandii*. *J. Bacteriol.* **143**, 1086-1089.

Basu, P., Katterle, B., Andersson, K. K. and Dalton, H. (2003). The membrane-associated form of methane mono-oxygenase from *Methylococcus capsulatus* (Bath) is a copper/iron protein. *Biochem. J.* **369**, 417-427.

Bayle, D., Wangler, S., Weitzenegger, T., Steinhilber, W., Volz, J., Przybylski, M., Schafer, K. P., Sachs G. and Melchers, K. (1998). Properties of the P-type ATPases encoded by the *copAP* operons of *Helicobacter pylori* and *Helicobacter felis*. *J. Bacteriol.* **180**, 317–329.

Behling, L. A., Hartsel, S. C., Lewis, D. E., DiSpirito, A. A., Choi, D. W., Masterson, L. R., Veglia, G. and Gallagher, W. H. (2008). NMR, mass spectrometry and chemical evidence reveal a different chemical structure for methanobactin that contains oxazolone rings. *J. Am. Chem. Soc.* **130**, 12604-12605.

Belova, S. E., Baani, M., Suzina, N. E., Bodelier, P. L. E., Liesack, W., and Dedysh, S. N. (2011). Acetate utilization as a survival strategy of peat-inhabiting *Methylocystis* spp. *Environ. Microbiol. Rep.* **3**, 36-46.

Berestovskaya, J. J., Kotsyurbenko, O. R., Tourova, T. P., Kolganova, T. V., Doronina, N. V., Golyshin, P. N. and Vasilyeva, L. V. (2011). *Methylorosula polaris* gen. nov., sp. nov., a new aerobic, facultatively methylotrophic psychrotolerant bacterium from tundra wetland soil. *Int. J. Syst. Evol. Microbiol.* doc: ijs.0.007005-0v1-ijs.0.007005-0.

Berson, O. and Lidstrom, M. E. (1996). Study of copper accumulation by the type I methanotroph *Methylomicrobium albus* BG8. ***Environ. Sci. Technol.* 30**, 802-809.

Berson, O. and Lidstrom, M. E. (1997). Cloning and characterization of corA, a gene encoding a copper repressible polypeptide in the type I methanotroph, *Methylomicrobium albus* BG8. *FEMS Microbiol. Lett.* **148**, 169-174.

Bissig, K. D., Wunderli-Ye, H., Duda, P. and Solioz, M. (2001). Structure-function analysis of purified *Enterococcus hirae* CopB copper ATPase, effect of Menkes/Wilson disease mutation homologues. *Biochemical. J.* **357**, 217-223.

Bodrossy, L., Holmes, E. M., Holmes, A. J., Kovacs, K. L. and Murrell, J. C. (1997). Analysis of 16S rRNA and methane monooxygenase gene sequences reveals a novel group of thermotolerant and thermophilic methanotrophs, *Methylocaldum* gen. nov. *Arch. Microbiol.* **168**, 493-503.

Borisov, Vitaliy B., Robert B. Gennis, James Hemp, and Michael I. Verkhovsky (2011). The Cytochrome *bd* respiratory oxygen reductases. *Biochim. Biophys. Acta* **1807**, 1398-1413.

Borodina, E., Nichol, T., Dumont, M. G., Smith, T. J. and Murrell., J. C. (2007). Mutagenesis of the" leucine gate" to explore the basis of catalytic versatility in soluble methane monooxygenase. *Appl. Environ. Microbiol.* **73**, 6460-6467.

Borneman, A. R., Bartowsky, E. J., McCarthy, J., and Chambers, P. J. (2010). Genotypic diversity in *Oenococcus oeni* by high-density microarray comparative genome hybridization and whole-genome sequencing. *Appl. Microbiol. Biotechnol.* **86**, 681-691.

Bowman, J. P., Jimenez, L., Rosario, I., Hazen, T. C. and Sayler, G. S. (1993a). Characterization of the methanotrophic bacterial community present in a trichloroethylene-contaminated subsurface groundwater site. *Appl. Environ. Microbiol.* **59**, 2380-2387.

Bowman, J. P., Sly, L. I., Nichols, P. D. and Hayward, A. (1993b). Revised taxonomy of the methanotrophs, description of *Methylobacter* gen. nov., emendation of *Methylococcus*, validation of *Methylosinus* and *Methylocystis* species, and a proposal that the family Methylococcaceae includes only the group I methanotrophs. *Int. J. Syst. Bacteriol.* **43**, 735-753.

Bowman, J. P., Sly, L. I. and Stackebrandt, E. (1995). The phylogenetic position of the family Methylococcaceae. *Int. J. Syst. Bacteriol.* **45**, 182-185.

Bowman, J. P., McCammon, S. A. and Skerratt, J. H. (1997). *Methylosphaera hansonii* gen. nov., sp. nov., a psychrophilic, group I methanotroph from Antarctic marine-salinity, meromictic lakes. *Microbiol.* **143**, 1451-1459.

Bratina, B. J., Brusseau, G. A. and Hanson, R. S. (1992). Use of 16S rRNA analysis to investigate phylogeny of methylotrophic bacteria. *Int. J. Syst. Bacteriol.* **42**, 645.

Brusseau, G.A., Tsien, H.-C., Hanson, R.S., and Wackett, L.P. (1990). Optimization of trichloroethylene oxidation by methanotrophs and the use of a colorimetric assay to detect soluble methane monooxygenase activity. *Biodegradation* **1**, 19-29.

Bublitz, M., Morth, J. P. and Nissen, P. (2011). P-type ATPases at a glance. *J. Cell Sci.* **124**, 2515-2519.

Burkhead, J. L., Reynolds, K. A. G., Abdel-Ghany, S. E., Cohu, C. M. and Pilon, M. (2009), Copper homeostasis. *New Phytol.* **182**, 799–816.

Burrows, K. J., Cornish, A., Scott, D. and Higgins, I. J. (1984). Substrate specificities of the soluble and particulate methane monooxygenases of *Methylosinus trichosporium* (OB3b). *J. Gen. Microbiol.* **130**, 3327-3333.

Butcher, P. D. (2004) Microarrays for *Mycobacterium tuberculosis*. *Tuberculosis* **84**, 131-137.

Cardy, D. L. and Murrell, J. C. (1990). Cloning, sequencing and expression of the glutamine synthetase structural gene (*glnA)* from the obligate methanotroph *Methylococcus capsulatus* (Bath). *J. Gen. Microbiol.* **136**, 343-352.

Cardy, D. L., Laidler, V., Salmond, G. P. and Murrell, J. C. (1991). The methane monooxygenase gene cluster of *Methylosinus trichosporium*, cloning and sequencing of the *mmoC* gene. *Arch. Microbiol.* **156**, 477-483.

Cavet, J. S., Borrelly, G. M. and Robinson, N. J. (2003). Zn, Cu and Co in cyanobacteria: selective control of metal availability. *FEMS Microbiol Rev* **27**, 165–181.

Chalabi, N., Satih, S., Delort, L., Bignon, Y. J., and Bernard-Gallon, D. J. (2007). Expression profiling by whole-genome microarray hybridization reveals differential gene expression in breast cancer cell lines after lycopene exposure. *Biochim. Biophys. Acta*. **1769**, 124-130.

Chan, H., Babayan, V., Blyumin, E. and other authors (2010). The P-type ATPase superfamily. *J. Mol. Biol. Biotechnol.* **19**, 5-104.

Chiemchaisri, C., Chiemchaisri, W., Kumar, S. and Wicramarachchi, P. N. (2012). Reduction of methane emission from landfill through microbial activities in cover soil: A brief review. *Crit. Rev. Environ. Sci. Technol.* **4**, 412-434.

Chinenov, Y. V. (2000). Cytochrome c oxidase assembly factors with a thioredoxin fold are conserved among prokaryotes and eukaryotes**.** *J. Mol. Med.* (*Berl*). **78**, 239-242.

Chistoserdov, A. Y., Chistoserdova, L. V., McIntire, W. S. and Lidstrom, M. E. (1994) Genetic organization of the *mau* gene cluster in *Methylobacterium extorquens* AM1: complete nucleotide sequence and generation and characteristics of *mau* mutants. *J. Bacteriol.* **176**, 4052–4065.

Chistoserdova, L. (2011). Modularity of methylotrophy, revisited. *Environ. Microbiol.* **13**, 2603–2622.

Choi, D. W., Kunz, R. C., Boyd, E. S. and other authors (2003). The membrane-associated methane monooxygenase (pMMO) and pMMO-NADH, quinone oxidoreductase complex from *Methylococcus capsulatus* (Bath). *J. Bacteriol.* **185**, 5755-5764.

Choi, D. W., Antholine, W. E., Do, Y. S. and other authors (2005). Effect of methanobactin on the activity and electron paramagnetic resonance spectra of the membrane-associated methane monooxygenase in *Methylococcus capsulatus* (Bath). *Microbiology* **151**, 3417-3426.

Choi, D. W., Corbin, J. Do, Y. S. Semrau, J. D. Antholine, W. E. Hargrove, M. S. Pohl, N. L. Boyd, E. S. Geesey, G. G. and Hartsel S. C. (2006). Spectral, kinetic, and thermodynamic properties of Cu (I) and Cu (Ii) binding by methanobactin from *Methylosinus trichosporium* (OB3b). *Biochemistry* **45**, 1442-1453.

Choi, D. W., J. D. Semrau, W. E. Antholine, S. C. Hartsel, R. C. Anderson, J. N. Carey, A. M. Dreis, E. M. Kenseth, J. M. Renstrom, and L. L. Scardino (2008). Oxidase, superoxide dismutase, and hydrogen peroxide reductase activities of methanobactin from Types I and II Methanotrophs. *J. Inorg. Biochem.* **102**, 1571-1580.

Choi, D. W., Bandow, N. L., McEllistrem, M. T. and other authors (2010). Spectral and thermodynamic properties of methanobactin from gamma-proteobacterial methane oxidizing bacteria, a case for copper competition on a molecular level. *J. Inorg. Biochem.* **104**, 1240-1247.

Cicerone, R. J. and Oremland, R. S. (1988). Biogeochemical aspects of atmospheric methane. *Global Biogeochem. Cy.* **2**, 299-327.

Colby, J., Dalton, H. and Whittenbury, R. (1975). An improved assay for bacterial methane mono-oxygenase, some properties of the enzyme from *Methylomonas methanica*. *Biochem. J.* **151**, 459-462.

Colby, J., Stirling, D. I. and Dalton, H. (1977). The soluble methane mono-oxygenase of *Methylococcus capsulatus* (Bath). Its ability to oxygenate n-alkanes, n-alkenes, ethers, and alicyclic, aromatic and heterocyclic compounds. *Biochem. J.* **165**, 395-402.

Cook, K. L. and Sayler, G. S. (2003). Environmental application of array technology, promise, problems and practicalities. *Curr. Opin. Biotech.* **14**, 311-318.

Copp, J., N. and Neilan, B. A. (2006). The phosphopantetheinyl transferase superfamily: Phylogenetic analysis and functional implications in cyanobacteria. *Appl. Environ. Microbiol.* **72**, 2298-2305.

Cox, C. D., K. L. Rinehart, M. L. Moore, and J. C. Cook (1981). Pyochelin: novel structure of an iron-chelating growth promoter for *Pseudomonas aeruginosa*. *Proc. Natl. Acad. Sci. USA* **78**, 4256-4260.

Crombie, A (2011) Metabolism of methane and propane, and the role of the glyoxylate bypass enzymes in *Methylocella silvestris* BL2**.** PhD thesis submitted to School of Life Sciences, University of Warwick.

Crombie, A., and Murrell, J. C. (2011). Development of a system for genetic manipulation of the facultative methanotroph *Methylocella silvestris* BL2. *Meth. Enzymol.* **495**, 119-133.

Crutzen, P. J. (1994). Global budgets for non-CO_2 greenhouse gases. *Environ. Monit. Assess.* **31**, 1-15.

Csaki, R., Bodrossy, L., Klem, J., Murrell, J. C. and Kovacs, K. L. (2003). Genes involved in the copper-dependent regulation of soluble methane monooxygenase of *Methylococcus capsulatus* (Bath), cloning, sequencing and mutational analysis. *Microbiology* **149**, 1785-1795.

Cunliffe, M., Schaefer, H., Harrison, E., Cleave, S., Upstill-Goddard, R. and Murrell, J.C. (2008). Phylogenetic and functional gene analysis of the bacterial and archaeal communities associated with the surface layer of an estuary. *ISME J.* **2**, 776-789.

Dalton, H. (2005). The Leeuwenhoek lecture the natural and unnatural history of methane-oxidizing bacteria. *Philos. Trens. Roy. Soc. B.* **360**, 1207-1222.

D'Argenio, D. A. and Miller, S. I. (2004). Cyclic di-GMP as a bacterial second messenger. *Microbiology* **150**, 2497-2502.

Davies, S. L. and Whittenbury, R. (1970). Fine structure of methane and other hydrocarbon-utilizing bacteria. *J. Gen. Microbiol.* **61**, 227-232.

DeChaine, E. G. and Cavanaugh, C. M. (2006). Symbioses of methanotrophs and deep-sea mussels (Mytilidae, Bathymodiolinae). *Molecul. Basis Symb.* **41**, 227-249.

Dedysh, S. N., Khmelenina, V. N., Suzina, N. E., Trotsenko, Y. A., Semrau, J. D., Liesack, W. and Tiedje, J. M. (2002). *Methylocapsa acidiphila* gen. nov., sp. nov., a novel methane-oxidizing and dinitrogen-fixing acidophilic bacterium from *Sphagnum* bog. *Int. J. Syst. Evol. Microbiol.* **52**, 251.

Dedysh, S. N., Liesack, W., Khmelenina, V. N., Suzina, N. E., Trotsenko, Y. A.,

Semrau, J. D., Bares, A. M., Panikov, N. S., and Tiedje, J. M. (2000). *Methylocella palustris* gen. nov., sp. nov., a new methane-oxidizing acidophilic bacterium from peat bogs, representing a novel subtype of serine-pathway methanotrophs. *Int. J. Syst. Bacteriol.* **50**, 955-969.

Dedysh, S. N., Panikov, N. S. and Tiedje, J. M. (1998). Acidophilic methanotrophic communities from *Sphagnum* peat bogs. *Appl. Environ. Microbiol.* **64**, 922-929.

Dennis, J. J. and Zylstra, G. J. (1998). Plasposons: Modular self-cloning minitransposon derivatives for rapid genetic analysis of Gram-negative bacterial genomes. *Appl. Environ. Microbiol.* **64**, 2710-2715.

DiSpirito, A. A., Zahn, J. A., Graham, D. W., Kim, H. J., Larive, C. K., Derrick, T. S., Cox, C. D. and Taylor, A. (1998). Copper-binding compounds from *Methylosinus trichosporium* (OB3b). *J. Bacteriol.* **180**, 3606-3613.

Donadio, S. and Katz, L. (1992). Organization of the enzymatic domains in the multifunctional polyketide synthase involved in erythromycin formation in *Saccharopolyspora erythraea*. *Gene* **111**, 51-60.

Dorrell, N., Mangan, J. A., Laing, K. G., Hinds, J., Linton, D., Al-Ghusein, H., Barrell, B. G., Parkhill, J., Stoker, N. G., Karlyshev, A. V., Butcher, P. D., and Wren, B. W. (2001). Whole-genome comparison of *Campylobacter jejuni* human isolates using a low-cost microarray reveals extensive genetic diversity. *Genome Res.* **11**, 1706-1715.

Dumont, M. G. (2004). Diversity, mutagenesis and recombinant expression of the soluble methane monooxygenase. PhD Thesis, University of Warwick, UK.

Dunfield, P. F., Khmelenina, V. N., Suzina, N. E., Trotsenko, Y. A. and Dedysh, S. N. (2003). *Methylocella silvestris* sp nov., a novel methanotroph isolated from an acidic forest cambisol. *Int. J. Syst. Evol. Microbiol.* **53**, 1231-1239.

Dunfield, P. F., Yuryev, A., Senin, P. and other authors (2007). Methane oxidation by an extremely acidophilic bacterium of the phylum *Verrucomicrobia*. *Nature* **450**, 879-882.

Dunfield, P.F., Belova, S.E., Vorob'ev, A.V., Cornish, S.L., and Dedysh, S.N. (2010). *Methylocapsa aurea* sp. nov., a facultative methanotroph possessing a particulate methane monooxygenase, and emended description of the genus *Methylocapsa*. *Int. J. Syst. Evo.l Microbiol.* **60**, 2659-2664.

Duperron, S., Halary, S., Lorion, J., Sibuet, M. and Gaill, F. (2008). Unexpected co occurrence of six bacterial symbionts in the gills of the cold seep mussel *Idas* sp.(Bivalvia, Mytilidae). *Environ. Microbiol.* **10**, 433-445.

Dworkin, M. and Foster, J. W. (1956). Studies on *Pseudomonas methanica* (Sohngen) nov. comb. *J. Bacteriol.* **72**, 646-659.

Ehmann, D. E., Shaw-Reid, C. A., Losey, H. C. and Walsh, C. T. (2000). The EntF and EntE adenylation domains of *Escherichia coli* enterobactin synthetase: sequestration and selectivity in acyl-amp transfers to thiolation domain co-substrates. *Proc. Natl. Acad. Sci. USA*, **97**, 2509- 2514.

Eisenreich, W., Menhard, B., Hylands, P. J., Zenk, M. H. and Bacher, A. (1996). Studies on the biosynthesis of taxol: the taxane carbon skeleton is not of mevalonoid origin**.** *Proc. Natl. Acad. Sci. USA*, **93**, 6431-6436.

El Ghazouani, A., Basle, A., Firbank, S. J., Knapp, C. W., Gray, J., Graham, D. W. and Dennison, C. (2011). Copper-binding properties and structures of methanobactins from *Methylosinus trichosporium* (OB3b). *Inorg. Chem*. **50**, 1378-1391.

Elango, N., Radhakrishnan, R., Froland, W. A., Wallar, B. J., Earhart, C. A., Lipscomb, J. D. and Ohlendorf, D. H. (1997). Crystal structure of the hydroxylase component of methane monooxygenase from *Methylosinus trichosporium* (OB3b). *Protein Sci.* **6**, 556-568.

Ellis, K. E., Seidel, J., Einsle, O. and Elliott, S. J. (2011). *Geobacter sulfurreducens* cytochrome c peroxidases: electrochemical classification of catalytic mechanisms. *Biochemistry* **50**, 4513–4520.

Eren, E., Kennedy, D. C., Maroney, M. J. and Argüello, J. M. (2006). A novel regulatory metal binding domain is present in the C terminus of *Arabidopsis* Zn^{2+}-ATPase HMA2. *J. Biol. Chem*. **281**, 33881-33891.

Fan, B. and Rosen, B. P. (2002). Biochemical characterization of CopA, the *Escherichia coli* Cu(I)-translocating P-type ATPase. *J. Biol. Chem*. **6**, 46987-46992.

Ferenci, T., Strom, T. and Quayle, J. R. (1975). Oxidation of carbon monoxide and methane by *Pseudomonas methanica*. *J. Gen. Microbiol*. **91**, 79-91.

Fink, A. L. (1999). Chaperone-mediated protein folding. *Physiol. Rev***. 79**, 425-449.

Finking, R. and Marahiel, M. A. (2004). Biosynthesis of nonribosomal peptides 1. *Annu. Rev. Microbiol***. 58**, 453-488.

Fitch, M. W., Graham, D. W., Arnold, R. G., Agarwal, S. K., Phelps, P., Speitel, G. E., Jr. and Georgiou, G. (1993). Phenotypic characterization of copper-resistant mutants of *Methylosinus trichosporium* (OB3b). *Appl. Environ. Microbiol.* **59**, 2771-2776.

Fjellbirkeland, A., Kleivdal, H., Joergensen, C., Thestrup, H. and Jensen, H. B. (1997). Outer membrane proteins of *Methylococcus capsulatus* (Bath). *Arch. Microbiol*. **168**, 128-135.

Fjellbirkeland, A., Kruger, P. G., Bemanian, V., Hogh, B. T., Murrell, J. C. and Jensen, H. B. (2001). The C-terminal part of the surface-associated protein MopE of

the methanotroph *Methylococcus capsulatus* (Bath) is secreted into the growth medium. *Arch. Microbiol.* **176**, 197-203.

Fleige, S., and Pfaffl, M.W. (2006). RNA integrity and the effect on the real time qRT-PCR performance. *Mol. Aspects Med.* **27**, 126-139.

Fliermans, C. B., Phelps, T. J., Ringelberg, D., Mikell, A. T. and White, **D. C.** (1988). Mineralization of trichloroethylene by heterotrophic enrichment cultures. *Appl. Environ.Microbiol.* **54**, 1709-1714.

Foster, J. W. and Davis, R. H. (1966). A methane-dependent coccus, with notes on classification and nomenclature of obligate, methane-utilizing bacteria. *J. Bacteriol.* **91**, 1924-1931.

Fox, B. G., Froland, W. A., Dege, J. E. and Lipscomb, J. D. (1989). Methane monooxygenase from *Methylosinus trichosporium* (OB3b). Purification and properties of a three-component system with high specific activity from a type II methanotroph. *J. Biol. Chem*. **264**, 10023-10033.

Frangipani, E., and Haas, D. (2009). Copper acquisition by the SenC protein regulates aerobic respiration in *Pseudomonas aeruginosa* PAO1. *FEMS Microbiol. Lett*. **298**, 234–240.

Franke, S., Grass, G. and Nies, D. H. (2001). The product of the *ybdE* gene of the *Escherichia coli* chromosome is involved in detoxification of silver ions. *Microbiology* **147,** 965-972.

Froland, W. A., Andersson, K. K., Lee, S. K., Liu, Y. and Lipscomb, J. D. (1992). Methane monooxygenase component B and reductase alter the regioselectivity of the hydroxylase component-catalyzed reactions. A novel role for protein-protein interactions in an oxygenase mechanism. *J. Biol. Chem*. **267**, 17588-17597.

Fru, E. C. (2011). Copper biogeochemistry: A cornerstone in aerobic methanotrophic bacterial ecology and activity? *Geomicrobiol. J.* **28**, 601-614.

Fujimoto, M., Yamada, A., Kurosawa, J., Kawata, A., Beppu, T., Takano, H. and Ueda, K. (2011), Pleiotropic role of the Sco1/SenC family copper chaperone in the physiology of *Streptomyces*. *Microbiol Biotechnol.* doi: 10.1111/j.1751-7915.2011.00319.x.

Gaetke, L. M. and Chow, C. K. (2003). Copper toxicity, oxidative stress, and antioxidant nutrients. *Toxicology* **15**, 147-163.

Gao, X., Wang, P. and Tang, Y. (2010). Engineered polyketide biosynthesis and biocatalysis in *Escherichia coli*. *Appl. Microbiol. Biotechnol.* **88**, 1233-1242.

Garcia-Contreras, R., Celis, H. and Romero, I. (2004). Importance of *Rhodospirillum rubrum* H^+-pyrophosphatase under low energy conditions. *J. Bacteriol.* **186**, 6651–6655.

Ge, Z., Hiratsuka, K., and Taylor, D.E. (1995). Nucleotide sequence and mutational analysis indicate that two *Helicobacter pylori* genes encode a P-type ATPase and a cation binding protein associated with copper transport. *Mol. Microbiol.* **15**, 97-106.

Geymonat, E., L. Ferrando, and S. E. Tarlera (2011). *Methylogaea oryzae* gen. nov., sp. nov., a mesophilic methanotroph isolated from a rice paddy field. *Int. J. Syst. Evol. Microbiol.* **61**, 2568-2572.

Gilbert, B. and Frenzel, P. (1995). Methanotrophic bacteria in the rhizosphere of rice microcosms and their effect on porewater methane concentration and methane emission. *Biol. Fert. Soils* **20**, 93-100.

Gilbert, B., McDonald, I. R., Finch, R., Stafford, G. P., Nielsen, A. K. and Murrell, J. C. (2000). Molecular analysis of the *pmo* (particulate methane monooxygenase) operons from two type II methanotrophs. *Appl. Environ. Microbiol.* **66**, 966-975.

Glerum, D. M, Shtanko, A. and Tzagoloff, A. (1996). ScO-1 and ScO-2 act as high copy suppressors of a mitochondrial copper recruitment defect in *Saccharomyces cerevisiae*. *J. Biol. Chem*. **23**, 531-535.

Gonzalez-Guerrero, M., Raimunda, D., Cheng, X. and Arguello, J. M. (2010). Distinct functional roles of homologous Cu+ efflux ATPases in *Pseudomonas aeruginosa*. *Mol. Microbiol.* **78**, 1246-1258.

Göthel, S. F., and M. A Marahiel (1999). Peptidyl-prolyl cis-trans isomerases, a superfamily of ubiquitous folding catalysts. *Cell. Mol. Life Sci.* **55**, 423-436.

Green, M. J., and Hill, H.A. (1984). Chemistry of dioxygen. *Meth. Enzymol.* **105**, 3–22.

Green, J., Prior, S. D. and Dalton, H. (1985). Copper ions as inhibitors of protein C of soluble methane monooxygenase of *Methylococcus capsulatus* (Bath). *Eur. J. Biochem*. **153**, 137-144.

Green, P. N. (1992). Taxonomy of methylotrophic bacteria, In *Microbiol growth on C1 compounds*, p. 23–84. Edited by J. C. Murrell and D. P. Kelley, Intercept Press, Ltd., Andover, United Kingdom.

Grosse, S., Laramee, L., Wendlandt, K. D., McDonald, I. R., Miguez, C. B. and Kleber, H. P. (1999). Purification and characterization of the soluble methane monooxygenase of the type II methanotrophic bacterium *Methylocystis* sp. strain WI 14. *Appl. Environ. Microbiol.* **65**, 3929.

Gunther, M. R., P. M. Hanna, Mason, R. P., and Cohen M. S. (1995). Hydroxyl radical formation from cuprous ion and hydrogen peroxide: a spin-trapping study. *Arch. Biochem. Biophys*. **316**, 515–522.

Hahne, H., Mader, U., Otto, A., Bonn, F., Steil, L., Bremer, E., Hecker, M. and Becher, D. B. (2010). A comprehensive proteomics and transcriptomics analysis of *Bacillus subtilis* salt stress adaptation. *J. Bacteriol.* **192**, 870.

Hakemian, A. S. and Rosenzweig, A. C. (2007). The biochemistry of methane oxidation. *Annu. Rev. Biochem.* **76**, 223-241.

Halsey, T. A., Vazquez-Torres, A., Gravdahl, D. J., Fang, F. C. and Libby, S. J. (2004). The ferritin-like Dps protein is required for *Salmonella enterica* serovar *typhimurium* oxidative stress resistance and virulence. *Infect. Immun.* **72**, 1155-1158.

Han, B., Chen, Y., Abell, G., Jiang, H., Bodrossy, L., Zhao, J., Murrell, J. C. and Xing, X. H. (2009a). Diversity and activity of methanotrophs in alkaline soil from a Chinese coal mine. *FEMS Microbiol. Ecol.* **70**, 196-207.

Han, B., Su, T., Wu, H., Gou, Z., Xing, X. H., Jiang, H., Chen, Y., Li X, and Murrell, J. C. (2009b). Paraffin oil as a "methane vector" for rapid and high cell density cultivation of *Methylosinus trichosporium* (OB3b). *Appl. Microbiol. Biotechnol.* 83669-77.

Hanahan D. (1983). Studies on transformation of *Escherichia coli* with plasmids, *J. Mol. Bio.* **166**, 557–80.

Hanson, R. S. and Hanson, T. E. (1996). Methanotrophic bacteria. *Microbiol. Rev.* **60**, 439-471.

Harley, C.B., and Reynolds, R.P. (1987). Analysis of *E. coli* promoter sequences. *Nucl. Acids Res.* **15**, 2343-2361.

Hassani, B. K., Astier, C., Nitschke, W., and Ouchane, S. (2010). CtpA, a copper-translocating P-type ATPase involved in the biogenesis of multiple copper-requiring enzymes. *J. Biol. Chem.* **285,** 19330–19337.

Helland, R., Fjellbirkeland, A., Karlsen, O. A., Ve, T., Lillehaug, J. R. and Jensen, H. B. (2008). An oxidized tryptophan facilitates copper-binding in *Methylococcus capsulatus*-secreted protein MopE. *J. Biol. Chem.* **283**, 13897-13904.

Henckel, T., Friedrich, M. and Conrad, R. (1999). Molecular analyses of the methane-oxidizing microbial community in rice field soil by targeting the genes of the 16S rRNA, particulate methane monooxygenase, and methanol dehydrogenase. *Appl. Environ. Microbiol.* **65**, 1980-1990.

Herrero, M. de Lorenzo, V. and Timmis, K. N. (1990). Transposon vectors containing non-antibiotic resistance selection markers for cloning and stable chromosomal insertion of foreign genes in gram-negative bacteria. *J. Bacteriol.* **172**, 6557-6567.

Heyer, J., Berger, U., Hardt, M., and Dunfield, P.F. (2005). *Methylohalobius crimeensis* gen. nov., sp. nov., a moderately halophilic, methanotrophic bacterium isolated from hypersaline lakes of Crimea. *Int. J. Syst. Evol. Microbiol.* **55**, 1817-

1826.

Hickman, J. W., Tifrea, D. F. and Harwood, C. S. (2005). A chemosensory system that regulates biofilm formation through modulation of cyclic diguanylate levels. *Proc. Natl. Acad. Sci. USA*. **102**, 14422.

Hinton, J. C. D., Hautefort, I., Eriksson, S., Thompson, A. and Rhen, M. (2004). Benefits and pitfalls of using microarrays to monitor bacterial gene expression during infection. *Curr. Opin. Microbiol.* **7**, 277-282.

Holmes, A. J., Owens, N. J. and Murrell, J. C. (1995). Detection of novel marine methanotrophs using phylogenetic and functional gene probes after methane enrichment. *Microbiology***141**, 1947-1955.

Huffman, D. L., Huyett, J., Outten, F. W., Doan, P. E., Finney, L. A., Hoffman, B. M. and O'Halloran T. V (2002). Spectroscopy of Cu(II)-PcoC and the multicopper oxidase function of PcoA, two essential components of *Escherichia coli pco* copper resistance operon. *Biochemistry* **4**, 10046-1055.

Iguchi, H., Yurimoto, H. and Sakai. Y. (2010). Soluble and particulate methane monooxygenase gene clusters of the Type I methanotroph *Methylovulum miyakonense* Ht12. *FEMS Microbiol. Lett*. **312**, 71-76.

Iguchi, H, Yurimoto, H. and Sakai, Y. (2011). *Methylovulum miyakonense* gen. nov., sp. nov., a type I methanotroph isolated from forest soil. *Int. J. Syst. Evol. Microbiol*. **61**, 810-815.

Im, J., Lee, S. W., Yoon, S., DiSpirito, A. A., and Semrau, J. D. (2010). Characterization of a novel facultative *Methylocystis* species capable of growth on methane, acetate and ethanol. *Environ. Microbiol. Rep*. **3**, 174-181.

Ingraham, J. L., Maaloe, O. and Neidhardt, F. C. (1983). Growth of the bacterial cell. Sunderland, MA: Sinauer Associates.

Islam, T., Jensen, S., Reigstad, L. J., Larsen, Ø. and Birkeland, N. K. (2008). Methane oxidation at 55 ºC and pH 2 by a thermoacidophilic bacterium belonging to the *Verrucomicrobia* phylum. *Proc. Natl. Acad. Sci. USA*, **105**, 300.

Jenal, U. (2004). Cyclic di-guanosine-monophosphate comes of age: a novel secondary messenger involved in modulating cell surface structures in bacteria? *Curr. Opin. Microbiol.* **7**, 185-191.

Jenal, U. and Malone, J. (2006). Mechanisms of cyclic-di-GMP signalling in bacteria. *Annu. Rev. Genet*. **40**, 385-407.

Jiang, H., Chen, Y., Jiang, P., Zhang, C., Smith, T. J., Murrell, J. C. and Xing, X. H. (2010). Methanotrophs, multifunctional bacteria with promising applications in environmental bioengineering. *Biochem. Eng. J*. **49**, 277-288.

Junemann, S. Cytochrome *bd* terminal oxidase. (1997). *Biochim. Biophys. Acta*. **1321**, 107-127.

Kalyuzhnaya, M., Khmelenina, V., Suzina, N., Lysenko, A. and Trotsenko, Y. A. (1999). New methanotrophic isolates from soda lakes of the southern Transbaikal region. *Microbiology* **68**, 592-600.

Kaneko, T., Minamisawa, K., Isawa, T., Nakatsukasa, H., Mitsui, H., Kawaharada, Y., Nakamura, Y., Watanabe, A., Kawashima, K. and Ono, A. (2010). Complete genomic structure of the cultivated rice endophyte sp. B510. *DNA Res*. **17**, 37-50.

Karlsen, O. A., Berven, F. S., Stafford, G. P., Larsen, O., Murrell, J. C., Jensen, H. B. and Fjellbirkeland, A. (2003). The surface-associated and secreted MopE protein of *Methylococcus capsulatus* (Bath) responds to changes in the concentration of copper in the growth medium. *Appl. Environ. Microbiol*. **69**, 2386-2388.

Karlsen, O. A., Kindingstad, L., Angelskar, S. M. and other authors (2005). Identification of a copper-repressible c-type heme protein of *Methylococcus capsulatus* (Bath). A member of a novel group of the bacterial di-heme cytochrome c peroxidase family of proteins. *FEBS J*. **272**, 6324–6335.

Karlsen, O. A., Lillehaug, J. R. and Jensen, H. B. (2008). The presence of multiple c-type cytochromes at the surface of the methanotrophic bacterium *Methylococcus capsulatus* (Bath) is regulated by copper. *Mol. Microbiol*. **70**, 15-26.

Karlsen, O. A., Larsen, Ø. and Jensen, H. B. (2011).The copper responding surfaceome of *Methylococccus capsulatus* Bath. *FEMS Microbiol Lett*. **323**, 97-104.

Kennedy, J., Auclair, K., Kendrew, S. G., Park, C., Vederas, J. C. and Richard Hutchinson, C. (1999). Modulation of polyketide synthase activity by accessory proteins during lovastatin biosynthesis. *Science* **284**, 1368.

Kenney, G. E., and Rosenzweig. A. C. (2011). Chemistry and biology of the copper chelator methanobactin. *ACS Chem. Biol.* DOI: 10.1021/cb2003913.

Khmelenina, V., Starostina, N., Tsvetkova, M., Sokolov, A., Suzina, N. and Trotsenko, Y. A. (1996). Methanotrophic bacteria in saline reservoirs of Ukraine and Tuva. *Microbiology* **65**, 609-615.

Kim, H. J., Graham, D. W., DiSpirito, A. A., Alterman, M., Galeva, N., Asunskis, D., Sherwood, P. and Larive, C. K. (2004). Methanobactin, a copper-acquisition in methane-oxidizing bacteria. *Science* **305**, 1612 - 1615.

Kitmitto, A., Myronova, N., Basu, P. and Dalton, H. (2005). Characterization and structural analysis of an active particulate methane monooxygenase trimer from *Methylococcus capsulatus* (Bath). *Biochemistry* **44**, 10954-10965.

Knapp, C. W., Fowle, D. A, Kulczycki, J. Roberts, E. A. and Graham, D. W. (2007). Methane monooxygenase gene expression mediated by methanobactin in the presence of mineral copper sources. *Proc. Natl. Acad. Sci. USA* **104**, 12040–12045.

Kohli, R. M., Trauger, J. W., Schwarzer, D., Marahiel, M. A. and Walsh, C. T. (2001). Generality of peptide cyclization catalyzed by isolated thioesterase domains of nonribosomal peptide synthetases. *Biochemistry* **40**, 7099-7108.

Korostelev, A., Asahara, H., Lancaster, L., Laurberg, M., Hirschi, A., Zhu, J., Trakhanov, S., Scott, W. G. and Noller, H. F. (2008). Crystal structure of a translation termination complex formed with release factor RF2. *Proc. Natl. Acad. Sci. USA* **105**, 19684-19689.

Kothapalli, R., Yoder, S., Mane, S. and Loughran, T. (2002). Microarray results, how accurate are they? *BMC Bioinformatics* **3**, 22.

Kremer, M., L. (2006). Promotion of the fenton reaction by Cu^{2+} ions: Evidence for intermediates. *I. J. Chem. Kinetics* **38**,725-736.

Krentz, B. D., Mulheron, H. J., Semrau, J. D. and other authors (2010). A comparison of methanobactins from *Methylosinus trichosporium* (OB3b) and *Methylocystis* strain SB2 predicts methanobactins are synthesized from diverse peptide precursors modified to create a common core for binding and reducing copper ions. *Biochemistry* **49**, 10117-10130.

Krogh, A., Larsson, B., von Heijne, G. and Sonnhammer, E. L. (2001). Predicting transmembrane protein topology with a hidden Markov model: application to complete genomes. *J. Mol. Biol.* **305**, 567–580.

Kulczycki, E., Fowle, D. A., Knapp, C., Graham, D. W. and Roberts, J. A. (2007). Methanobactin-promoted dissolution of Cu-substituted borosilicate glass. *Geobiology* **5**, 251–263.

Kulczycki, E., Fowle, D. A., Kenward, P. A., Leslie, K., Graham, D. W. and Roberts, J. A. (2010). Stimulation of methanotroph activity by Cu-substituted borosilicate glass. *Geomicrobiol. J.* **28**, 1–10.

Leadbetter, E. R. (1974). Family Methylomonadaceae, In: Bergey's Manual of Determinative Bacteriology, 8th edn. pp. 267-269. Edited by Buchanan and Gibbons, The Williams and Wilkins company, Baltimore.

Leahy, J. G., Batchelor, P. J., and Morcomb, S. M. (2003) Evolution of the soluble diiron monooxygenases. *FEMS Microbiol. Rev*. **27**, 449-479.

Leary, S. C., Cobine, P. A., Kaufman, B. A., Guercin, G. H., Mattman, A., Palaty, J., Lockitch, G., Winge, D. R., Rustin, P., Horvath, R. and Shoubridge, E. A. (2007). The human cytochrome c oxidase assembly factors SCO1 and SCO2 have regulatory roles in the maintenance of cellular copper homeostasis. *Cell Metab*. **5**, 9–20.

Leary, S. C. (2010). Redox regulation of ScO protein function: Controlling copper at a mitochondrial crossroad. *Antioxid. Redox Signal.* **1**, 1403-1416.

Ledala, N., Sengupta, M., Muthaiyan, A., Wilkinson, B. J. and Jayaswal, R. (2010). Transcriptomic response of *Listeria monocytogenes* to iron limitation and Fur mutation. *Appl. Environ. Microbiol.* **76**, 406-416.

Lelieveld, J. O. S., Crutzen, P. J., and Dentener, F. J. (1998) Changing concentration, lifetime and climate forcing of atmospheric methane. *Tellus B* **50**, 128-150.

Lewinson, O., Lee, A. T. and Rees, D. C (2009). A P-type ATPase importer that discriminates between essential and toxic transition metals. *Proc. Natl. Acad. Sci. USA*, **106**, 4677-4682.

Li, Y. and R. Müller (2009). Non-modular polyketide synthases in myxobacteria. *Phytochem*. **70**, 1850-1857.

Lieberman, R. L. and Rosenzweig, A. C. (2005). Crystal structure of a membrane bound metalloenzyme that catalyses the biological oxidation of methane. *Nature*. **434**,177-182.

Lloyd, J. S., De Marco, P., Dalton, H. and Murrell, J. C. (1999a). Heterologous expression of soluble methane monooxygenase genes in methanotrophs containing only particulate methane monooxygenase. *Arch. Microbiol.* **171**, 364-370.

Lloyd, J. S., Finch, R., Dalton, H. and Murrell, J. C. (1999b). Homologous expression of soluble methane monooxygenase genes in *Methylosinus trichosporium* (OB3b). *Microbiol.* **145**, 461-470.

Lorenz, W. W., Alba, R., Yu, Y. S., Bordeaux, J. M., Simoes, M. and Dean, J. F. (2011). Microarray analysis and scale-free gene networks identify candidate regulators in drought-stressed roots of loblolly pine (*P. taeda* L.). *BMC Genomics* **12**:264-280.

Lontoh, S. and J. D. Semrau (1998). Methane and trichloroethylene degradation by *Methylosinus trichosporium* (OB3b) expressing particulate methane monooxygenase. *Appl. Environ. Microbiol.* **64**, 1106-1114.

Ludwig, W. and Schleifer, K. (1994). Bacterial phylogeny based on 16S and 23S rRNA sequence analysis. *FEMS Microbiol. Rev*. **15**, 155-173.

Lutsenko, S. and Petris, M. (2003). Function and regulation of the mammalian copper-transporting ATPases, insights from biochemical and cell biological approaches. *J. Memb. Biol.* **191**, 1-12.

Maeshima, M. (2000). Vacuolar H^+-pyrophosphatase. *Biochim. Biophys. Acta*. **1465**, 37–51.

March, P. E., Lerner, C. G., Ahnn, J., Cui, X. and Inouye, M. (1988). The *Escherichia coli* Ras-like protein (Era) has GTPase activity and is essential for cell growth. *Oncogene*. **2**, 539-44.

Martin, H. and Murrell, J. C. (1995). Methane monooxygenase mutants of *Methylosinus trichosporium* constructed by marker-exchange mutagenesis. *FEMS Microbiol. Lett*. **127**, 243-248.

Marzi, S, Myasnikov A. G, Serganov, A., Ehresmann, C., Romby, P., Yusupov, M. and Klaholz, B. P (2007). Structured mRNAs regulate translation initiation by binding to the platform of the ribosome. *Cell*. **130**, 1019-31.

Matsushita, K., Takaki, Y., Shinagawa, E., Ameyama, M. and Adachi, O. (1992). Ethanol oxidase respiratory chain of acetic acid bacteria: reactivity with ubiquinone of pyrroloquinoline quinone-dependent alcohol dehydrogenase purified from *Acetobacter aceti* and *Gluconobacter suboxydans*. *Biosci. Biotechnol. Biochem*. **56,** 304–310.

Mattatall, N. R., Jazairi, J. and Hill, B. C. (2000). Characterization of YpmQ, an accessory protein required for the expression of cytochrome c oxidase in *Bacillus subtilis*. *J. Biol. Chem*. **15**, 28802-9.

McDaniel, R., Ebert-Khosla, S., Hopwood, D. A. and Khosla, C. (1993). Engineered biosynthesis of novel polyketides. *Science* **262**, 1546-1550.

McDonald, I. R., Kenna, E. M. and Murrell, J. C. (1995). Detection of methanotrophic bacteria in environmental samples with the PCR. *Appl. Environ. Microbiol*. **61**, 116-121.

McDonald, I. R. and Murrell, J. C. (1997). The particulate methane monooxygenases gene *pmoA* and its use as a functional gene probe for methanotrophs. *FEMS Microbiol. Lett*. **156**, 205-210.

McDonald, I. R., Uchiyama, H., Kambe, S., Yagi, O. and Murrell, J. C. (1997). The soluble methane monooxygenase gene cluster of the trichloroethylene-degrading methanotroph *Methylocystis* sp. strain M. *Appl. Environ. Microbiol*. **63**, 1898-1904.

Medvedkova, K., Khmelenina, V. and Trotsenko, Y. A. (2007). Sucrose as a factor of thermal adaptation of the thermophilic methanotroph *Methylocaldum szegediense* O-12. *Microbiol*. **76**, 500-502.

Meister, M., Saum, S., Alber, B. E., and Fuchs, G. (2005). L-Malyl-coenzyme A/β-methylmalyl-coenzyme A lyase is involved in acetate assimilation of the isocitrate lyase-negative bacterium *Rhodobacter capsulatus J. Bacteriol*. **187**, 1415-1425.

Miller, D. A., Luo, L., Hillson, N., Keating, T. A. and Walsh, C. T. (2002). Yersiniabactin synthetase: A four-protein assembly line producing the nonribosomal peptide/polyketide hybrid siderophore of *Yersinia pestis*. *Chem. Biol*. **9,** 333-344.

Murrell, J. C. (1992). Genetics and molecular biology of methanotrophs. *FEMS Microbiol. Rev*. **8**, 233-248.

Murrell, J. C. (1994). Molecular genetics of methane oxidation. *Biodegradation* **5**, 145-159.

Murrell, J. C., Gilbert, B. & McDonald, I. R. (2000). Molecular biology and regulation of methane monooxygenase. *Arch Microbiol* **173**, 325-332.

Murrell, J. C. and McDonald, I. R. (2000). Methylotrophy, In Encyclopedia of Microbiology, vol. 3, pp. 245–255. Edited by J. Lederberg, Academic Press, Inc., New York, N. Y.

Nielsen, A. K., Gerdes, K., Degn, H. and Murrell, J. C. (1996). Regulation of bacterial methane oxidation, transcription of the soluble methane mono-oxygenase operon of *Methylococcus capsulatus* (Bath) is repressed by copper ions. *Microbiol.* **142**, 1289-1296.

Nielsen, A. K., Gerdes, K. and Murrell, J. C. (1997). Copper-dependent reciprocal transcriptional regulation of methane monooxygenase genes in *Methylococcus capsulatus* and *Methylosinus trichosporium*. *Mol. Microbiol.* **25**, 399-409.

Nguyen, H. H., Elliot, S. J., Kent, B. H. & 10 other authors (1996). The biochemistry of the particulate methane monooxygenase. In Microbiol Growth on C_1 , Compounds, pp. 150-158. Edited by M. E. Lidstrom and F. R. Tabita. Dordrecht, Kluwer.

Odermatt, A., Suter, H. Krapf, R. and Solioz, M. (1992). An ATPase operon involved in copper resistance by *Enterococcus hirae*. *Ann. NY. Acd. Sci.* **671**, 484-484.

Okubo, Y., Skovran, E., Guo, X., Sivam, D., and Lidstrom, M. E. (2007). Implementation of microarrays for *Methylobacterium extorquens* AM1. *OMICS J. Integr. Biol.* **11**, 325-340.

Olano, C., Méndez, C. and Salas, J. A. (2010). Post-PKS tailoring steps in natural product-producing actinomycetes from the perspective of combinatorial biosynthesis. *Nat. Prod. Rep.* **27**, 571-616.

Oldenhuis, R., Vink, R. L., Janssen, D. B., and Witholt, B. (1989). Degradation of chlorinated aliphatic hydrocarbons by *Methylosinus trichosporium* (OB3b) expressing soluble methane monooxygenase. *Appl. Environ. Microbiol.* **55**, 2819-2826.

Op den Camp, H. J. M., Islam, T., Stott, M. B., Harhangi, H. R., Hynes, A., Schouten, S., Jetten, M. S. M., Birkeland, N. K., Pol, A. and Dunfield, P. F (2009). Environmental, genomic and taxonomic perspectives on methanotrophic *Verrucomicrobia*. *Environ. Microbiol. Rep*. **1**, 293-306.

Osman, D. And Cavet, J. S. (2008). Copper homeostasis in bacteria. *Adv. Appl. Microbiol.* **65**, 217-247.

Outten, F. W., Outten, C. E., Hale, J. And O'Halloran T. V. (2000). Transcriptional activation of an *Escherichia coli* copper efflux regulon by the chromosomal MerR homologue, *cueR*. *J. Biol. Chem*. **275**, 31024-31029.

Pace, N., Stahl, D., Lane, D. and Olsen, G. (1986). The analysis of natural microbial populations by ribosomal RNA sequences. *Adv. Microbiol. Ecol*. **9**, 1-55.

Paulus, A. and de Vries, S. (2011). Energy conversion and conservation by cytochrome oxidases, In Copper-Oxygen Chemistry 1st edn., pp. Edited by K. D. Karlin and S. Itoh, John Wiley and Sons, Inc., Hoboken, N. J, USA.

Pearson, A. R., De la Mora-Rey, T., Graichen, M. E., Wang, Y. T., Jones, L. H., Marimanikkupam, S., Agger, S. A., Grimsrud, P. A., Davidson, V. L. and Wilmot, C. M. (2004). Further insights into quinone cofactor biogenesis: probing the role of *mauG* in methylamine dehydrogenase tryptophan tryptophylquinone formation. *Biochem*. **43,** 5494-5502, 2004.

Perri, A. and Hsu, S. (2003). A review of thalidomide's history and current dermatological applications. *Dermatol. Online J*. **9**, 1-13.

Petersen, J. M. and Dubilier, N. (2009). Methanotrophic symbioses in marine invertebrates. *Environ. Microbiol. Rep*. **1**, 319-335.

Phelps, P. A., Agarwal, S. K., Speitel, G. E. and Georgiou, G. (1992). *Methylosinus trichosporium* (OB3b) mutants having constitutive expression of soluble methane monooxygenase in the presence of high levels of copper. *Appl. Environ. Microbiol*. **58**, 3701-3708.

Phung, L. T., Ajlani, G. and Haselkorn, R. (1994). P-type ATPase from the cyanobacterium *Synechococcus* 7942 related to the human Menkes and Wilson disease gene products. *Proc. Natl. Acad. Sci. USA* **91**, 9651-9654.

Pol, A., Heijmans, K., Harhangi, H. R., Tedesco, D., Jetten, M. S. M. and den Camp, H. J. M. O. (2007). Methanotrophy below pH 1 by a new *Verrucomicrobia* species. *Nature* **450**, 874-878.

Prazeres, S., Moura, J. J. G., Moura, I., Gilmour, R., Goodhew, C., Pettigrew, G. W., Ravi, N. and Huynh, B. H. (1995). Mössbauer characterization of *Paracoccus denitrificans* cytochrome *c* peroxidase**.** *J. Biol. Chem*. **270**, 24264 - 24269.

Prior, S. and Dalton, H. (1985a). Acetylene as a suicide substrate and active site probe for methane monooxygenase from *Methylococcus capsulatus* (Bath). *FEMS Microbiol. Lett*. **29**, 105-109.

Prior, S. D. and Dalton, H. (1985b). The effect of copper ions on membrane content and methane monooxygenase activity in methanol-grown cells of *Methylococcus capsulatus* (Bath). *J. Gen. Microbiol.* **131**, 155-163.

Pyle, A. M. (2008). Translocation and unwinding mechanisms of RNA and DNA helicases. *Annu. Rev. Biophys*. **37**, 317-336.

Raghoebarsing, A. A., Smolders, A. J. P., Schmid, M. C. and other authors (2005). Methanotrophic symbionts provide carbon for photosynthesis in peat bogs. *Nature*. **436**, 1153-1156.

Rahalkar, M., Bussmann, I. and Schink, B. (2007). *Methylosoma difficile* gen. nov., sp. nov., a novel methanotroph enriched by gradient cultivation from littoral sediment of Lake Constance. *Int. J. Syst. Evol. Microbiol.* **57**, 1073-1080.

Rahman Md. T., Crombie, A., Chen, Y., Stralis-Pavese, N., Bodrossy, L., Meir, P. McNamara, N. P. and Murrell, J. C. (2011) Environmental distribution and abundance of the facultative methanotroph *Methylocella*. *The ISME J*. **5**, 1061-1066.

Ramos, J. L., Martinez-Bueno, M., Molina-Henares, A. J., Teran, W. Watanabe, K., Zhang, X., Gallegos, M. T., Brennan, R. and Tobes R. (2005). The TetR Family of transcriptional repressors. *Microbiol. Molecul. Biol. Rev*. **69**, 326-356.

Rensing, C., Fan, B., Sharma, R., Mitra, B. and Rosen, B. P. (2000). CopA: an *Escherichia coli* Cu (I)-translocating P-type ATPase. *Proc. Nat. Acad. Sci. USA*, **97**, 652–656.

Rensing, C. and Grass, G. (2003). *Escherichia coli* mechanisms of copper homeostasis in a changing environment. *FEMS Microbiol. Rev*. **27**, 197-213.

Rhodius, V., Van Dyk, T. K., Gross, C. and LaRossa, R. A. (2002). Impact of genomic technologies on studies of bacterial gene expression. *Ann. Rev. Microbiol.* **56**, 599-624.

Rigby, K., Cobine, P. A., Khalimonchuk , O. and Winge, D. R. (2008). Mapping the functional interaction of Sco1 and Cox2 in cytochrome oxidase biogenesis**.** *J. Biol. Chem*. **30**, 15015-1522.

Roggentin, P., Rothe, B., Kaper, J. B., Galen, J., Lawrisuk, L., Vimr, E. R. and Schauer, R (1989). Conserved sequences in bacterial and viral sialidases. *Glycoconj. J*. **6**, 349-353.

Rondon, M. R., Ballering, K. S. and Thomas M. G. (2004). Identification and Analysis of a siderophore biosynthetic gene cluster from *Agrobacterium tumefaciens* C58. *Microbiol*. **150**, 3857-3866.

Rosenzweig, A. C., Frederick, C. A., Lippard, S. J. and Nordlund, P. (1993). Crystal structure of a bacterial non-haem iron hydroxylase that catalyses the biological oxidation of methane. *Nature* **366**, 537-543.

Rosenzweig, A. C., Brandstetter, H., Whittington, D. A., Nordlund, P., Lippard, S. J. and Frederick, C. A. (1997) Crystal structures of the methane monooxygenase hydroxylase from *Methylococcus capsulatus* (Bath): implications for substrate gating and component interactions. *Proteins*, **29**, 141-152.

Röttig, M., Medema, M. H., Blin, K., Weber, T., Rausch, C. and Kohlbacher, O. (2011). NRPSpredictor2—a web server for predicting NRPS adenylation domain specificity. *Nucleic Acids Res*. **39**, W362-W367.

Saenkham, P., Vattanaviboon, P. and Mongkolsuk, S. (2009). Mutation in *sco* affects cytochrome c assembly and alters oxidative stress resistance in *Agrobacterium tumefaciens*. *FEMS Microbiol Lett*. **293**, 122-129.

Sambrook, J., and Russell, D.W. (2001). Molecular cloning: A laboratory manual. New York: Cold Spring Harbor Laboratory Press

Sambrook, J., E. F. Fritsch, and T. Maniatis. (1989). Molecular cloning: a laboratory manual, 2nd edn. Cold Spring Harbor Laboratory, Cold Spring Harbor, New York.

Saxena, B., M. Modi, and V. V. Modi (1986). Isolation and characterization of siderophores from *Azospirillum lipoferum* D-2. *J. Gen. Microbiol*. **132**, 2219-2224.

Scanlan, J., M. G. Dumont, and J. C. Murrell (2009). Involvement of MmoR and MmoG in the transcriptional activation of soluble methane monooxygenase genes in *Methylosinus trichosporium* (OB3b). *FEMS Microbiol. Lett*. **301**, 181-187.

Schafer, A., Tauch, A., Jager, W., Kalinowski, J., Thierbach, G. and Puhler, A. (1994). Small mobilizable multi-purpose cloning vectors derived from the *Escherichia coli* plasmids pK18 and pK19: selection of defined deletions in the chromosome of *Corynebacterium glutamicum*. *Gene* **145**, 69-73.

Schauer, K., Gouget, B., Carriere, M., Labigne, A. and de Reuse, H. (2007). Novel nickel transport mechanism across the bacterial outer membrane energized by the TonB/ExbB/ExbD machinery. *Mol. Microbiol*. **63**, 1054-1068.

Schena, M., Shalon, D. Davis, R. W. and Brown P. O. (1995). Quantitative monitoring of gene expression patterns with a complementary DNA microarray. *Science*. **270**, 467-470.

Scheutz C, Kjeldsen P, Bogner JA, De Visscher A, Gebert J, Hilger HA, Huber-Humer M and Spokas K (2009). Microbial methane oxidation processes and technologies for mitigation of landfill gas emissions. *Waste Manage. Res*. **27**, 409–455.

Schirmer, A., R. Gadkari, C. D. Reeves, F. Ibrahim, E. F. DeLong, and C. R. Hutchinson. (2005). Metagenomic analysis reveals diverse polyketide synthase gene clusters in microorganisms associated with the marine sponge *Discodermia dissoluta*. *Appl. Environ. Microbiol*. **71,** 4840-4849.

Schulze M. and Rödel, G. (1988). *scO-1*, a yeast nuclear gene essential for accumulation of mitochondrial cytochrome c oxidase subunit II. *Mol. Gen. Genet*. **3**, 492–498.

Schwan, W. R., Warrener, P. Keunz, E, Stover C. K and Folger, K. R. (2005). Mutations in the *cueA* gene encoding a copper homeostasis P-type ATPase reduce the pathogenicity of *Pseudomonas aeruginosa* in mice. *Int. J. Med. Microbiol.* **295**, 237–242.

Segal, E., Shapira, M., Regev, A., Peter, D., Botstein, D., Koller, D., Friedman, N. (2003). Module networks: identifying regulatory modules and their condition-specific regulators from gene expression data. *Nat. Genet*. **34**, 166–176.

Selbitschka, W., Niemann, S., and Pühler, A. (1993). Construction of gene replacement vectors for Gram-bacteria using a genetically modified *sacRB* gene as a positve selection marker. *Appl. Microbiol. Biotechnol.* **38**, 615-618.

Semrau, J. D., Chistoserdov, A., Lebron, J. and other authors (1995). Particulate methane monooxygenase genes in methanotrophs. *J. Bacteriol.* **177**, 3071-3079.

Semrau, J. D., DiSpirito, A. A. and Yoon, S. (2010). Methanotrophs and copper. *FEMS Microbiol. Rev*. **34**, 496-531.

Shah, S., Vaidehi K. and Anjana, D (1992). Isolation and characterization of siderophore, with antimicrobial activity, from *Azospirillum lipoferum* M. *M. Curr. Microbiol.* **25**, 347-351.

Shcolnick, S. and Keren, N. (2006). Metal homeostasis in cyanobacteria and chloroplasts. Balancing benefits and risks to the photosynthetic apparatus. *Plant Physiol.* **141**, 805–810.

Shigematsu, T., Hanada, S., Eguchi, M., Kamagata, Y., Kanagawa, T. and Kurane, R. (1999). Soluble methane monooxygenase gene clusters from trichloroethylene-degrading *Methylomonas* sp. strains and detection of methanotrophs during in situ bioremediation. *Appl. Environ. Microbiol.* **65**, 5198-5206.

Shimamoto, T. and Inouye, M. (1996). Mutational analysis of Era, an essential GTP-binding protein of *Escherichia coli*. *FEMS Microbiol. Lett*. **1**, 57-62.

Simon, R., Priefer, U. and Pühler, A. (1983). A broad host range mobilization system for *in-vivo* genetic engineering - Transposon mutagenesis in Gram-negative bacteria. *Bio-Technology* **1**, 784-791.

Simossis, V. A. and Heringa, J. (2005). PRALINE: a multiple sequence alignment toolbox that integrates homology-extended and secondary structure information. *Nucleic Acids Res*. **33**, W289-W294.

Sitthisak, S., Howieson, K., Amezola, C. and Jayaswal, R. K. (2005). Characterization of a multicopper oxidase gene from *Staphylococcus aureus*. *Appl. Environ. Microbiol.* **71**, 5650-5653.

Smith, K. S., Costello, A. M. and Lidstrom, M. E. (1997). Methane and trichloroethylene oxidation by an estuarine methanotroph, *Methylobacter* sp. strain BB5.1. *Appl. Environ .Microbiol.* **63**, 4617-4620.

Smith, T. J., Slade, S. E., Burton, N. P., Murrell, J. C. and Dalton, H. (2002). Improved system for protein engineering of the hydroxylase component of soluble methane monooxygenase. *Appl. Environ. Microbiol.* **68**, 5265-5273.

Smith, T. J., and Dalton. H. (2004). Biocatalysis by methane monooxygenases and its implications for the petroleum industry. In Petroleum biotechnology, developments and perspectives p. 177–192. Edited by R. Vazquez- Duhalt and R. Quintero-Ramirez: Elsevier, Amsterdam, The Netherlands.

Smith, T. J. and Murrell, J. C. (2009). Methanotrophy/methane oxidation. In Encyclopedia of Microbiology, 3rd edn, Vol. 3, pp. 293-298. Edited by M. Schaechter: Elsevier.

Smith, T. J. and Murrell, J. C. (2010). Methanotrophs. In: Encyclopaedia of Industrial Biotechnology, Bioprocess, Bioseparation and Cell Technology, pp 1-13, Edited by M. C. Flickenger: John Wiley and Sons.

Smith. T. J., Trotsenko, Y. A. and Murrell, J. C. (2010). Physiology and biochemistry of the aerobic methane oxidizing bacteria. In Handbook of Hydrocarbon and Lipid Microbiology, Vol. 2, pp. 767-780. Edited by K. N. Timmis, Berlin: Springer-Verlag.

Smith, T. J. and Murrell, J. C. (2011). Mutagenesis of soluble methane monooxygenase. In: Methods in methane metabolism, Methods in Enzymology vol. 495, pp 135-147. Edited by A. C. Rosenzweig and S. W. Ragsdale: Elsevier.

Solioz, M., and Odermatt, A. (1995). Copper and silver transport by CopB-ATPase in membrane vesicles of *Enterococcus hirae*. *J. Biol. Chem*. **270**, 9217-9221.

Solioz, M. and Stoyanov, J. V. (2003). Copper homeostasis in *Enterococcus hirae*. *FEMS Microbiol Rev* **27**, 183-195.

Solioz M, Abicht H. K, Mermod, M. Mancini, S. (2010). Response of Gram-positive bacteria to copper stress. *J. Biol. Inorg. Chem*. **15**, 3–14.

Söhngen, N. L. (1906). Über Bakterien, welche Methan als Kohlenstoffnahrung und Energiequelle gebrauchen. *Centr. Bakt. Parasitenk., Abt. II*, **16**, 513-517.

Speich, N., and Trüper. H. G. (1988). Adenylylsulfate reductase in a dissimilatory sulfate-reducing *Archaebacterium*. *J. Gen. Microbiol.* **134**, 1419- 1425.

Stafford, G. P., Scanlan, J., McDonald, I. R. and Murrell, J. C. (2003). *rpoN*, *mmoR* and *mmoG*, genes involved in regulating the expression of soluble methane monooxygenase in *Methylosinus trichosporium* (OB3b). *Microbiol*ogy **149**, 1771-1784.

Stanley, S. H., Prior, S. D., Leak, D. J. and Dalton, H. (1983). Copper stress underlies the fundamental change in intracellular location of methane monooxygenase in methane oxidizing organisms, studies in batch and continuous cultures. *Biotechnol. Lett*. **5**, 487-492.

Stainthorpe, A. C., Murrell, J. C., Salmond, G. P., Dalton, H. and Lees, V. (1989). Molecular analysis of methane monooxygenase from *Methylococcus capsulatus* (Bath). *Arch. Microbiol.* **152**, 154-159.

Stainthorpe, A. C., Lees, V., Salmond, G. P. C., Dalton, H. & Murrell, J. C.(1990). The methane monooxygenase gene cluster of *Methylococcus capsulatus* (Bath). *Gene* **91**, 27-34.

Staunton, J. and Weissman, K. J. (2001). Polyketide biosynthesis: a millennium review. *Nat Prod. Rep*. **18**, 380-416.

Stein, L.Y., Yoon, S., Semrau, J. D., DiSpirito, A. A., Crombie, A., Murrell, J. C. And other authors (2010). Genome sequence of the obligate methanotroph *Methylosinus trichosporium* strain (OB3b). *J. Bacteriol.* **192**, 6497-6498.

Stoecker, K., Bendinger, B., Schoning, B., Nielsen, P. H., Nielsen, J. L., Baranyi, C., Toenshoff, E. R., Daims, H. and Wagner, M. (2006). Cohn's *Crenothrix* is a filamentous methane oxidizer with an unusual methane monooxygenase. *Proc. Natl. Acad. Sci. USA*, **103**, 2363-2367.

Stoyanov, J. V., Hobman, J. L. and Brown, N. L. (2001). CueR (YbbI) of *Escherichia coli* is a MerR family regulator controlling expression of the copper exporter CopA. *Mol. Microbio*logy **39**, 502–512.

Stolyar, S., Costello, A. M., Peeples, T. L. and Lidstrom, M. E. (1999). Role of multiple gene copies in particulate methane monooxygenase activity in the methane oxidizing bacterium *Methylococcus capsulatus* (Bath). *Microbiol.* **145**, 1235-1244.

Stolyar, S., Franke, M. and Lidstrom, M. E. (2001). Expression of individual copies of *Methylococcus capsulatus* (Bath) particulate methane monooxygenase genes. *J. Bacteriol.* **183**, 1810-1812.

Sullivan, J. P., Dickinson, D. and Chase, H. A. (1998). Methanotrophs, *Methylosinus trichosporium* (OB3b), sMMO, and their application to bioremediation. *Crit. Rev. Microbiol.* **24**, 335-373.

Sultana, A., P. Kallio, Jansson, A., Wang, J. S., Niemi, J., Mäntsälä, P. and Schneider, G. (2004). Structure of the polyketide cyclase snoal reveals a novel mechanism for enzymatic aldol condensation. *EMBO J.* **23**, 1911-1921.

Summer, K. H., J. Lichtmannegger, N. Bandow, D. W. Choi, A. A. DiSpirito, and B. Michalke (2011). The biogenic methanobactin is an effective chelator for copper in a rat model for Wilson disease. *J. Trace Elem. Med. Bio.* **25**, 36-41.

Swem, D. L., Swem, L. R., Setterdahl, A. and Bauer, C. E. (2005). Involvement of SenC in assembly of cytochrome c oxidase in *Rhodobacter capsulatus*. *J. Bacteriol.* **187**, 8081-808.

Tal, R., Wong, H. C., Calhoon, R. and other authors (1998). Three *cdg* operons control cellular turnover of cyclic di-GMP in *Acetobacter xylinum*: genetic organization and occurrence of conserved domains in isoenzymes. *J. Bacteriol.* **180**, 4416.

Tamura, K., Peterson, D., Peterson, N., Stecher, G., Nei, M. & Kumar, S. (2011). MEGA5: Molecular Evolutionary Genetics Analysis using Maximum Likelihood, Evolutionary Distance, and Maximum Parsimony Methods. *Mol. Biol. Evol. Evol.* Doi: 10.1093/molbev/msr121.

Teitzel, G. M, Geddie, A. De Long, S. K, Kirisits, M. J., Whiteley, M. and Parsek, M. R. (2006). Survival and growth in the presence of elevated copper: transcriptional profiling of copper stressed *Pseudomonas aeruginosa*. *J. Bacteriol.* **188**, 7242–7256.

Tellez, C. M., K. P. Gaus, D. W. Graham, R. G. Arnold, and R. Z. Guzman (1998). Isolation of copper biochelates from *Methylosinus trichosporium* (OB3b) and soluble methane monooxygenase mutants. *Appl. Environ. Microbiol.* **64**, 1115-1122.

Theisen, A. R., Ali, M. H., Radajewski, S., Dumont, M. G., Dunfield, P. F., McDonald, I. R., Dedysh, S. N., Miguez, C. B. and Murrell, J. C. (2005). Regulation of methane oxidation in the facultative methanotroph *Methylocella silvestris* BL2. *Mol. Microbiol.* **58**, 682-692.

Theisen, A. R. and Murrell, J. C. (2005). Facultative methanotrophs revisited. *J. Bacteriol.* **187**, 4303-4305.

Thompson, A. K., Smith, D., Gray, J., Carr, H. S., Liu, A. M., Winge, D. R., and Hosler, J. P. (2010). Mutagenic analysis of Cox11 of *Rhodobacter sphaeroides*: insights into the assembly of Cu_B of cytochrome c oxidase. *Biochemistry* **49**, 5651–5661.

Tinberg, C. E., and S. J. Lippard (2009). Revisiting the mechanism of dioxygen activation in soluble methane monooxygenase from *Methylococcus capsulatus* (Bath): Evidence for a multi-step, proton-dependent reaction pathway. *Biochemistry* **48**, 12145-12158.

Tinberg, C. E., and S. J. Lippard (2011). Dioxygen activation in soluble methane monooxygenase. *Acc. Chem. Res.* **44,** 280–288.

Tischler, A. D. and Camilli, A. (2004). Cyclic diguanylate (c-di-GMP) regulates *Vibrio cholerae* biofilm formation. *Molec. Microbiol.* **53**, 857-869.

Tischler, A. D. and Camilli, A. (2005). Cyclic diguanylate regulates *Vibrio cholerae* virulence gene expression. *Infect. Immun.* **73**, 5873.

Tottey, S., Rich, P. R., Rondet, S. M. and Rosbinson, N. J. (2004). Two Menkes-type ATPases supply copper for photosynthesis in *Synechocystis* PCC 6803. *J. Biol. Chem*. **276,** 19999-20004.

Trotsenko, Y. A and Murrell, J. C. (2008). Metabolic aspects of aerobic obligate methanotrophy. *Adv. Appl. Microbiol.* **63**, 183-229.

Tsien, H. C., Brusseau, G. A., Hanson, R. S. and Waclett, L. P. (1989). Biodegradation of trichloroethylene by *Methylosinus trichosporium* (OB3b). *Appl Environ Microbiol* **55**, 3155-3161.

Tsuji, K., Tsien, H., Hanson, R., DePalma, S., Scholtz, R. and LaRoche, S. (1990). 16S ribosomal RNA sequence analysis for determination of phylogenetic relationship among methylotrophs. *J. Gen. Microbiol.* **136**, 1-10.

Tsubota, J., Eshinimaev, B., Khmelenina, V. N., and Trotsenko, Y. A. (2005). *Methylothermus thermalis* gen. nov., sp. nov., a novel moderately thermophilic obligate methanotroph from a hot spring in Japan. *Int. J. Syst. Evol. Microbiol.* **55**, 1877-1884.

Tsukada, S., Aono, T., Akiba, N., Lee, K. B., Liu, C. T., Toyazaki, H., and Oyaizu, H. (2009). Comparative genome-wide transcriptional profiling of *Azorhizobium caulinodans* ORS571 grown under free-living and symbiotic conditions. *Appl. Environ. Microbiol.* **75**, 5037-5046.

Ukaegbu, U. E., Henery, S., and Rosenzweig, A. C (2006). Biochemical characterization of MmoS, a sensor protein involved in copper-dependent regulation of soluble methane monooxygenases. *Biochemistry* **45**, 10191-10198.

Ukaegbu, U. E., and A. C. Rosenzweig (2009). Structure of the redox sensor domain of *Methylococcus capsulatus* (Bath) MmoS. *Biochemistry* **48**, 2207-2215.

Valnot, I., Osmond, S., Gigarel, N., Mehaye, B., Amiel, J., Cormier-Daire, V., Munnich, A., Bonnefont, J. P., Rustin, P. and Rötig, A. (2000). Mutations of the *scO-1* gene in mitochondrial cytochrome c oxidase deficiency with neonatal-onset hepatic failure and encephalopathy. *Am. J. Hum. Genet*. **67**, 1104-9.

Vigliotta, G., Nutricati, E., Carata, E. and other authors (2007). *Clonothrix fusca* Roze 1896, a filamentous, sheathed, methanotrophic γ-proteobacterium. *Appl. Environ. Microbiol.* **73**, 3556-3564.

Vorholt, J. A., Marx, C. J., Lidstrom, M. E., and Thauer R. K. (2000). Novel formaldehyde-activating enzyme in *Methylobacterium extorquens* AM1 required for growth on methanol. *J. Bacteriol.* **182**, 6645-6650.

Vorholt, J. A. (2002). Cofactor-dependent pathways of formaldehyde oxidation in methylotrophic bacteria. *Arch. Microbiol.* **178**, 239-249.

Vorobev, A. V., Baani, M., Doronina, N. V., Brady, A. L., Liesack, W., Dunfield, P. F. and Dedysh, S. N. (2010). *Methyloferula stellata* gen. nov., sp. nov., an acidophilic, obligately methanotrophic bacterium possessing only a soluble methane monooxygenase. *Int. J. Syst. Evol. Microbiol.* **61**, 2456-63.

Voskoboinik, I., Strausak, D., Greenough, M., Brooks, H., Petris, M., Smith, S., Mercer, J. F. and Camakaris, J. (1999). Functional analysis of the N-terminal CXXC metal-binding motifs in the human Menkes copper-transporting P-type ATPase expressed in cultured mammalian cells. *J. Biol. Chem.* **274**, 22008.

Wang, Y., Graichen, M. E., Liu, A., Pearson, A. R., Wilmot, C. M. and Davidson, V. L. (2003) MauG, a novel diheme protein required for tryptophan tryptophylquinone biogenesis. *Biochem*istry **42**, 7318–7325.

Ward, N., Larsen, O., Sakwa, J., Bruseth, L., Khouri, H., Durkin, A. S., Dimitrov, G., Jiang, L., Scanlan, D., Kang, K. H., Lewis, M., Nelson, K. E., Methe B. A., Wu, M., Heidelberg, J. F., Paulsen, I. T., Fouts, D., Ravel, J., Tettelin, H., Ren, Q., Read, T., DeBoy, R. T., Seshadri, R., Salzberg, S. L., Jensen, H. B., Birkeland, N. K., Nelson, W. C., Dodson, R. J., Grindhaug, S. H., Holt, I., Eidhammer, I., Jonasen, I., Vanaken, S., Utterback, T., Feldblyum, T. V., Fraser, C. M., Lillehaug, J. R. and Eisen, J. A. (2004). Genomic insights into methanotrophy, the complete genome sequence of *Methylococcus capsulatus* (Bath). *PLoS Biol* **2**, e303.

Whittenbury, R., Phillips, K. C. and Wilkinson, J. F. (1970). Enrichment, isolation and some properties of methane-utilizing bacteria. *J. Gen. Microbiol.* **61**, 205-218.

Whittenbury, R., and Krieg, N. R. (1984). Family IV. *Methylococcaceae* fam. nov. In Bergey's Manual of Systematic Bacteriology, pp. 256-261. Edited by N. R. Krieg and J. G. Holt. Baltimore, The Williams and Wilkins Co.

Winder, R. (2004). Methane to biomass. *Chem. Ind-London* 17-19.

Wise, M. G., McArthur, J. V. and Shimkets, L. J. (1999). Methanotroph diversity in landfill soil, isolation of novel type I and type II methanotrophs whose presence was suggested by culture-independent 16S ribosomal DNA analysis. *Appl. Environ. Microbiol.* **65**, 4887-4897.

Wise, M. G., McArthur, J. V. and Shimkets, L. J. (2001). *Methylosarcina fibrata* gen. nov., sp. nov. and *Methylosarcina quisquiliarum* sp. nov., novel type 1 methanotrophs. *Int. J. Syst. Evol. Microbiol.* **51**, 611-621.

Woese, C. R. (1987). Bacterial evolution. *Microbiol. Mol. Biol. Rev.* **51**, 221-271.

Wolfrum, T. and Stolp, H. (1987). Comparative studies on 5 S RNA sequences of RuMP-type methylotrophic bacteria. *Syst. Appl. Microbiol.* **9**, 273-276.

Woodland, M. P. and Dalton, H. (1984). Purification and characterization of component A of the methane monooxygenase from *Methylococcus capsulatus* (Bath). *J. Biol. Chem.* **259**, 53-59.

Wuebbles, D. J., and Hayhoe, K. (2002). Atmospheric methane and global change. *Earth-Sci. Rev*. **57**, 177-210.

Xin, J. Y., Cui J. R., Niu J. Z., Hua S. F., Xia C. G., Li S. B., Zhu L. M. (2004). Production of methanol from methane by methanotrophic bacteria. *Biocatal. Biotrasfor*. **22,** 225-229.

Yoon, S., Kraemer, S. M., DiSpirito, A. A. and Semrau, J. D. (2010). An assay for screen microbial cultures for chalkophore production. *Environ. Microbiol.* **2**, 295 - 303.

Yoon, S., DiSpirito, A. A., Kraemer, S. M. and Semrau, J. D. (2011). A simple assay for screening microorganisms for chalkophore production. *Meth. Enzymol.* **495**, 248 - 259.

Yu, S. S., Chen, K. H., Tseng, M. Y., Wang, Y. S., Tseng, C. F., Chen, Y. J., Huang, D. S. and Chan, S. I. (2003). Production of high-quality particulate methane monooxygenase in high yields from *Methylococcus capsulatus* (Bath) with a hollow-fiber membrane bioreactor. *J. Bacteriol*.**185**, 5915-5924.

Yun, C. W., Tiedeman, J. S., Moore, R. E. and Philpott, C. C. (2000). Siderophore-iron uptake in *Saccharomyces cerevisiae*. identification of ferrichrome and fusarinine transporters. *J. Biol. Chem*. **275**, 16354- 59.

Zahn, J. A., Arciero, D. M., Hooper, A. B. and Dispirito, A. A. (1996). Cytochrome *c* of *Methylococcus capsulatus* (Bath). *Euro. J. Biochem*. **240**, 684–691.
Zahn, J. A. and DiSpirito, A. A. (1996). Membrane associated methane monooxygenase from *Methylococcus capsulatus* (Bath). *J. Bacteriol*. **178**, 1018-1029.